Alma Mater Studiorum – Università di Bologna

DOTTORATO DI RICERCA IN

MECCANICA E SCIENZE AVANZATE DELL'INGEGNERIA

CICLO XXX

Settore Concorsuale di afferenza: 09/A1 Ingegneria Aeronautica, Aerospaziale e Navale

Settore Scientifico disciplinare: ING-IND/05 Impianti e Sistemi Aerospaziali

Design, development and testing of a GPS-based navigation sub-system for microsatellites missions

Presentata da: Alfredo Locarini

Coordinatore Dottorato   Relatore

Prof. Marco Carricato   Prof. Paolo Tortora

Esame finale anno 2018

Dedicated to my father

Abstract

The topic of spacecraft navigation can be addressed using different approaches, which can be grouped in ground based or space-based techniques. Previous space missions demonstrated that GPS-based navigation brings several advantages in terms of costs reduction of the whole mission and the possibility to obtain the position information in real-time on-board, making it directly available to all other sub-systems. While major spacecraft missions can easily host any model of the several spaceborne receivers available on the market, finding a GPS-based navigation solution for small satellite platforms is not an easy task, due to the limited budget, development time and available volume, typical of this kind of missions. Following the design philosophy of sub-systems for small satellites, this thesis presents the development process of a GPS-based navigation device for future low-cost missions, that aims at representing an ideal trade-off between high quality positioning in space and fast and cost effective manufacturing. The entire PhD work was carried out in the framework of the ESEO project, a microsatellite mission sponsored by ESA education office, and this thesis covers the entire design process of the GPS receiver, which will be launched as secondary payload on-board of this spacecraft. As part of a real space mission, this thesis describes all steps of the development, following the tight ESEO spacecraft schedule. Hardware and software design is described, focusing on the main solutions adopted to meet the typical reliability requirements of space applications. The GPS-based navigation payload underwent a long test campaign to assess its capability to operate in the space environment and the navigation algorithm was validated with the support of GPS signal simulators. The payload described herein is currently in the final development phases and its proto-flight model will be integrated soon within the ESEO platform, expected to be launched in Q4 2018. The results of the development and testing phases shown herein indicate that accurate and autonomous real-time orbit determination is a viable option also for microsatellite platforms, meeting stringent requirements in terms of development costs, and mass, volume and power availability. It is expected that this findings will eventually become flight proven during the ESEO in-orbit operations.

CONTENTS

LIST OF FIGURES

LIST OF TABLES

LIST OF ACRONYMS

C/A	Coarse Acquisition
COTS	Commercial Off-The-Shelf
CVCM	Collected Volatile Condensable Materials
EBB	Elegant Bread-Board
ECSS	European Cooperation for Space Standardization
EKF	Extended Kalman Filter
EMC	Electro-Magnetic Compatibility
ESA	European Space Agency
ESEO	European Student Earth Orbiter
GNSS	Global Navigation Satellite System
GPS	Ground Positioning System
HW	Hardware
LEO	Low Earth Orbit
MEO	Medium Earth Orbit
MRR	Manufacturing Readiness Review
OBDH	On Board Data Handling
PFM	Proto-Flight Model
PPS	Precise Positioning Service
QR	Qualification Review
SA	Selective Availability
S/C	Spacecraft
SPS	Standard Position Service
SW	Software
TMC	Total Mass Loss
TRR	Test Readiness Review
USART	Universal Asynchronous Receiver-Transmitter
WGS-84	World Geodetic System 1984

1 INTRODUCTION

1.1 Background and Motivation

Satellite-aided navigation technology was born with the purpose of providing position, velocity and time information to a user on the surface of the Earth. Starting from this idea, this technology evolved and laid the basis for the development of new services, like survey, surveillance, safety and rescue. At the same time satellite navigation technology proved to be suitable for the use also as instrument for scientific investigation, like terrestrial geodesy. The Ground Positioning System (GPS) is the first and the most widely used satellite navigation system. Originally intended for military purpose only, its development dates back to 1970 and its positioning concept was based on the previous radio navigation techniques implemented with terrestrial transmitters, while the first GPS operative satellite was launched in 1978. Starting from 1983 the service was open also to civil users and from 1991 was accessible from everywhere in the world. In the beginning, it was providing two different services: Standard Position Service (SPS), available for every user, and Precise Positioning Service (PPS), much more precise and for restricted use of the US Army. GPS, along with any other satellite navigation service, is composed of 3 segments:

- user, i.e. the sensor capable to lock satellite signal along with broadcasted data to calculate position and velocity;

- ground segment, a network of transmitting and receiving stations spread around the world, that provide 24/7 monitoring of the constellation status and performs tracking and operations of the GPS satellites. Periodic updates of satellites ephemeris and satellite clock correction are uploaded using five ground antennas every 12 hours;

- space segment, a constellation that was originally meant to include 24 satellites in circular Medium Earth Orbit (MEO) around the Earth with orbit radius of around 26.600 km and orbital period of 11 hours and 58 minutes. Satellites are distributed in 6 orbital planes with 55° of relative inclination to the equatorial orbit and inside each orbit they are separated from each other by 60°. The constellation now counts over 30 satellites with some inactive satellites ready to replace other satellites that goes out of service.

In the years, space segment underwent several improvements, providing new services and signal quality, with different generations of satellites being used for GPS service. In their current configuration, satellites of the GPS constellation transmits several types of signals distributed among three frequencies:

- L1 frequency [1575.42 MHz]: it includes Coarse/Acquisition (C/A) code and L1C signal for civil use; encrypted precision P(Y) code and M signal, for military purpose

- L2 frequency [1227.60 MHz]: it includes civil L2C signal and military P(Y) code

- L5 frequency [1176.45 MHz]: it includes L5 signal meant for civil use and safety purpose.

Until May 2000 the Selective Availability (SA) artificial degradation was affecting the civil signal accuracy to advantage US and allies military usage of GPS service. Nowadays, after de-activation of SA, the quality of the performance of the navigation sensors operating only on civil signals is good enough to be adapted to a wide range of demanding applications. The GPS geodetic reference is the WGS-84 (World Geodetic System 1984) and was introduced to enable GPS use, along with GPS System Time that differs from Coordinated Universal Time (UTC) by an integer number of seconds. Currently many satellite constellations are operative for navigation purpose at different stages of the development and they constitute the Global Navigation Satellite System network, including: GPS (USA), GLONASS (Russia), Beidou (China), Galileo (Europe), IRNSS (India), QZSS (Japan), along with several GNSS augmentation services, meant to support GNSS network and enhance its performance.

Parallel to the development of new techniques and technologies for terrestrial applications, GPS navigation was also adapted in the years for the use on-board of aircrafts and spacecrafts in Low Earth Orbit (LEO). The issue of autonomous navigation on-board of satellites has always been of great interest in the space sector, as the default practice for most missions foresees ground support for orbital determination, which results in an increase in mission costs, as well as the inability to obtain on-board real-time position data. The use of GPS-based navigation is the most direct solution to this problem, mainly in LEO orbit, where the operating altitude allows for excellent coverage by GPS constellation. Furthermore, with autonomous navigation, data are immediately available to all the other spacecraft subsystems, which can benefit of the precise knowledge of the position in real-time during the mission.

Many successful LEO missions benefited of autonomous GNSS navigation and in some of them the GNSS sensors covered a key role in the mission scientific purpose. Some of the most remarkable missions are: Topex/POSEIDON, for the oceans mapping and topography; GOCE and GRACE missions, for the accurate measurement of Earth gravity field and geoid; MetOP, a polar-orbiting weather satellite; SRTM, for high resolution topography. In order to satisfy the demanding technical requirements of the major missions, several GPS receivers were specifically developed for space applications. This new class of space-born receivers offers technical features and performance that are usually related and customized for the satellite platform hosting the GNSS receiver. Even if for space embedded applications the receiver design shall always reflect the specific spacecraft mission length, weight and available power, for major missions, like the ones listed before, the on-board technical resources do not usually represent a great constraint. Some of the most used and high performance space-born GNSS receivers for LEO spacecraft are listed in Table 1 with a brief overview of their technical details (where available):

Table 1: List of Spaceborn GNSS receivers

Receiver	Developer	Signals	Dimensions And Weight (kg)	Power consumption	Achievable Accuracy	Nominal Costs
BlackJack	NASA JPL	C/A, P1, P2, LA, L1, L2	3.2 kg	15 W	10-15 m	N/A
IGOR	BRE	C/A, P1, P2, LA, L1, L2	4.6 kg	16 W	10-15 m	500 k€
GRAS	Saab	C1,P1,P2 LA,L2	10 – 30 kg	50 W	20 m	2 M€
Lagrange	Laben	C1,P1,P2 LA,L2	5.2 kg	30 W	8 m	700 k€
TopStar 3000G2	Alcatel	C1, L2C LA, L2	N/A	N/A	5 m	N/A
IGPS-A	AAE	C1,P1,P2 LA,L2	N/A	N/A	5-10 m	N/A
OEM4-G2L	Novatel	C1, P2 LA,L2	50 g	1.5 W	14 m	10 k€

With the current state of the art of spaceborn GNSS receiver it is possible to easily achieve a GPS based real-time orbit determination with an accuracy of 10 m for LEO application, but it can be further improved by filtering techniques, based on reduced-dynamic philosophy. Although the presented examples demonstrates a wide and advanced use of GNSS navigation in space, the common receivers implement an expensive and complex architectural solution, that is not nearly applicable to micro- and nano- class of satellites missions, that play a key role in the current and future frontiers of space industry and research.

1.2 Thesis Breakdown

The research project presented in this thesis focused on development of a navigation sub-system based on a relatively simple and cost-effective hardware architecture, in order to meet the requirements of reduced budget and development time, typical of small satellite platforms. The main purposes of this work include the validation in space environment of commercial off the shelf (COTS) technologies for the tracking and demodulation of the GPS signal and the assessment of the performance of two real-time navigation algorithms, designed to provide different levels of accuracy. The selected commercial component under test is a GPS L1 baseband processor from Novatel, model OEM 615. This device is integrated with a dedicated navigation computer specifically designed with techniques and methods typical of space systems industry and its positioning performance is supported by the application software, in order to provide a reliable high quality navigation solution for micro- and nano- class of satellites. This thesis presents the design and testing phases and challenges that led to the development of a first prototype of the sub-system based on the mentioned philosophy, that was prepared for the European Space Agency (ESA) ESEO mission. This thesis is organized as follows:

Chapter 2: **GNSS Navigation in Low Earth Orbit**. This section provide a brief overview of the fundamentals of space segment design, focusing on small satellite missions features. The main topic of satellite navigation will be addressed, with a particular emphasis on receivers on-board of low Earth orbiting satellites.

Chapter 3: ESEO GPS Payload architecture. This chapter introduces the work performed on the design and development of the GPS Payload. A description of the device architecture and layout is included and the main, commercial and custom, functional parts are presented, motivating the design choices.

Chapter 4: Hardware design and testing. This chapter presents the mechanical and electrical hardware design process, description of the long test campaign performed on the device, in order to validate the design and qualify it for launch

Chapter 5: Application software development and validation. This chapter includes the description of the design and validation of the application software, hosted by the navigation computer. All software components are presented into details, highlighting how they perform every single task required to the custom navigation computer.

Chapter 6: Conclusions. In the final section, main outcomes of this project are resumed and some comments are provided as conclusions about the status of the project, along with next steps and future possible improvements.

2 GPS NAVIGATION IN LOW EARTH ORBIT

Satellites operating in Low Earth Orbit (LEO), between 200 and 2000 km, are particularly useful for a wide range of applications, such as remote sensing, communication, gravimetric and magneto-metric sensing, oceanography, atmospheric study and search and rescue operations. The accurate knowledge of their position is very important for the successful accomplishment of their mission. The possibility to use GPS navigation devices to precisely estimate the orbit of LEO satellites in real-time introduced great advantages for the space industry, in terms of overall mission costs and management:

- simpler implementation with respect to classical orbit determination methods based on terrestrial radiometric tracking, because it is not necessary anymore to measure and process satellite position on ground to perform operations on the spacecraft;

- mission overall costs reduction, because reduced ground support means less costs related to manpower needed to perform orbit determination;

- possibility to make data produced on-board directly available for the use in real-time by other sub-systems, to speed up scientific products availability time.

For this reason, GNSS receivers for satellite orbit determination became a common solution in recent satellite design, since it provides continuous satellite tracking and low-noise measurements on-board of a spacecraft user. The possibility to have high accuracy navigation on-board, also open to new operative scenarios, e.g. satellites formation flight, in order to achieve more complex mission tasks, like parallel group measures or for interferometry purpose. To develop a GPS-based navigation technology meant to operate on-board of satellites, the design process shall take into account both space systems design and satellite navigation issues. The principles of satellite-based navigation can adapted to be used on-board of spacecrafts by applying low level modifications with respect to terrestrial applications. Some difficulties arises when the target platform is a small satellite, where the reduced economical and power resources translate to strong constraints to the design and development process.

2.1 Small satellite platforms

In the last decades, a growing interest was shown by space industry and research towards small satellite platforms. They represent a simple and versatile instrument to access space, allowing the execution of missions characterized by reduced budget and development time, if compared to classical bigger class of space missions. Although at the beginning of the small satellites age, their dimensions translated into strong constraints to mission performance expectations, today this technological limit is removed by the current state of the art in the miniaturization process of sensors and sub-systems. The so called "small satellites" cover a category of

platforms from 0.1 kg up to 500 kg, but the categories of major interest from the scientific and industrial point of view are the micro- and nano- satellites (Table 2).

Table 2: Small class of satellite platforms

Category	Mass (kg)	
Mini satellite	100 to 500	
Micro satellite	**10 to 100**	
Nano satellite	**1 to 10**	
Pico satellite	0.1 to 1	
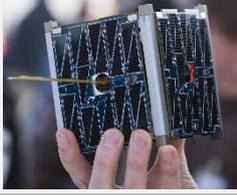
These platforms represent the perfect solution for space projects or applications carried out by universities, research centres or small companies, because small satellites missions can be entirely managed with a reduced budget. At the same time, they can be a useful resource also for the aerospace industry, thanks to the increasing quality of their performance and because they can be considered a fundamental step in the process to facilitate the access to space applications and research, with a consequent rise of the number of satellites developed and launched every year (Figure 1). Market forecasts, based on small satellites launches of the past years, show an increasing trend, so that many light launchers dedicated to small platforms are currently under development, in order to maximize the economic advantage derived from their use. In fact, the weight of a spacecraft represents a driving economical factor for space missions, with a launch cost per kilo between 10k$ and 50k$. For small satellite platforms with low budget sometimes the cost of the launch can be comparable to the cost of the entire space segment and mission management. For this reason one important design factor in the development of small satellite sub- systems is the research of lightweight solutions. Small satellites are suitable to be used as small orbital laboratory for microgravity experiments that do not need a big test chamber, for testing of new technologies and materials, to validate new instruments or sub-systems that will be used in future missions or to perform scientific monitoring and sensing, whose quality can satisfy a wide range of missions. This growing interest for small spacecrafts generated the need of adequate sub-systems, whose development philosophy shall be comparable to the small platform that hosts them.

Projections based on announced and future plans of developers and programs indicate as many as 3,000 nano/microsatellites will require a launch from 2016 through 2022.

Source: SpaceWorks Enterprises, Inc.
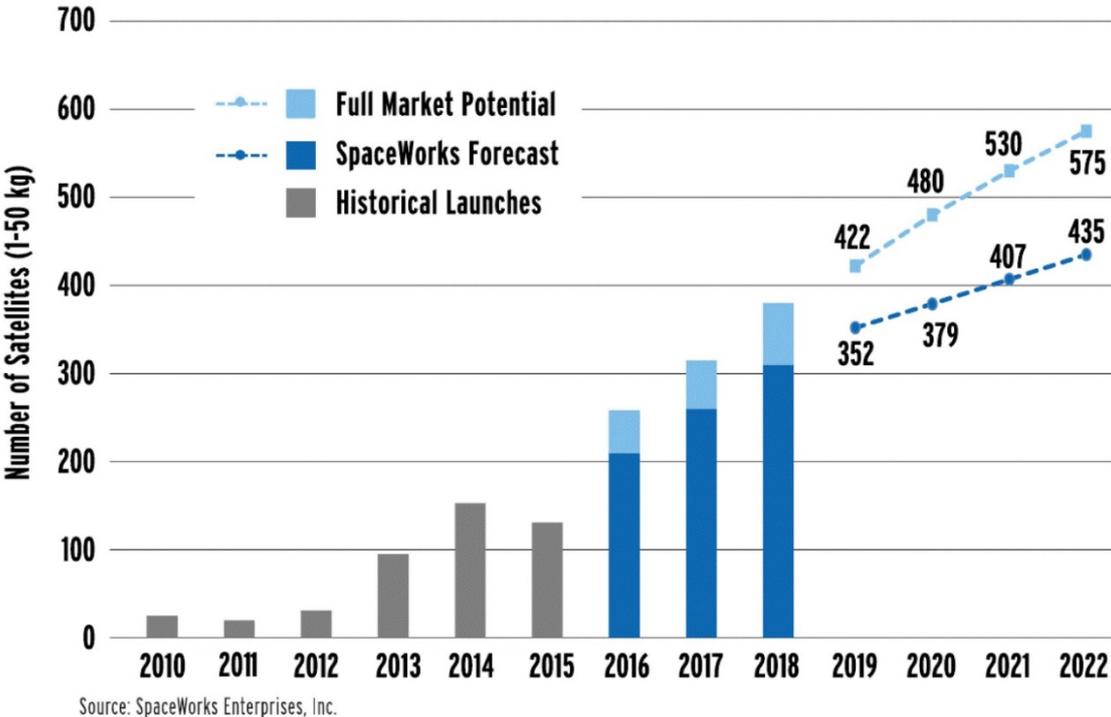
Figure 1: Nano- and micro- satellites launch history and forecast (source : SpaceWork Enterprises, Inc))

Beside size and budget issues, usually the architecture complexity of this type of systems is considerably lower with respect to bigger satellites, that translates in reduced available power on-board, that represents another strong constraint in the design phase. Due to their suitability to be used inside a constellation or group launch missions, small satellites may benefit of precise orbit determination, to enable new mission concepts for low orbits. Nevertheless, it is not possible to apply the same principles and the already proven technology of space-born GNSS receivers to small satellite platforms. In fact, they usually features many channels and multiple frequencies, providing high performance, but resulting at the same time not adapt to small spacecrafts missions, in terms of size, mass, power request and costs. For the mentioned reasons, in this case a different approach is required and, in this respect, the use of receivers based on COTS chipsets, with limited number of channels and capability to manage single frequency observations, may significantly reduce both development time and cost [23]. Considering such a simpler architecture, it is possible to obtain power levels compatible with the few tens of Watt available on-board and a solution that fits the reduced volume and mass limits of the structure for the target class of spacecrafts. On the other hand, in order to guarantee a good quality of the performance, COTS-based receivers shall implement quite sophisticated processing S/W running on a dedicated computing unit. The increasing available embedded computational resources allows the implementation of more sophisticated navigation techniques, like the reduced dynamic filtering approach, for this class of spacecraft.

2.2 Space segment design

The design and development process of devices for space application is regulated by severe technical requirements that are mostly related to the operative environment and for this reason widely different from terrestrial application design. Typical space projects development phases are briefly described in Table 3.

Table 3: Space system development process

Phase A: Feasibility	This phase includes feasibility study expressed as conceptual design and Preliminary Requirements Review
Phase B: Detailed definition	This phase covers complete sub-system level requirements definition, technology demonstration, and preliminary design, along with the subsystem requirements specification. It includes System Requirements Review and Preliminary Design Review.
Phase C: Detailed design and manufacturing drawings	This phase covers detailed design process and manufacturing preparation, including the Critical Design Review.
Phase D: Manufacturing, Assembly, Integration and Verification	This phase covers sub-system models manufacturing and validation through a test campaign, which includes functional, performance and environmental tests. After assembly and integration of the flight model with the satellite platform, qualification level tests are performed in order to obtain acceptance of the flight hardware for the launch. It includes also Manufacturing Readiness Review (MRR), Test Readiness Review (TRR), Qualification Review (QR), Acceptance Review (AR), Flight Readiness Review (FRR).
Phase E: Utilization	This phase covers the launch preparation activities, including launch and early orbit phase, commissioning phase (E1) and routine operations phase (E2). Usually ends with Launch Readiness review (LRR).
Phase F: Operations	This phase covers includes satellite missions procedures.

Usually sub-systems that are launched as payloads on-board of spacecrafts are not subjected to all typical design reviews foreseen for platform parts. For this project the following design verifications were applied, along with periodical status updated, by ESA and SITAEL officers: CDR, Software CDR (SW CDR), Manufacturing Readiness Review (MRR), Test Readiness Review (TRR).

This PhD work is included in the GPS Payload development process covering Phase C and Phase D of the project and started from the results of the graduation work performed by the same author of this thesis during the previous year [10], which included requirements definition, preliminary design (Phase B) of the electronic and mechanical hardware parts, and thermal analysis.

The main issues that need to be addressed during space sub-systems design [36], typical of the space operational environment, are:

- *Space radiations*: this aspect represents the main threat to electronic circuits on-board of spacecrafts. This ionizing radiation, present in space in form of high energy particles (e.g. neutrons, protons and gamma rays), includes: particles trapped in the Earth magnetic field, galactic cosmic radiation and solar particles events. Their action can affect electronics in two forms: Total Dose, failures linked to constant and repeated particles impact and collection of charge over time; Single Events, concentrated and instantaneous event that can lead to sudden catastrophic failure. This aspect is usually the main driving factor when designing electronic devices for space and represents the main reason for the application of restrictive reliability requirements that shall be accurately tailored.

- *Thermal environment*: spacecrafts operating in low Earth orbit, usually complete an entire revolution around the planet in almost 90-100 minutes. Since half of the orbit is considered to be in eclipse and half in sunlight, this means that every 45-50 minutes the satellite experiences an external temperature range from -25° C to 75°C. This represents a considerable thermal stress to the spacecraft subsystems, leading to degradation of the performance up to possible failures of some electronic components.

- *Low pressure and outgassing behaviour*: due to the very low external pressure of the space environment, it is necessary to accurately consider stresses in pressurized tanks and some types of battery models, along with the outgassing behaviour of some materials. The outgassing phenomenon affects mainly polymeric materials, because the high pressure difference may lead to expulsion of gas bubbles enclosed in the material, with subsequent diffusion of plastic powder that may deposit on other surfaces and affect nominal operations of sensors and other components.

- *Launch vibrations*: even if only for the short period of the launch, the sub-system experiences strong vibrations and for this reason it shall implement an adequate protective enclosure that is also needed as mechanical interface with the rest of the spacecraft. The external chassis shall guarantee sub-system integrity during the launch to ensure nominal operations of the system itself and the rest of the spacecraft during the mission.

Almost all of the mentioned aspects were covered with dedicated requirement during the development of the GPS receiver, object of this thesis, and each requirement was addressed by dedicated design solution or to be tested through an adequate test campaign [11]. There are also several other aspects to be taken into account, whose effect can be critical for specific space applications, but for the purpose of this thesis and for the relative smaller relevance for this project, they were not addressed into details: UV rays effects, atomic oxygeon erosion, plasma charge, microgravity condition.

2.3   GPS signal in space

In the previous chapter the main problems of the space missions design applicable to the development of a GPS-based navigation system, were presented. Following the same philosophy, in this section the GPS-based navigation features and the main difficulties and differences with respect to terrestrial applications are listed and briefly introduced. The GPS-based autonomous navigation on-board of spacecraft presents several aspects that appear different from ground application, with respect to hardware resources and signal characteristics. In this chapter only the issues applicable to the case of a small satellite mission are considered, considering only 1 zenith pointing GPS antenna and the spacecraft attitude fixed on three axes:

- *COCOM Limitations*: if a COTS front-end is used as core chipset for a GPS-based navigation device, it is necessary to take into account possible application by the manufacturer of the so-called COCOM limits. This software constraint, that can be implemented in several ways, inhibits GPS receiver functionality when it detects user speed above 1000 knots (1900 km/h) and height above 60000 feet (18 km). The reason behind this choice is for defence purpose, in order to avoid GPS-based navigation to be used for intercontinental ballistic missiles.

- *Doppler shift*: considering typical terrestrial applications the expected frequency shift of the incoming GPS signal due to the Doppler effect is expected to be from -5 kHz to up to 5 kHz. Using Unibo GPS signal software simulator, a scenario of a spacecraft in LEO orbit at about 500 km of altitude was set. The maximum Doppler values in module, affecting L1 frequency, for each available PRN appeared in the field of view, over a simulation time of 2 days, were calculated and displayed in Figure 2. Figure 3 shows instead all Doppler values affecting the signal received by 4 GPS satellites, PRN 12, 15, 19 and 22 during their appearance time in the field of view. The simulated data suggest that for receivers on board of LEO spacecraft, the possible range of Doppler values can cover values of up to one order of magnitude more then terrestrial applications.
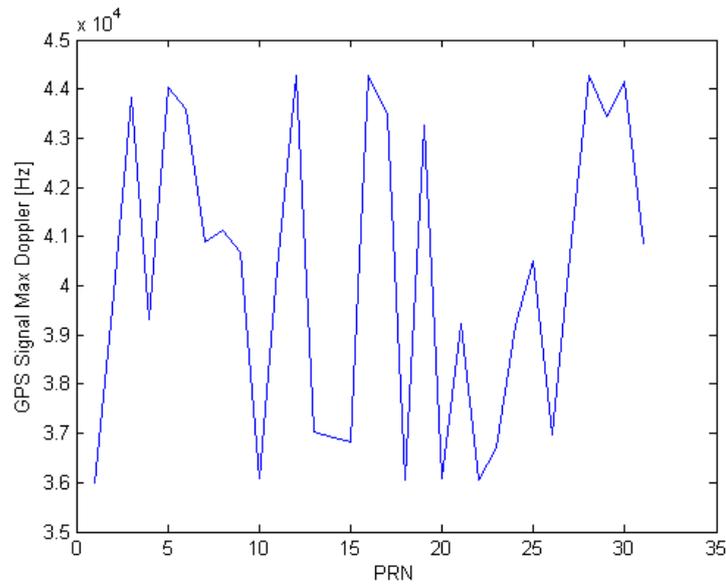
Figure 2 : Max Doppler values for each PRN satellite in the field of view obtained after a 2-days simulation
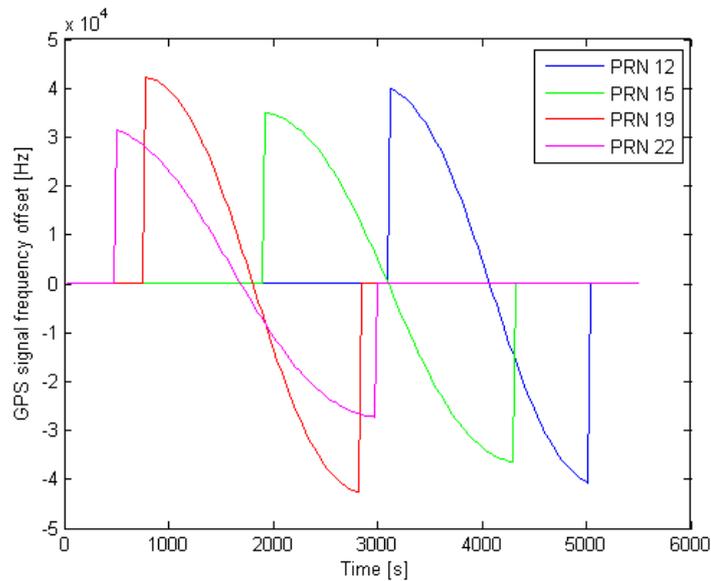
Figure 3: Simulated Doppler values of the GPS signal as experienced by a LEO receiver

As it is possible to see from the simulated values, for a receiver on-board of a LEO satellites moving at a speed of 6-7 km/s, the Doppler shift can reach values of up to one order of magnitude higher than the signal received on the surface of the Earth. This can be a problem during the signal acquisition phase, that can translate in longer acquisition times and, in case of a COTS chipset, the impossibility to lock the signal.

- *Embedded Electronics compatibility*: as already mentioned in previous sections, designing a GPS-based navigation sub-system for space applications implies facing the issue of limited power resources available on-board. While this problem is common to every embedded terrestrial application, on-board of spacecrafts it is even more critical. Since the only rechargeable power source is linked to solar panels, the

24

entire power design of the spacecraft is really critical and usually the amount of power dedicated to subsystems is lower than terrestrial applications and this is particularly true if the navigation sub-systems operates as a payload. Furthermore since the GPS receiver is connected to the platform data and power bus, that interfaces also all the other sub-systems, it shall meet a series of strict electrical and EMC (Electro-Magnetic Compatibility) requirements in order to avoid that a wrong behaviour or failures propagate to the rest of the spacecraft.

- *Computational limitations*: quite linked to the previous issue, also computational resources represents a limiting factor for space applications sub-systems. Due to the less volume and power available within the spacecraft platform, it is not possible to host high performing chipset and memory resources. This represents a driving factor when trying to implement sophisticated navigation algorithms, like the reduced dynamic filter, because on-board processor cannot afford the processing of excessively complex models and considerable computational loads. Furthermore, the models implemented inside reduced dynamic navigation filters usually includes many perturbations terms in order to provide a good estimation of the trajectory, so some approximations is needed to obtain an acceptable rate of fix processing.

- *Physical size and mass limitations*: as already discussed in Section 2.1, this aspect is a typical design factor of space applications and is not linked to the portability of the whole system, like happens for terrestrial applications, but to the actual volume available inside the spacecraft platform and to the cost of the launch. This factor limits the hardware extension and the subsequent achievable performance. If we consider a small satellite mission, these constraint become main design drivers and trade-offs shall be find to match limitations and data quality requirements.

- *Testing*: the issue of validation of GPS-based navigation devices for any application can be addressed by direct testing of the nominal functionality and performance in the real operative environment or, where this is not applicable, through the use of signal simulators. While usually in static or dynamic terrestrial and aircraft applications, the direct test in operative environment is not a problem, for receivers on-board of spacecrafts this is less trivial. Due to the costs and development time of a space mission for technology demonstration, it is necessary to perform extensive ground validation, using GPS signal simulators. Most of the commercial simulators include the possibility to set a spacecraft scenario. The issue with this approach is related to the accuracy of the orbital model included in the simulator, which sometimes is not well described in manuals. In fact, in order to test navigation filters that implements a model of the spacecraft of the trajectory, it is not easy to assess the actual performance and perform fine tuning, if the reference accuracy is not perfectly known.

3 ESEO GPS PAYLOAD ARCHITECTURE

Usually the validation process of sub-systems specifically designed for spacecraft is less trivial, with respect to terrestrial applications, because of the difficulty to simulate the operative conditions of the device. For this reason each new sub-system shall be tested in space as an experiment (payload), and only after assessing the actual performance, it can be used in future missions as part of the platform of the spacecraft. In particular, following the Technology Readiness Level (TRL) chart, used for assessing the reliability of a new technology and its suitability to be widely used in future missions, the GPS-based navigation sub-system, object of this thesis, can only reach TRL 7 out of 9, considering only the ground validation. Since this PhD project was carried out in the framework of the ESEO (European Student Earth Orbiter) project, that foresees the final launch of a spacecraft for new technologies testing purpose, this is a great opportunity to rise the TRL level of this GPS sub-system and making it ready to be integrated in future satellite platforms.

3.1   ESEO Project

ESEO is a micro-satellite class mission, sponsored by the Education Office of the European Space Agency, designed to operate in Low Earth Orbit, around 500 km height (Table 4).

Table 4: ESEO Spacecraft overview

Mass	50 Kg	
Altitude	523 km	
LTAN	10:30	
Eccentricity	0.001	
Attitude	Nadir pointing	
Dimension	33x33x63 cm	
TMTC	UHF: 437 MHz (DL) 435.5 MHz (UL)	
Scientific data	S Band (DL only)	
Launch (TBC)	Q4 2018	

This mission is designed with the purpose to involve students and researchers from several European universities and research centres, in the design and development of new satellite technology to be tested on-board of a micro- class spacecraft. Several European universities are involved in the project, and their effort is

focused on the payloads and experiments that will operate on-board, while the Italian company SITAEL (formerly ALMASpace) is the prime contractor for the platform.

The main scientific purposes of this satellite are:

- Earth imaging performed by one of the main payloads, which is a camera developed to take pictures of educational outreach.

- Measurement of the radiation levels along the orbit using a Langmuir probe and a TriTel three-axis dosimeter.

- Technology demonstration: several secondary payloads are carried on-board.

The University of Bologna contributes providing one of the secondary payloads for technology demonstration, a GPS-based navigation sub-system designed for satellites applications (Figure 4), and a ground station for mission telemetry and control.
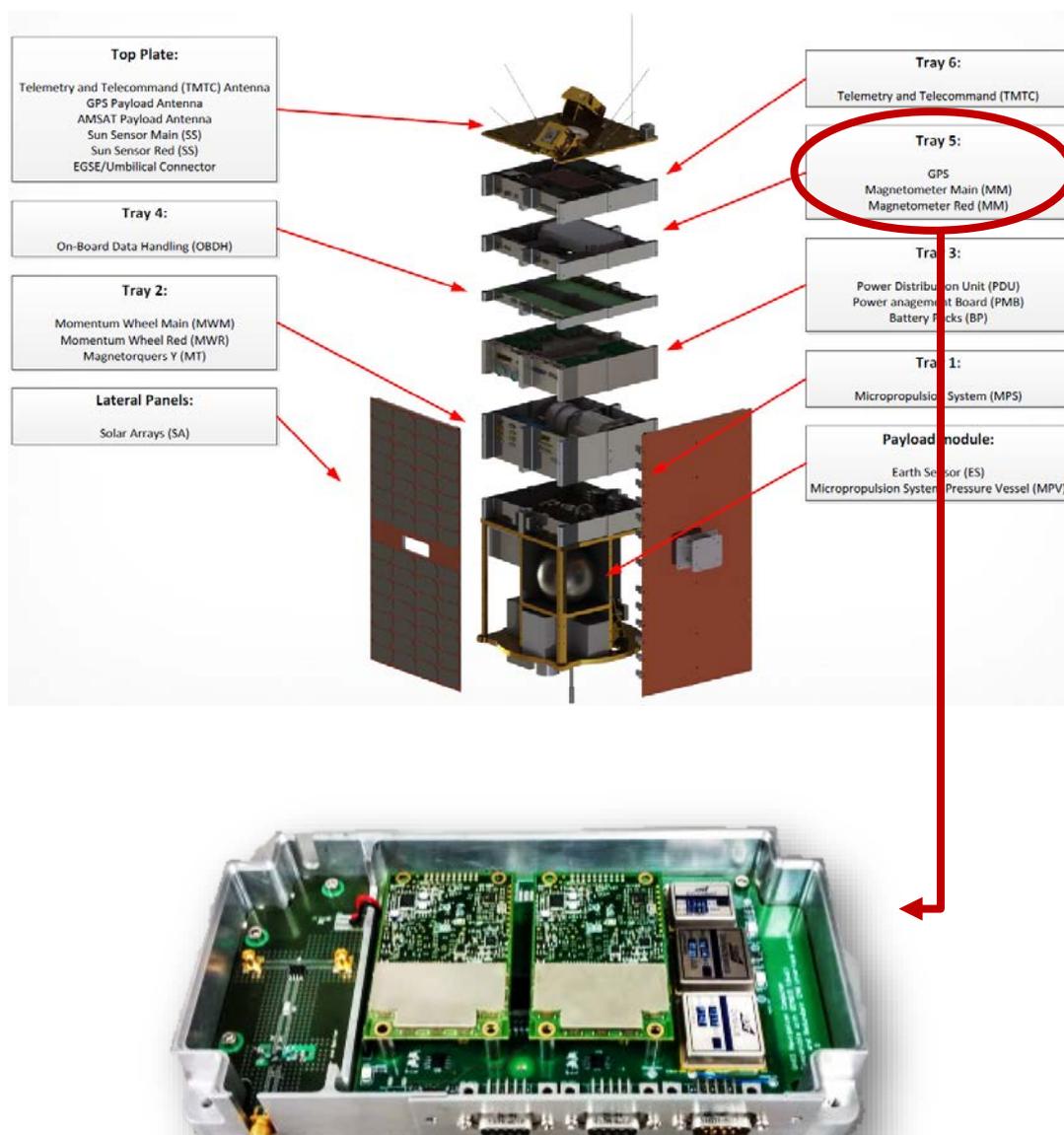
Figure 4: ESEO GPS Payload

The main purposes of the GPS Payload mission are:

- <u>verification in space environment</u> of the functionality of COTS navigation technology, commonly used in terrestrial GPS receivers

- <u>determination of the actual positioning accuracy</u> achievable by a commercial receiver in space using sophisticated navigation algorithms

The ESEO spacecraft is expected to be launched in sun-synchronous orbit by the end of 2018.

This project covered the part of development of the ESEO navigation payload, from the end of the master thesis work to the payload delivery for the integration within the satellite. Since this PhD project was carried out in the framework of an ESA space mission, it was organized following typical space missions schedule and obligations, including formal project reviews by ESA, weekly updates to ESA and SITAEL technical officers, periodic delivery of updated technical documentation about design and test campaign status along with the resolution of actions asked by ESA.

During this PhD project, the following technical documents were generated and delivered to ESA, in order to satisfy product assurance standards as indicated by ECSS-Q-ST-70C:

- *Design Definition File (DDF):* this is the main document of the project and was delivered several times with updated design and development status. It includes the complete list of sub-system level technical requirements, general payload features, electrical parts and components lists, extensive and detailed description of hardware and software design of the payload.

- *Experiment Interface Document part B (EIDB):* this document represents a fast reference to check for GPS Payload requirements compliancy. Every single requirement of the list is addressed with a short description of the compliance method (review of design or test). It presents also external interfaces description and resumes the payload general features.

- *Software Architectural Design Documentation (SWADD):* while in the DDF the software is only generally described, this document provides appropriate insight at code level, with accurate definition of source files and software packages.

- *House Keeping data and Telecommands description file (HKTC):* since the payload is no longer directly accessible from ground once integrated within the spacecraft platform, in order to perform operations, monitor the payload status and download scientific data during the mission, data shall be organized on-board as House Keeping or Scientific data packages and a set of telecommands was defined and implemented inside the application software.

- *Declared Mechanical Parts List (DMPL) and Declared Materials List (DML):* these two documents include the list of all parts and materials used inside the payload, in order to allow easy and quick quality check on materials or components.

- *User Manual (UM):* This document includes information about RF, data and power connectors, power-on information, mechanical interfaces, payload handling instructions that an external user may need, while using this sub-system.

- *Test Plan (TP):* it includes the complete list of tests the are part of the acceptance and qualification level test campaign. All tests included in the TP shall be performed in order to be compliant with the technical requirements.

- *Test Procedures (TPRO):* for each test included inside the TP, a dedicated detailed test procedure ad checklist was generated, in order to allow for a fast check of compliancy of the test architecture and correct implementation of methods and procedures.

- *Test Reports (TREP):* following the same philosophy of the TP, for each test performed on the GPS Payload a detailed report was produced showing the correct implementation of the procedure and the results along with comments about the results.

3.2 GPS Payload functional components

Although this device was specifically developed for the ESA ESEO mission, it was designed with the idea to create a general GPS navigation sub-system that can be used also in other micro- satellite platforms with minor HW and SW modifications, in order to meet the general technical requirements and make it a strategical element per small satellite industry [11]. The basic idea behind this project was to develop a *low-cost solution* for GPS positioning in space capable of produce *high quality data*. This design philosophy was implemented by selecting some common and simple COTS parts to be coupled with a dedicated processing computer and performing navigation software. The purpose was to provide a navigation service for satellites with the following features:

- **on-board**: direct measurements, no ground based radiometric tracking

- **sub-meter accuracy**: using a Kalman filter with a very accurate model of the s/c dynamics

- **in real-time**: no post-processing phase on ground

- **COTS components**: testing commercial technology in order to lower the *costs* and time of manufacturing

For this project the selected COTS component is the baseband processor, allowing for a better focus in the design on the observables processing part. Due to the harsh space environment, the choose of critical parts among COTS offer rises serious reliability issues. In this case the verification of COTS functionality and robustness in orbit is part of the ESEO GPS Payload mission purpose, however some solutions have been implemented: cold redundancy on critical component and electrical hardware protection. For this mission, a single frequency GPS-only base band processor, was selected and the reason of the choice of such a simple commercial components are:

- *Reduced price*: since the aim is to provide a cost-effective navigation subsystem for satellite missions with low budget, it is important to assess functionality and accuracy achievable in space with components that do not features high performance. However, the choice was also driven by the outcomes of the study of Montenbruck that demonstrated that a single frequency receiver can provide high accuracy positioning, if data are adequately processed.

- *Reduced power consumption*: a baseband processor capable to perform multi constellation processing on many channels and on different frequencies usually requires an amount of power that is not always available on-board of small satellites.

- *Replacement of the COTS component:* this project should be considered a starting point and many future improvements has been considered for future implementations of this navigation sub-system. One version foresees the replacement of the COTS baseband processor with a custom one, specifically designed for small satellite missions. For this reason, the development of a custom device that shall handle only one constellation signals and only one frequency and code, would be easier and faster.

The sub-system architecture includes four main functional units connected together (Figure 5): a commercial model of the baseband receiver has its communication interface connected to a custom computer in order to exchange commands (from the external computer to the COST front-end) and raw data (from the COTS front-end to the external computer). The commercial baseband processor has also radiofrequency interface that is connected a GPS antenna, placed externally, through a custom PCB that includes an low noise amplifier, to amplify the incoming GPS signal and make it compatible with the sensitivity range of the baseband processor.
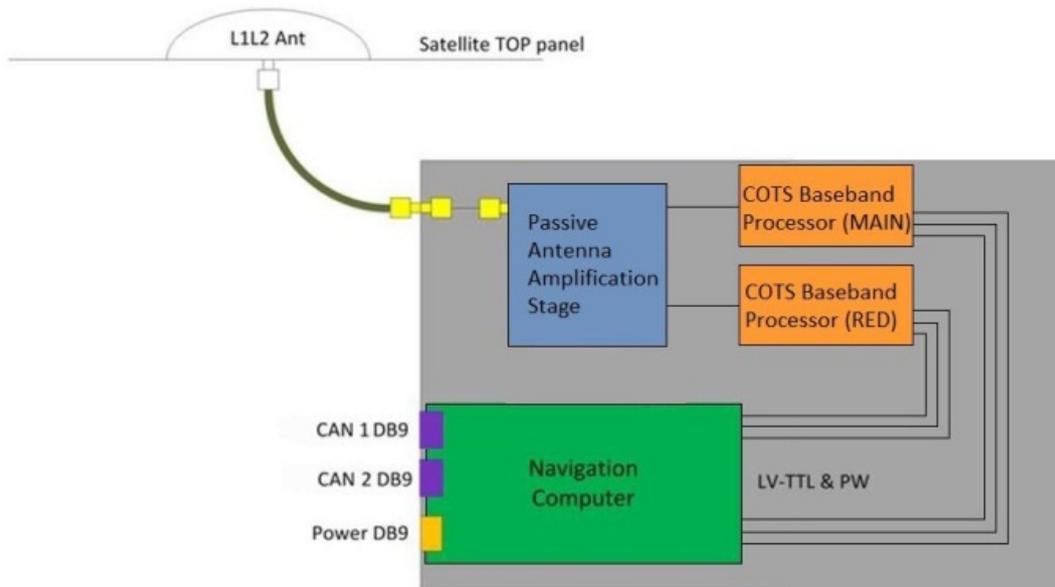
Figure 5: ESEO GPS Payload architecture

The mentioned main components that compose the GPS payload are presented in the next sections with their technical features.

3.2.1 COTS Baseband processor

The selected component is the model OEM 615 from Novatel [21], a GNSS receiver designed for terrestrial applications. This model is available in several versions, but the one used for this project is the simplest implementation (part number OEM615V-G1S-B0G-TT0), for the project philosophy explained in previous sections: GPS signal, single frequency L1, 16 channels. Although it is a complete receiver and it is able to perform PVT (position, velocity and time) navigation, inside this project it is used only for the GPS signal acquisition and processing phase, to test the GPS Payload navigation algorithms with raw GPS observables. The main products expected by this device are the raw observables, in terms of pseudorange and carrier phase, which are then processed by an external device. Its main technical details are listed in Table 5.

Table 5: COTS front-end component details

Frequency	L1 GPS	
Version	OEM	
Raw data	Yes	
Data update frequency	Up to 20Hz	
Dimensions	46 x 71 x 11 mm	
Weight	24g	
Voltage supply	3.3Vdc ± 5%	
Power consumption	Typically 1W	
Data Interface	LVTTL	
Acceptable RF input level	-122.0 to -87 dBm	

Since it is a critical component for the missions success, several reliable design solutions were applied in the GPS Payload architecture. To meet reliability requirements, two identical models of the same receiver were included inside the Payload. They are used in cold double redundancy: only one of them is operating at the same time and they are switched only in case a detected failure of the active receiver. Also some other reliability solutions were applied, but they were implemented on the other parts connected to the OEM 615 receiver, in order to avoid that a failure of the commercial part propagates externally to the GPS Payload and damages other spacecraft subsystems.

3.2.2 Navigation PC

This computer was specifically designed for this application and represents the core of the whole ESEO GPS Payload. It performs several tasks:

- Communication with Novatel front-ends

- Real-time processing of raw GPS observables

- Electrical and mechanical interface with the front-end

- Communication with S/C on-board data handling (OBDH)

- Payload power management

- Monitoring of COTS front-end functionality

- Telecommands handling

- Scientific and Housekeeping data collection

It is based on a STM32F407 microcontroller with ARM Cortex M4 core, which hosts the application software, including the navigation filters (Table 6). It implements USART communication interfaces and socket connectors to match the ones on the COTS front-end. To perform data exchange with the rest of the satellite

two DB9 connectors and CAN communication protocol were used, including 2 CAN transceivers. Another DB9 connector is used as power interface: incoming unregulated power passes through a voltage regulation stage, including two isolated DC/DC converters, which distributes power to the "data part" and "radiofrequency part" of the Payload. Right before the voltage regulator, an EMI filter is included to reduce conducted electromagnetic interference from the GPS payload to the rest of the satellite. Also a thermal sensing circuit is included: sensors, two 10K ohm Panasonic thermistor ERTJ1VG103FA, are placed to the external enclosure surface and on the top plane of the PCB, close to DC-DC converters.

Table 6: Navigation Computer component details

Power consumption	0.83 W	
Dimensions	208 x 108 mm	
Mass	0.159 kg	
Input Voltage	18 V – 25.5 V	
Data circuit voltage	3.3 V	
RF circuit voltage	5 V	
Max clock frequency	168MHz	
Processor speed	1.25DMPIS/MHz	
Flash memory	1024 kbytes	
SRAM memory	192 Kbytes	
ADC	24 analog channels with 12 bits of resolution	

To address reliability issues, several solutions were implemented during the Navigation PC design phase:

- Use of components with flight heritage: DC-DC converters, EMI filters, CAN transceivers, non volatile EEPROMs

- CAN communication cold double redundancy

- Overvoltage protection circuit: the sensing circuit detects the overvoltage condition, it activates the latch circuit that disables the DC/DC converters output.

- Current limiter circuit: avoids that a wrong behavior of one of the two front-ends damages the navigation computer; the circuit can be enabled with a digital output from the microcontroller, providing the power at 3.3V to the front-end. In case of anomaly in the current absorption, the circuit automatically disables the power to the front-end, allowing the microcontroller to switch to the redundant one.

3.2.3 GPS Antenna

The selected component is a patch antenna from Sensor Systems, series S67-1575 [20], that has flight heritage from previous space missions (e.g. CHAMP, GRACE) and, for this reason, provides confidence of correct functionality and was not covered by any reliability requirement. The antenna will be mounted on top external surface of the ESEO S/C that, according to the satellite expected attitude, will always be zenith pointing: considering also to the radiation pattern, geometry of the satellite and the antenna itself, the multipath effect is expected to be very low. The selected component is the passive single frequency version, that features reduced size and weight (Table 7).

Table 7: GPS antenna component details

Dimensions	90 x 90 x 15 mm	
Mass	0.170 kg	
Frequency	1575.42 MHz (L1)	
Gain	3 dBic (Zenith)	
Polarization	RHCP	
Tmeperature	-55 to 85	
Vibration	10 G	

3.2.4 Amplification stage

Since the selected antenna does not provide integrated pre- amplification of the signal, a custom PCB was design to support the antenna during signal reception. This amplification stage is placed between the navigation computer and the antenna and is used to amplify the GPS signal coming from the antenna and address the signal to the two different front-ends in double redundancy (Table 8). To perform this task it includes a Low Noise Amplifier (LNA), component PMA-545G2 from Mini Circuits, a bandpass filter and a power splitter. This PCB presents 3 SMA RF connectors, one for antenna cable connection and two for COTS front-ends cables connection. Power for the whole Payload is handled by the Navigation computer and is provided to the amplification stage through internal cables soldered to a wire pad

Table 8: Amplification stage component details

Power Consumption	1.05 W	
Dimensions	90 x 90 x 15 mm	
Mass	0.170 kg	
Input frequency range	1.1 and 1.6 GHz	
LNA Gain	30.4 dB	
Insertion loss (splitter + filter)	2.4 dB	
LNA Noise figure	1 dB	
Circuit Impedance	50 Ohm	
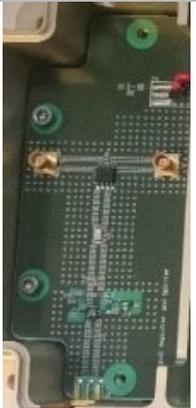
4 HARDWARE DESIGN AND TESTING

Following the schedule of activities agreed with ESA and the prime contractor SITAEL, the GPS Payload design flow was organized as follows:

1. Hardware design

2. Test campaign

3. Application software development

4. Application software debug and performance assessment

As already anticipated in previous chapters, the master thesis work of the author covered part of the first point of the previous list [10], in particular the first iteration of hardware design, following ESA requirements. During the PhD period, the design was refined and finalized, after several iterations with ESA and the company SITAEL, manufacturer of ESEO spacecraft platform. In this chapter, the results of the electronic and mechanical design are presented separately, while all verification sessions performed on the GPS Payload are included in a dedicated section. The first part the design phase focused on both electronic and mechanical hardware parts and included:

- Navigation computer PCB design

- Amplification stage PCB design

- External mechanical enclosure design

- Manufacturing files generation and delivery to external companies for production

4.1 Electronic H/W

The Altium Designer software was used to design the navigation computer and amplifications stage PCBs. The project of the navigation computer includes separated schematics for the main circuits grouped for functionality:

- Power supply management and overvoltage detection circuit

- Microcontroller and EEPROMs

- CAN interface

- External connectors

- Current Limiter circuit

- Thermal sensing circuit

Once generated the board file (.brd) from schematics, the routing procedure was performed (Figure 6). Where possible, since for most of the circuits there is a perfect copy introduced to implement the double redundancy of the front-end, the twin circuits were routed and placed symmetrically, to speed up the check process. The final board features 4 layers, top and bottom for components soldering and two internal plane to distribute power and ground. Ground layer was divided in three regions connected each other with 0 ohm resistor, to avoid disturbance propagation to each other: analog ground region, digital ground region and input ground region.
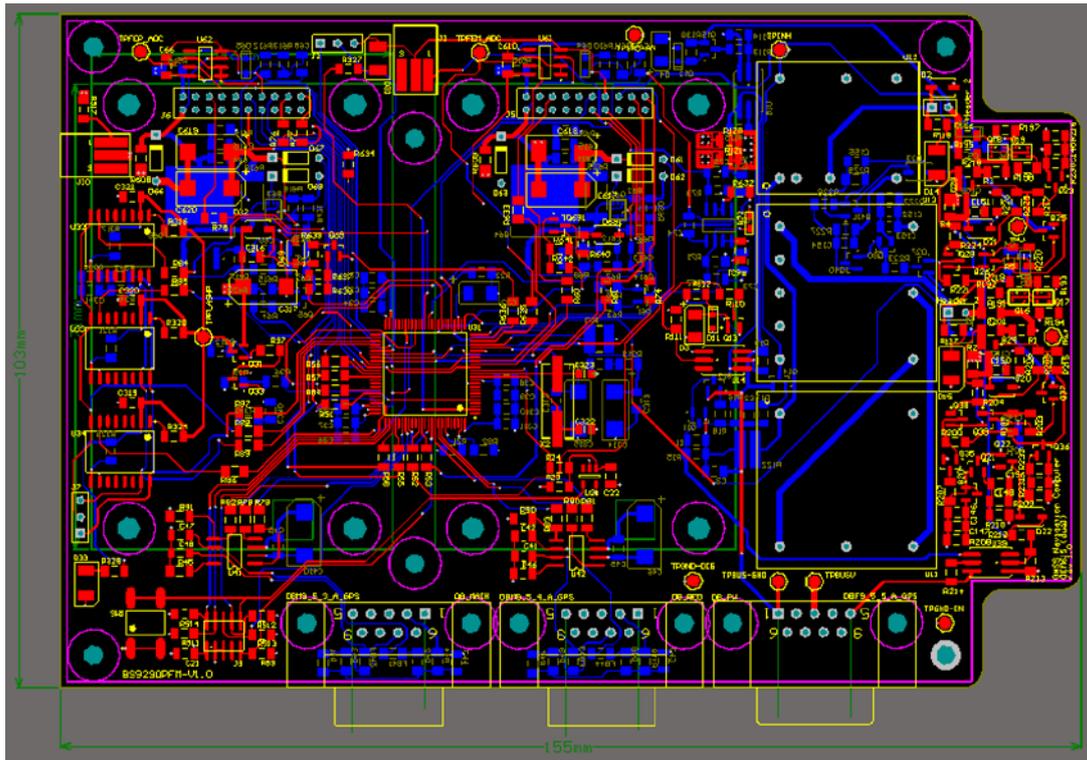
Figure 6 : Navigation computer board (all layers)

The routing and components placement in the centre of the board was performed taking into account to position of the two COTS front-ends. In fact the navigation computer is designed to implement both electrical and mechanical interface for the front-ends (Figure 7). Some space was left around the four mechanical interface points of the front-ends, in order to avoid the PCBs spacers to cover or touch electronic components on the top surface.
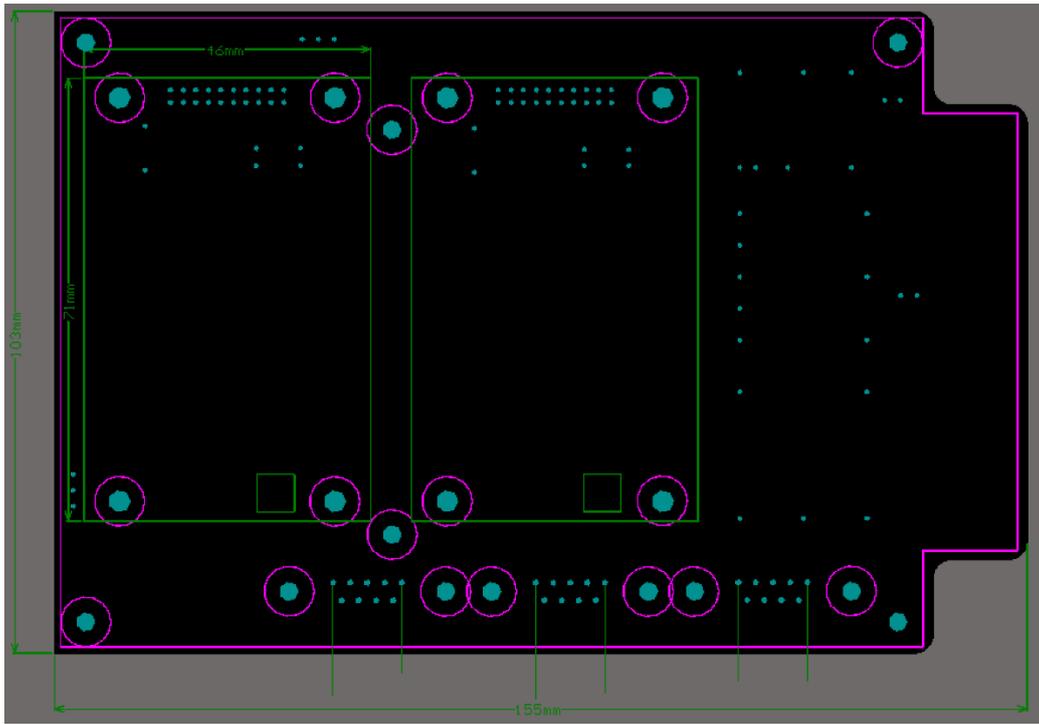
Figure 7: COTS Front-end interface

Figure 8 shows the 3D model obtained from the Altium board files.
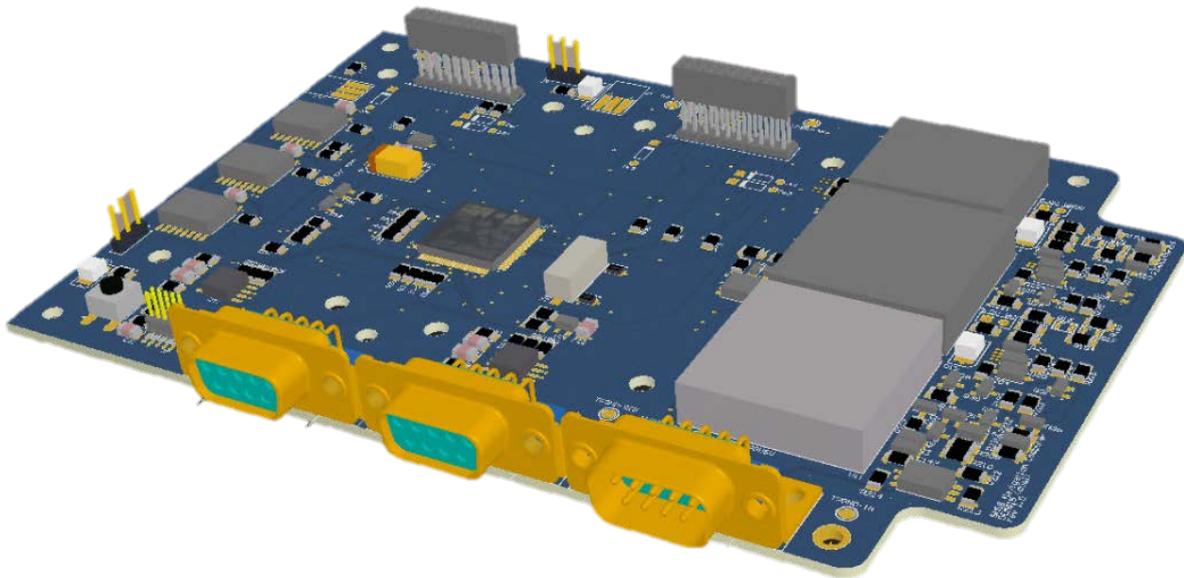
Figure 8: Navigation computer 3D model

The amplification stage drawing was simpler, due to the fewer amount of components involved, but with greater attention to components routing and PCB fabrication rules, because it is designed for radiofrequency purpose (Figure 9).
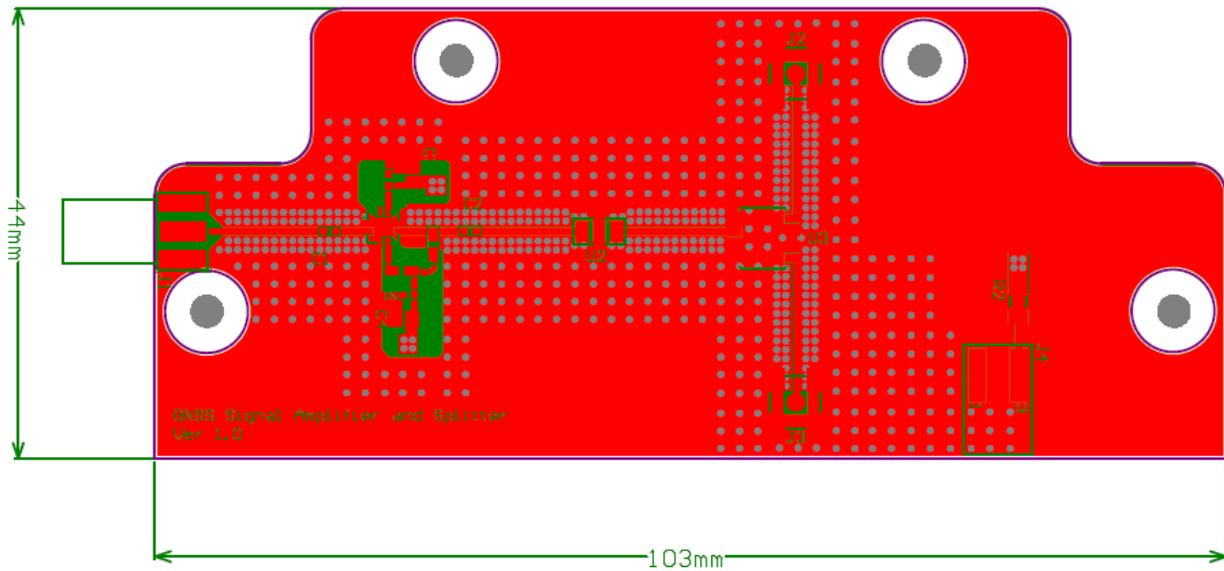
Figure 9 : Amplification stage board (all layers)

Figure 10 shows the 3D model obtained from Altium board files.
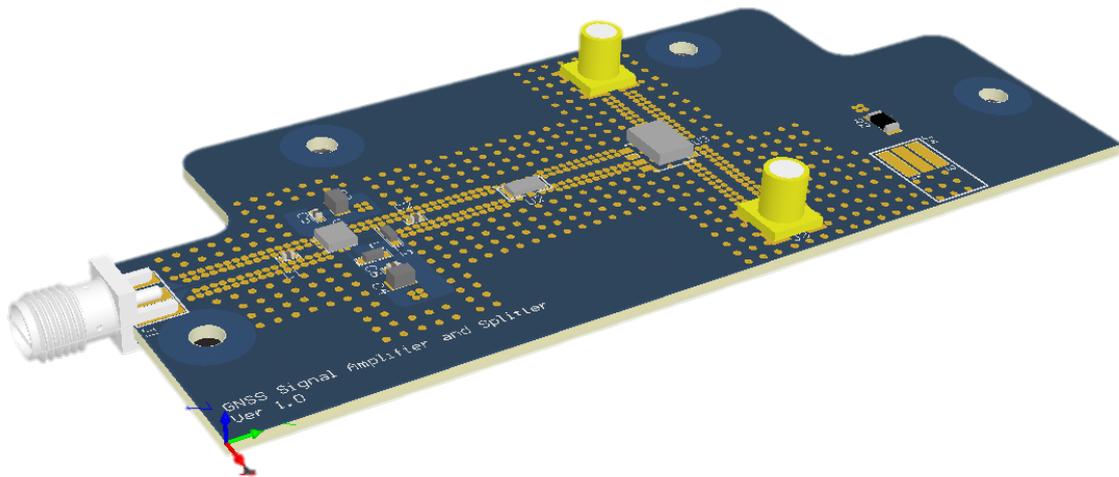
Figure 10: Amplification stage 3D model

4.2 Mechanical H/W

Even if the GPS Payload mission main task is performed by the Navigation computer and other PCBs, they shall be housed inside an enclosure, in order to guarantee their integrity during launch, to ease integration with the spacecraft, to provide grounding with the rest of the spacecraft and to partially contribute to Payload protection from radiative environment. Enclosure size, and subsequent PCBs dimensions, were linked to the volume dedicated to payloads by the spacecraft platform manufacturer. The enclosure is composed of three main parts: an empty box, a mask for DB9 connectors and a cover plate, which represents the top panel of the enclosure (Figure 11, Figure 12, Figure 13 and Figure 14). The selected material for the three mechanical parts is the aluminum alloy 7075 and an alodine 1200 treatment was applied on the external surfaces, according to dedicated aerospace materials guidelines [38]. The used material is an alloy of aluminum and zinc that is widely used for the structural parts in the aerospace industry, because it matches the need of low weight mechanical parts with high mechanical resistance and low thermal dilatation, that for the strong thermal cycles experienced during the mission can be an issue. Alodine coating is commonly used on structures that are connected to the ground planes of PCBs that are exposed to external environment, in order to maintain unaltered in time their electrical properties. In fact due to the oxidizing process of aluminum external surfaces, the low resistivity property of the enclosure can be affected and could represent an issue for PCBs correct functionality, if no protective coating is applied. To meet outgassing specifications Payload external protection material and potential coatings shall not emit particles due to the very low external pressure. In order to provide information about materials outgassing properties, Total Mass Loss (TMC) value and Collected Volatile Condensable Materials (CVCM) factors are commonly used, according to the dedicated ECSS (European Cooperation for Space Standardization) [37], and they represents the total mass expelled and the amount of that material that condensed on a collector. While the aluminum outgassing behaviour is neglectable, the alodine 1200 TMC value and CVCM value are respectively 0.51% and 0, that are compliant with the 1% ECSS acceptance level. The final 3D model of the enclosure was developed using Solidworks software during , from Dessault Systems and manufacturing files were produced from this model. The main part of the enclosure implements two separated housings for the custom boards, that are partially isolated by separating plate. A large rectangular hole in the separating plate was necessary to allow wiring between the front-end mounted on the navigation computer and the antenna amplification stage. PCBs were shaped to perfectly fit the entire 2D space inside the enclosure, with 1 mm margin (Figure 15). Due to the reduced space inside the plane of the ESEO spacecraft tray that hosts the GPS Payload, the height of the chassis is designed to include the two front-ends stacked over the navigation computer, without exceeding the 30 mm of height available until the upper tray. To use all available space between two spacecraft trays, the cover plate implements countersunk holes, to let the screws head to not add more thickness. The use of the little front plate acting as a DB9 connector mask, was necessary to allow easy placement of the navigation computer, considering the reduced tolerance of the PCB housing designed inside the lower chassis. This little plate will be used to cover the rectangular space cut from the front surface of the chassis, once that the PCBs will be in place.
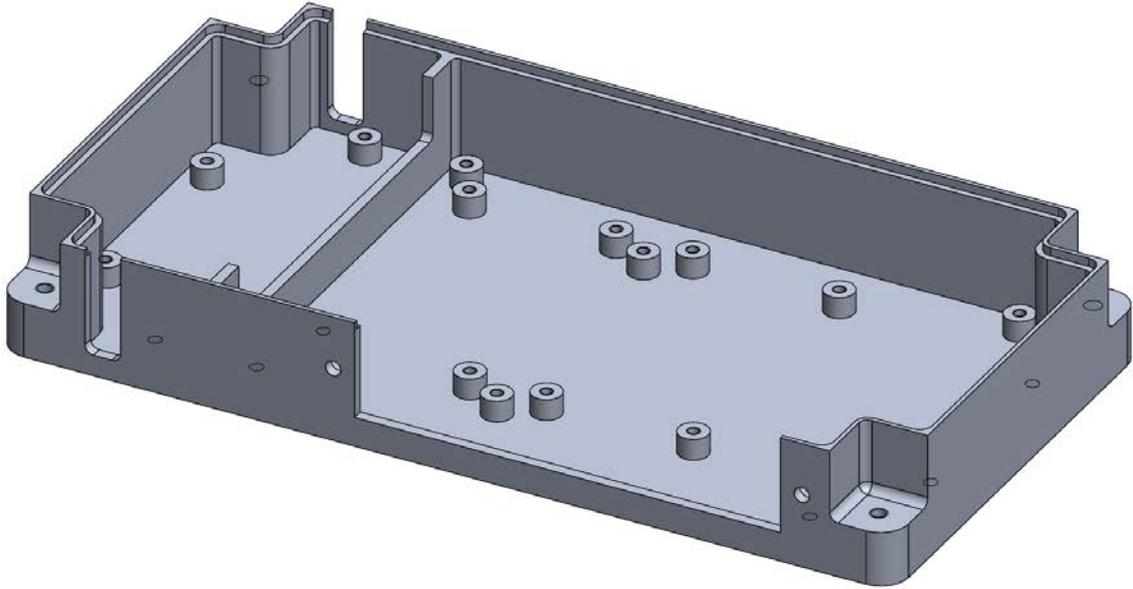
Figure 11: GPS Payload bottom chassis
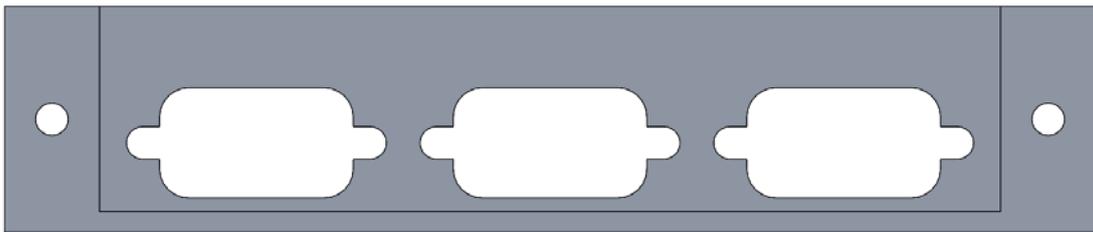
Figure 12: GPS Payload front plate
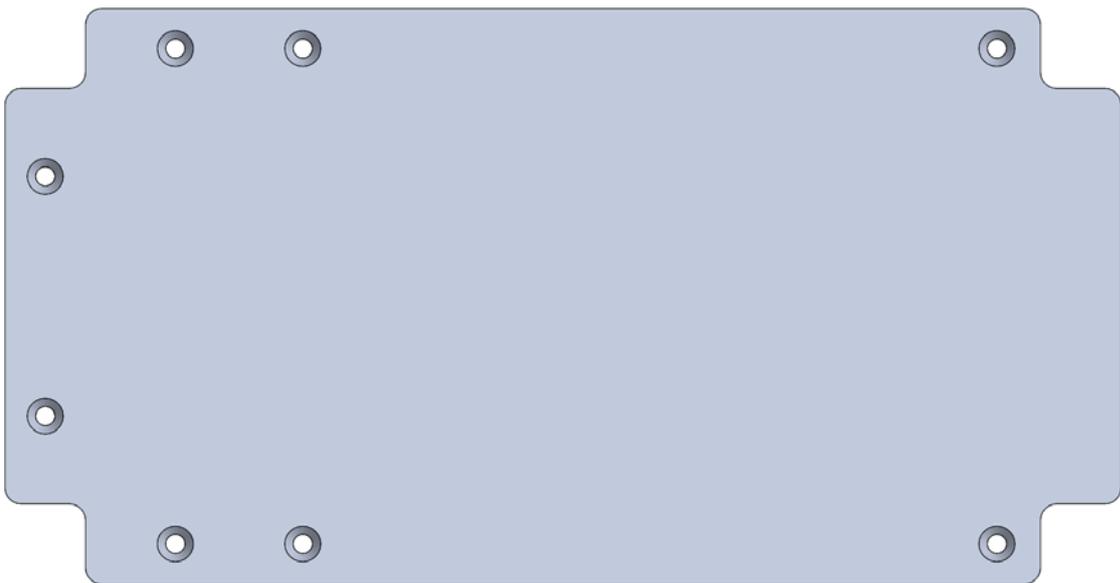
Figure 13: GPS Payload upper plate
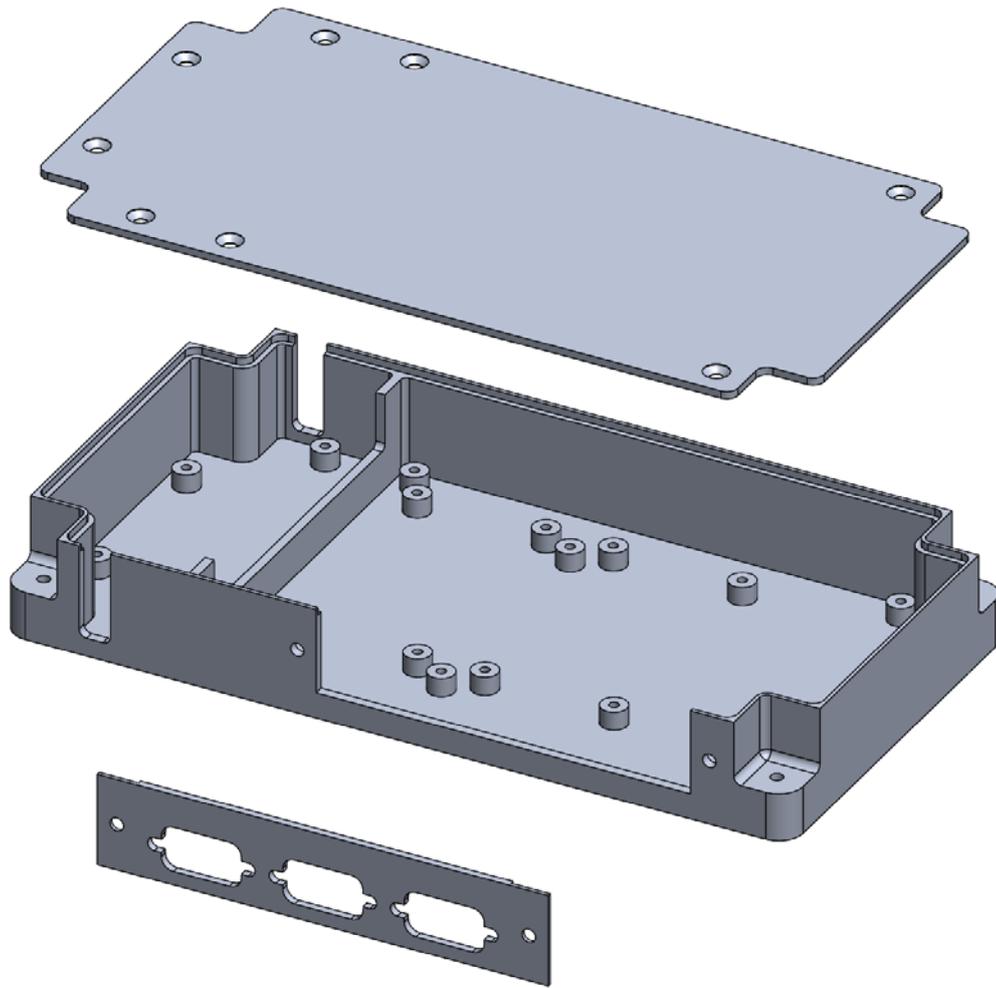
Figure 14: GPS Payload enclosure
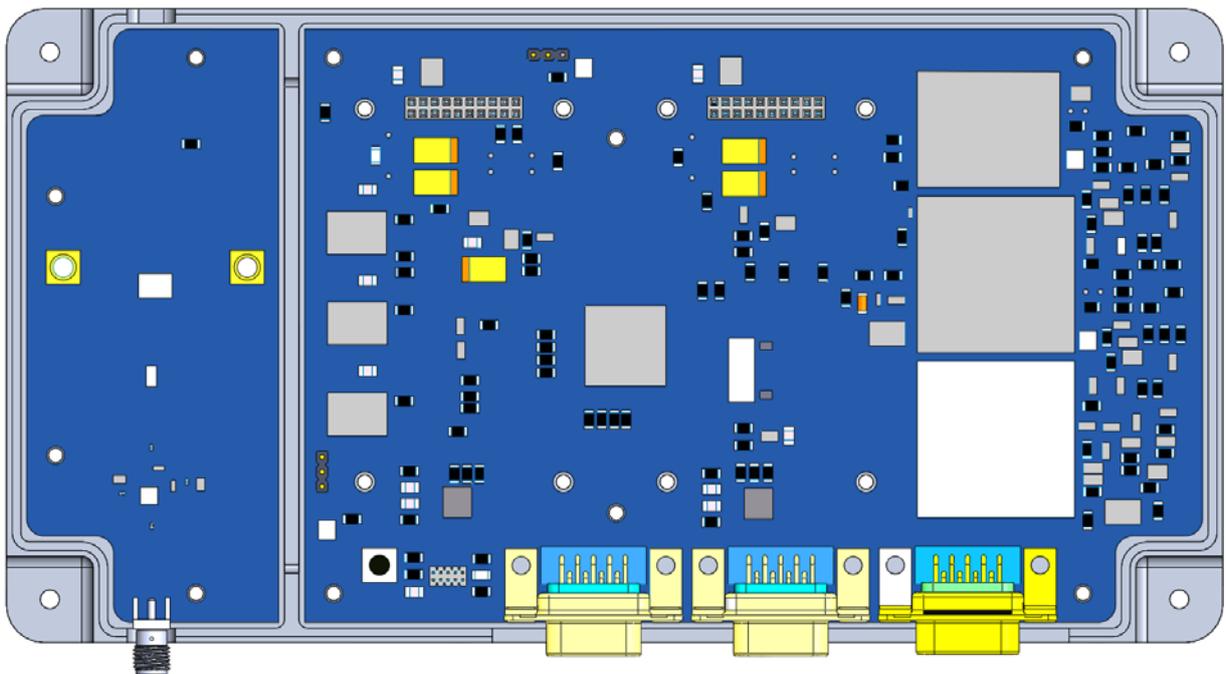
Figure 15: Custom PCB placed in dedicated housings

Short columns rises from the internal bottom surface to provide fix points to the PCBs, placed in order to not interfere electrically with the routes and vias of the bottom face of the navigation computer. Colums also includes M3 threaded holes to fix PCBs and and cover plate.

For matters of easy vertical placement and installation of the amplification stage and due to the need to include venting holes to satisfy the pressure difference requirement, two symmetrical holes were applied on lateral walls (Figure 16). Considering that one hole will be covered by the tray's wall, the actual venting area is referred to the hole on the opposite side with respect to the SMA connector, equal to 104.73 mm^2. Since the volume of the payload is less than 1 liter (0.693 l), the dimensions of the venting holes are compliant with the requirements.
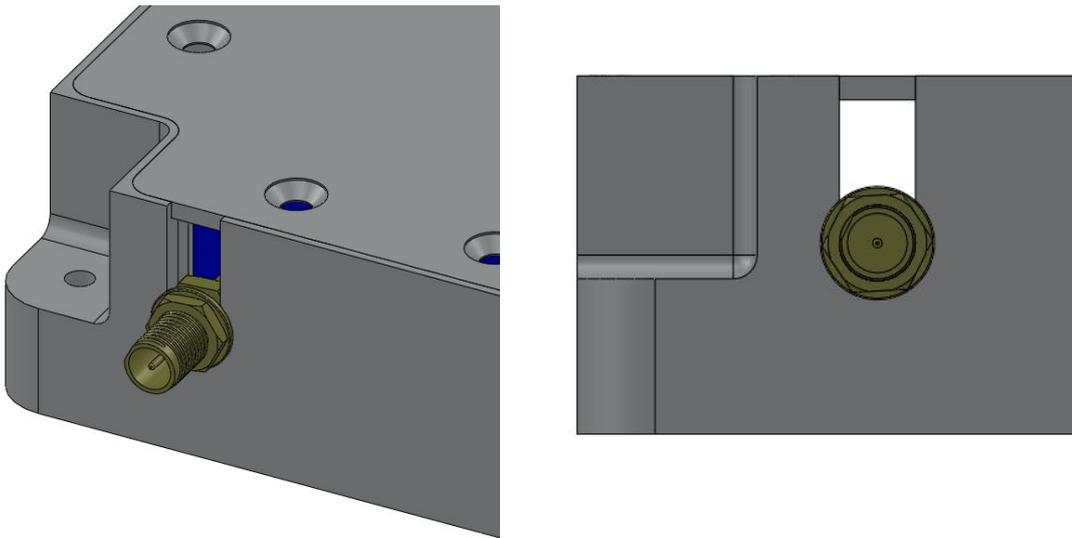
Figure 16: Venting holes

Cylindrical spacers with length of 13 mm and 30 mm were added respectively between the front-ends and the navigation computer and between the navigation computer and the cover plate to improve internal rigidity of the whole payload.

The main technical details of different parts of the enclosure are included in Table 9.

Table 9: Mechanical parts technical features

	Size	**Weight**
Lower Chassis	210 mm x 110 mm x 30 mm	274.19 g
DB9 mask	120 mm x 25 mm x 2 mm	10.08 g
Cover plate	208 mm x 108 mm x 2 mm	120.15 g
Spacers	8 x 13 mm and 8 x 20 mm	21.04 g
Total Weight	425.46 g	

4.3 Final Payload H/W

In order to develop the payload hardware and software verification plan, the ESEO spacecraft model philosophy was used as reference [19]. Figure 17 shows a summary of the adopted ESEO model philosophy together with planned verification and milestones.
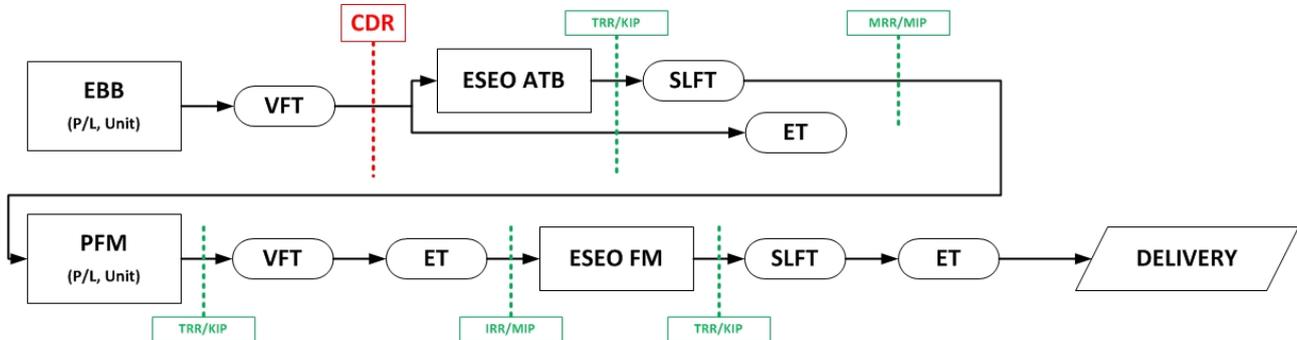
Figure 17 : ESEO model and verification philosophy

Two different models of the GPS Payload were produced, following indications included in the ESEO model philosophy and payloads Test Plan [12]:

- *The Elegant breadboard (EBB):* two EBBs already produced and they were intended to be used for validation of the hardware design and as H/W support for coding of the firmware. The first prototype was used to perform acceptance level test campaign on the hardware. The second EBB, with minor updates, was used as workbench for the application software development and testing.

- *The Proto Flight Model (PFM):* considering the outcomes from the test campaign performed on the H/W, some minor changes were applied and another model was produced. The proto-flight model is the final payload, that will be integrated with the flight model of the spacecraft and will be launched.

Each model shall be subjected to a series of verifications that can be grouped in the following areas:

- Verification and Functional Tests (VFT), with the aim to validate the hardware and software design though dedicated test oriented to the sub-system mission

- Environmental Tests (ET), meant to verify the capability of the sub-system to be operative in space environment

- SLFT (System Level Functional Tests), including integrated system tests, EM compatibility, functional tests, system validation tests;

Furthermore, the sub-system design and development progress was constantly subjected to review by ESA technical officers, in order to assess compliance with ESA quality standards. The review plan included: Critical Design Review (CDR), Test Readiness Review (TRR) and Manufacturing Readiness Review (MRR).

4.3.1 Payload integration and operations intruction

The design process that led to the development and manufacturing of the GPS Payload EBB and PFM models was an iterative work that started from the sub-system level technical requirements and involved electrical design of the custom PCBs, mechanical design of the external enclosure and hardware validation. The final result of this iterative process is the 3D model of the complete GPS Payload shown in Figure 18, Figure 19 and Figure 20.

Figure 18: Complete GPS Payload rendering
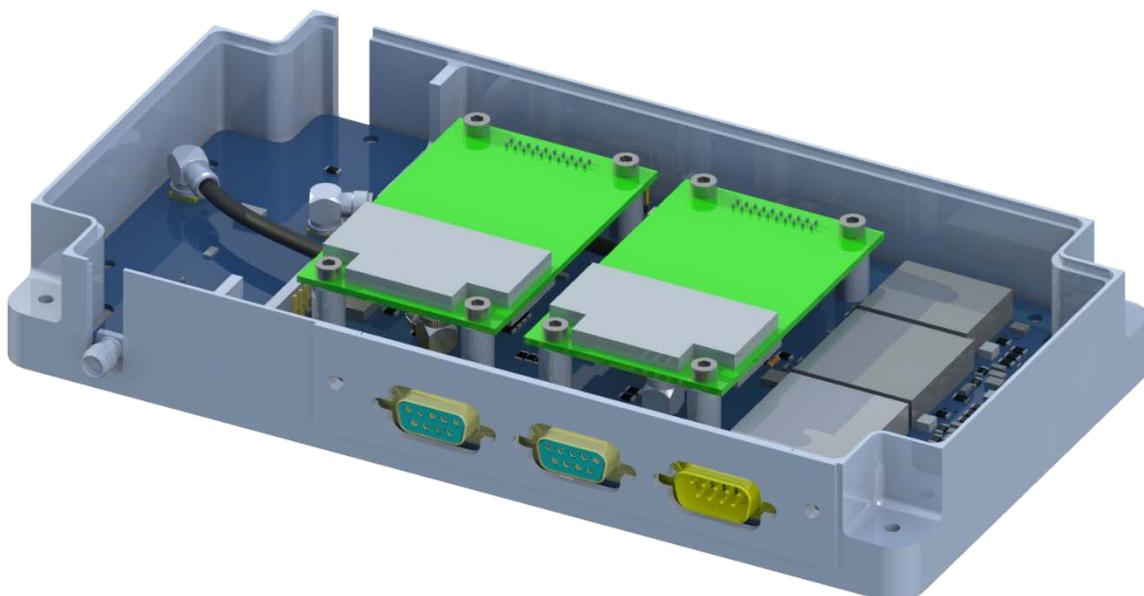
Figure 19: Complete GPS Payload rendering with no cover plate
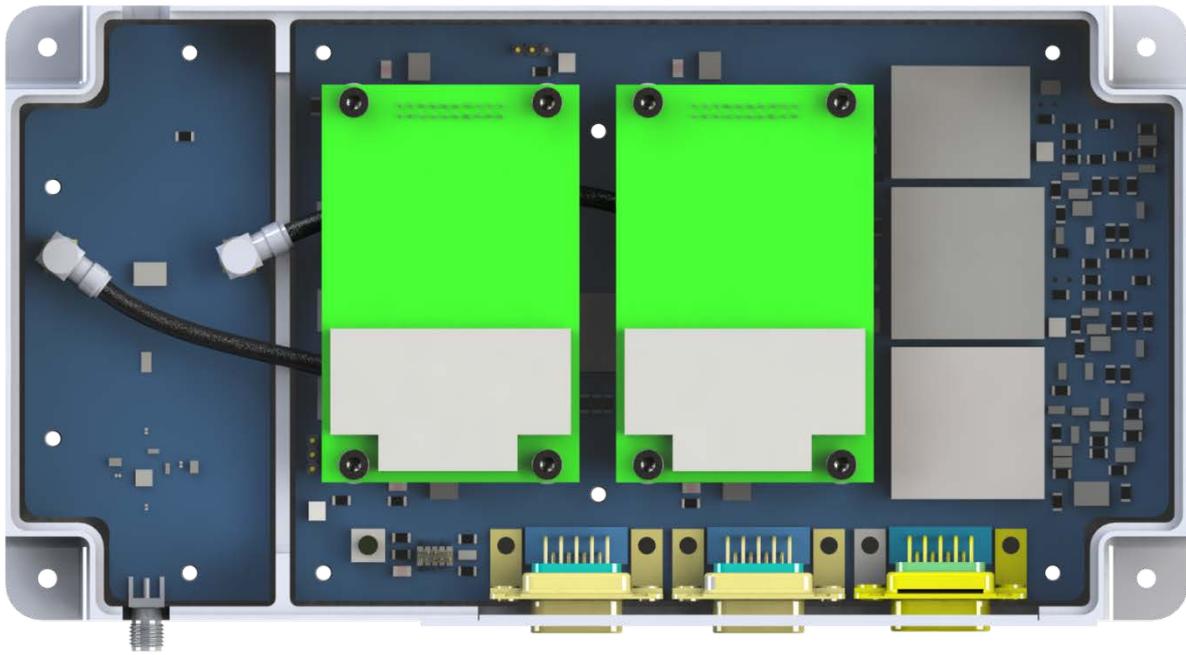
Figure 20 Complete GPS Payload rendering, top view

GPS Payload integration procedure is organized in the following steps [17]:

1. Insertion of amplification stage and navigation computer from above, and placement in dedicated housing inside the main chassis. The two PCBs shall be placed in the same moment, because they are physically connected by two short wires for power and ground, soldered on dedicated pads. Navigation computer is then preliminary fixed with internal screw to threaded holes of two chassis columns.

2. Integration of the two COTS front-ends with the Navigation computer (Figure 21). Connection of the baseband processor to the two SMA connectors on the antenna amplification stage, where the GPS signal coming from the antenna is addressed. Two internal short rf cables are used to bring the signal to the front-ends. Apart from the power and ground wires mentioned before that are soldered, rf cables represent the only internal cables connection included in the payload, reducing the risk of disconnection during the launch. In fact no data connection is needed between amplification stage and navigation computer, while communication between front-ends and navigation computer is exploited using sockets interface. Front-ends are then mechanically fixed using 8 screws and 13 mm spacers. In Figure 22 internal mechanical and electrical interfaces are displayed on the top surface of the navigation computer: blue circles shows the mechanical interface with COTS front-ends; orange circles highlight the position of the two first fix points for the front-end with the chassis; yellow circles displays the mounting holes used to fix both navigation computer and cover plate with lower chassis, using 20mm spacers; red rectangles show the connectors for power and ground with amplification PCB (and the left border) and for front-end electrical interface (the two sockets on the upper border)
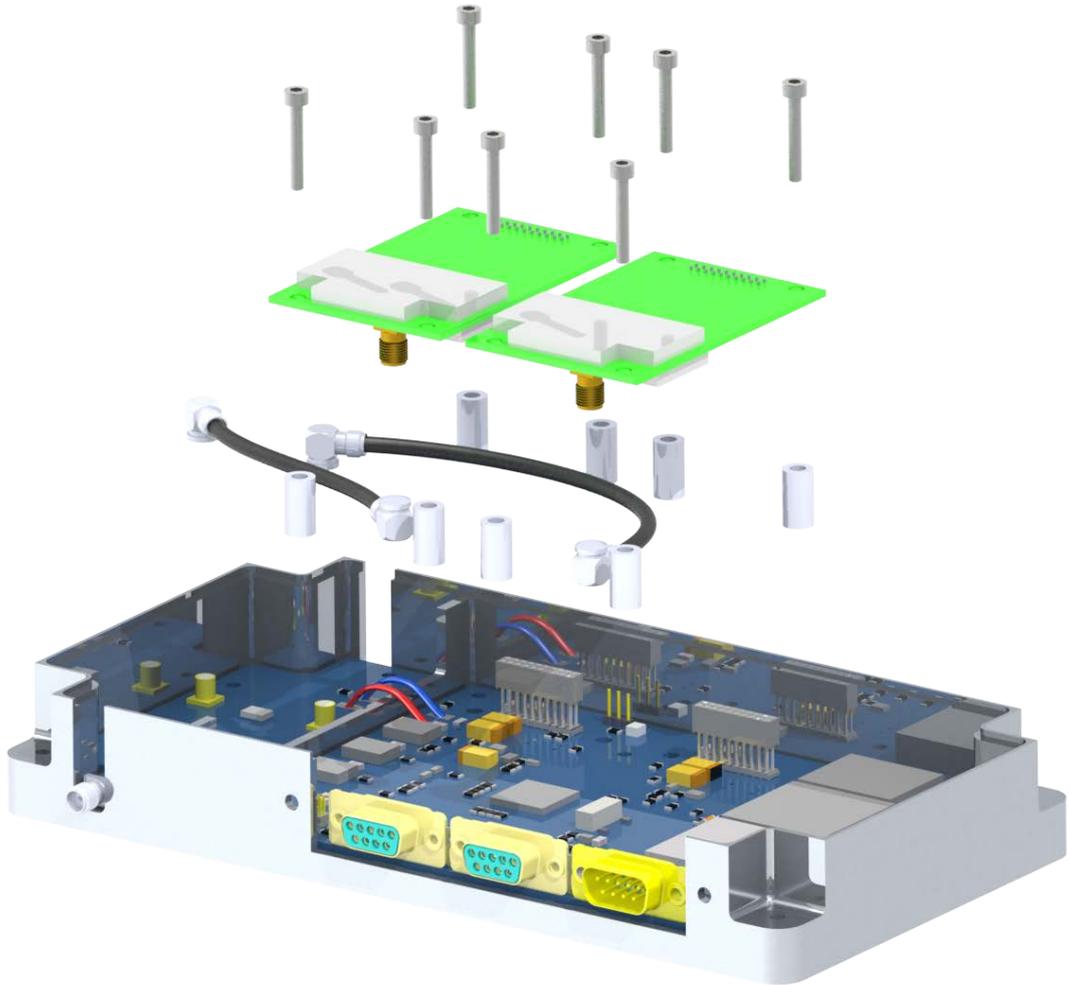
Figure 21: COTS front-end integration
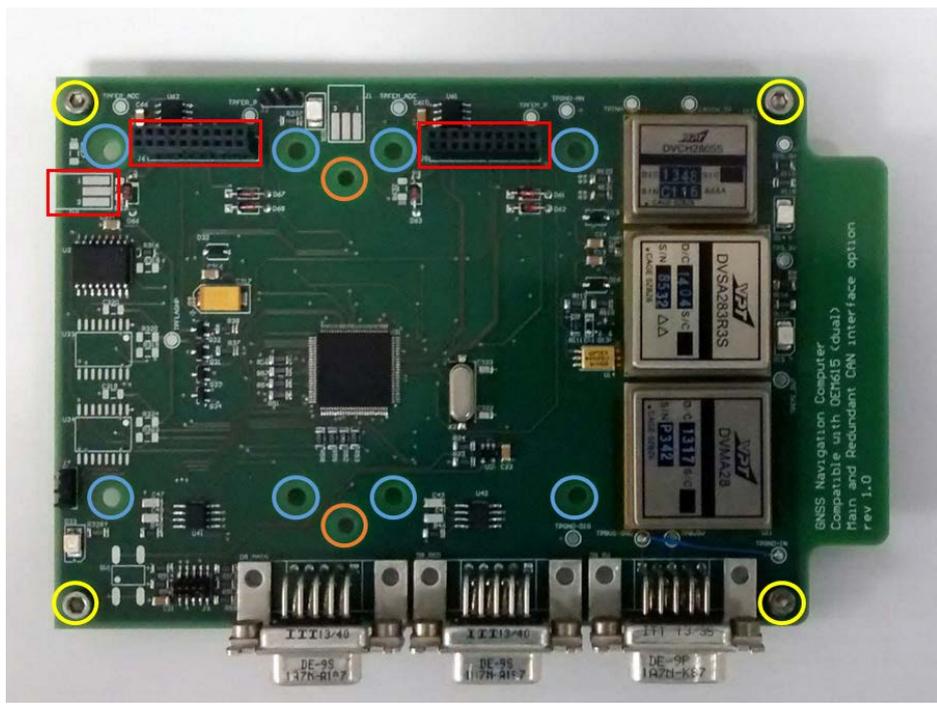
Figure 22: Navigation computer mechanical and electrical interfaces

3. Once that all COTS and custom PCBs are placed and connected inside the lower chassis, the GPS Payload is completed with top cover and and DB9 mask, fixed with screws. Before placing the top cover, the 20 mm spacers are included inside the enclosure between the navigation computer and the plate, around each of the countersunk screws (Figure 23).
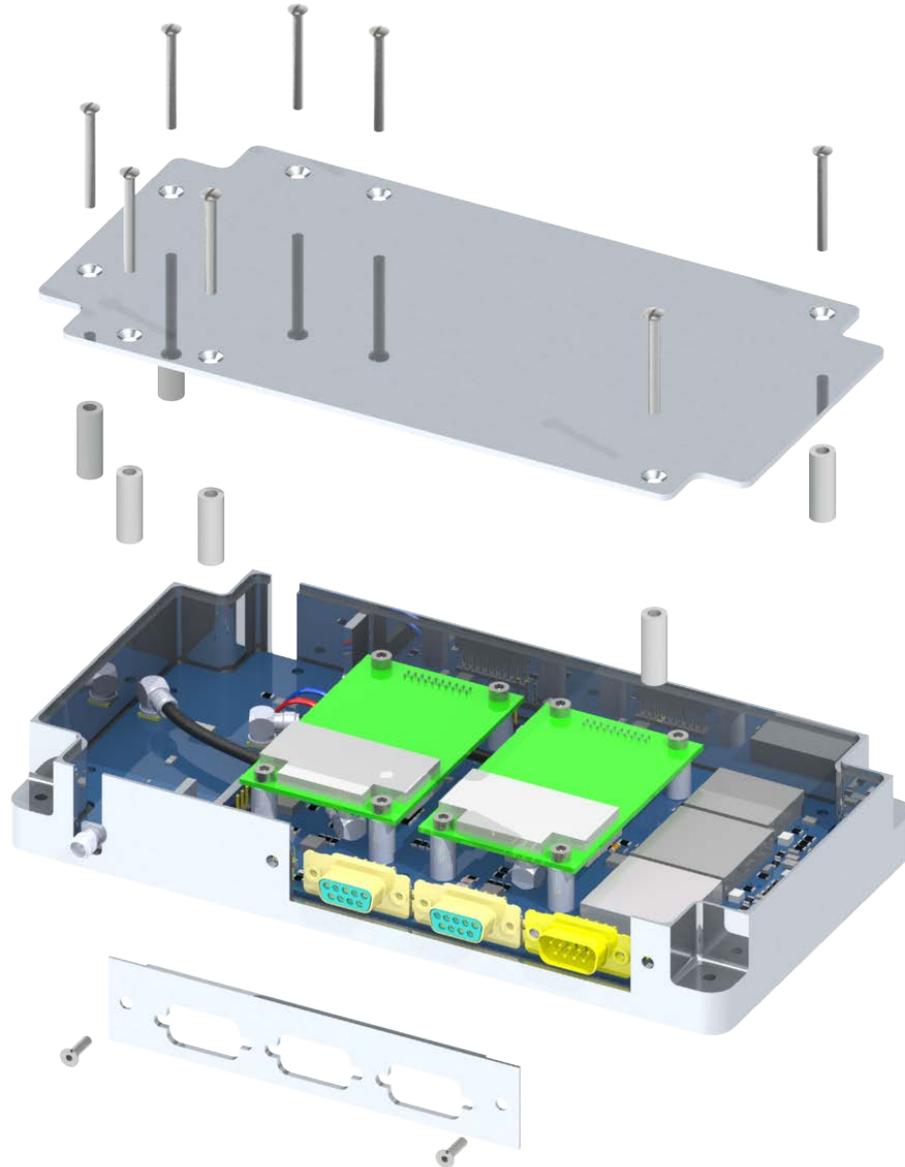
Figure 23: GPS Payload integration

4. Once integrated, in order to install the GPS Payload within the ESEO tray, four M4 threaded holes were foreseen at the corners of the chassis. External SMA connector shall be connected to GPS antenna cable and DB9 connector mated with CAN main and redundant bus and power source. In Figure 24 external mechanical and electrical interfaces are shown: in the yellow circle the 4 mechanical interface with ESEO spacecraft tray are highlighted; within green circles the three external DB9 connectors are shown and in blue the external connector for the antenna.
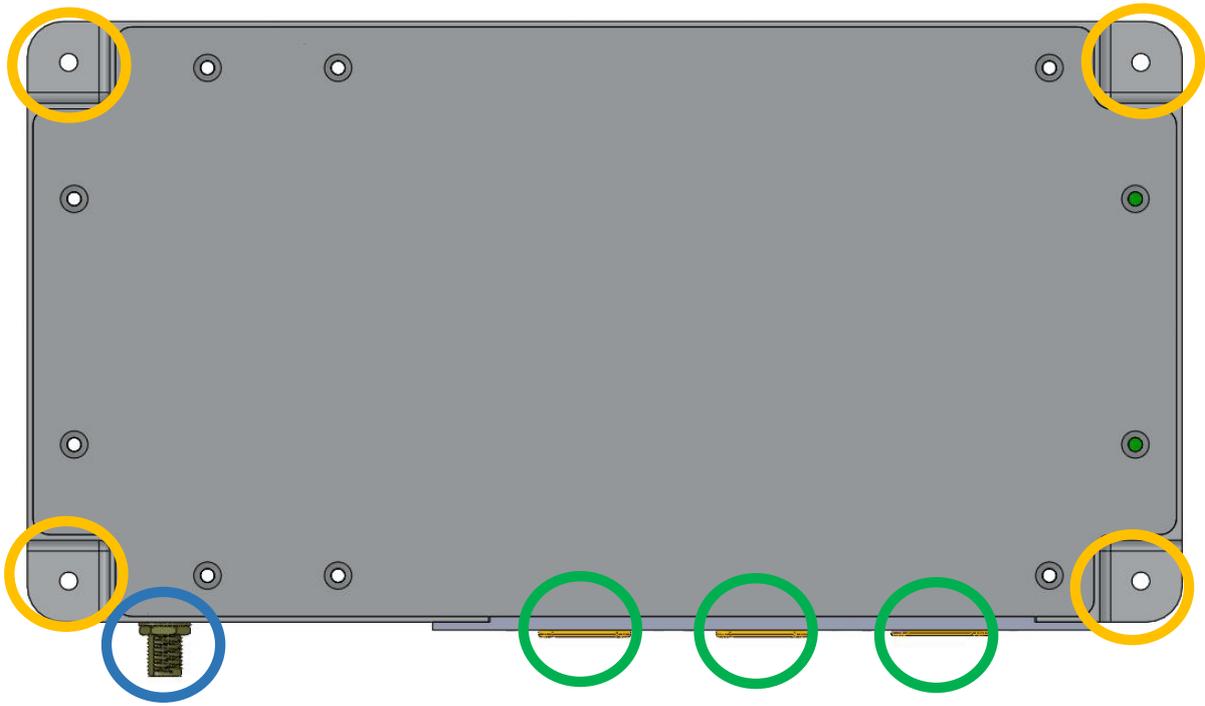
Figure 24: GPS Payload external interfaces

The GPS payload is designed to operate with external power source, so it does not implement battery packs, because as a payload it's operations are not considered fundamental for the ESEO mission success. Furthermore, due to power management issues, it will not be always active, tracking satellite position continuously. For the experiments on-board, a working schedule was defined, as long as their idle cycles.

Since it is foreseen to be powered on only for testing its performance and since these periods will be reduced, it is designed to be externally controlled: to turn on the device, the ESEO platform just need to manage the power to the dedicated interface using a female DB9 connector (Figure 25).
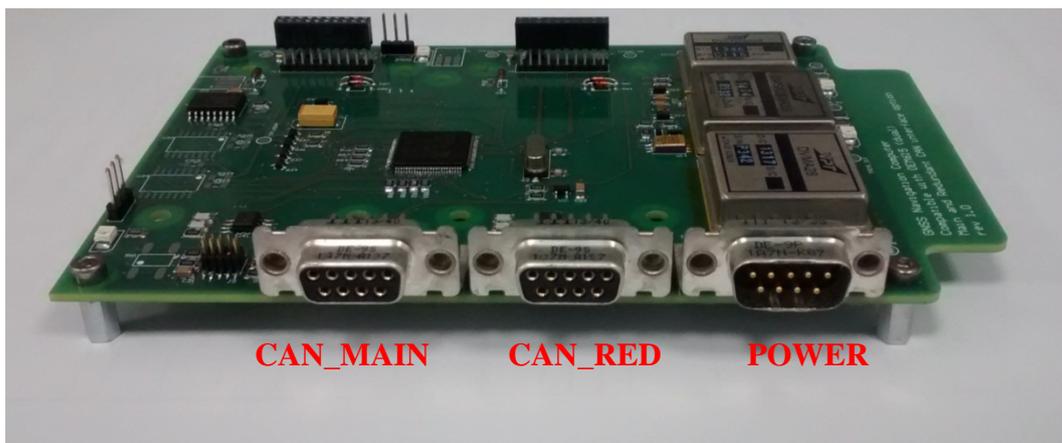
Figure 25: GPS EBB DB9 connectors

No other commands shall be provided to the GPS Payload Navigation computer in order to enable position fixes. According to the payload's scientific purpose, this subsystem shall not be turned off until a failure is

detected on the payload itself or on the platform, during GPS Payload idle cycle. In fact the payload shall continuously collect data during the period indicated by its mission specification. The firmware, implemented inside the microcontroller of the payload, is able to manage autonomously several hardware and software failures and anomalies. Only in one case it is foreseen the payload's automatic power-off: once an overvoltage is detected either on the 3.3V and 5V circuit, the DC/DC regulators output will be inhibited by the overvoltage protection circuit, so the payload power shall be turned off and on again by the ESEO OBDH, in order to restore the correct functionality.Figure 26, Figure 27, Figure 28 and Figure 29 display the second EBB model, used for software testing. It is slightly different from the first EBB model, for some minor changes after HW test campaign.

Figure 26: EBB model of the GPS Payload including model of the GPS antenna

Figure 27: Complete EBB model of the GPS Payload

Figure 28: Complete EBB model of the GPS Payload, connectors view

Figure 29: GPS Payload during application software programming and test

No pictures of the PFM model are included, because it was in the final production and verification phase at at the moment of the writing of this document. However, the final model is almost identical to the second EBB used for software development and validation, shown in previous pictures, a part from minor changes represented by the exclusion of external diagnostic interface and status leds, that were meant to be used only during the functional validation of the design.

4.4 Dynamic loads simulation

The mechanical design of a sub-system meant to operate on-board of a spacecraft is not driven only by the need to implement all necessary mechanical interface with the satellite platform, but its main task is focused on the development of a device able to withstand the launch period, dominated by a strong dynamic load environment. In particular the external structure and the overall payload layout shall be chosen accurately in order to avoid that the normal frequencies are too close to the launch load frequency and that the frequency response of the structure does not includes stresses or displacements that can critically affect nominal operations. To validate hardware mechanical design for this purpose, usually a procedure that includes finite elements analysis (FEM) and subsequent vibration test is foreseen. Although some preliminary FEM analysis were performed during the very early phases of the enclosure design, a more accurate simulation was necessary, considering the final 3D model, obtained after the conclusion of the detailed design of both electronic and hardware parts. The simplification of the 3D geometry interested only the parts considered not critical to assess a conservative and reliable frequency response indication of the Payload layout. To perform these simulations, a slightly de-featured 3D geometry of the payload obtained from Solidworks in .STEP format was imported inside the Ansys software, typically used to perform physical simulations.

Materials data obtained from ESA and NASA databases were grouped in three categories and applied to the relative parts of the model:

- Alluminum 7075 for the lower chassis (Figure 30).
- FR4-copper composite material for the navigation computer, amplification stage and COTS baseband processors (Figure 31).
- Stainless steel AISI 304 for the spacers between navigation computer and the two front-ends (Figure 32)
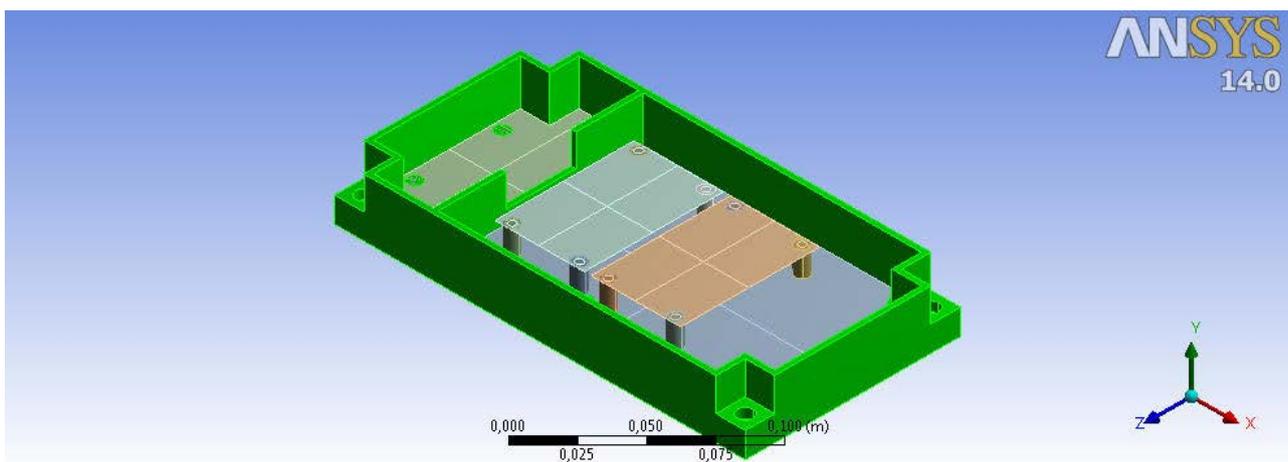
Figure 30: Aluminum 7075 parts
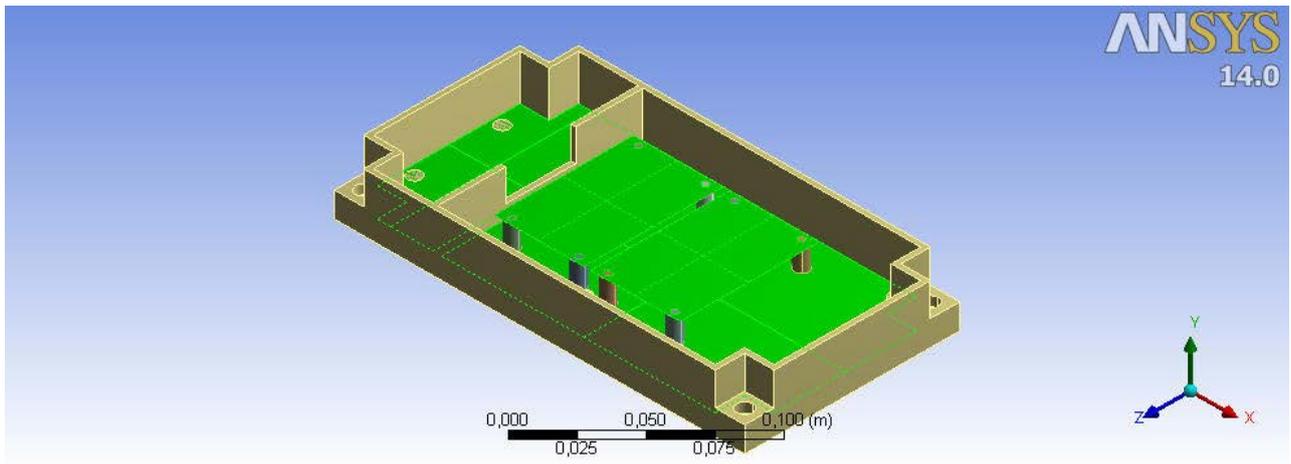
Figure 31: FR4-copper parts
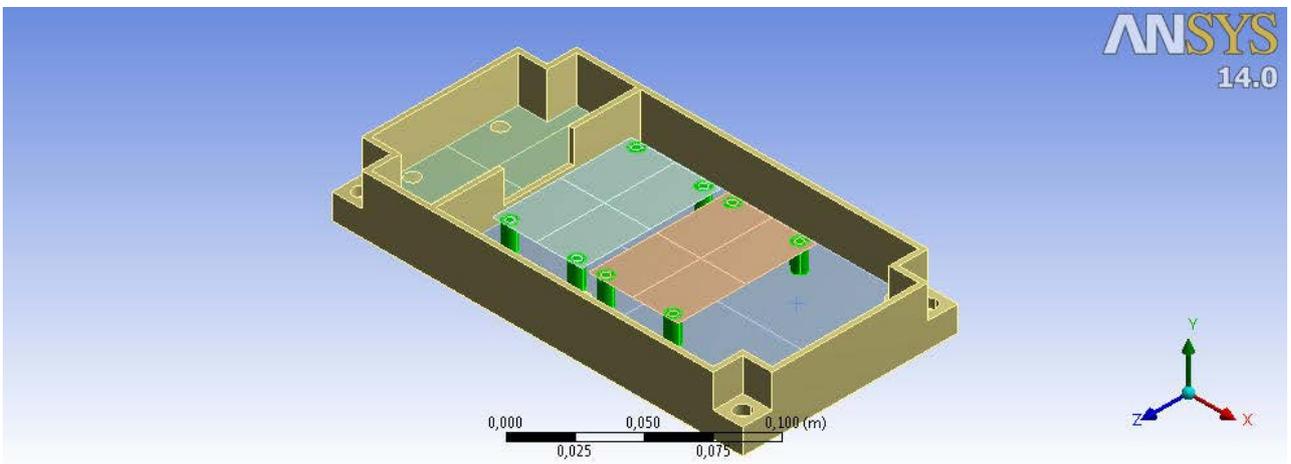
Figure 32: Stainless steel parts

After material assignement contraints and bonding contacts were applied at the interface points between the main parts (Figure 33). In the details :

- Fixed support constraint to the four external holes of the chassis, where the GPS Payload is mechanically fixed to the ESEO tray

- Bonding contact between chassis and the two custom PCBs through the embedded columns and between the baseband processors and navigation computer through the 8 spacers
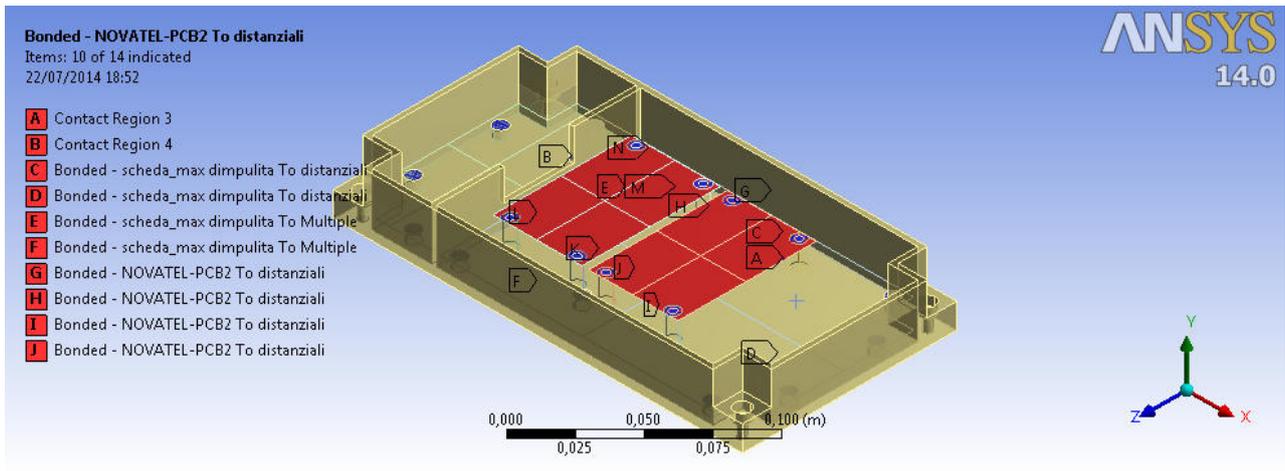
Figure 33: Contact regions

A mesh of approximately 170k nodes was applied on the 3d geometry, with elements of 3 mm, using solid elements for the enclosure and spacers and shell elements for the PCBs (Figure 34). The size of the elements, which determined the number of nodes, was chosen as first approximation equal to the minimum dimension included in the 3d model, i.e. the thickness of the lateral walls of the enclosure. Considering the relative simplicity of the de-featured 3D model used for the simulations, this solutions was adopted as acceptable trade off between the computational capacity available and need of a fine mesh to obtain reliable results.
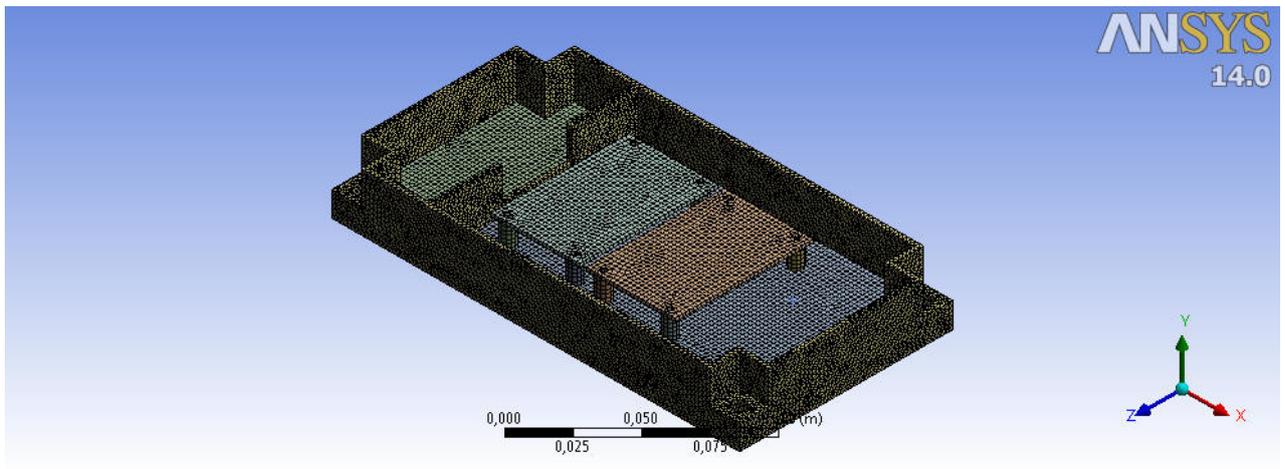
Figure 34: Mesh applied to 3D model

In order to validate the hardware design and assess the need for any modifications, the outcomes of the analyses performed are multiplied by margins and safety factors following the margin policy indicated in ECSS-E-ST-32-10C and then the final stress values are compared to materials resistance properties. These safety factors, whose combination is used to create the stresses coefficients, are included in Table 10.

Table 10: Safety factors

Coefficients components	Values
Model factor, Km	1.2
Project factor, Kp	1.1
Factor of safety, yield stresses, FOSY	1.1
Factor of safety, ultimate stresses, FOSU	1.25
Acceptance level factor, KA	1.1
Qualification level factor, KQ	1.25

Margins of safety are then calculated for both the yielding, MOSy, and ultimate loads, MOSu, cases as the fraction between the material tensile strength and the maximum stress multiplied by the related factors. If the obtained value is higher then 1, i.e. the margin is positive, the likelihood of the mechanical design is demonstrated and no further action is needed, until environmental test campaign verification.

4.4.1 Modal analysis

The first simulation was a modal analysis useful to assess that the natural frequencies of the GPS Payload are far enough from critical values that can be experienced during the launch. Dedicated requirement states that the modes frequencies shall be higher than 200 Hz. Table 11 includes the frequencies obtained from the analysis for the first 10 modes and all of them are compliant with the reference value.

Table 11: Modal analysis outcomes

Mode	1	2	3	4	5	6	7	8	9	10
Frequency [Hz]	509.02	781.82	862.47	1001.8	1067.2	1312.8	1380.7	1390.3	1426	1567

Figure 35, Figure 36, Figure 37, Figure 38 and Figure 39 display the results of the modal analysis for the first 5 modes.
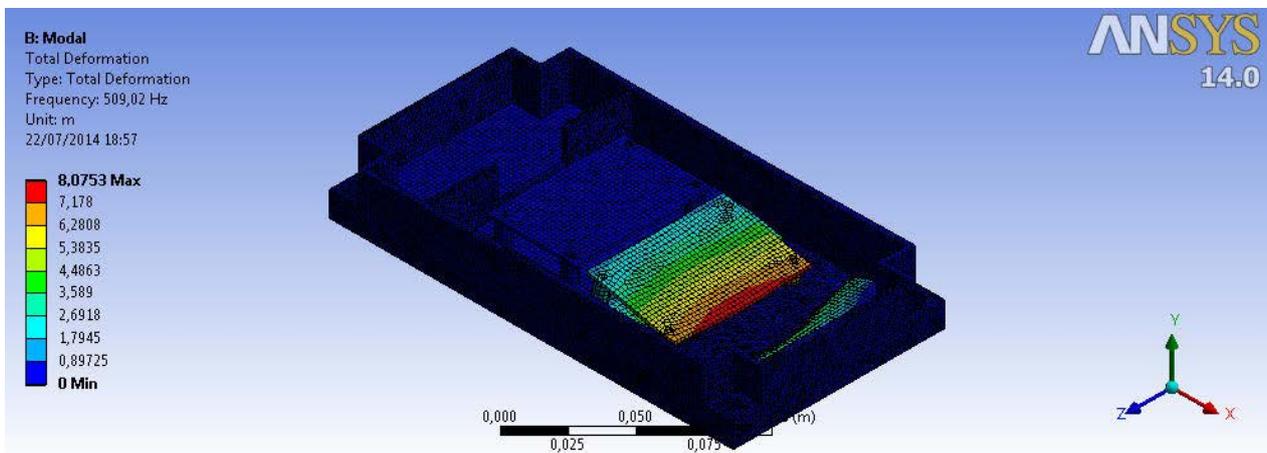
Figure 35: First mode deformation

54
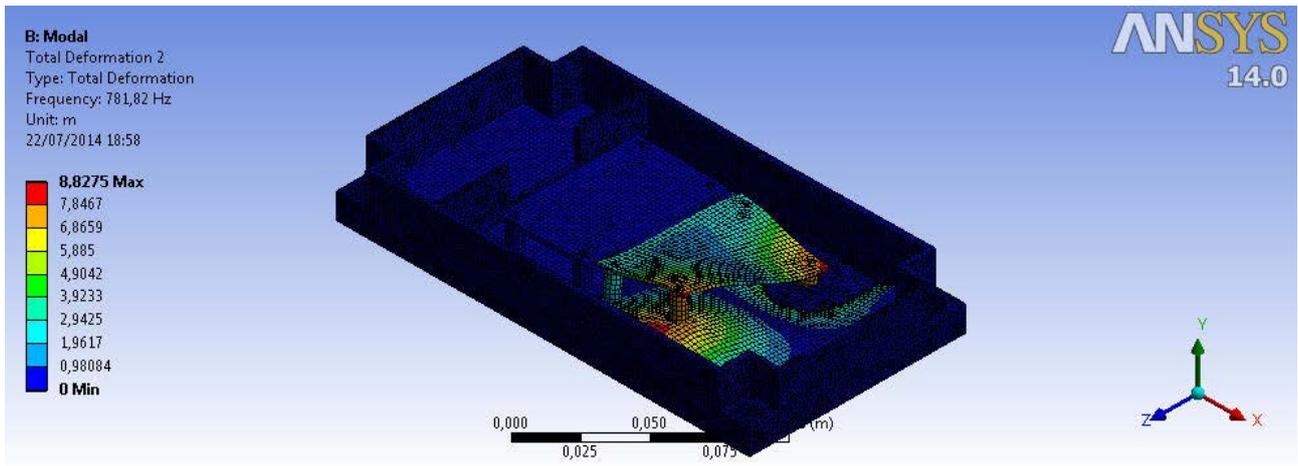
Figure 36: Second mode deformation
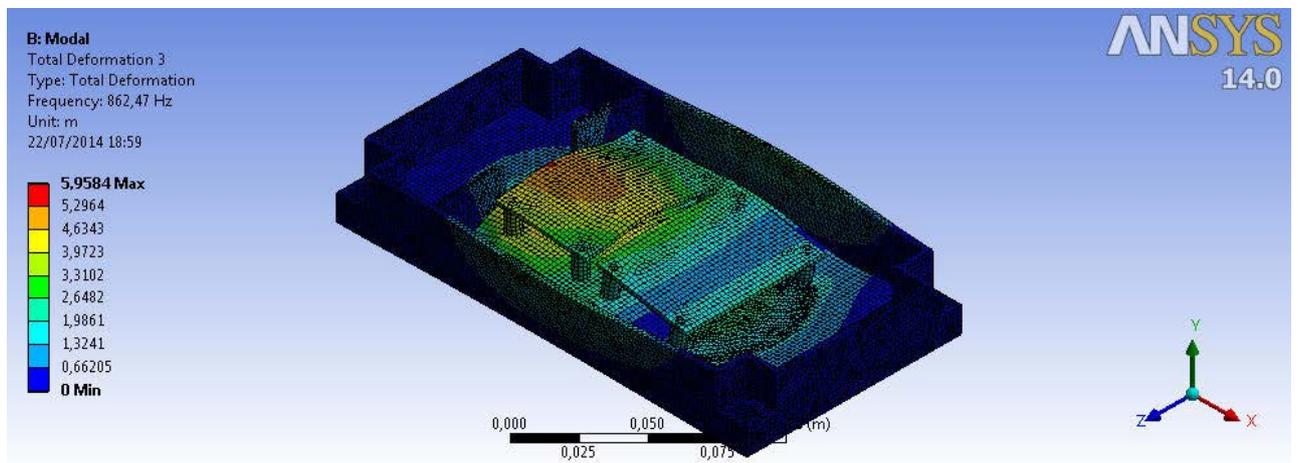
Figure 37: Third mode deformation
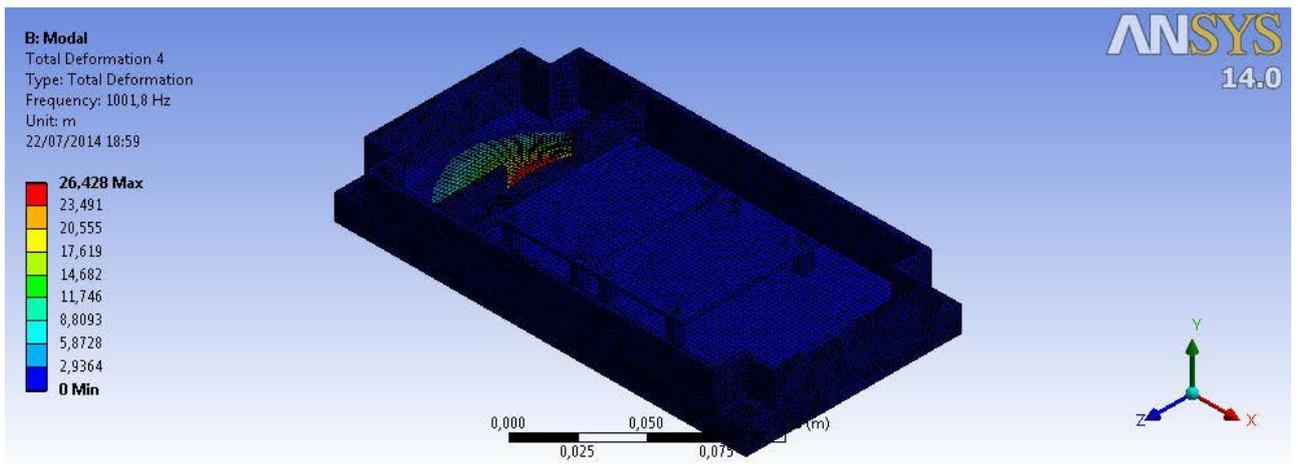
Figure 38: Fourth mode deformation
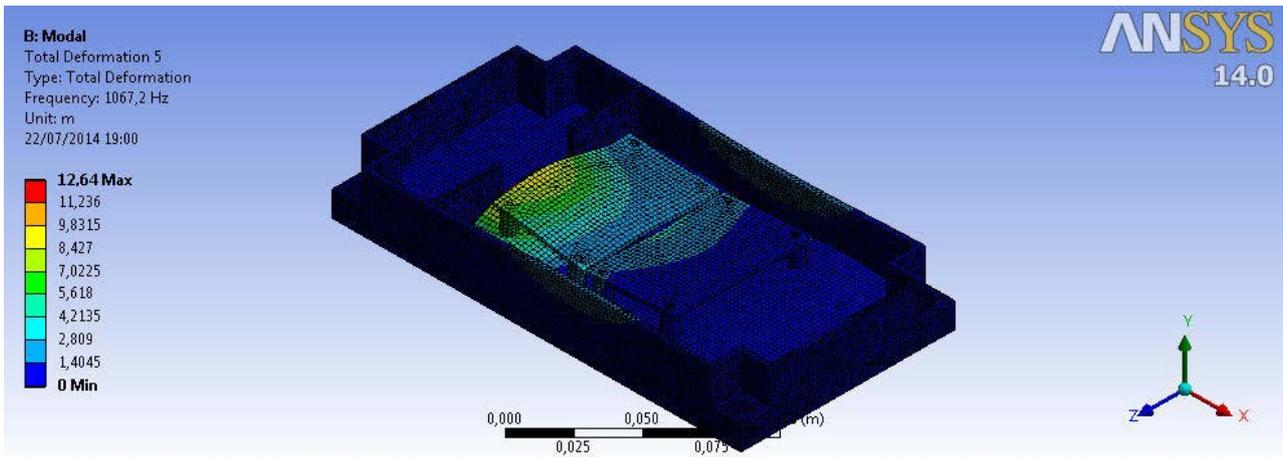
Figure 39: Fifth mode deformation

4.4.2   Sine analysis

Since vibration simulation is generally used to assess the sub-system structural response in presence of dynamic loads in the low frequency range with high constant amplitude . This analysis includes a swipe of the loads frequency from a quasi-static condition (Figure 40), in this case 5 Hz, to 100Hz, as requested by technical requirements. The amplitude for the entire frequency range is fixed to the qualification level of 16g and was applied in all three axes. This value was obtained by a previous analysis performed by SITAEL officers at system level on the ESEO platform to assess the acceleration amplification at sub-systems interfaces.
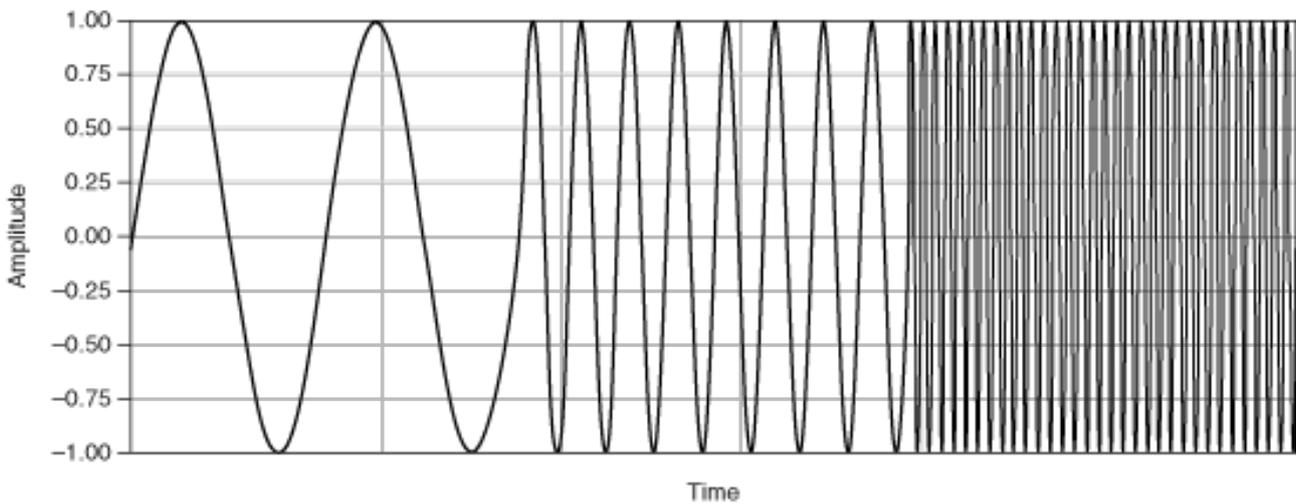
Figure 40: Sine analysis typical profile

The output of the simulation expressed in stresses calculated at 100Hz are displayed in Figure 41, Figure 42, Figure 43respectively for X, Y and Z axes.
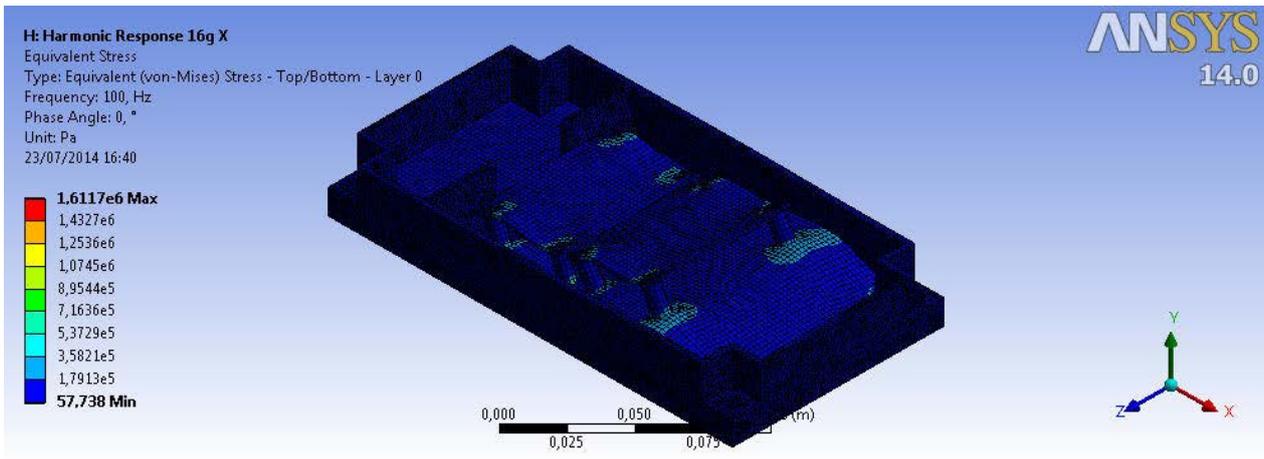
Figure 41: Sine vibrations stresses, X axis
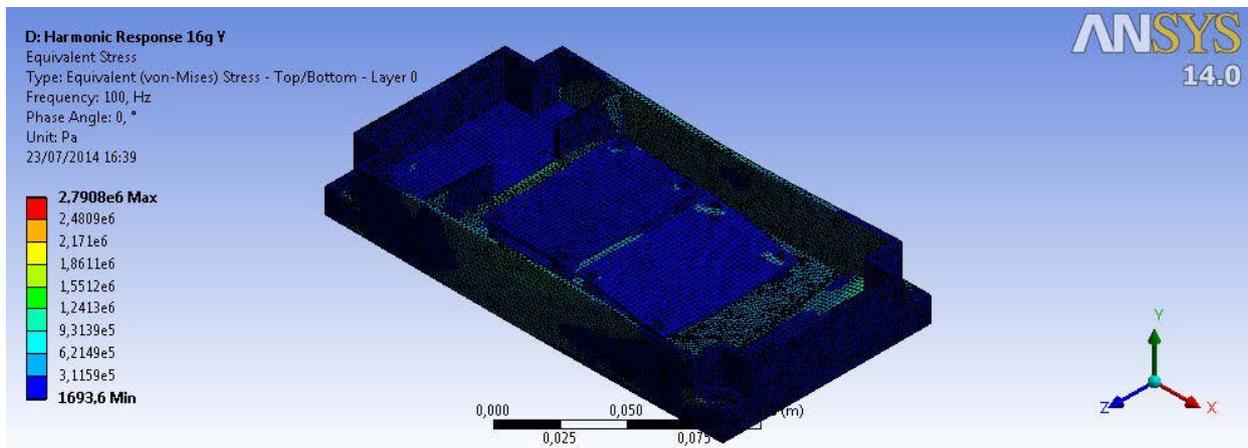
Figure 42: Sine vibrations stresses, Y axis
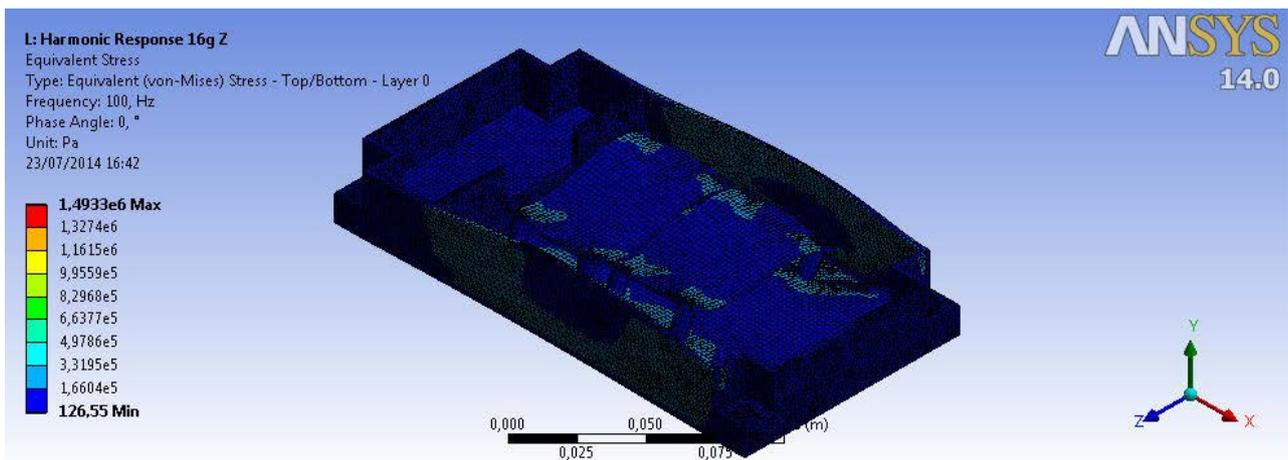
Figure 43: Sine vibrations stresses, Z axis

Margins of safety are then calculated for both the yielding and ultimate loads cases:

$$MOS_{yeld} = \frac{\sigma_{yeld}}{\sigma_{max}K_mK_pK_qFOS_{yeld}} - 1 = 51.33$$

$$MOS_u = \frac{\sigma_u}{\sigma_{max}K_mK_pK_qFOS_u} - 1 = 52.87$$

4.4.3   Random vibrations analysis

Random vibration scenario was applied to the GPS Payload 3D model to assess its response and generated stresses in presence of a high frequency random dynamic loads, whose distribution follows the power spectral density profile (PSD) obtained as output from the ESEO spacecraft system level analysis. The simplified profile with related acceleration power spectral density values used for this simulation is included in Table 12.

Table 12 : Random vibration analysis spectrum

Frequency [Hz]	20	100	300	2000
ASD [g2/Hz]	0.105	0.525	0.525	0.023

The PSD profile was applied along each axes and the 3σ stresses obtained as output are displayed in Figure 44, Figure 45 and Figure 46.
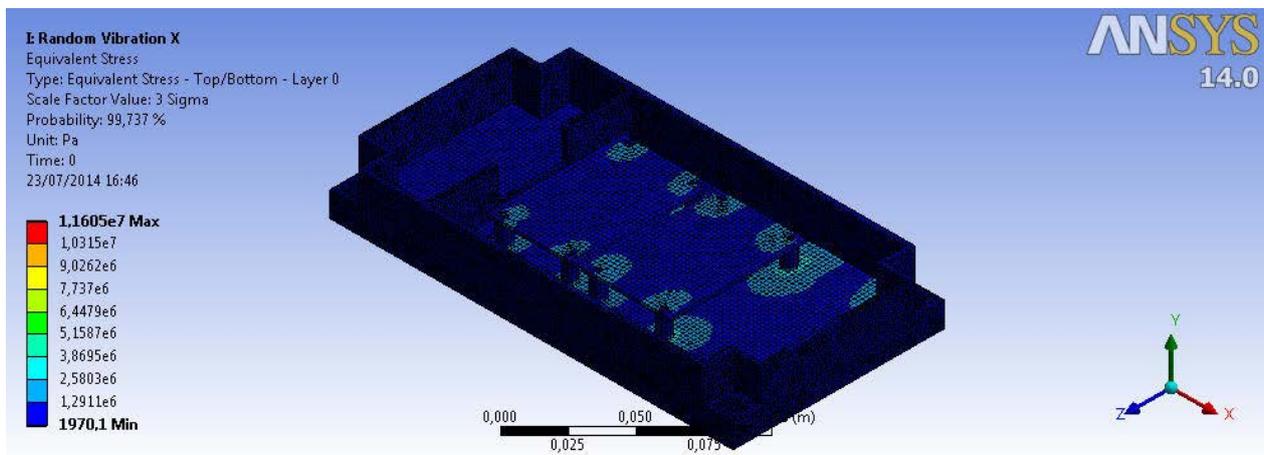
Figure 44: Random vibrations stresses, X axis
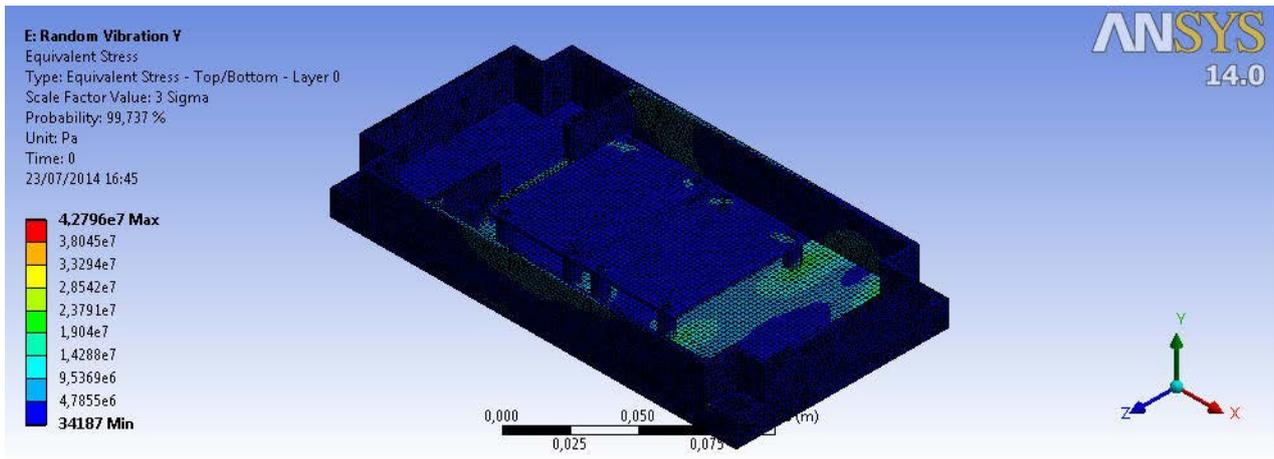
Figure 45: Random vibrations stresses, Y axis
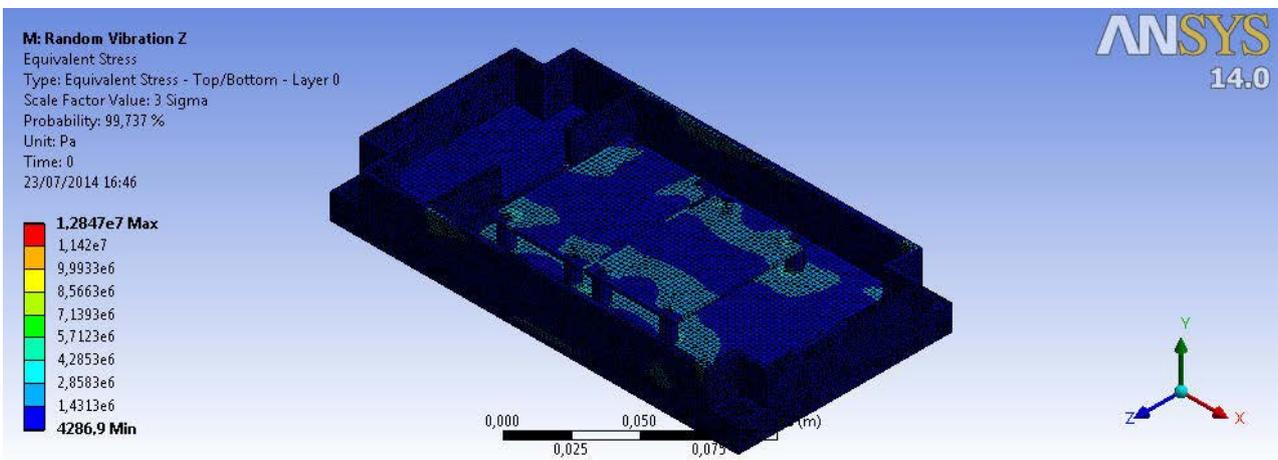
Figure 46: Random vibrations stresses, Z axis

The minimum margins of safety were calculated for both yielding and ultimate scenario:

$$MOS_y = \frac{\sigma_y}{\sigma_{max} K_p K_m K_q FOS_y} - 1 = 2.41$$

$$MOS_u = \frac{\sigma_u}{\sigma_{max} K_p K_m K_q FOS_u} - 1 = 2.51$$

4.4.4 Shock analysis

A shock analysis was performed in order to assess the entity of stresses generated on the GPS Payload in presence of dynamic load at high frequency and amplitude, experienced for a very short time, simulating impact of events like launcher stages separation. The shock profile, called Shock Response Spectrum (SRS), used for this simulation was obtained from the analysis performed at system level by SITAEL company and is included in:

Frequency [Hz]	30	100	1000	1500	4000	5000	10000
SRS [g]	2.5	30	750	1000	1500	1500	750

Stresses are reported in the following pictures respectively with acceleration applied in the X, Y and Z axis (Figure 47, Figure 48 and Figure 49). For each case the yield margin of safety and the ultimate margin of safety are assessed.
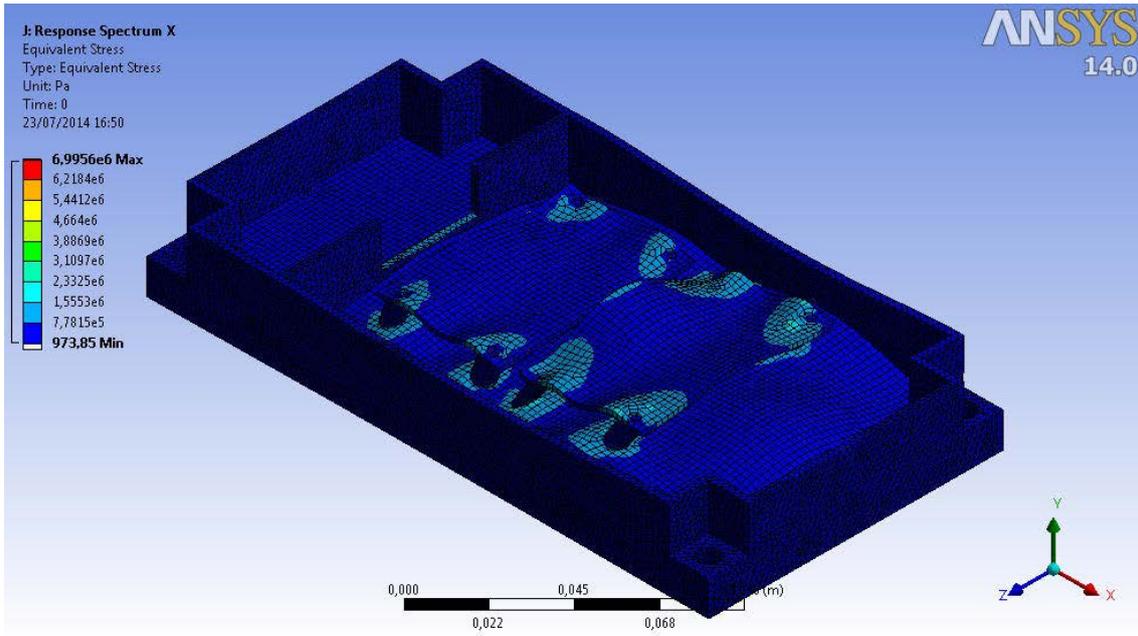
Figure 47: Shock stresses, X axis
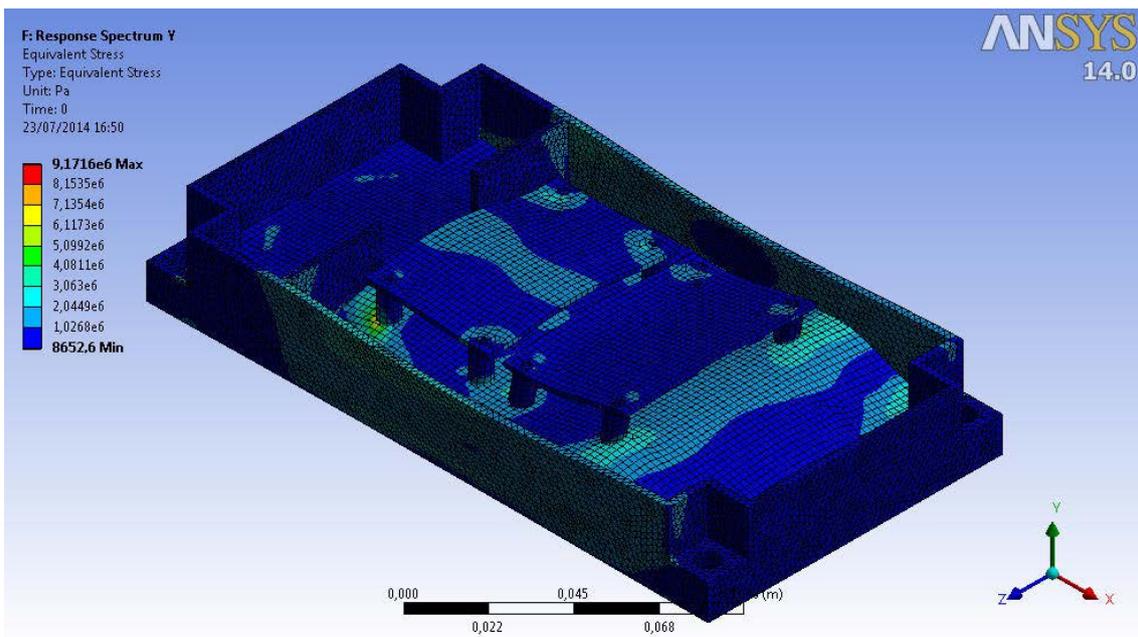
Figure 48: Shock stresses, Y axis

60
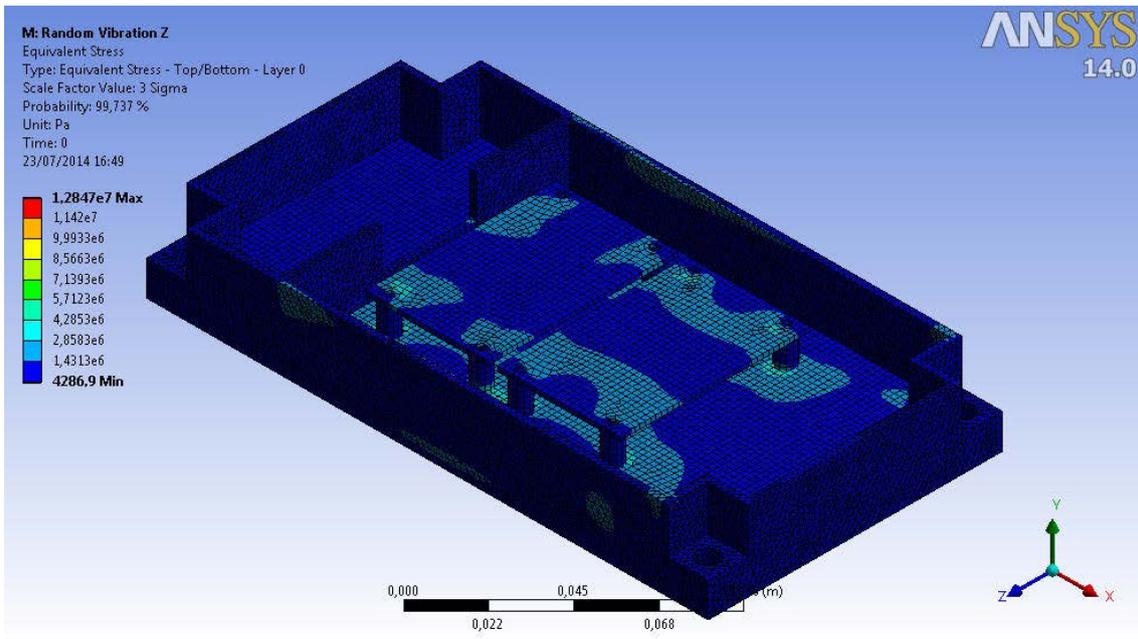
Figure 49: Shock stresses, Z axis

The minimum MOSy and MOSu are calculated below:

$$MOS_y = \frac{\sigma_y}{\sigma_{max}K_pK_mK_qFOS_y} - 1 = 10.3$$

$$MOS_u = \frac{\sigma_u}{\sigma_{max}K_pK_mK_qFOS_u} - 1 = 10.7$$

4.4.5   Frequency response

A frequency response analysis was carried out to assess the behavior of the Payload in presence of vibration environment of 1g of amplitude applied with sine profile with frequency variation between 5 Hz and 2000 Hz. Payload response was inspected in six internal critical points, namely at PCBs and interface points (Figure 50) in order to understand from the output accelerations if the internal layout shall be modified in order to reduce the accelerations experienced by some of its parts.
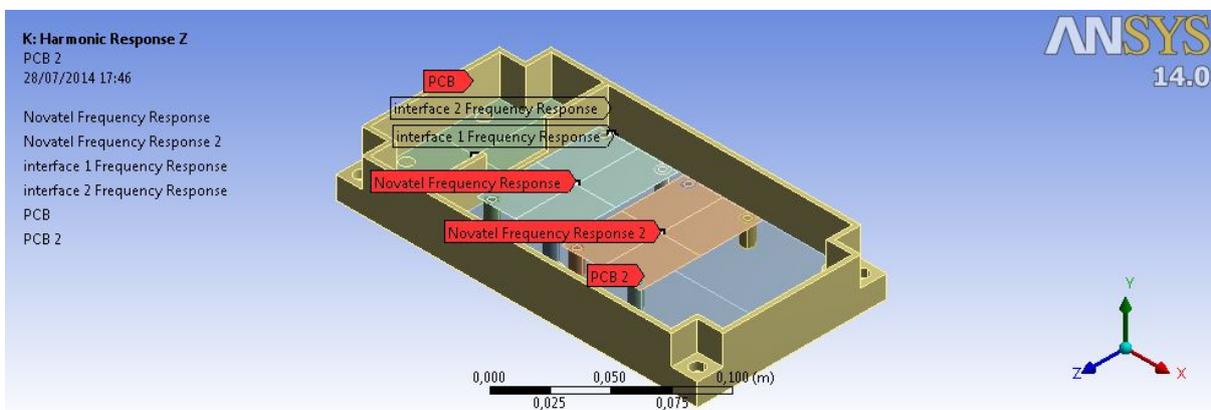
Figure 50: Acceleration control points

61

The responses in terms of acceleration with the input acceleration along X, Y and Z axes are reported down below for each one of the control points ().
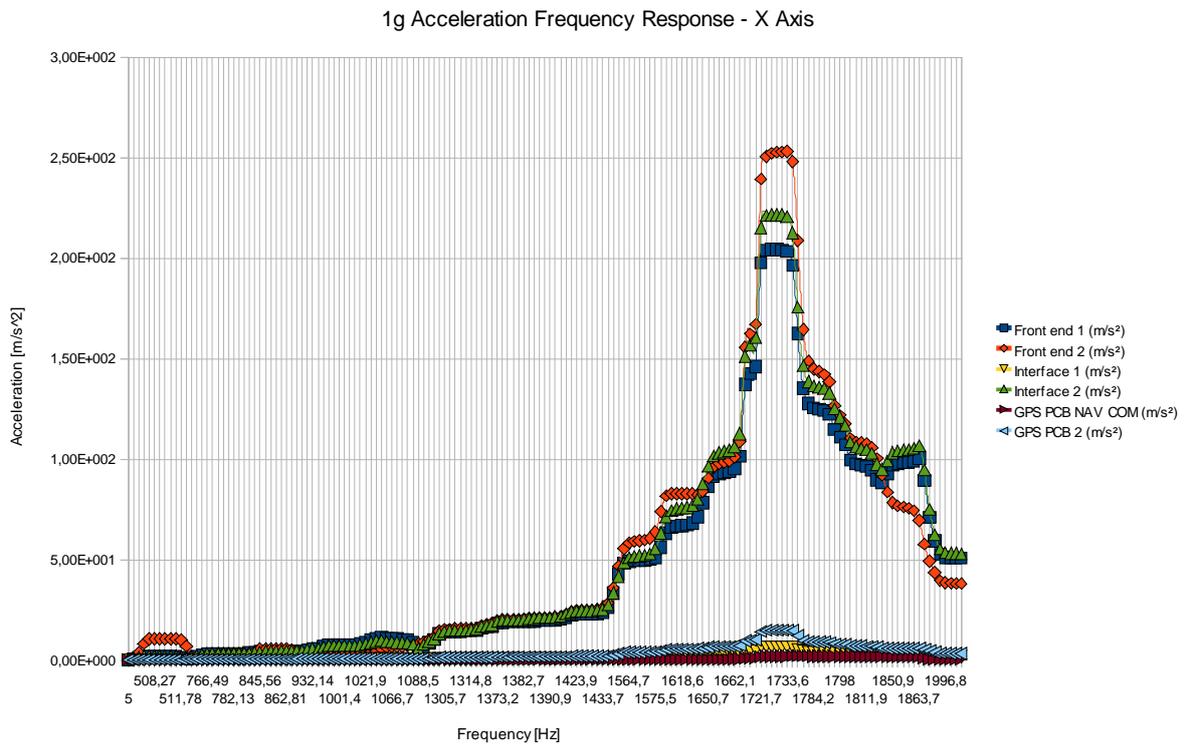
Figure 51: Acceleration response at the control points, X axis
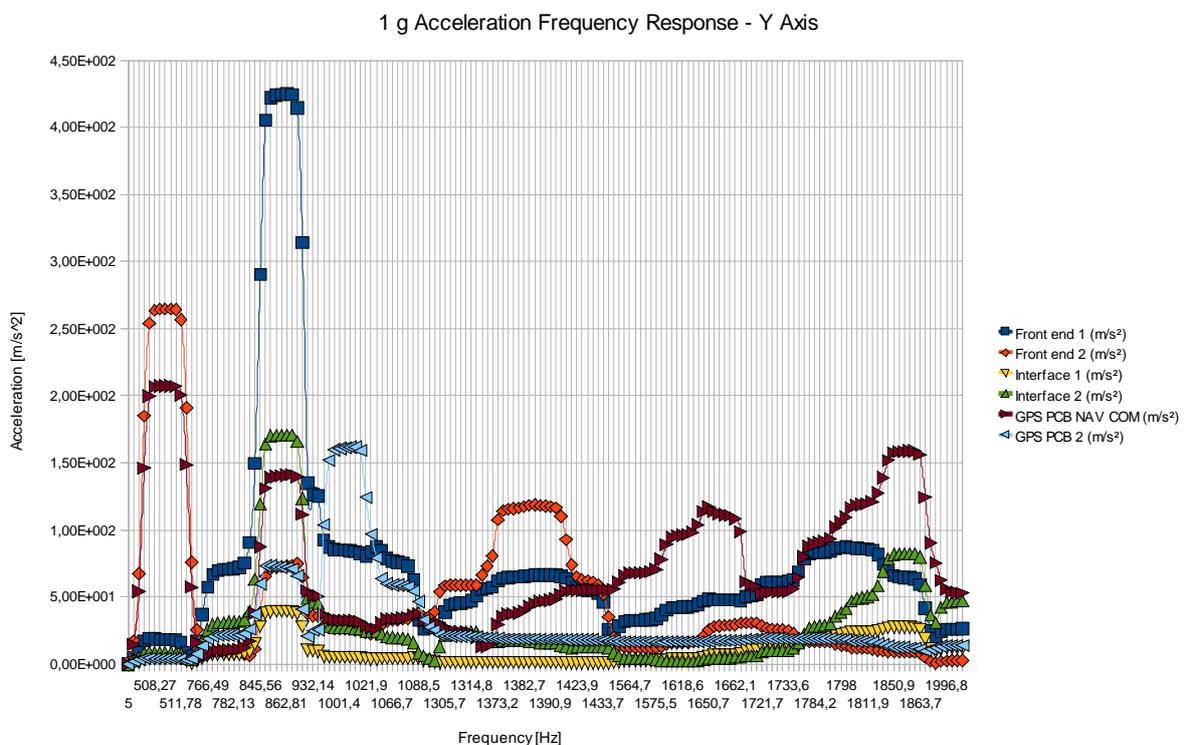
Figure 52: Acceleration response at the control points, Y axis
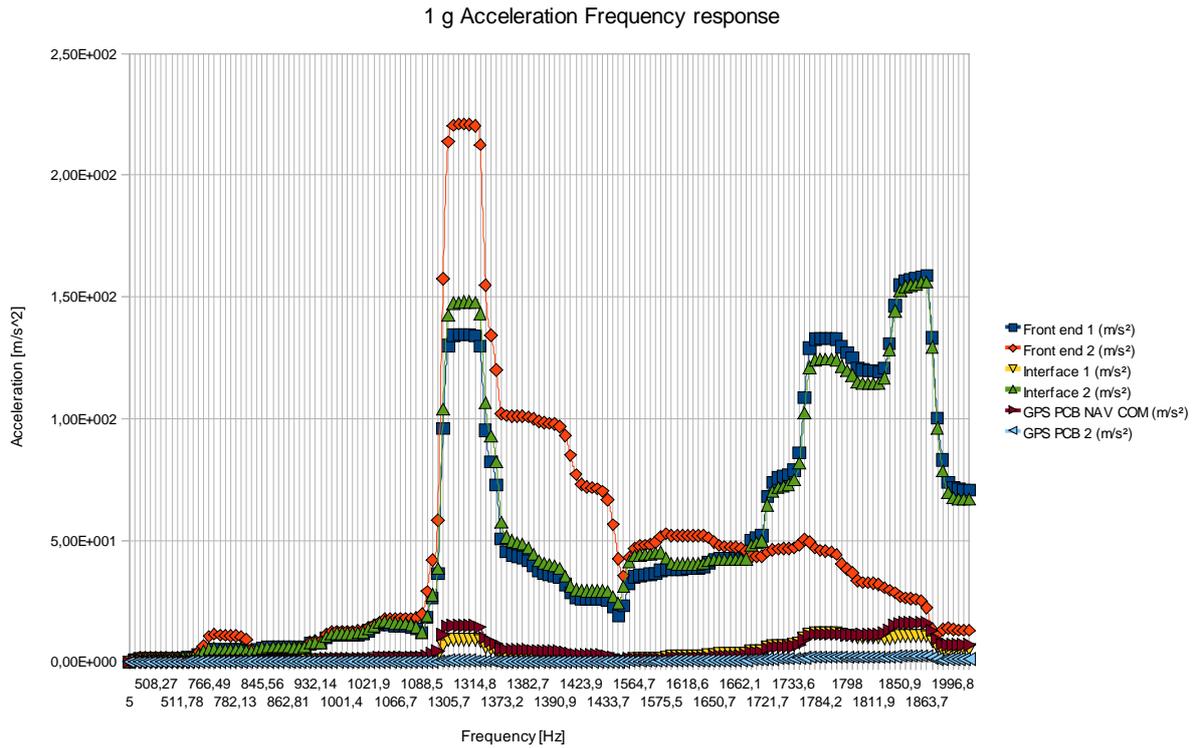
Figure 53: Acceleration response at the control points, Z axis

4.4.6 Fail safe analysis

GPS payload was also verified with the fail safe approach: only three of the four interface points with the tray were considered, lefting the fourth one floating, in order to simulate the screw breakage. Using the same model and settings of the previous simulations, only the random vibrations along th three axis were run again. Figure 54, Figure 55 and Figure 56show the results in terms of stresses and deformations along the three axis.
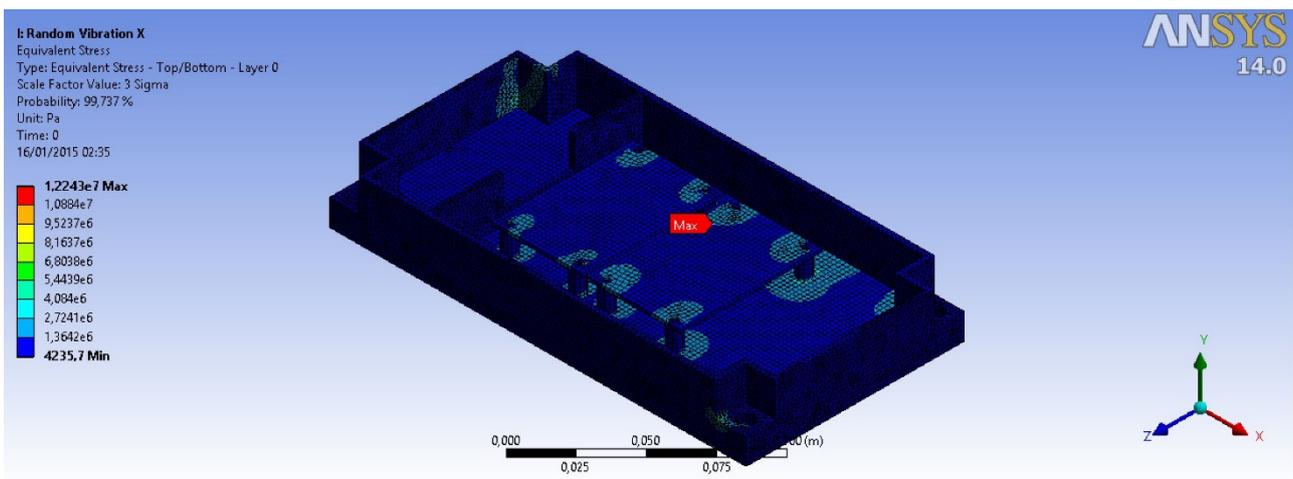
Figure 54 : Fail Safe analysis stresses, X axis
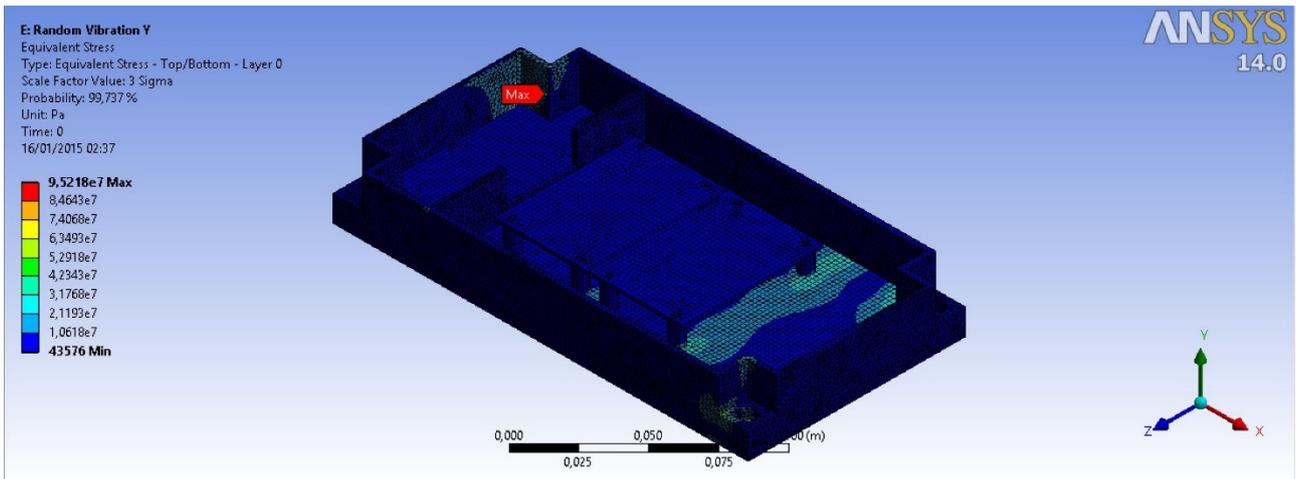
Figure 55: Fail Safe analysis stresses, Y axis
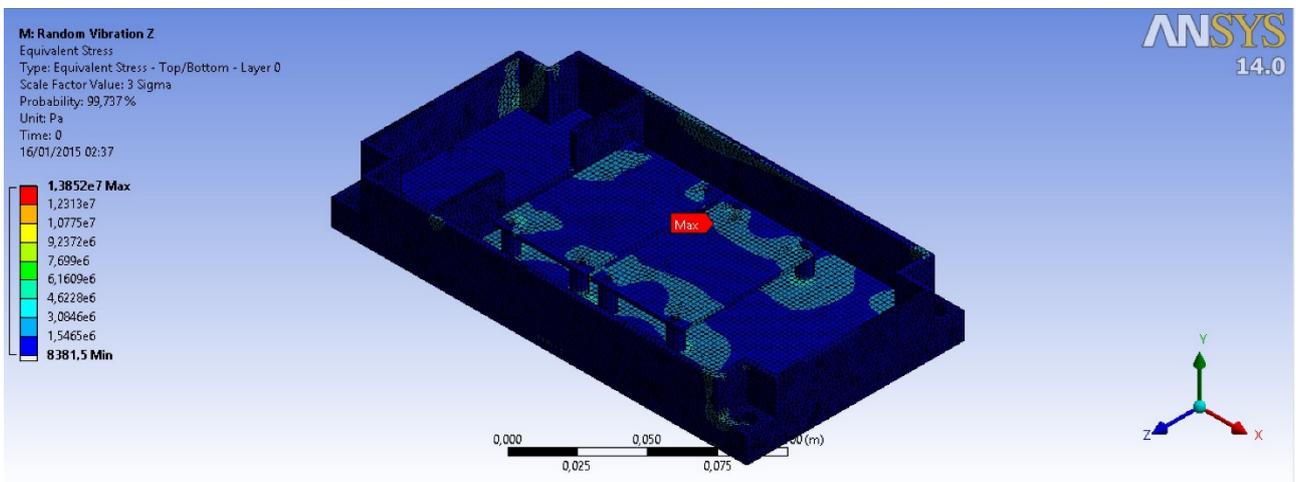
Figure 56: Fail Safe analysis stresses, Z axis

Since the maximum stresses were obtained during the simulation of the random vibration along the Y axis, it was studied to evaluate the margins of safety. The maximum value was applied to one of the four fixation points, as shown in Figure 57:
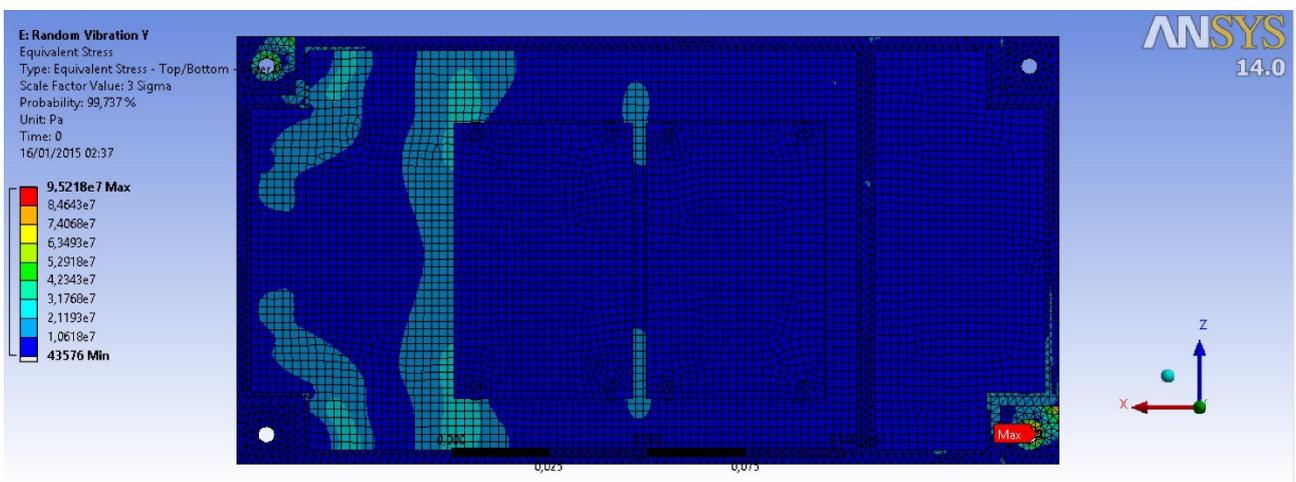
Figure 57: Max stress value

The minimum MOSy and MOSu have been calculated as:

$$MOS_y = \frac{\sigma_y}{\sigma_{max} K_p K_m K_q FOS_y} - 1 = 0.5334$$

$$MOS_u = \frac{\sigma_u}{\sigma_{max} K_p K_m K_q FOS_u} - 1 = 0.5785$$

The static loads, SL$_{random}$, related to the random vibration analysis can be evaluated from the simulation data along the three axis, using the following equation:

$$SL_{random} = MOS_y \cdot 3 \cdot RMS = 27.8 \, g$$

where RMS is included in the EID-B document and is equal to 17.38.

4.4.7 Mechanical analysis results

From of the mechanical simulations the following conclusions can be given:

- Modal analysis: since the first mode has a frequency higher than 200 Hz, the model is compliant with the requirements.

- High level low frequency response: both the yeld and ultimate minimum margin of safety are positive, so the model is compliant with the mechanical requirements.

- Random Vibrations: both the yeld and ultimate minimum margin of safety are positive, so the model is compliant with the mechanical requirements.

- Shock: both the yeld and ultimate minimum margin are positive, so the model is compliant with the mechanical requirements.

- Deformation: in order to verify if the displacement level in Y direction is acceptable, it was considered the Steinberg empirical value as a reference. It is calculated considering the limit displacement value of a PCB obtained under a certain component (Figure 58).
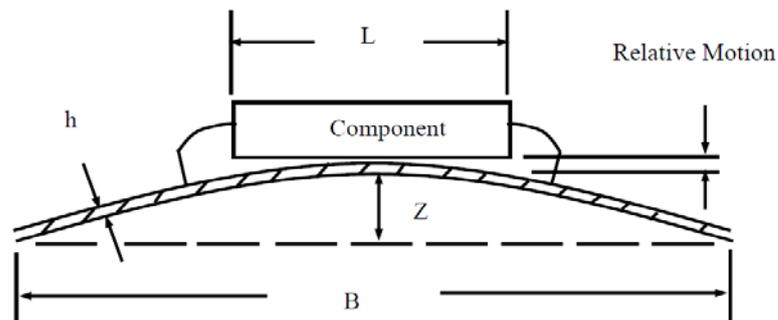
Figure 58: Component under bending motion

This component was chosen as the one that provide the minimum value for the Steinberg empirical formula [39], between the one included in the design:

$$Z_{3\sigma\ limit} = \frac{0.00022 \cdot B}{C \cdot h \cdot r \cdot \sqrt{L}} = 0.015\ in = 0.38\ mm$$

with:

C = constant related to the electronic component = 1.26 (microcontroller)

B = length of the circuit board parallel to the chosen component = 103 mm (in this case the component has the same length in the plane, so was used the short side for a more conservative analysis) = 4 in

L = length of the electronic component = 14 mm = 0.55 in

h = circuit board thickness = 1.6 mm = 0.063 in

r = relative position factor for the component mounted on the board = 1 (component placed in the middle of the board)

For the verification, it is considered the maximum deformation value in Y direction as a result of the random vibration analysis: 0.368 mm. Since the max deformation obtained from the simulations is lower than the Steinberg value, the displacement is acceptable and the model is compliant with the requirements.

This dynamic loads analyses are meant just to provide preliminary insight about the likelihood of the mechanical design and to assess potential first level of iterations of design review. Vibration test are mandatory to totally validate the design and the GPS Payload layout, before proceeding with the production of the proto flight model.

4.6 Hardware Test Campaign

Test campaigns are a critical part of the overall space mission project, in order to verify and ensure that the product final performance meets the quality requirements and to rise confidence of proper functionality of the device during its operative life. The test philosophy adopted for the ESEO GPS Payload is in accordance with the reference standard ECSS-E-10-03A. All technical requirements generated at sub-system level were addressed with adequate verification method:

- Inspection: used to determine conformance to requirements without the use of special laboratory equipment, procedures, test support items or services.
- Review of design: validation by evidence from design documents of correct implementation of requirements indications and guidelines.
- Analysis: theoretical or empirical evaluation of the behaviour of the payload. It makes use of technical methods such as engineering analysis, statistics and qualitative analysis, analogue modelling, computer and hardware simulations.
- Test: verification by technical means, such as the use of special equipment and instrumentation, following determined principles and procedures.

The requirements with test and inspection methods were grouped thematically, in order to define accurate test procedures to follow during the test campaign. Every single action, as described in this section, performed during the test sessions was intended to satisfy a specific requirement.

Differently from other applications, space systems cannot be repaired in their operative environment, a part from historical and specific events (e.g. Hubble Space Telescope). For this reason, every device that will be launched in space undergoes several testing stages and almost every relevant aspect of the space environment is replicated on ground to assess sub-system compatibility. In space missions test campaigns, functional tests are usually performed inside the so called environmental tests. This leads to test sessions that require very long time to be prepared and concluded, and, in order to be compliant with Product Assurance requirements from national space agencies, they foresee very precise and comprehensive test procedures. Starting from the set of sub-system level technical demands, test criteria and test requirements are derived, and then a Test Plan is produced. The test plan purpose is:

- Provide a brief description of all tests phases;
- Objectives and the role of each test;
- Declaration test facilities and equipment;

For every test included in the Test Plan several new documents were produced:

- Test Procedure: to govern the execution of all tests, enlist the technical requirements that are covered by that specific test, highlighten how the each step of the procedure satisfies a requirement, provide a detailed procedure of actions to perform and a checklist to use during the test session and record results and notes.

- Test Report: Detailed description of test session and results. Scans of test checklist used during the session is included.

Since for this project mostly parts and components with no heritage were considered, the GPS Payload shall achieve the qualification for flight through the test campaign. In order to carry out all the functional verifications on equipment that is not intended to be launched, two types of model were used (Table 13).

The GPS payload testing strategy is based upon the protoflight (PFM) philosophy, in order to reduce time and costs of the development, by producing a reduced number of models. The GPS payload PFM is intended to be integrated in the ESEO Spacecraft Flight Model exclusively to proceed the final proto-qualification campaign at system level.

So far, for testing purpose EBB models of every functional components were used and the final complete EBB of the GPS Payload was provided for integration with ESEO AVB to perform verification of all the requirements at system level up to the proto-qualification. For what concerns the COTS Front-end, the two models without COCOM limitations are considered PFM, while a third component of the same type but with COCOM limits was purchased to perform most of the tests on the GPS Payload. The PFM front-end were just used to verify their functionality on ground and during functional tests with GPS simulators, because the EBB was useless for this purpose.

Table 13: ESEO GPS receiver hardware matrix

Subsystem/instrument and equipment	EBB	PFM
COTS front-end (OEM615V-G1S-B0G-TT0) - Baseband ASIC processor - Signal tracking microcontroller	1	2
Navigation computer - Isolated DC-DC section with OVP - Navigation processor - Data interfaces	2	1
COTS Antenna S67-1575-20	1	1
Metallic enclosure	1	1
Connectors/Cables	1	1

The tests performed so far on the GPS Payload can be grouped under the following areas:

- Electrical test (EBB)

- Environmental test (EBB)

  - Thermal/vacuum qualification test

  - Vibration qualification test

- Firmware Functional test (EBB)

  - Front-end functionality

- Telecommands exchange

- Housekeeping data exchange

- Operational modes

- Application software test (EBB/PFM)

  - Full functions

  - Navigation algorithms

The test campaign was performed in different places:

- SITAEL S.p.A facilities: all electrical and environmental test at sub-system level were carried out at the Forlì and partially Bari facilities of the company prime contractor of the ESEO project. In particular several laboratory equipment was available to perform the tests: bench instruments and tools for electrical verifications, thermal chamber, electrodynamic shaker.

- Istituto Superiore Mario Boella (ISMB): first sessions of functional tests were performed at ISMB facility in Turin, Italy. For this test the GNSS signal simulator NAVX was kindly conceded by ISMB to assess the performance of the application software.

- Nottingham Geospatial Institute (NGI): to verify the performance of the Reduced Dynamic Filter the Spirent Simulator was kindly made available by NGI. Thanks to this finale verification period was possible to achieve an acceptable tuning of the filter and verification of the application software.

4.6.1 Electrical test

The present section describes the procedure and results of the confidence test on the ESEO GPS Navigation Computer EBB board. The purpose of this test was to verify to correct implementation of hardware requirements during the design phase. The electrical functionality of the Navigation Computer board was tested, without uploading the application software and without connecting the COTS front-end. General dimensions, DC-DC control and operation, overvoltage protection operation and in rush current measurements are some of the tests that were carried out on the board and the results were collected inside a report [30], provided to ESA for review purpose. Several hardware aspects were checked, in order to verify also that the GPS Payload is compatible with safety and product assurance requirements and will not represent a threat for other subsystems. Among others, the following aspects were checked: interfaces and PCB connectors, including mechanical, power and CAN interfaces; capability of the unit to work properly with the power source, including correct functionality after power cut-off and reset; functionality of the voltage protection and current limiting circuits. The Table 14 provides a schematic overview about test conditions and settings:

Table 14: Test conditions and settings

Test conditions and levels	- Temperature: ambient - Pressure: ambient - DC-DC primary voltage: - TP1: 18V +0V/-1V - TP2: 25,2V +1V/-0V - TP3: cut-off DC-DC primary voltage ripple: 1% of nominal ±0.01V
Tools and facilities	- Power source - Digital multimeter - Digital Caliber - Oscilloscope - Female DB9 power connector with cables and plugs to be connected to the power source - Cable with plug to be connected to the power source equipped with probe on one end and with a push button with series resistor 1 cable with plug to be connected to the power source equipped with probe on one end, and with a series capacitor of 5000 uF.

This test was performed inside the SITAEL S.p.A cleanroom with regulated environmental properties. Also the laboratory equipment to perform the test was kindly made available by SITAEL company.

Test setup is shown in Figure 59.
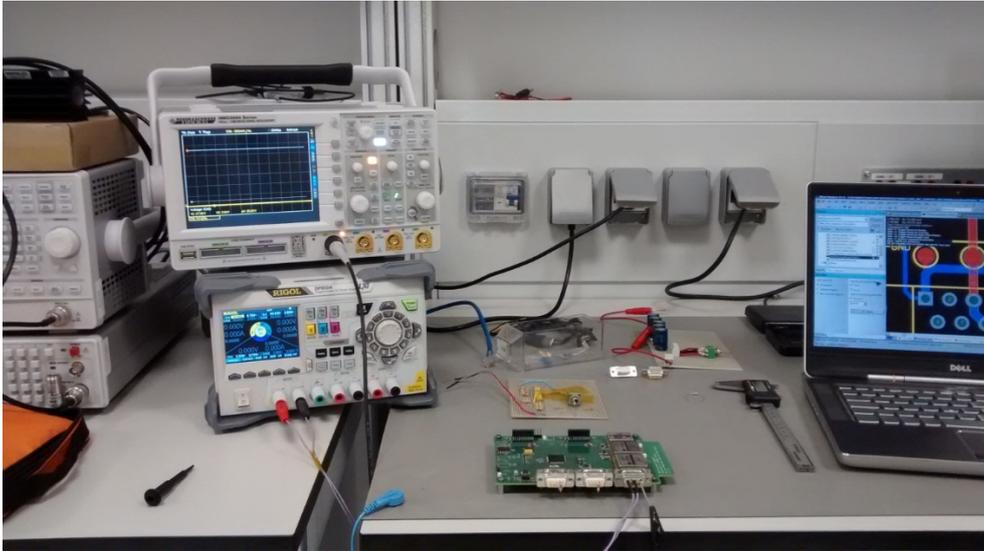
Figure 59 : Electrical test set up

According to the procedure written for this test, each step of verification included several activities, from direct inspection of evident hardware properties to electrical measurements of several aspects of navigation computer board. These activities were planned according to the specific hardware requirements. Since this test was the first performed on the custom designed hardware, the unit under test was the first EBB model produced, that was slightly different from the second EBB and final PFM. In fact, also thanks to this verification, some review of the design was applied between the production of the two EBB models.

4.6.1.1 Visual inspection

In order to satisfy some technical requests, a simple direct visual inspection of the board was sufficient. It covered the verification of: the presence of fixing holes, adequate connectors and their labels, overall board dimensions, absence of interferences and the capability to easily mate and de-mate connectors.
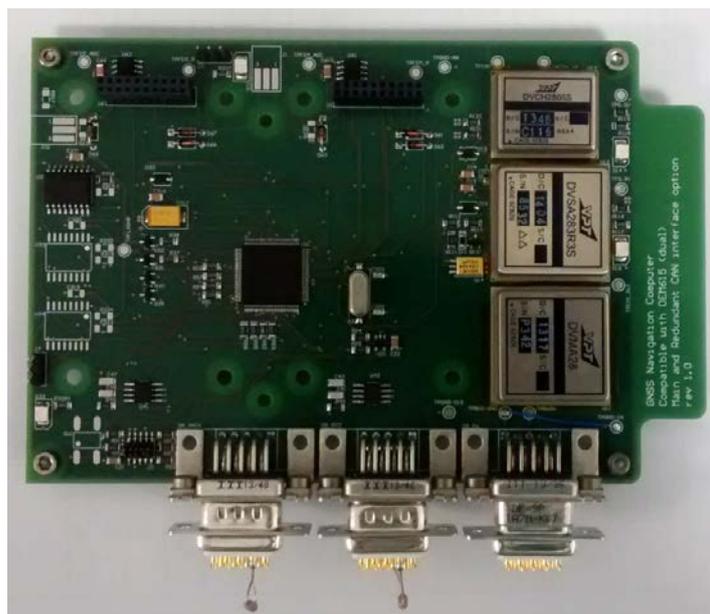
Figure 60: Board with mated connectors, during inspection

4.6.1.2   Electrical measurements

During preliminary design phase, estimations of several electrical properties of the payload in form a budgets were required, based only on available information from the datasheets of parts or single components. The core and more critical result expected from this verification, from the hardware design point of view, was the assessment of actual electrical performance of the navigation computer and the whole GPS Payload. The procedure used to perform this test [13] was repeated to assess PCBs integrity after every environmental test. Most of the following measurements were performed with the aid of a digital multi-meter.

First of all the external connector pins continuity and isolation was verified, to ensure that no failure will occur when connecting the Payload to external power and communication buses. After fixing the Nav PC board to the external chassis, the DC resistance between primary voltage connection and secondary ground/chassis was measured, along with the connection between primary bus ground and secondary ground/chassis. The detected resistance was over 99 MOhm, which guarantees adequate isolation of input power lead and return from chassis. The amplification stage was then added to the main board, in order to perform voltage and power measurements (Table 15).
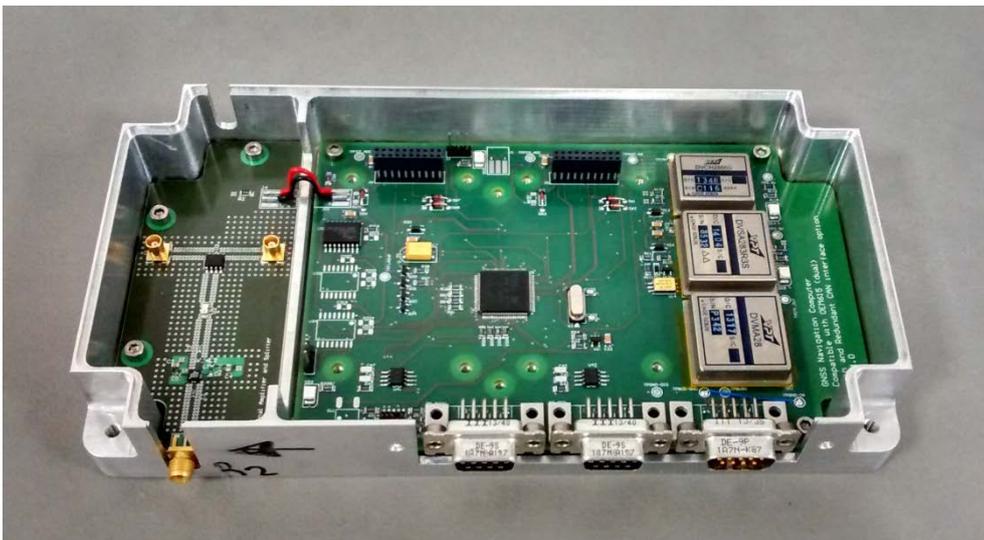
Figure 61: Custom designed functional parts assembled for verification

Requirements states that the subsystems and units shall be designed to operate without performance degradation, considering unregulated power supply bus with voltage in the range 18V to 25.2V ±1%. The unit primary was then first powered with 18V and then with 25.2V and current consumption values were collected with and without the amplification stage, in order to obtain separated values for both boards. Since two LEDs at the DC-DC outputs were used in the first EBB to visually verify that the board is operating properly, also pure current consumption was calculated, considering that they will not be mounted on the PFM.

Table 15: Power consumption measurements

Vin	Current	Power
18.28 V (Nav PC Only)	0.058A	1.060W
25.40 V (Nav PC Only)	0.055A	1.397W
18.28 V (Nav PC + Amp)	0.108A	1.974W
25.40 V (Nav PC + Amp)	0.088A	2.235W
18.28 V (Nav PC + Amp - LEDs)	0.095A	1.737W
25.40 V (Nav PC + Amp - LEDs)	0.075A	1.905W

Note that the measured power consumption values do not include the COTS front-ends: the measurements are just referred to the custom design boards, whose absorption behaviour need to be empirically assessed. The output voltage of the voltage regulation stage was also measured with the oscilloscope, along with voltage ripple (Table 16).

Table 16 : Voltage and ripple measurements

Vin	3.3V DC DC	5 V DC DC
18.28 V	3.36V	5.05V
25.40 V	3.36V	5.05V
Ripple Std	0.016V	0.017V
Ripple p-p	0.100 V	0.110 V

The power source was also removed and then the unit was switched on again to assess that no damage or limitation occurs upon inadvertent switch off.

4.6.1.3 Overvoltage protection circuit functionality

The overvoltage protection solution effectiveness was verified with an external circuit that generates a temporary overvoltage condition on the DC-DC output, simulating a failure of a component or the effect of space radiations (Figure 62). The external overvoltage simulator consists of capacitors connected in series with the PSU and the capacitor output is used to generate the transient overvoltage.
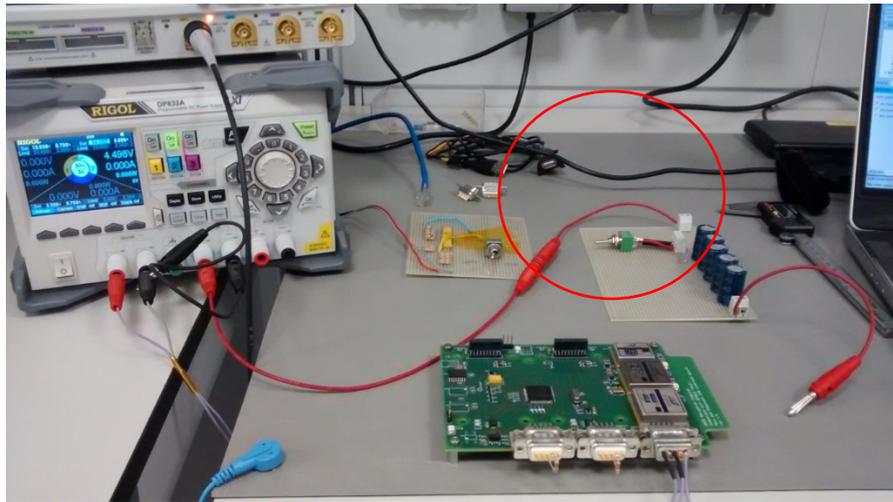
Figure 62: Overvoltage test

A spike voltage of 4.0V and 6.3V was caused respectively on the 3.3V circuit and the 5.0V part. During the test the correct functionality of the protection circuit was checked on the DC-DC INHIBIT pin, obtaining a change time from high to low level of 49 us.
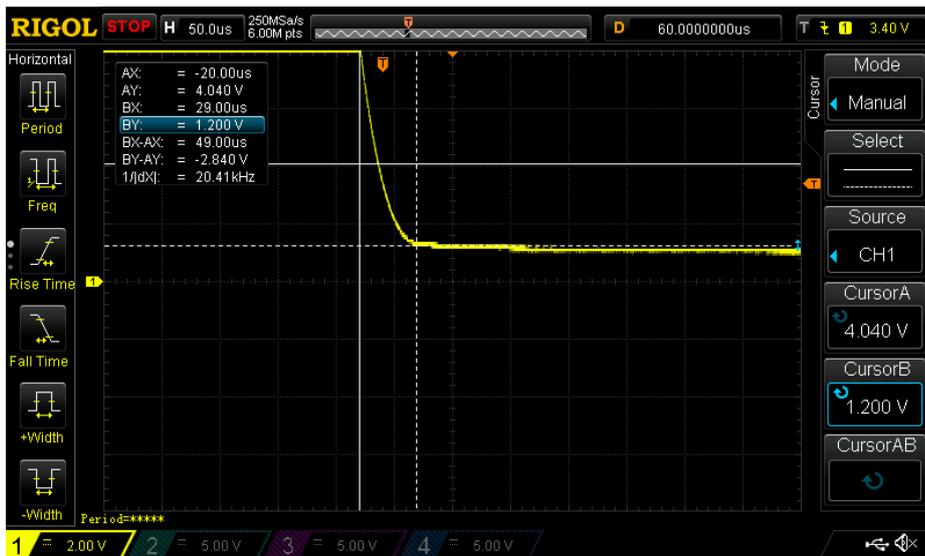
Figure 63: INHIBIT signal during overvoltage test

After the overvoltage occurs, the board was switched OFF and switched ON again acting directly on the power supply, in order to check that the correct operations were restored and the overvoltage protection was disabled.

4.6.1.4 Current limiter circuit functionality

Also the current limiter circuit was verified with an additional dummy board in order to simulates the load of the front-end (Figure 64). The board is designed to reproduce a static load equivalent to 10.6 Ohm plus an inrush current of about 6A for 10us (reported on the COTS front-end datasheet). Then a switch with 1 Ohm resistor is included to simulate a short circuit, result of space radiation effect on the COTS device.
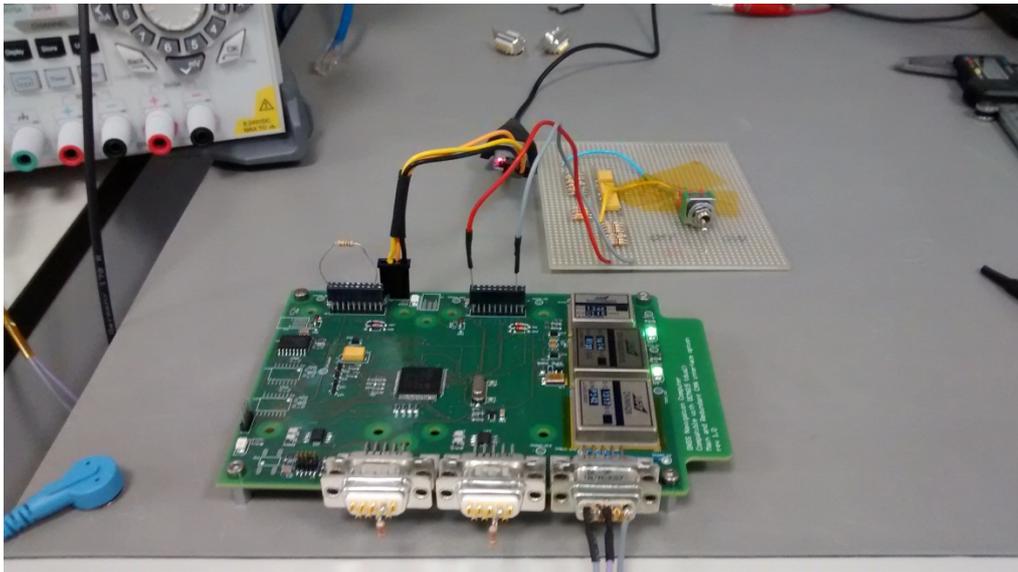
Figure 64: Current limiter circuit test

The dummy COTS front-end is switched ON by the microcontroller: both the behaviors at startup and in the event of a short circuit were monitored on the oscilloscope screen (Figure 65 and Figure 66). The current imposed by the CL was calculated as the voltage difference on the CL sensing resistor.
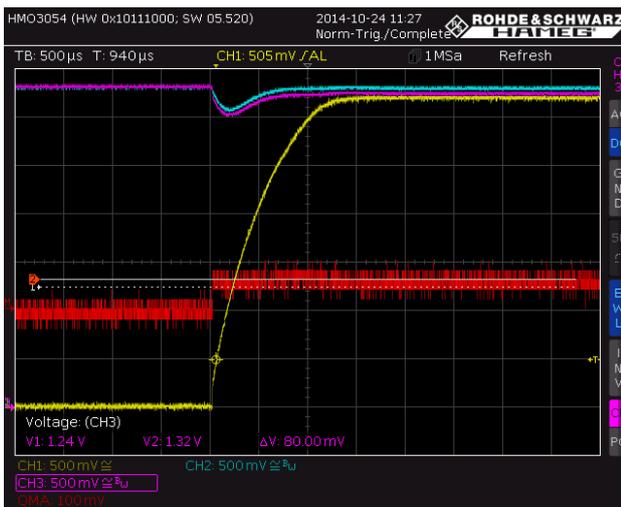
Figure 65: Output voltage (yellow) and voltage across the sensing resistor (red) during power ON
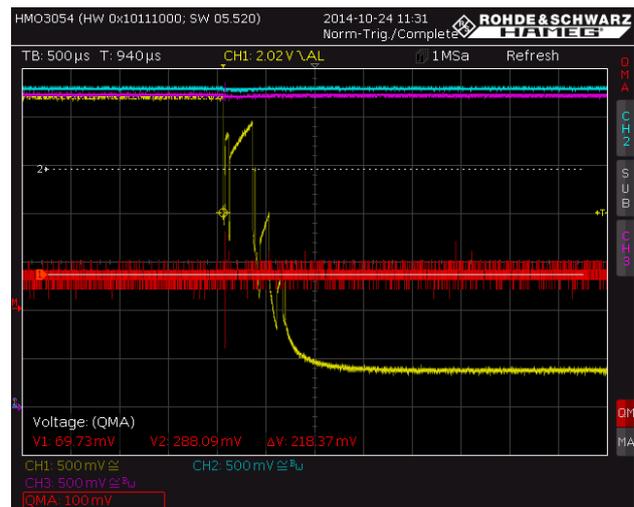
Figure 66: Output voltage (yellow) and voltage across the sensing resistor (red) during short circuit condition

Analyzing the data it was clear that the current limiter was designed a little bit too tight: the limitation current that triggered the limiting behavior was around 380 mA, while steady state current required by the front-end is 305 mA. This leads the circuit to work at the edge of limitation even during steady state conditions with the nominal current absorption. This critical behavior was confirmed when a model of the COTS front-end was mounted on the navigation-board: due to transient current absorption by the front-end during power up, the limiting circuit used to activate reactively disabling the front-end functionality before reaching steady state

conditions. For this reason minor changes were applied to the design of this part of the circuit, in order to perform adequate tuning of the sensing resistor.

4.6.2   Baseband Processor Test

This test represented a critical step in the definition of the final payload architecture, it involved the verification of COTS front-end behavior. The goal of this series of tests was not the assessment of the positioning performance of the commercial receiver, but the characterization of its behavior in terms of reactivity, multi-log timing capability, log message structure and, most important, space application compatibility. Using the developer firmware document as a reference [3], several ground test were performed in order to identify the useful logs to be used during the real mission that shall be implemented inside the Navigation computer application software. Ground tests were conducted inside the SITAEL facility in Forlì, Italy, using a replacement equipment for the custom boards: a Novatel Development Board with electrical and mechanical interfaces for each OEM family receivers and an active antenna from Sensor Systems. This choice was dictated by the need to reduce the possible sources of errors in the Payload architecture chain, as at that point of the design the custom boards were not yet well tested.
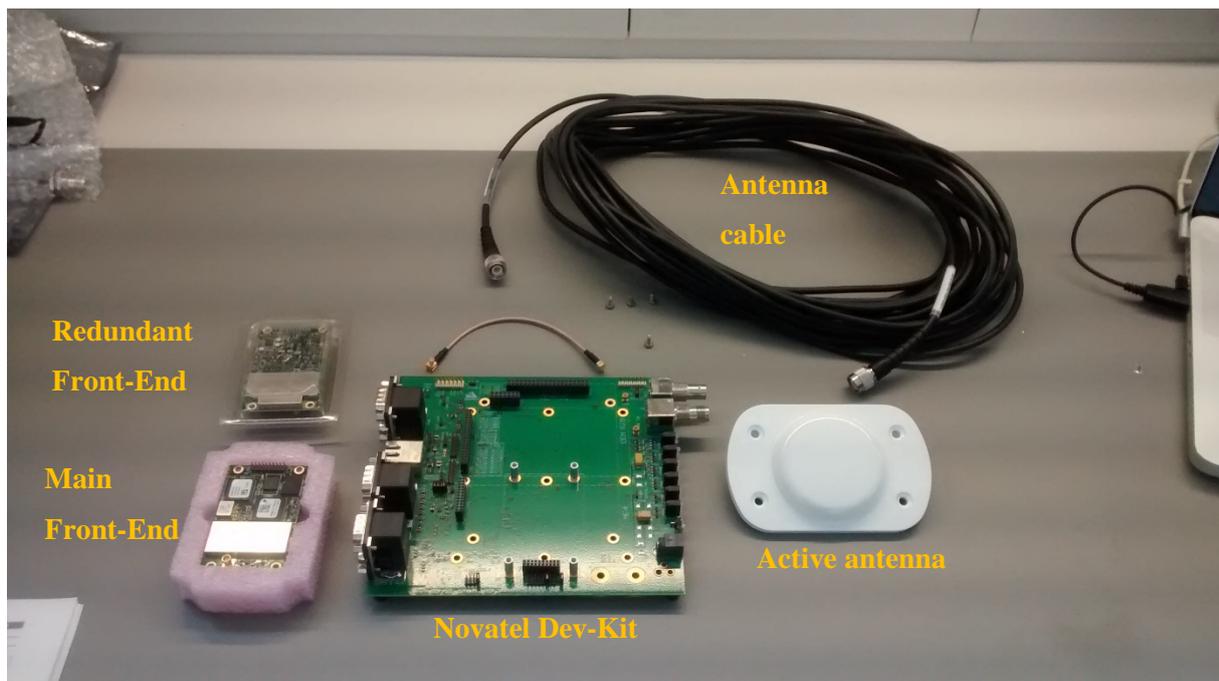
Figure 67: Ground COTS front-end test equipement

This series of tests was performed by using the Novatel Connect software [22] to send command, test logs and monitor the receiver behaviour (Figure 68 and Figure 69). A subset of commands and logs was derived in order to cover all possible data or funcionality that could be needed during the GPS Payload lifetime to carry out successfull mission. Based on sub-system level and GPS Payload specific requirements [34], a test procedure was derived to verify the main tasks required by the Navigation computer to the COTS front-end are [14]:

- Acquisition of GPS signal of at least 4 satellites while moving on-board of a LEO satellite
- Provide raw GPS observations as output : Pseudorange and Carrier Phase. These parameters shall be provided upon explicit request or with a pre-defined timing.
- Provide GPS constellation satellites ephemeris upon request and then every time an updated ephemeris set of parameters is available
- Provide self-diagnostic indications about receiever hardware and software internal status, including board temperature measurement, errors or failures, clock steering status
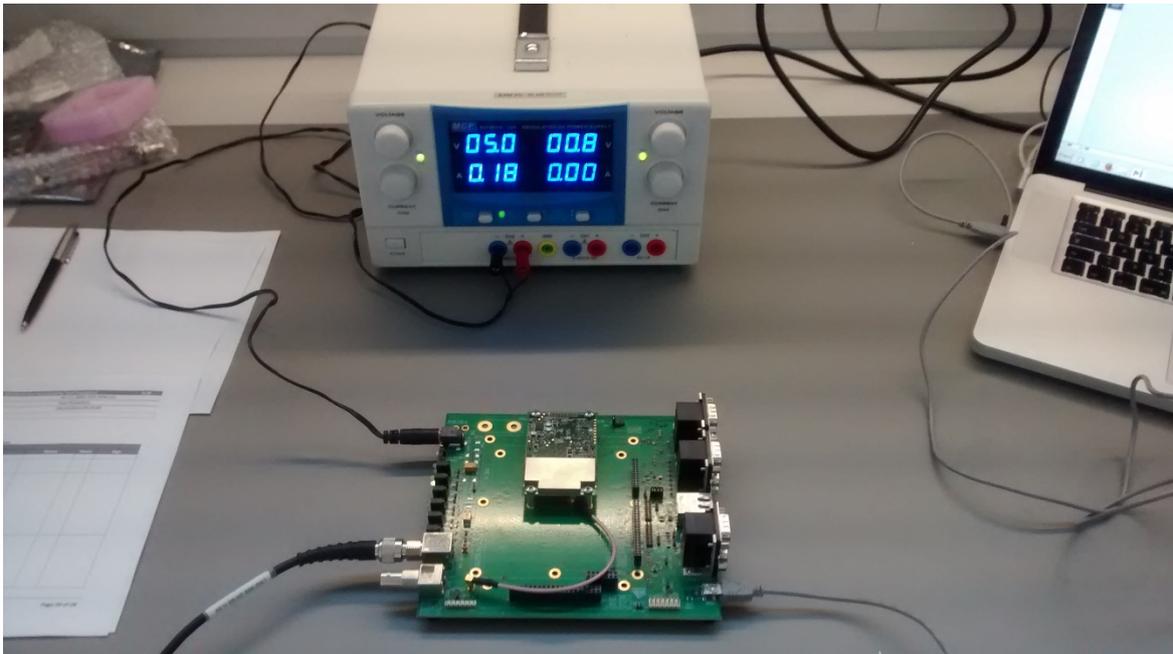
Figure 68: COTS front-end ground tests: indoor equipment

Figure 69: COTS front-end ground tests: outdoor equipment

The final set of commands and logs selected to achieve GPS Payload mission includes 6 commands that were implemented successively inside the application software in order to provide realtime information to the navigation computer. Table enlist the chosen commands, along with a brief description and their use inside the navigation software.

Table 17: Mission command and logs list

Command of log name	Description	Utilization description
ASSIGN / ASSIGNALL	This command allows to set each receiving channel of the front-end to scan the incoming signal from the antenna for a single PRN code, with dedicated frequency parameters. For the chosen PRN, each channel can be set to scan signal with a specific frequency offset, whose range is -100kHz/100kHz, and considering a frequency window around the central value to compensate for uncertainties or errors, whose range is 0/10000 kHz. The ASSIGNALL command can be used to set all channels at the same time. The forced setting of each signal can be undo by sending the command with the "AUTO" suffix.	Used in a dedicated routine, before the activation of the infinite loop. It will handle channel assignement until a stable link with at least 4 satellites is obtained. This mean that this command will be sent systematically, different every time, following a predetermined pattern of change of parameters to scan the entire expected range of frequencies.
TRACKSTAT	This log request is useful to check tracking channels status and functionality. It provides overall solution status for quick inspection of tracking process and for each channel other useful details such as tracked PRN, channel tracking status, pseudorange (if available), doppler shift used to scan incoming signal, C/N0.	This log is used in combination with the ASSIGN command to have complete control on the tracking functionality of the front-end. During the acquisition phase, assign command and trackstat log are alternated: first channels parameters are assigned and then tracking status is checked to verify if PRN signal is obtained.
GPSEPHEM	It provides GPS satellites ephemeris in form of orbital parameters set. It includes every information needed to reconstruct GPS satellite orbit and estimate position	This log is called right after the front-end initialization, and before entering the main loop. It is set to provide input to the navigation computer not under a

	at the current epoch. During the first call after power on, this log provides a set of satellite ephemeris that is already saved inside the receiver memory, that is updated once new data are obtained from the GPS constellation.	certain timing, but every time that the ephemeris set of a satellite is updated. Data obtained from the log is arranged in an array that is provided to the navigation algorithm to perform position computation.
RXSTATUS	This instruction asks the front-end for information about the receiver status. It provides complete and accurate data about the front-end hardware and software functionality, in form of words of flags, thematically grouped. It covers: receiver error, receiver status, communication ports status and memory status.	This request is set to ask rxstatus log every 30 seconds, during the main opeartive loop, after front-end and navigation computer initialization. In particular, the error word and status word are extrapolated from the log and saved as housekeeping data. They can be downloaded directly on ground using telecommands to monitor the active front-end status.
HWMONITOR	This log request Information about the hardware status of the receiver. Usually this log provides the output of different embedded sensors, but for the OEM615 model it only include temperature measure. However it is sufficient for the GPS Payload purpose, because voltage and current values are monitored externally by the Navigation Computer	This request is set to ask hwmonitor log every 30 seconds, during the main opeartive loop, after front-end and navigation computer initialization. In particular, temperature information is extrapolated from the log and saved as housekeeping data. It can be downloaded directly on ground using telecommands, to monitor the front-end temperature, along with other temperature measurements collected by the navigation computer inside the chassis.
RANGE	This log includes several information about channels that are actually tracking a PRN signal. Once called, this log includes a set of parameters for every tracking channel, exluding the ones that are still searching for a link, including : psudorange mesurement, psudorange standard deviation, carrier phase	This request is set to ask range log every 30 seconds, during the main opeartive loop, after front-end and navigation pc initialization. This log provides GPS raw observations that are used as input by the navigation algorithms to process the receiver position. From the received set

		measurement, carrier phase standard deviation, doppler, C/N0. This is the perfect log to obtain raw GPS measurements, to process with external algorithms.	of data, pseudorange and carrierphase information are extrapolated and used to generate PVT service. The two measurements for each PRN, are then saved, along with C/N0 value, as housekeeping data. They can be downloaded directly on ground using telecommands to perform precise processing on ground.
	TIME	This log provides time reference and clock corrections: It includes: receiver clock model status, estimation of receiver clock offset and standard deviation, GPS time offset from UTC, UTC time.	This request is set to ask time log every 30 seconds, during the main opeartive loop, after navigation pc and front-end initialization. Time information obtained from this log is used to evaluate GPS satellites position starting from the orbital parameters set. It is also used to timetag epochs raw and processed information, helping to save the set of housekeeping data.

4.6.3   Baseband Processor Simulator Test

Once assessed COTS front-end functionality in nominal ground tests, it is necessary to validate its performance in mission-like environment. In fact, also from the GPS signal acquisition point of view, a space scenario could introduce some difficulties, mostly linked to the signal frequency shift caused by the Doppler effect experienced when the receiver is moving at very high speed, which for a LEO satellite is around 6/7 km/s. The resulting frequency offset can be higher, with respect to terrestrial applications, of up to one order of magnitude. Considering that the selected COTS component was designed for terrestrial applications and no indications are provided by the manufacturer about possible implementation on-board of a spacecraft, it was necessary to characterize its behavior in presence of space-like GPS signal. This test was conducted inside the ESA ESTEC facility, using the SPIRENT GNSS signal simulator. Using the available equipment it was possible to simulate a receiver under typical LEO spacecraft motion and then to receive the related GPS signal by connecting the COTS front-end to the simulator output connector. For this test the COTS front-end was mounted on the Novatel development board, that provides all necessary standard electrical and rf interfaces and connectors, necessary to operate with the SPIRENT simulator (Figure 70, Figure 71 and Figure 72).
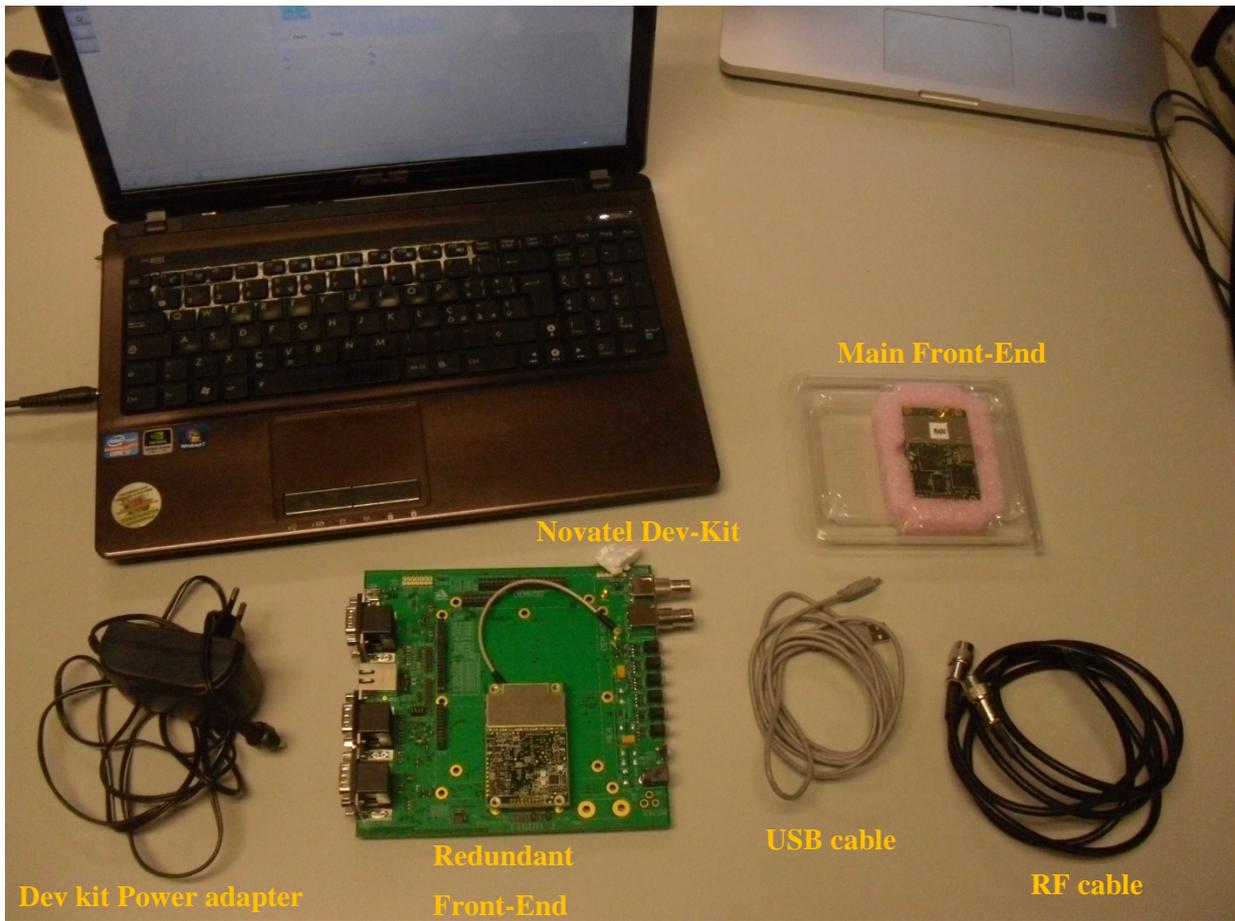
Figure 70: Test Equipment
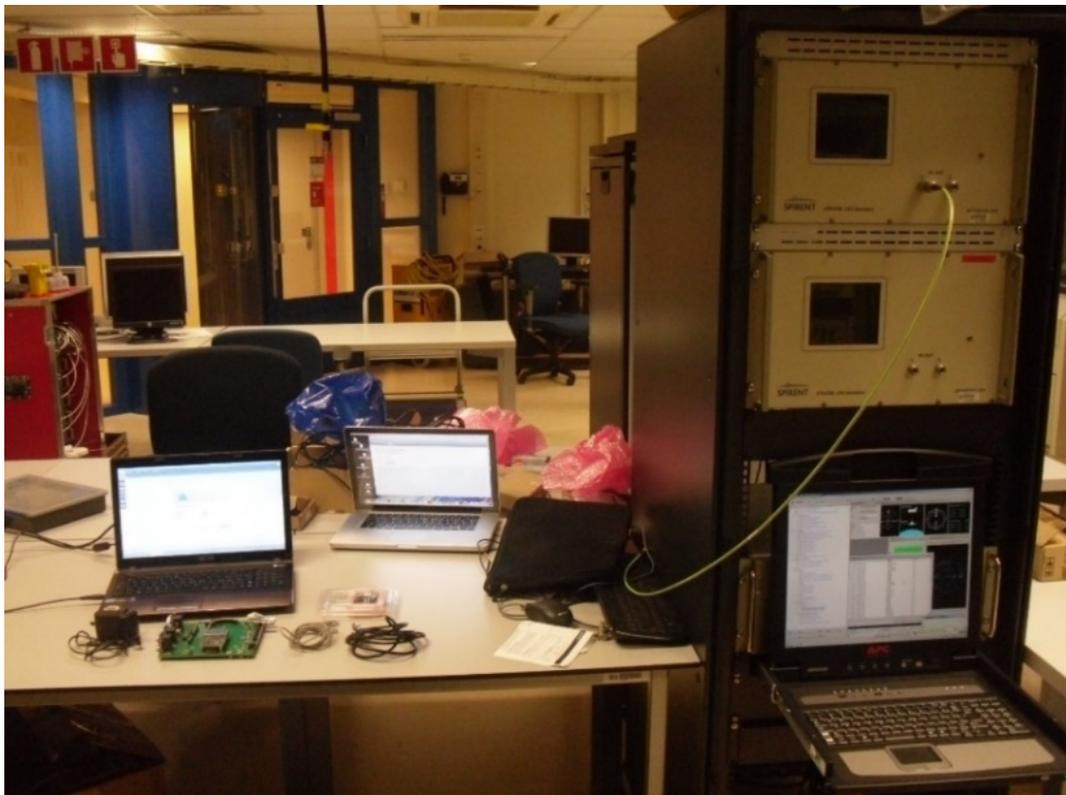
Figure 71 : SPIRENT Simulator
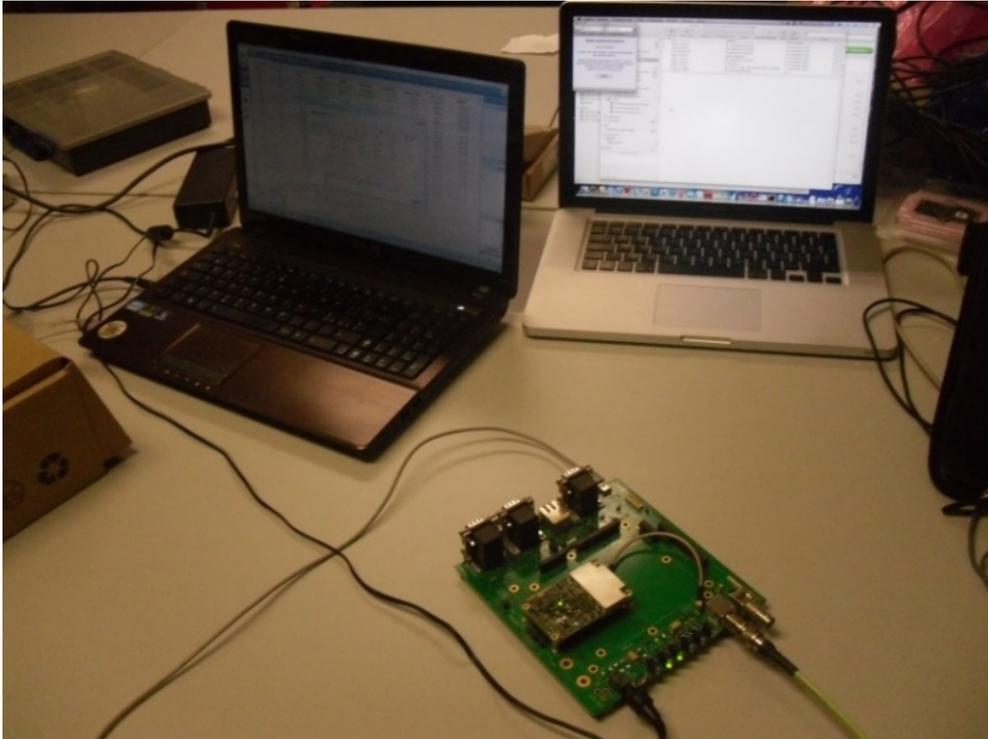
Figure 72: COTS front-end under test

Since this test was focused on the COTS front-end functionality, it was not mandatory to test the complete GPS Payload, including also navigation computer, amplification stage and external enclosure. The COTS front-end models used for this verification were the ones with removed COCOM limitations: both main and redundant components were tested to assess correct functionality and the same procedure described below was repeated also for the second front-end. The scenario was set to simulate a spacecraft in Low Earth Orbit with the following orbital settings:

- Reference frame = ECI

- Semi major axis = 6904 km = 6904827 m

- Inclination angle = 97.47884 deg

- Right ascension of the ascending node= 137.34 deg

- Eccentricity = 0.00135

- Mean anomaly = 25 deg (random) o 292

- Argument of perigee = 67.74183 deg

The attitude of the spacecraft was set as fixed Earth pointing, with the antenna on the opposite surface, in Zenith pointing. Once the scenario was ready, the COTS front-end, mounted on the development board, was connected to simulator output connector and to the laptop to monitor the behavior in real-time.

After power on of the device, it was left free to execute automatic built in initialization routines and signal tracking. Commands were set using the manufacturer's software and channels status was checked from a dedicated window inside the Novatel GUI: after several minutes of testing none of the channels was able to find any of the PRN signals. Although a long GPS link acquisition time is quite normal after every power on, checking on the tracking window it was clear that a major factor of this lack of link was the low frequency offset used to scan incoming signal for PRN codes. This is the evidence that the acquisition software has been optimized for terrestrial application, without including the extended range of Doppler for space applications.

To help the receiver lock the GPS signal, the forced setting strategy was adopted, thanks to the ASSIGN command, already tested in previous ground tests. Looking at the SPIRENT simulator GUI, the available PRN and relative Doppler at the beginning of a new simulation were used to perform a pre-setting of receiver channels. After starting the simulation, as expected, this time the receiver was able to lock signal in a few minutes. The behaviour of the channels was than monitored through the Advanced Tracking Window:

- Figure 73 shows the status of the channels before the starting of the simulation.Even if no signal is present, it is possible to notice that the channels are scanning the signal with the higher range of frequency offset, following the forced setting.

- During the simulation, after few seconds, the receiver obtained the complete GPS link and the position was processed, as shown in Figure 74.

- Then the additional command ASSIGN AUTO was sent, in order to turn all channels to the automatic assignment and to allow the receiver to autonomously arrange the previous channels to search other PRN codes once that old satellites disappeared from the field of view. As it is possible to see from Figure 75, the receiver maintains the GPS link in time after the re-arrangement of channels, setting to idle all redundant channels, not necessary for the position processing.

- Each test was performed for several minutes and, after the initial tracked satellites disappeared from the field of view, the receiver was able to automatically rearrange the channels to search and track new satellites with the right Doppler, as shown in Figure 76.

Channel	PRN	State	Doppler	CNO	Residual	Lock Time	Reject Code	Sys-Corr	Signal
0A	26	L1 Sky Sea...	42750				NA	GPS-P	L1C/A
1A	27	L1 Sky Sea...	32000				NA	GPS-P	L1C/A
2A	28	L1 Sky Sea...	19250				NA	GPS-P	L1C/A
3A	17	L1 Sky Sea...	-16500				NA	GPS-P	L1C/A
4A	2	L1 Sky Sea...	-30000				NA	GPS-P	L1C/A
5A	4	L1 Sky Sea...	-22000				NA	GPS-P	L1C/A
6A	15	L1 Sky Sea...	-35500				NA	GPS-P	L1C/A
7A	11	L1 Sky Sea...	-1000				NA	GPS-P	L1C/A
8A	21	L1 Sky Sea...	4000				NA	GPS-P	L1C/A
9A	23	L1 Sky Sea...	-2000				NA	GPS-P	L1C/A
10A	22	L1 Sky Sea...	-3000				NA	GPS-P	L1C/A
11A	24	L1 Sky Sea...	-2000				NA	GPS-P	L1C/A
12A	26	L1 Sky Sea...	1000				NA	GPS-P	L1C/A
13A	13	L1 Sky Sea...	4000				NA	GPS-P	L1C/A
14A	25	L1 Sky Sea...	-2000				NA	GPS-P	L1C/A
15A	14	L1 Sky Sea...	3500				NA	GPS-P	L1C/A
16A		Idle					NA	Geo-S	L1C/A
17A		Idle					NA	Geo-S	L1C/A
18A		Idle					NA	Geo-S	L1C/A
19A		Idle					NA	Geo-S	L1C/A

Figure 73: Channels behavior before starting the simulation

Channel	PRN	State	Doppler	CNO	Residual	Lock Time	Reject Code	Sys-Corr	S
0A	26	Lock	40030,3	47,0037	0,54321	46,8	Good	GPS-P	
1A	27	Lock	35669	47,2067	0,474133	61,9	Good	GPS-P	
2A	28	Lock	26967,4	47,4117	0,196251	49,84	Good	GPS-P	
3A	17	Lock	-10940,9	47,9676	-0,698959	52,59	Good	GPS-P	
4A	2	Lock	-29781,5	46,8878	0,037827	40,83	Good	GPS-P	
5A	4	Lock	-38351,9	46,7532	0,402237	47,18	Good	GPS-P	
6A	15	Lock	41276,5	46,4252	-1,58295	19,59	Good	GPS-P	
7A	11	L1 Sky Se...	-2500				NA	GPS-P	
8A	27	Lock	35669	47,2079		17,96	L1 Observ...	GPS-P	
9A	26	Lock	40030,3	47,0021		16,96	L1 Observ...	GPS-P	
10A	4	Lock	-38351,9	46,7531		19,38	L1 Observ...	GPS-P	
11A	17	Lock	-10940,9	47,9681		52,57	L1 Observ...	GPS-P	
12A	13	Lock	-31423,5	46,8845	0,0499452	12,6	Good	GPS-P	
13A	8	Lock	26024,1	46,8044	0,160319	22,46	Good	GPS-P	
14A	28	Lock	26967,4	47,4115		19,74	L1 Observ...	GPS-P	
15A	10	Lock	7495,26	47,7046	0,183131	38,7	Good	GPS-P	
16A		Idle					NA	Geo-S	
17A		Idle					NA	Geo-S	
18A		Idle					NA	Geo-S	
19A		Idle					NA	Geo-S	

Figure 74: Channels behaviour during the running of the simulation

Channel	PRN	State	Doppler	CNO	Residual	Lock Time	Reject Code	Sys-Corr	S
0A		Idle					NA	GPS-P	
1A		Idle					NA	GPS-P	
2A		Idle					NA	GPS-P	
3A		Idle					NA	GPS-P	
4A	2	Lock	-30323,6	46,8505	-0,0237738	67,83	Good	GPS-P	
5A		Idle					NA	GPS-P	
6A	15	Lock	41089,8	46,6452	-1,09002	46,59	Good	GPS-P	
7A		Idle					NA	GPS-P	
8A	27	Lock	34961,7	47,2144	0,213913	44,96	Good	GPS-P	
9A	26	Lock	39407,4	47,0757	0,492291	43,96	Good	GPS-P	
10A	4	Lock	-38706	46,7041	0,305631	46,38	Good	GPS-P	
11A	17	Lock	-12011,8	47,9661	-0,460785	79,57	Good	GPS-P	
12A	13	Lock	-32075,4	46,7876	0,0147893	39,59	Good	GPS-P	
13A	8	Lock	25234,5	46,8494	0,220482	49,46	Good	GPS-P	
14A	28	Lock	26161,8	47,5228	0,0279086	46,74	Good	GPS-P	
15A	10	Lock	5924,68	47,6654	0,152407	65,7	Good	GPS-P	
16A		Idle					NA	Geo-S	
17A		Idle					NA	Geo-S	
18A		Idle					NA	Geo-S	
19A		Idle					NA	Geo-S	

Figure 75: Channels behaviour after the auto-assignment command

Channel	PRN	State	Doppler	CNO	Residual	Lock Time	Reject Code	Sys-Corr	S
0A	16	Lock	32712,1	48,2549	0,31508	344,6	Good	GPS-P	
1A	1	Lock	31082,9	47,9671	0,0548299	274,6	Good	GPS-P	
2A	18	Lock	-38103,9	47,7066	0,633951	1804,59	Good	GPS-P	
3A	19	Lock	-19422,9	48,3112	-0,134245	1734,6	Good	GPS-P	
4A	22	Lock	-30707,3	48,6093	0,691679	1484,6	Good	GPS-P	
5A	21	Lock	-15080,2	47,6461	-1,51874	1434,59	Good	GPS-P	
6A	3	Lock	-5619,75	49,0646	-0,545988	1334,61	Good	GPS-P	
7A	6	Lock	-1277,32	49,0594	-0,377537	1234,61	Good	GPS-P	
8A		Idle					NA	GPS-P	
9A		Idle					NA	GPS-P	
10A		Idle					NA	GPS-P	
11A	14	Lock	7831,22	48,5754	0,596737	777,4	Good	GPS-P	
12A		Idle					NA	GPS-P	
13A		Idle					NA	GPS-P	
14A		Idle					NA	GPS-P	
15A		Idle					NA	GPS-P	
16A		Idle					NA	Geo-S	
17A		Idle					NA	Geo-S	
18A		Idle					NA	Geo-S	
19A		Idle					NA	Geo-S	

Figure 76: Channels behavior after several minutes of test

After the acquisition phase was completed, the complete GPS link and correct position processing were demonstrated by the two green leds turned on along the short edge of the dev kit (Figure 77). According to the dev kit manual, these leds indicates that at least four satellites are tracked and the GPS link is built. The front-end is then able to provide a valid position, that can be checked in the control window (Figure 78), along with other useful data to check consistency with the simulation scenario.
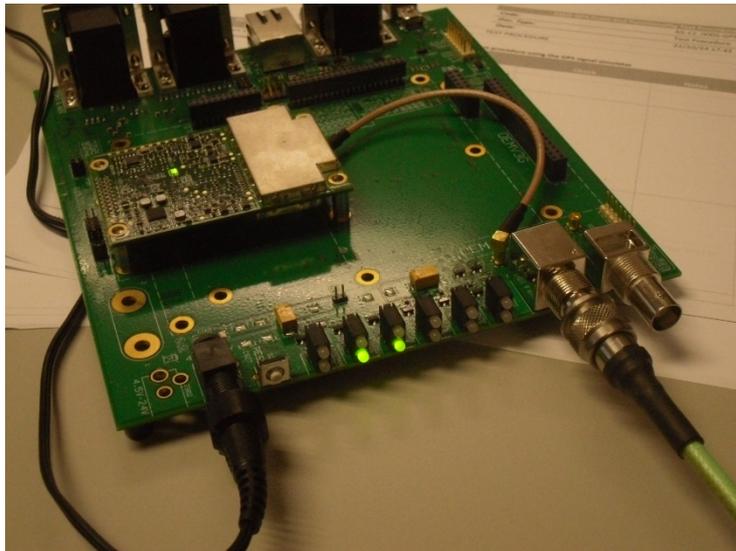
Figure 77: GPS link green leds
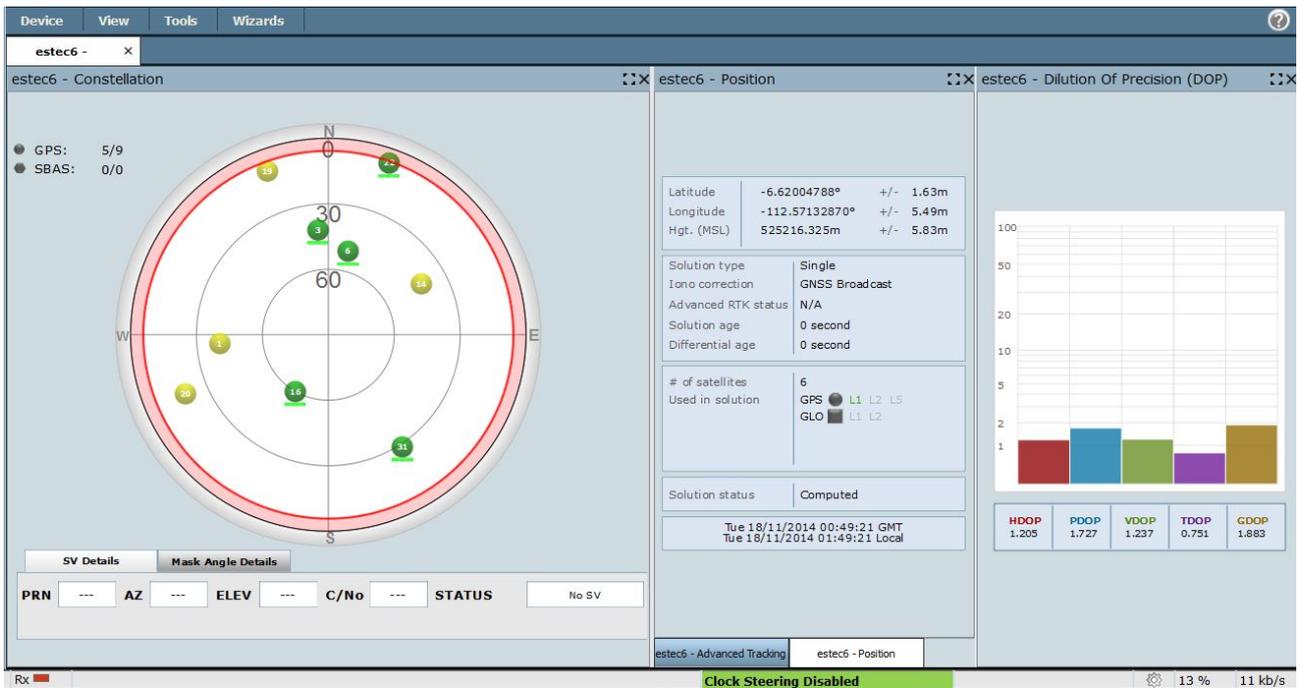
Figure 78: Control window

As it is possible to see from the Position and Velocity windows (Figure 79 and Figure 80) the receiver behavior is consistent with the LEO spacecraft scenario set using the simulator software: an height of 524881.736 m above mean sea level and a velocity 7674.5 m/s are reported by the monitoring windows.

Figure 79: Position window
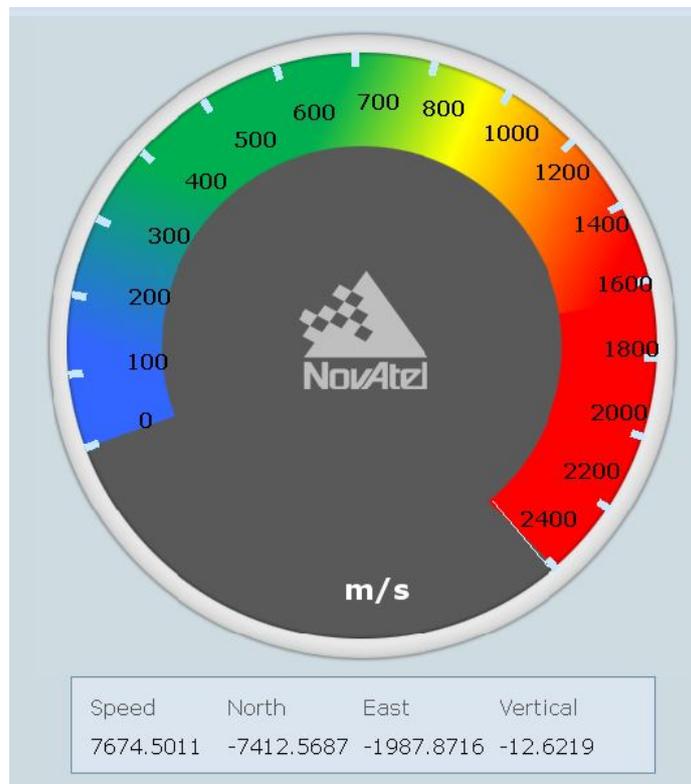
Figure 80: Velocity Window

Once assessed the correct solution evaluation performed by the receiver, a complete functional test of the mission logs was performed, by setting processing epochs every 30 seconds and checking the results to be coherent with the scenario [31].

This test provided evidence of the need of a forced setting of channels after every power on of the COTS front-end in space, to be sure that a complete GPS link will be established in a reasonable time. While during this verification this problem was avoided by setting the exact expected Doppler values for each PRN, this does not represent a solution for real-time embedded application, because exact values are not known in advance. For this reason, a dedicated setting routine was designed for the implementation inside the embedded software. This part of the code will be run during the initialization routine of the COTS front-ends and will scan the entire range of frequency offsets systematically. Its architecture and effectiveness assessment will be shown later in this document.

4.6.4 Communication Test

This test was intended to verify internal communication of the GPS Payload in flight configuration, with the COTS front-end integrated on the navigation computer. This test session was performed on ground, without the use of simulated observations, because the focus was not to assess navigation performance, but just to verify the application software architecture that hosts the two navigation algorithms. Test was conducted partially in the outdoor area close to the ALMASpace facility and partially inside the building (Figure 81 and Figure 82).
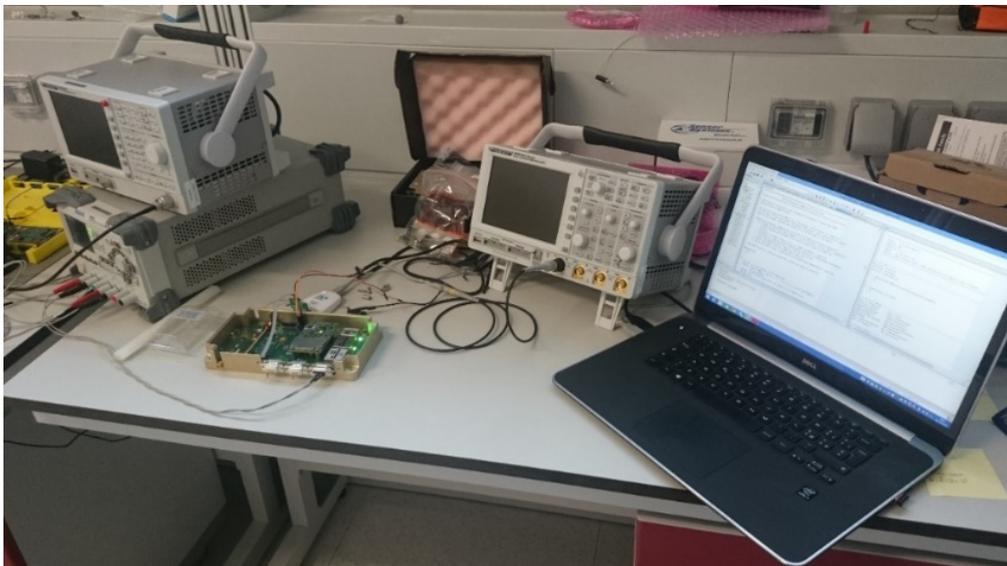
Figure 81: Indoor communication test

Figure 82: Outdoor communication test

The nominal functionality of the communication interface between the commercial receiver and the custom PCB was assessed. In particular all the mission-related commands and configurations identified during the previous test and reported in Table 17 were verified, together with the capability of the application software to handle log data while the front-end is operating in nominal behaviour. While during previous tests, the Novatel GUI was used to monitor to acquisition, tracking and observable generation of GPS signals as received by a static antenna mounted on ground, this time the Novatel software was replaced by an embedded software with the support of visual inspection to. To perform this test a basic firmware has been developed, in order to be able to check communications with the front-end. Using the navigation computer as an interface between the front-end and a laptop, commands and logs requests were sent from the terminal and the response was shown on the screen for visual check.

A first prototype of the code was written, including detailed log detection and data acquisition part, along with a rudimental a non-optimized implementation of the navigation filters. This code was written in C language using the dedicated development environment of ST, IAR Embedded Workbench, which was also used to test

different parts of code, in particular those for mission data reception and extrapolation, using the engineering model of the navigation computer. This version of the application software was useful to characterize the real-time behaviour of the payload, verifying the actual processing times and reaction to incoming new data from the Novatel front-end. This is a critical part of the code and of the same importance of the navigation part of the software. In order to be able to provide as output a set of position fixes every 30 seconds, the code must be able to manage up to 5 different logs incoming at the same time from the front-end with high reactivity and to perform a reliable data extrapolation in case of missing logs or incomplete set of data. To perform real-time visual inspection of the Payload behaviour, the application code was designed to transmit test data through an external diagnostic interface, specifically included in the hardware design for testing purpose. Basically, the test was focused on simulating a series of internally generated log request and the verification of the correct reception of the log instruction by the active front-end through 4 internal Universal Asynchronous Receiver-Transmitter (USART) communication ports: main and redundant port for both front-ends. This test was performed until a correct implementation of handling routines for all mission logs was demonstrated: first each single log request was tested separately with single call and scheduled call with time interval of 30 seconds; then all log were set active together at the same time, with their dedicated timing schedule, to verify the performance of the data handling routine while receiving more log in the same moment. The success criteria for each log was represented by the correct extrapolation of mission data from each log request, by performing visual checking of the navigation computer output on the Putty terminal.

This code and testing procedure, once the GPS Payload baseline functionality was assessed in nominal condition, was also useful for successive verification of the Payload integrity, after environmental test sessions.

Figure 83 shows the flow chart of the simplified version of the application software used for this test.
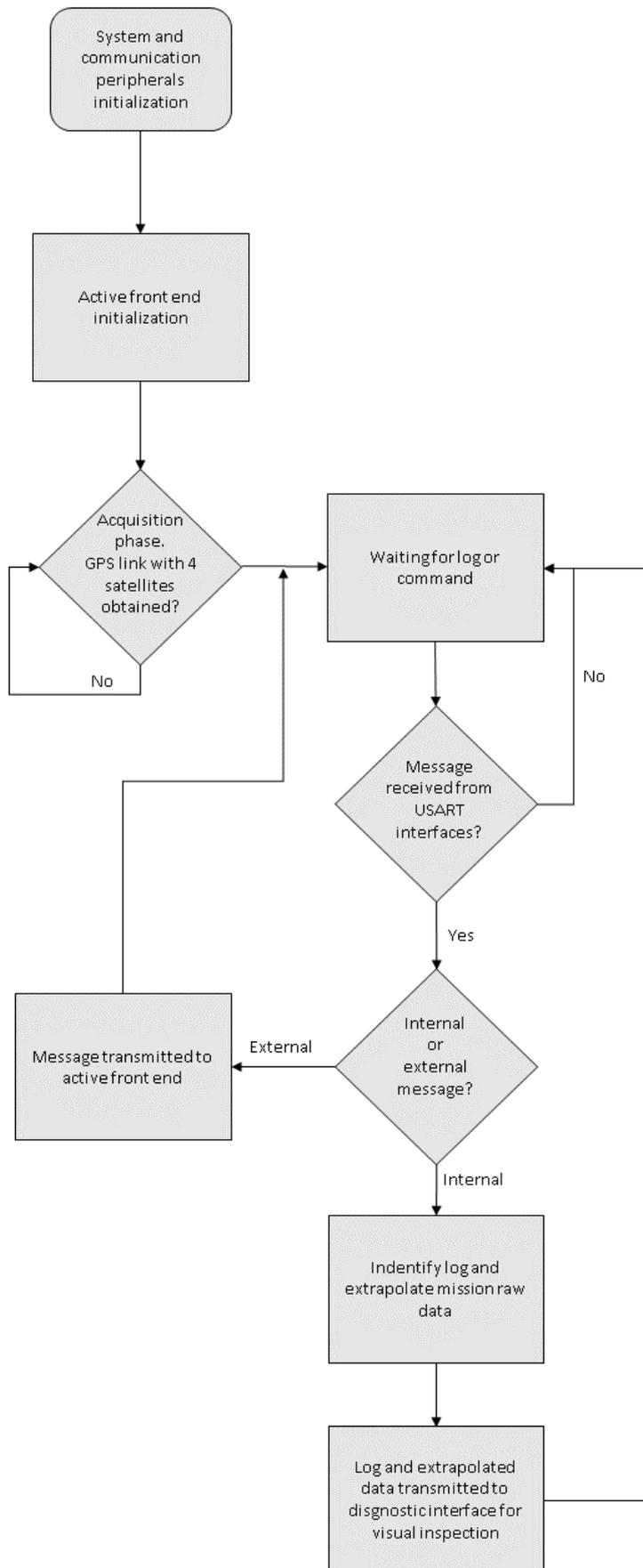
Figure 83: Communication test software flow chart

4.6.5   Thermal Test

Thermal test, as part of the environmental tests group, is intended to verify the behaviour and integrity of the hardware parts under extreme external conditions, close to the ones experienced in space. For this reason this test includes partially the procedures performed in the previous tests, to ensure that the device did not experience any degradation inside the thermal chamber. The verification was organized as follows:

- Functional and electrical verification during thermal test

- Electrical verification outside of the thermal chamber in normal environment

- Functional verification outside of the thermal chamber in normal environment

To perform this test a thermal chamber was used, that is able to control temperature and humidity inside a test chamber, where the unit under test is placed. The thermal chamber used for this test is the Discovery ES model, from Angelantoni ACS, available for the use inside the University of Bologna, with a test chamber of dimensions 601 mm x 810 mm x 694 mm (Figure 84).

Figure 84: ACS Discovery ES thermal chamber

The equipment under test was the complete payload in "flight configuration", in order to assess the functionality of the commercial baseband processor, to verify the thermal indications provided by the manufacturer, and the navigation computer, to determine if hardware changes were needed, to guarantee

correct operations under extreme external temperatures. To perform functional verifications during the thermal balance test, a laptop was used to send instructions and to monitor the payload's behaviour inside the chamber. During the thermal tests, temperature was monitored in different points of the Payload using sensors already implemented inside the hardware design. The first (TTP1) is soldered directly on the PCB and is displayed in Figure 85, near the unit DC-DC converter. The PCB is capable to acquire data also from an external temperature sensor that can be soldered using wires to the connector high lightened in Figure 86, and usually placed on the enclosure internal surfaces.
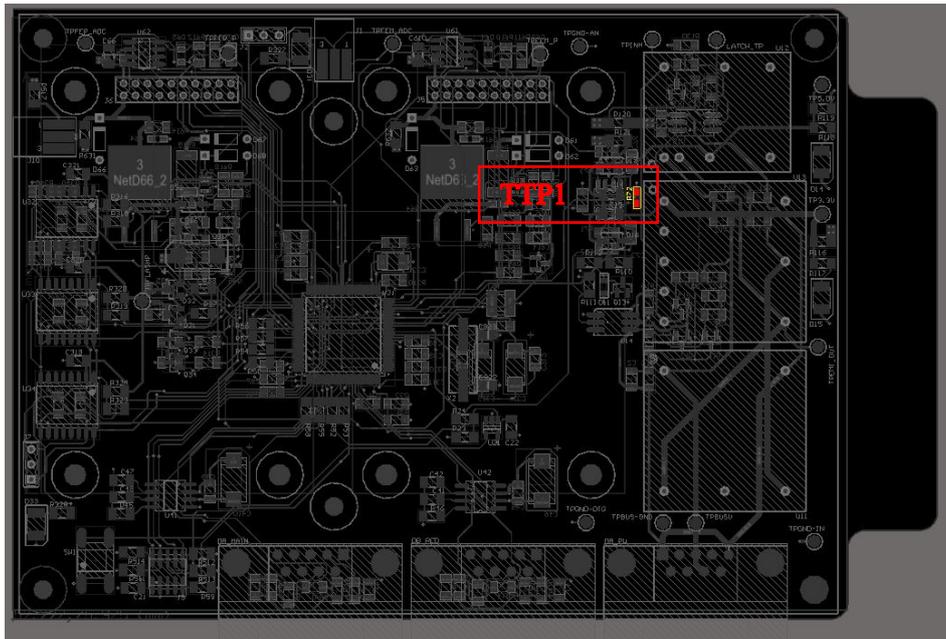
Figure 85: GPS Payload Thermal Test Point #1
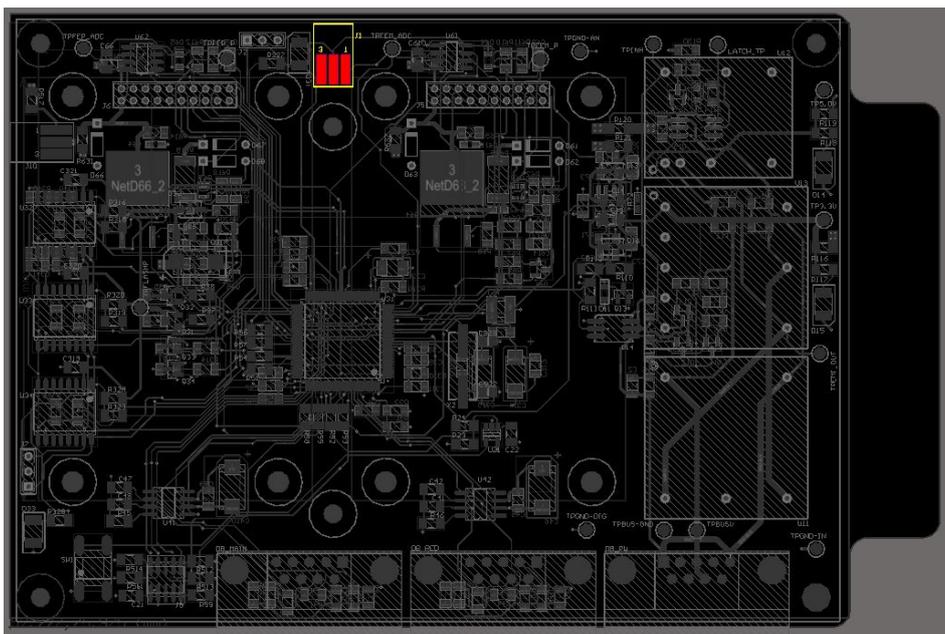
Figure 86: GPS Payload Thermal Test Point #2

The specific test performed is called "thermal balance test" and is meant to demonstrate the system capability to work safely at the operating temperature boundaries. Details of the test setting are included in Table 18.

Table 18 : Thermal balance test technical details

Requirement	Value
Maximum temperature	+70°C
Minimum temperature	-25°C
Maximum temperature variation slope (heating)	<20°/min
Maximum temperature variation slope (heating)	2/3 °/min
Pressure	<10^{-5} mbar
Maximum pressure variation slope	50 mbar/s
T_E	2h
T_R	2h
Stabilization criteria	1 °C/h
The temperature levels include the +/- 5°C margin	

The payload was first placed inside the test chamber, connected to external power and data cables, and then stabilized at -25 °C (Figure 87, Figure 89 and Figure 90)

Figure 87: Payload setting inside the thermal chamber

Figure 88: Payload wiring
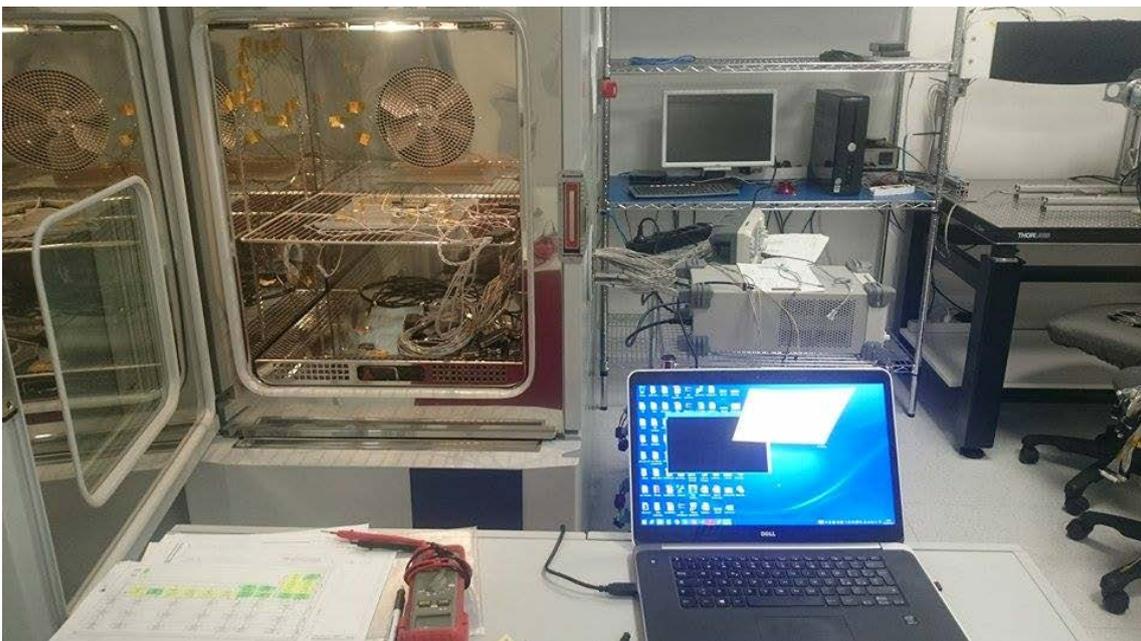
Figure 89: Payload wiring to external instruments

Figure 90: -25° test setting

Once that the thermal chamber was stabilized at the target temperature, the Payload was turned on and the procedure already used for electrical and functional tests, as described in Section 4.6.1 and Section 4.6.4, was repeated and the hardware behaviour was monitored for several minutes. Using the external connections, electrical verifications were possible thanks to the external power supply and digital oscilloscope (Figure 91). After the electrical test, Payload functional verification was performed using the laptop to send and receive commands and logs. Since during the test there was no possibility to provide an RF interface to a GPS antenna through the thermal chamber connections and since the thermal chamber is placed inside the SITAEL clean room, the functional tests performed during the thermal verifications did not provide log with signal-related data (pseudorange and carrier phase), so only the reduced version of the in-mission performances was assessed. However the results provided indications of correct functionality of the front end under extreme thermal conditions and the tested logs were received with correct timing and expected content.

Figure 91: External electrical verification equipment

For sake of brevity only the "HWMONITOR" log is reported herein, which provides the temperature detected by the front end embedded sensors (Figure 92).

```
<HWMONITOR COM1 0 91.0 UNKNOWN 0 870.000 004c0000 52db 12996
<    22
<      -24.000000000 100
<      0.000000000 200
<      0.000000000 305
<      -3.540204567e-38 405
<      -3.540239319e-38 505
<      -1.893644119e-38 605
<      -3.540240440e-38 705
<      -3.540239319e-38 805
<      0.000000000 905
<      0.000000000 a05
<      0.000000000 b05
<      -3.540225867e-38 c05
<      -3.540216898e-38 d05
<      0.000000000 e05
<      0.000000000 f05
<      -6.020907320e-37 1005
<      0.000000000 1105
<      0.000000000 1205
<      0.000000000 1305
<      0.000000000 1405
<      -3.540255014e-38 1505
<      -3.540226988e-38 1605
[COM1]
```

Figure 92: HWMONITOR log with temperature indication on the front end during -25° test

After the payload electrical and functional behaviour assessment for the "cold scenario", the thermal chamber was set to +70 °C, and the same verification procedure was repeated with the new external temperature condition (Figure 93).

Figure 93: 70° test setting

The front end functional test, performed inside the thermal chamber during the 70° scenario validation, provided coherent and correct results for all mission logs, even if with a reduced operational conditions due to the lack of GPS signal through the antenna connector. For sake of brevity only the "HWMONITOR" log is reported herein, which provides the temperature detected by the front end embedded sensors (Figure 94).

```
<HWMONITOR COM1 0 91.0 UNKNOWN 0 270.000 004c0000 52db 12996
<    22
<    71.000000000 100
<    0.000000000 200
<    0.000000000 305
<    -3.540204567e-38 405
<    -3.540239319e-38 505
<    -1.893644119e-38 605
<    -3.540240440e-38 705
<    -3.540239319e-38 805
<    0.000000000 905
<    0.000000000 a05
<    0.000000000 b05
<    -3.540225867e-38 c05
<    -3.540216898e-38 d05
<    0.000000000 e05
<    0.000000000 f05
<    -6.020907320e-37 1005
<    0.000000000 1105
<    0.000000000 1205
<    0.000000000 1305
<    0.000000000 1405
<    -3.540255014e-38 1505
<    -3.540226988e-38 1605
[COM1]
```

Figure 94: HWMONITOR log with temperature indication on the front end during 70° test

The results of the electrical verifications, performed during the two thermal test sessions inside the chamber, did not provide any evidence of severe degradation of the unit under test and the deviation of the electrical performances under the two extreme thermal conditions is within acceptable limits for the compliancy with technical requirements (Table 19).

Table 19: Power consumption measurements under extreme thermal conditions

Vin	Current (-25°)	Current (+70°)	Power (-25°)	Power (+70°)
18.0 V (Nav PC + Ampl + FE)	0.151 A	0.147 A	2.718 W	2.646 W
25.2 V (Nav PC + Ampl + FE)	0.111 A	0.114 A	2.797 W	2.873 W

The output voltage of the voltage regulation stage was also measured with the oscilloscope, along with voltage ripple (Table 20).

Table 20: Voltage and ripple measurements under extreme thermal conditions

Vin	3.3V (-25°)	3.3V (+70°)	5V (-25°)	5V (+70°)
Output Voltage (18.0 V)	3.34V	3.33V	5.05V	5.11V
Output Voltage (25.2 V)	3.33V	3.32V	5.05V	5.10V
Ripple Std (18.0 V)	0.044V	0.045V	0.041V	0.046V
Ripple Std (25.2 V)	0.043V	0.043V	0.046V	0.046V

In addition, the testing of the overvoltage protection circuit and current limiter circuit was performed, providing successful results and ensuring the high protection and reliability levels indicated in the technical requirements also under extreme external temperature conditions.

A final cycle of electrical and functional test was performed after the conclusion of the thermal balance test, outside of the chamber, to assess not only the absence of performance degradation under extreme conditions, but also that there were no consequences on the hardware after some minutes from the application of the high temperatures. In particular, functional test was performed using the GPS antenna in order to ensure also the correct operations of the radio-frequency part of the payload. These two type of verifications, followed the procedure presented in Section 4.6.1 and Section 4.6.4. For sake of brevity the results of the entire electrical and functional tests performed during and after the thermal verification is not reported in this document, but was included in dedicated test report submitted for review to ESA. However, the results demonstrated that the extreme external temperature conditions did not affect the performance of the payload, since no critical degradations were detected from the mission logs message and the electrical measurements were consistent with expectations and compliant with the technical requirements.

4.6.6   Vibration test

The second of the environmental tests performed on the EBB models is the vibration test and is a typical step of the validation of instruments for space applications. The reason of this test is related to the fact that every equipment integrated inside a spacecraft, shall resist, even if for a few minutes, to the dynamic loads transmitted by the rocket to the spacecraft during the launch. For this reason, the payload enclosure was designed in order to maintain the payload internal and external integrity during the launch, considering also the presence of internal wiring inside the enclosure. This test was intended to validate the mechanical design and FEM analysis by simulating the vibration environment using electrodynamic shakers. Two types of verifications were performed on the payload in each direction of the three orthogonal axes: high level sine vibration and random vibration environment. GPS Payload was assembled in flight configurations, completed with all mechanical parts. Test set up and shaker configuration was carried out by SITAEL operators at their facility in Mola di Bari, Italy and the results were provided to the University of Bologna to examine possible design actions [29]. Testing on Z axis and on the plane X-Y axes were performed separately with the support of the two different instruments, available at SITAEL centre in Mola di Bari, both of TIRA vibration test systems family. Before starting the vibration test, the GPS payload was fixed to the interface plate with the shaker and three accelerometers were applied in several points of the external enclosure to collect accelerations data (Figure 95 and).
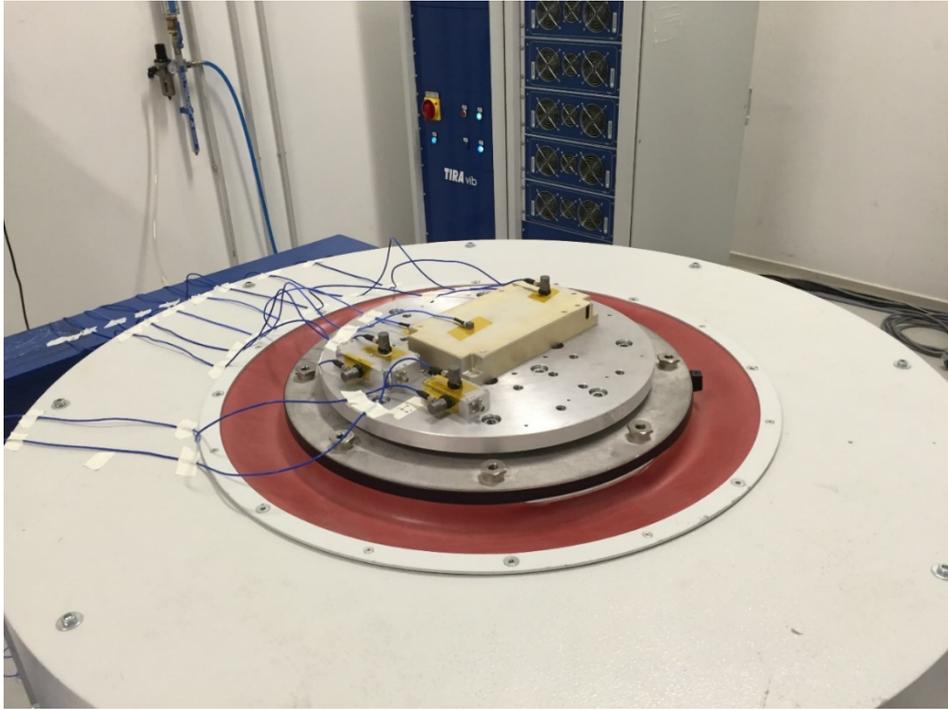
Figure 95: GPS Payload set up for Z axis loads #1
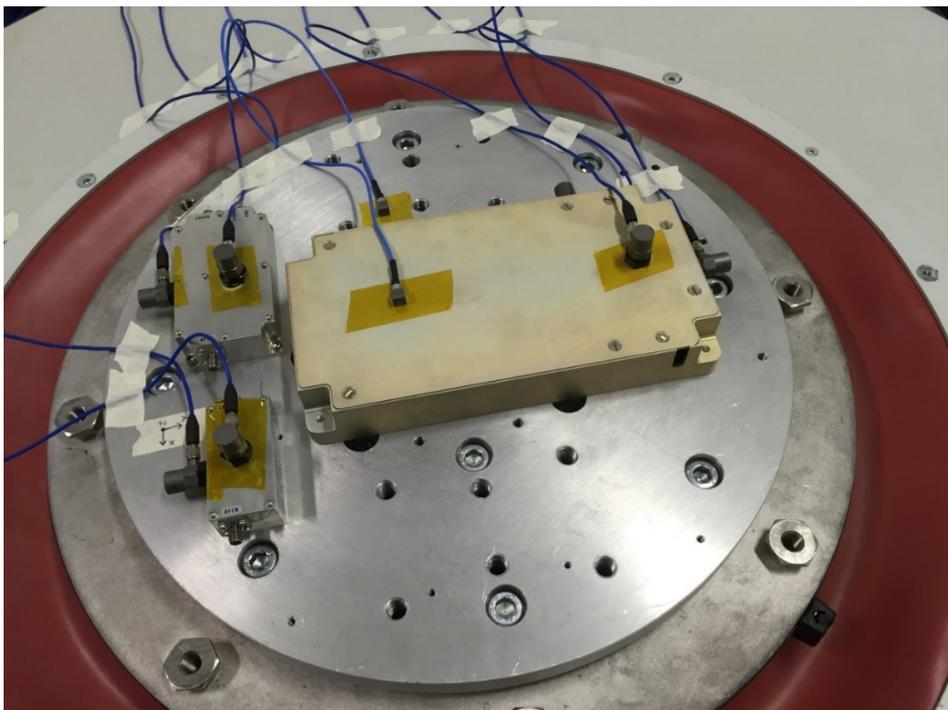
Figure 96: GPS Payload set up for Z axis loads #2

After test sessions on z axis were completed, the same set up procedure was repeated to fix the payload to the second shaker to perform validation along X and Y axes (Figure 97 and Figure 98).
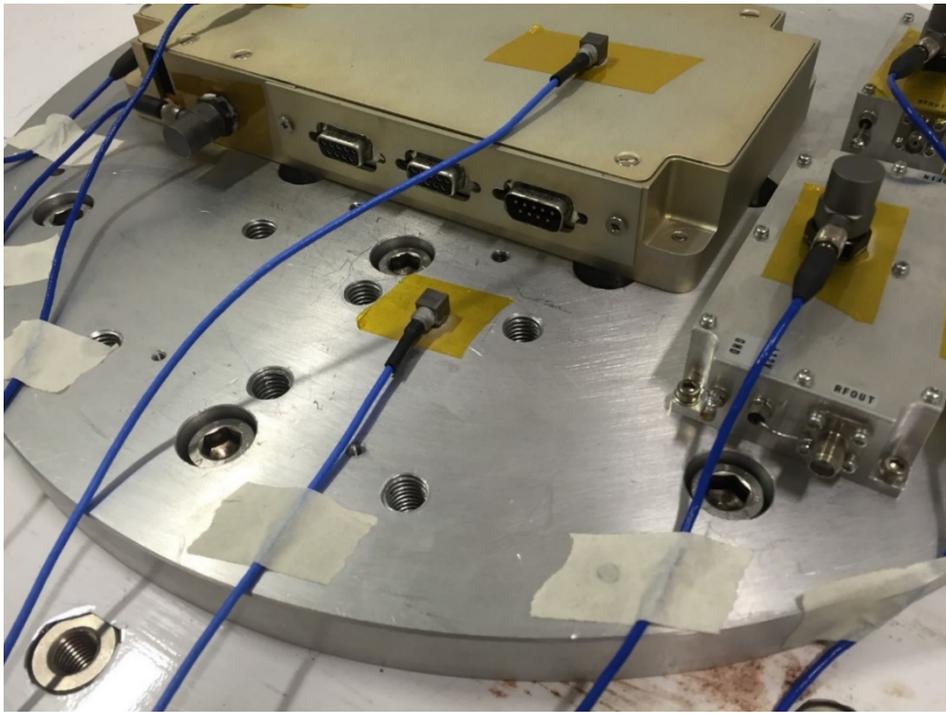
Figure 97: GPS Payload set up for X-Y axis loads #1
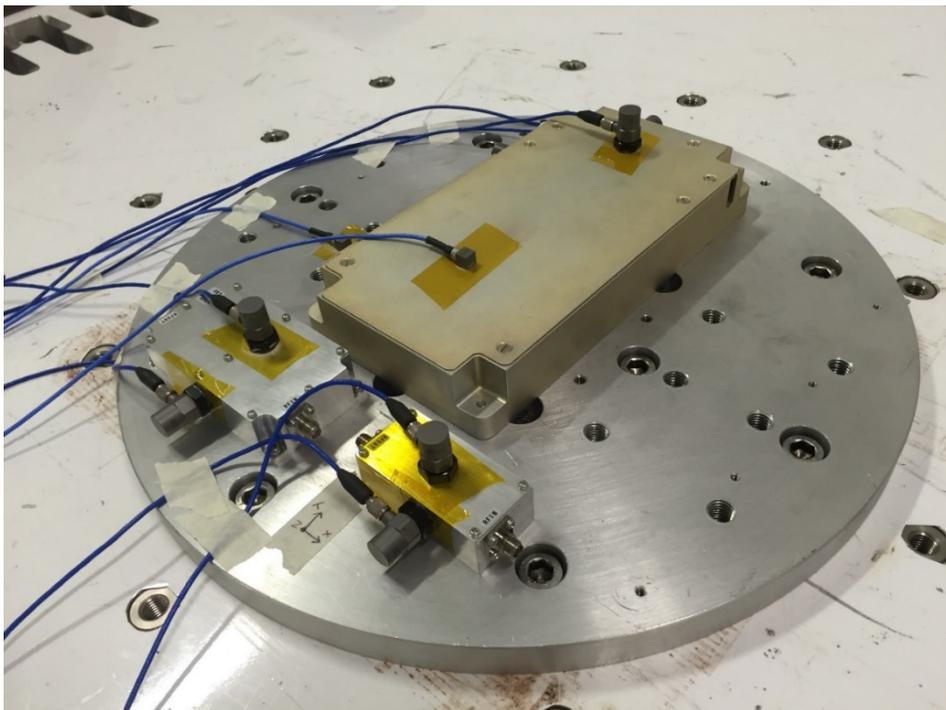
Figure 98: GPS Payload set up for X-Y axis loads #2

Before and after each test, resonance frequency shift inspection was carried out to ensure that no severe internal modifications happened after the application of the dynamic loads. In fact, if an internal loss of rigidity due to cracks or fixing loosening happens during the application of dynamic loads, that can lead to potential catastrophic failures, it can be detected from the analysis of the natural frequencies of the payload. Absence of marked frequency shift in the first four resonance frequencies is generally considered a successful result.

Z-axis test

During resonance search sessions described in Table 21, no marked frequency shift or related amplification variations were detected. The only notable event was represented by an additional frequency found at the end of the test, as result of decoupling of two eigenfrequency on the top of the GPS case. Despite the presence of this phenomenon, the frequency results were compliant with the requirements and the accurate visual inspection carried out after the test did not provide any evidence of deformation or damaging of the plate. A reasonable justification to the problem can be related to the possible untightening of the internal boards interface with the support columns. After the conclusion of the vibration tests, the device electrical and functional behavior was assessed following the procedures described in Sections 4.6.1 and 4.6.3, in order to verify if the decoupling of the natural frequencies resulted in a degradation of the mission-critical parameters. Since no deviation from nominal functionality was detected, the possible decoupling of the natural frequency detected during the test will not affect the correct operations of the Payload.

Table 21: Resonance search results – Y axis

Eigenfrequencies [Hz]	Test results – Resonance search				
	I	II	-	III	IV
Resonance search /1	388.2	724	-	962.5	1342
Resonance search /2	388.2	715.4	-	968.3	1342
Resonance search /3	403.6	713.3	877.1	1010	1347
Overall shift	+3.9%	-1.5%	-	+4.9%	+0.37%

X-axis test

During resonance search sessions described in Table 22, no marked frequency shift was found on the first resonance frequencies and related system amplifications.

Table 22: Resonance search results – X axis

Test results – Resonance search			
Eigenfrequencies [Hz]	I	II	III
Resonance search /1	1347	1583	1889
Resonance search /2	1351	1583	1889
Resonance search /3	1347	1500	1884
Overall shift	-	-5.2%	+0.26%

Y-axis test

During resonance search sessions described in Table 23, no marked frequency shift was found on the first resonance frequencies and related system amplifications.

Table 23: Resonance search results – Y axis

Eigenfrequencies [Hz]	Test results – Resonance search			
	I	II		III
Resonance search /1	874.5	1363	1583	1906
Resonance search /2	874.5	1367	1583	1906
Resonance search /3	866.7	1347	1583	1889
Overall shift	-0.89%	-1.2%	-	-0.37%

After the vibration test, once that the payload was brought back to the University of Bologna facilities for the final assessment, a series of electrical and functional tests was performed again on the payload, following the procedures described in Section 4.6.1 and Section 4.6.4. This final validation phase was meant to assess integrity of all hardware parts and wiring, though the comparison of electrical measurements with expected values and by interrogating the COTS front-ends with the mission set of logs and commands. Electrical verifications provided satisfactory results, providing measures compatible with technical requirements, demonstrating that the dynamic loads experienced during the vibration test did not affect overall payload functionality. The final visual inspection and the functional checks assessed that the payload successfully passed the vibration test. For sake of brevity the entire electrical and functional test results description is not reported in this document, but was included in dedicated test report submitted for review to ESA.

5 APPLICATION SOFTWARE DEVELOPMENT AND VALIDATION

The development of the application software represented a critical and extensive part of the GPS Payload project. Clearly the final output required to the application software is an estimation of the ESEO satellite position; however, to achieve this goal, several other aspects were covered, related to the interface with COTS components, i.e. the Novatel front-end. Furthermore, since this navigation sub-system will be operative on-board of a spacecraft, to allow all data produced on-board to be available to the users (other sub-systems and ground operators or scientists), other accessory code parts are necessary to manage external communication. According to the sub-system level technical requirements, the application software, hosted by the Navigation computer microprocessor, shall be able to perform the following tasks [16]:

- Payload hardware and software status monitoring

- Communication with COTS front-end and data extrapolation

- Position determination using navigation algorithms

- Handling of raw and processed data produced on-board, in order to make them available to other sub-systems and to ground users

5.1 Software development

The application software development covered the final part of the GPS Payload design process and started during the last phase of the hardware test campaign. The embedded code was written using the EBB models as HW support, to test it step-by-step during the development. The GPS Payload software was written in four stages:

1. Preliminary software with reduced operations, including only data acquisition implementation. This prototype was used during the hardware test campaign, to test correct hardware implementation of communication interfaces between the navigation computer and the COTS front-end. Its flow chart is displayed in Figure 83.

2. First prototype of the complete software. It included a draft version of all software main components, covering all software tasks from data acquisition to real-time processing.

3. Second prototype of the code, implementing a cleaned and advanced version of all previous modules and all necessary code parts to manage telecommands, housekeeping data and scientific data.

4. Flight version of the code: this is the final software, that was optimized for the mission, removing all software parts included in previous versions only for testing purposes.

The first prototype of the complete software was developed in C language, using the IAR Embedded Workbench, which provided straightforward debugging interface and memory management (Figure 99). This IAR development environment was considered ideal for the first stages of the application software development, allowing for a better insight and control of the hardware resources and to perform easier and faster debugging sessions of the software core components.
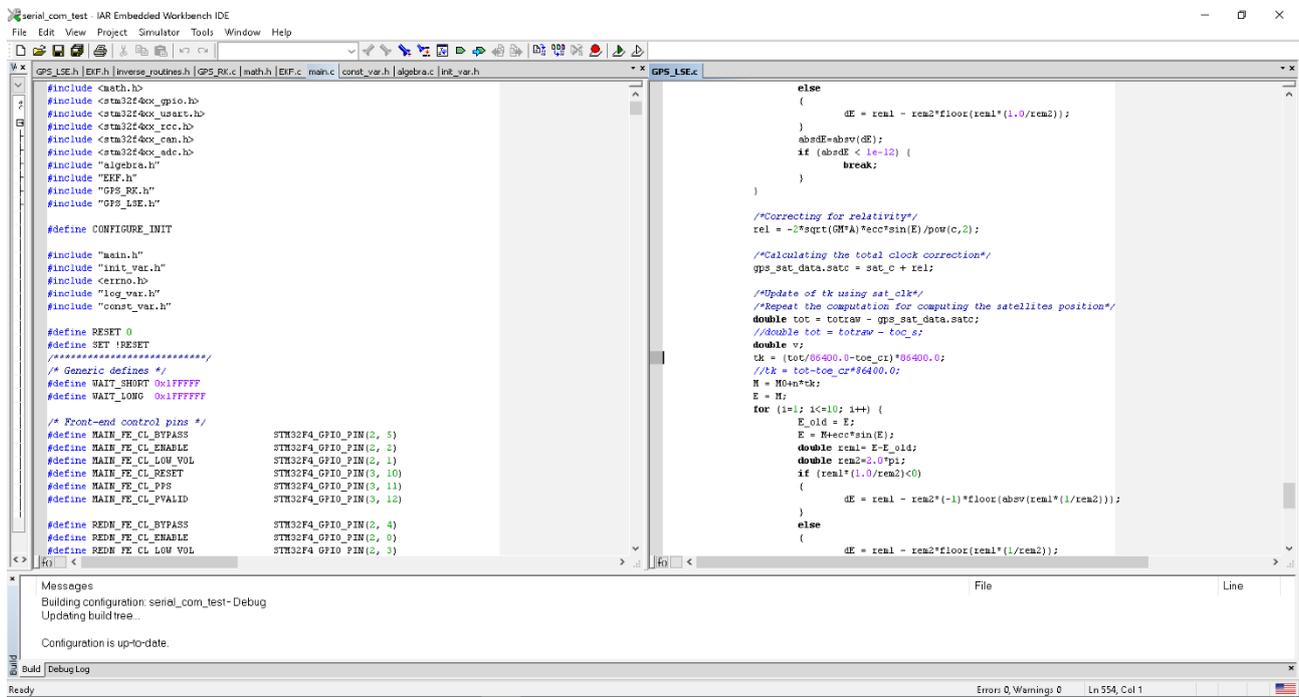
Figure 99: IAR Embedded Workbench

To develop the second prototype and the flight version of the software, the previous code was ported and adapted to RTEMS (Real-Time Executive for Multiprocessor Systems), an open source real-time operating system for embedded applications. This operating system was already implemented on-board of the other platform sub-systems of the ESEO spacecraft and was strongly recommended by the prime contractor company SITAEL, to facilitate software integration and interfacing between subsystems, and for payloads testing purpose during technical reviews. Furthermore, it allowed to implement the same drivers for CAN communication and other Board Support Packages (BSP) related to the management of components or parts of integrated circuits that are common to all subsystems and were developed and shared by the prime contractor company. This choice helped SITAEL achieving product assurance goals, by standardizing the low-level software packages for the sub-systems. Due to the different software packages available for RTEMS to handle the peripherals operations, the porting of the software meant a rewriting of several parts of the code, like microprocessor initialization and the communication ports handling. This second version of the software was coded and debugged using the Eclipse development environment, that allowed a constant connection to SITAEL online software resources database, available for the ESEO mission, in order to download updated versions of BSPs and to save the last versions of the GPS Payload application software (Figure 100).

105

During the development of the final software version, data management routines were also reviewed and expanded to include the complete set of data logs, required by the navigation computer. The second prototype of the application software was the one used to perform the software validation sessions to test correct real-time functionality and assess the positioning performance.
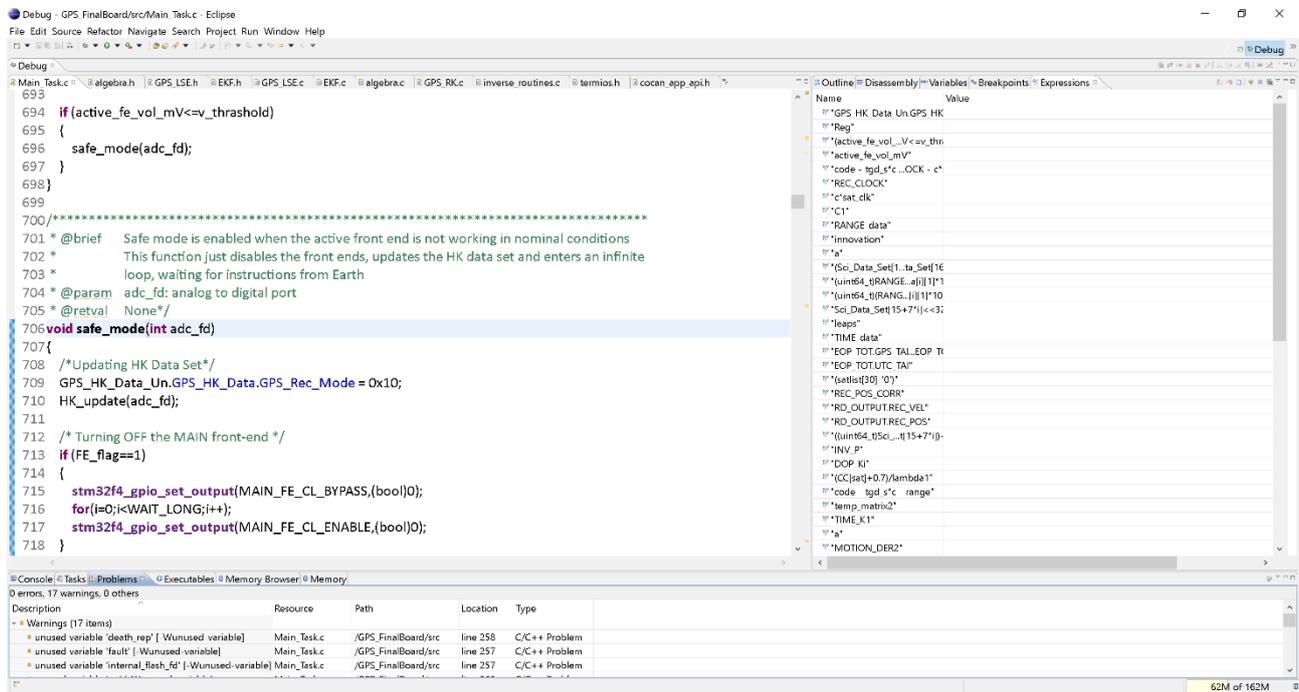
Figure 100: Eclipse development environment

5.1.1 Application software architecture

To perform all the tasks defined by technical requirements, the application software was designed to implement five main operational modes [Figure 101]:

- Initialization sequence: this software section is executed right after the receiver activation or watchdog reset and performs setting of main front-end functionalities, like registers and communication, followed by a series of hardware verifications, including CPU, memory verification and CAN controller.

- Front-ends power on and verification: this software component is activated after successful initialization or every time that the main functionalities are restored, after the trigger of the safe mode. This software state turns-on the front-end marked as active, waits for front-end initialization and verifies the corrects communication. It then configures the front-end to provide the requested log outputs and checks for front-end clock convergence. If the procedure fails, the application software enters the safe mode.

- Safe mode: this mode is activated in case of front-end failure, either functional or related to current limiter trigger. The front-end marked as active is turned-off. Software checks the number of front-end

106

fails and the time elapsed since the last safe mode activation. It then decides whether to turn-on again the same front-end or to switch to the redundant one.

- Kinematic positioning: it is the simplest navigation algorithm, a direct computation of the receiver position from the raw GPS observables, without filtering them using a dynamic model. The attainable accuracy is expected to be between 10-15 m 3D rms. If the active front-end works properly, the software starts generating position fixes in kinematic mode every 30 seconds and records the navigation mode outputs and raw observations history. Upon CAN request, the software provides a data pack including the last position and clock fixes and the last raw observations set.

- Reduced dynamic positioning: this algorithm is based on the integration of the raw observations with an accurate orbit model. According to the complexity of the orbit model and the selected observations combination, available studies in the literature suggest an expected accuracy of about 1m 3D rms [8]. This algorithm is activated with an external telecommand, switching from the default kinematic mode. It still produces position fixes every 30 seconds, but with a more sophisticated filter that provides a higher accuracy.
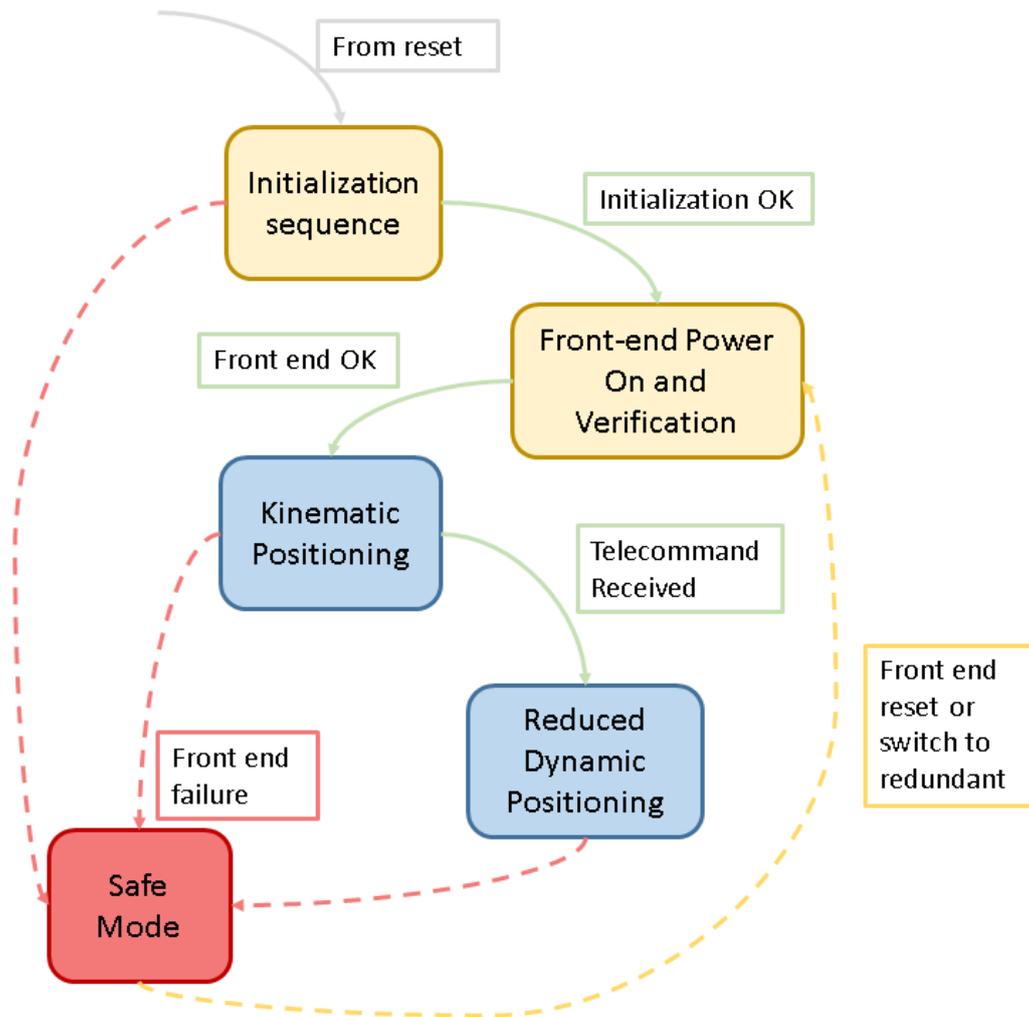
Figure 101 : Application software state machine

To provide a better insight of the software, another possible components classification is possible, related to the code packages, grouped by task affinity. This classification is presented below and is used to describe the software in details, highlighting also service code packages that are included and executed as part of different software states. In fact, many software sub-components are common to several modes, while others may be partially included in some main components but are thematically uncorrelated.

5.1.2   Initialization sequence

The navigation computer initialization sequence includes the first code instructions that are executed after every power on of the GPS Payload (Figure 102). This code component is in charge of:

- Configuration of on-chip registers

- Internal and external communication interfaces setting

- Verification of the various microcontroller peripherals, including CPU/FPU functionalities, interrupts, CAN controllers and external flash memory read/write.

Internal serial communication ports are initialized: considering that each of the two COTS front-ends implements two USART interfaces, one is configured as main, based on default instructions, and remains active until an error occurs. All USART port are initialized with 8 bit words, baudrate of 9600 bps and no stop bit. A fifth USART port, available on the navigation computer microprocessor, is also set to provide serial communication interface with an external terminal or laptop, for visual inspection of data management and processing during the runtime, to be used for debug and testing purpose. This additional USART port is set to communicate with baudrate of 115200 bps, and was excluded from the final version of the code, since the flight version of the software will not implement external serial communication and the related connector was removed from the flight model of the GPS Payload hardware.

For what concerns the external communication with other subsystems, CAN interfaces were implemented, that represents the main data bus of the ESEO platform. The decision behind the use of this communication protocol, that is typical of automotive and industrial sectors, resides inside its high reliability, mainly related to a reduced number of wires involved, that makes it particularly adapt for applications designed to operate in harsh environment, such as space applications. Furthermore, a reduction of wires means also lower mass and costs, that are driving factors of this project. Reliability of the communication between the GPS Payload and the OBDH, is improved by the heartbeat control. This functionality is enabled with the dedicated instruction inside the initialization sequence and allows to automatically provide the GPS Payload communication status with regular time intervals. In case of communication failure with GPS Payload, OBDH will switch to the redundant CAN bus to interface with the device affected by communication problems. Note that the GPS Payload will act as passive device (slave) on the CAN bus. This means that the payload will communicate through CAN ports only when explicit request or interrogation is received from the ESEO platform OBDH (master). The possible external interactions are reduced to a limited set of tasks:

- Reception of predetermined set telecommands

- Transmission of housekeeping data

- Transmission of scientific data

Initialization sequence ends with the update of the housekeeping data set, communicating that the initialization procedure is completed. Application software then proceeds with the execution of the front-end initialization phase and the main navigation tasks.
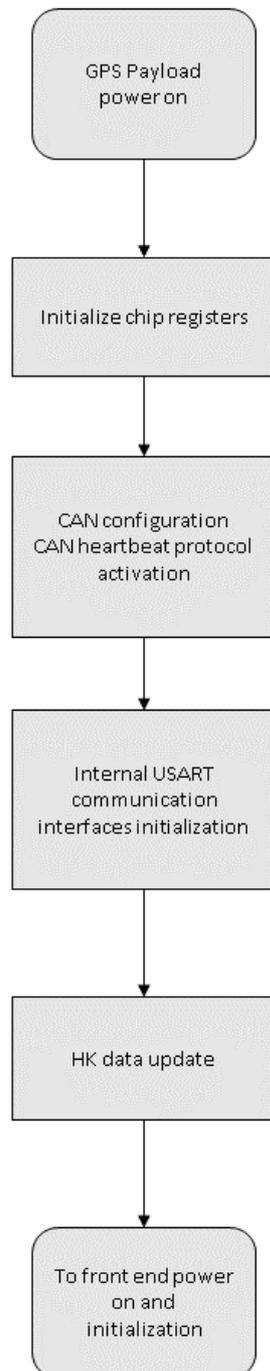
Figure 102: Initialization sequence flow chart

5.1.3 Front-end power on and verification

If the initialization routine is successfully executed, the application software first task is the management of the two front-ends activation and monitoring (Figure 103). This software section turns on the front-end marked as "active", after checking the content of the telecommands set: in fact, after power on, by default one of the two front-ends is selected as "main", but in case of different instructions provided through telecommands from ground, the redundant front-end is activated instead. Front-end initialization software component then checks COTS device current absorption and communication interfaces. If the current is below a fixed threshold and the communication is working properly, software configures the front-end for the mission with the desired parameters. Front-end clock convergence is constantly inspected until it indicates that a complete GPS link was established with at least four satellites. In fact, after the acquisition of the first GPS satellite, the front-end automatically corrects its internal clock to match the GPS time. During this operation, the raw observations may experience large jumps in their values due to the large error of the receiver clock. For this reason, the receiver waits for this correction before executing the orbit determination algorithm, to avoid large error in the position computation. According to the device firmware manual, the most common "clock words" that can be obtained are included in Table 24 and can be found in the header of every log.

Table 24: Clock words managed by application software

UNKNOWN	No information about internal clock offset with respect to GPS time. This is the standard clock message after power on, when no satellite is tracked.
COARSE	It means that the receiver time is valid, but the precision is coarse, because less than 4 GPS satellites are tracked.
FREEWHEELING	It means that for some reasons position is lost and the range bias cannot be calculated. This translates in the need of a reset action to the active front-end.
FINE	Time is valid and fine. It means that at least 4 GPS satellites signal is obtained

This software mode can be accessed also from other points of the code, namely every time that an internal or external warning indicates the need to switch the active front-end. The last part of this code section includes the setting of mission logs, right before entering the main loop and the navigation modes. It sends to the active front-end the following strings (see reference Table 17):

- "*log rangea ontime 30*": requests RANGE log with constant time interval of 30 seconds

- "*log timea ontime 30*": requests TIME log with constant time interval of 30 seconds

- "*log rxstatusa ontime 30*": requests e RXSTATUS log with constant time interval of 30 seconds

- "*log hwmonitora ontime 30*": requests HWMONITOR log with constant time interval of 30 seconds

- "*log gpsephemaa onchanged*": requests GPSEPHEM every time that the updated ephemeris of a GPS satellite are available
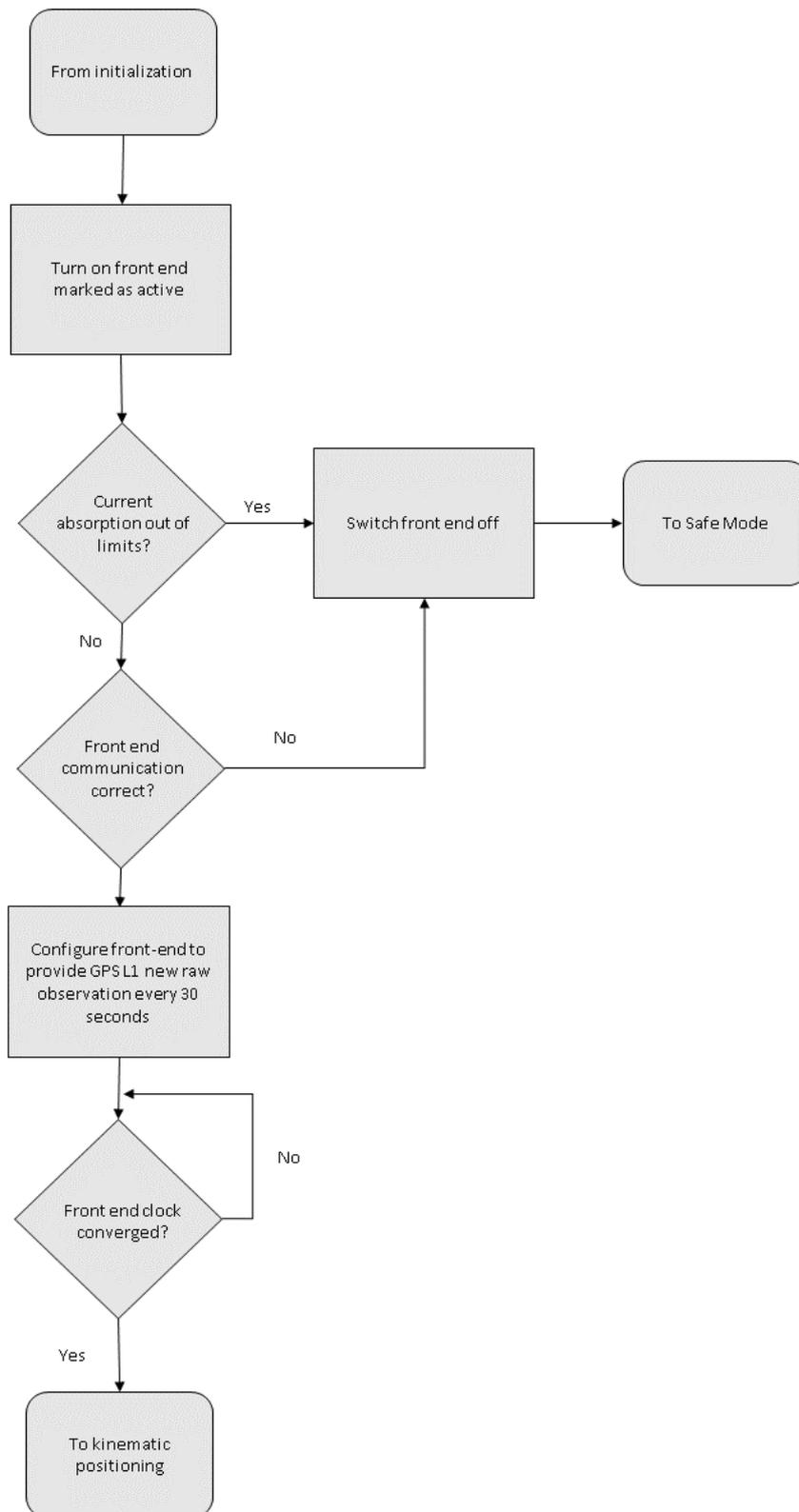
Figure 103: Front- end power on and verification flow chart

The main and most important part of the *front_end_init* function is the *GPS_init_routine* code: it implements the algorithm of forced setting, which is necessary to allow the active front-end to gain GPS link after power on. As demonstrated in Section 4.6.3, COTS front-end channels shall be set to scan GPS signal with and extended range of frequency offset. Considering that no information about PRN in the field of view or Doppler are available on-board in advance, before the beginning of the front-end initialization, the acquisition routine starts assigning PRN to each channel in numerical order. Since the maximum settable frequency margin is 10 kHz and considering that the possible frequency range of the incoming signal, due to the Doppler effect, is -45kHz/+45kHz, for every tracked PRN the entire range was scanned by varying the frequency offset of 10kHz every interval of 30 seconds. Considering a fixed value of 10kHz of frequency margin, different offset values are set from 0kHz to +40kHz and then from 0kHz to -40kHz. As it is possible to see from Figure 104, with this technique every receiver channel can cover every 20 seconds a range of 20kHz, with half of the range overlapped with the previous range. The entire possible range of frequencies can be scanned in 4 minutes and 30 seconds.
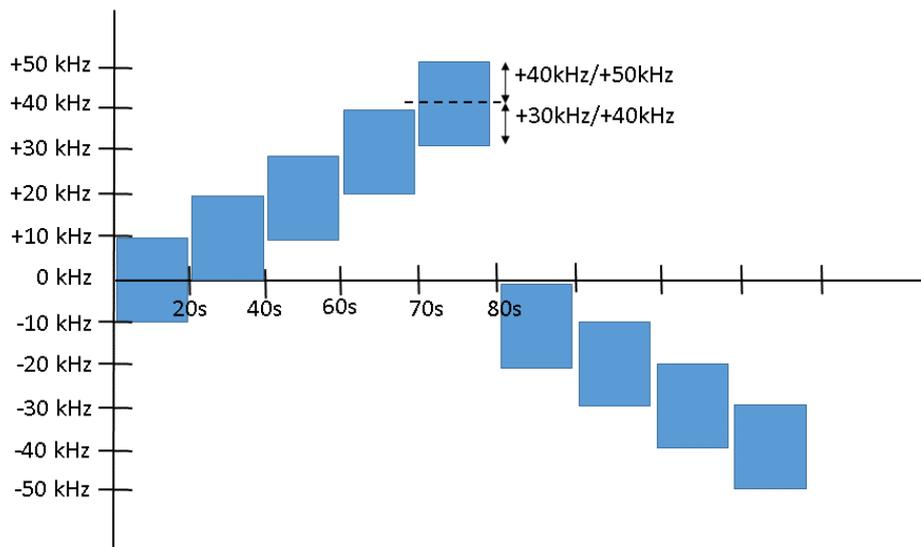
Figure 104: Frequency range scan

To check the channel tracking status, a trackstat log request is sent before starting the routine. Log is requested to provide tracking message every 30 seconds, so that it provides also timing reference to perform checking of the channel status. Every time that a trackstat log is received, every channel tracking word is checked to verify if the link with the PRN is established. For every channel, the frequency error value is modified every 30 seconds. If the channel will not find any PRN signal in the complete frequency range scanning interval, it is set to look for another PRN, starting again from 0kHz. The effectiveness of this method was assessed during the software testing sessions and the results are reported in Section 5.2. Figure 105 shows the flow chart of the channel setting routine. If the front-end initialization is executed correctly and no failure is detected, the software automatically enables the Kinematic Navigation Mode.
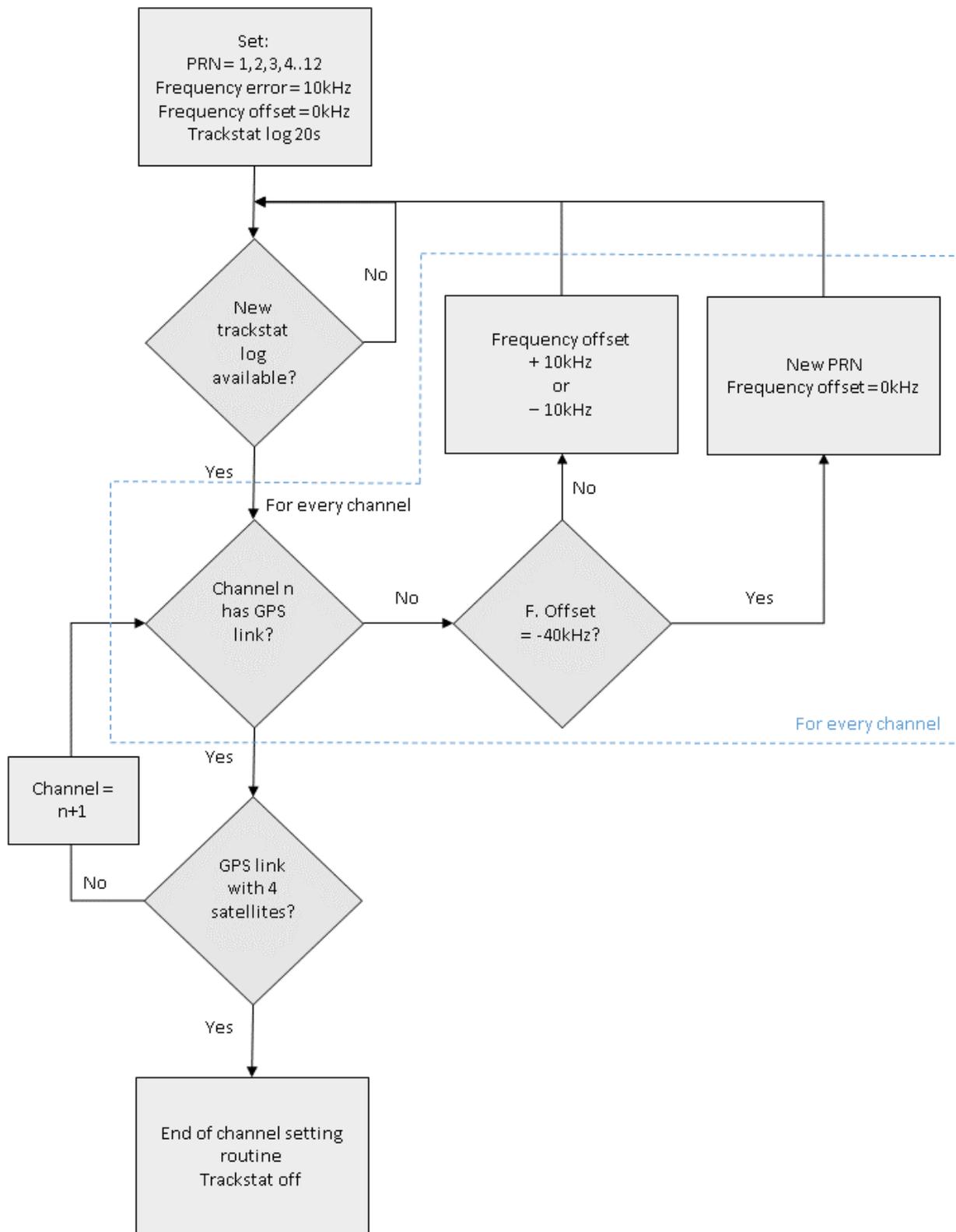
Figure 105: Channel setting routine flow chart

5.1.4 Data acquisition

The data acquisition software component includes all instructions that are necessary to manage COTS front-end data handling. It is in charge to analyze a received log message, recognize type of log, to extrapolate data, to perform a preliminary processing (where necessary), to arrange values inside dedicated arrays that are provided to the navigation algorithms. It is operative mainly inside the main loop, after the mission logs request are already sent to the Novatel component, but it is partially used also during the front-end acquisition routine, to handle the trackstat log. The core of this software component is the *log_analysis* routine, which inspects the received log message header to identify the log name. It then addresses the subsequent message to the dedicated sub component and their outputs are distributed to several other software components to perform the different ASW tasks:

- *trackstat_analysis*: extracts tracking status word for every channel involved acquisition phase and provides it back to the *GPS_init* routine that will decide whether or not to change channel settings.

- *time_analysis*: extracts UTC time and receiver clock error and provides them to the active navigation algorithm to process the ESEO position.

- *range_analysis*: extracts UTC time and receiver clock error and provides them to the active navigation algorithm to process the ESEO position.

- *gpsephem_analysis*: extracts UTC time and receiver clock error and provides them to the active navigation algorithm to process the ESEO position.

- *rxstatus_analysis*: extracts the error status word and the receiver status word and provides them to the *GPS_HK* software component, in charge to handle the housekeeping data collection.

- *hwmonitor_analysis*: extracts the COTS front-end temperature and provides it to the *GPS_HK* software component, in charge to handle the housekeeping data collection.

Figure 106 provides a rapid graphical idea of the relation between data acquisition component and the rest of the application software.
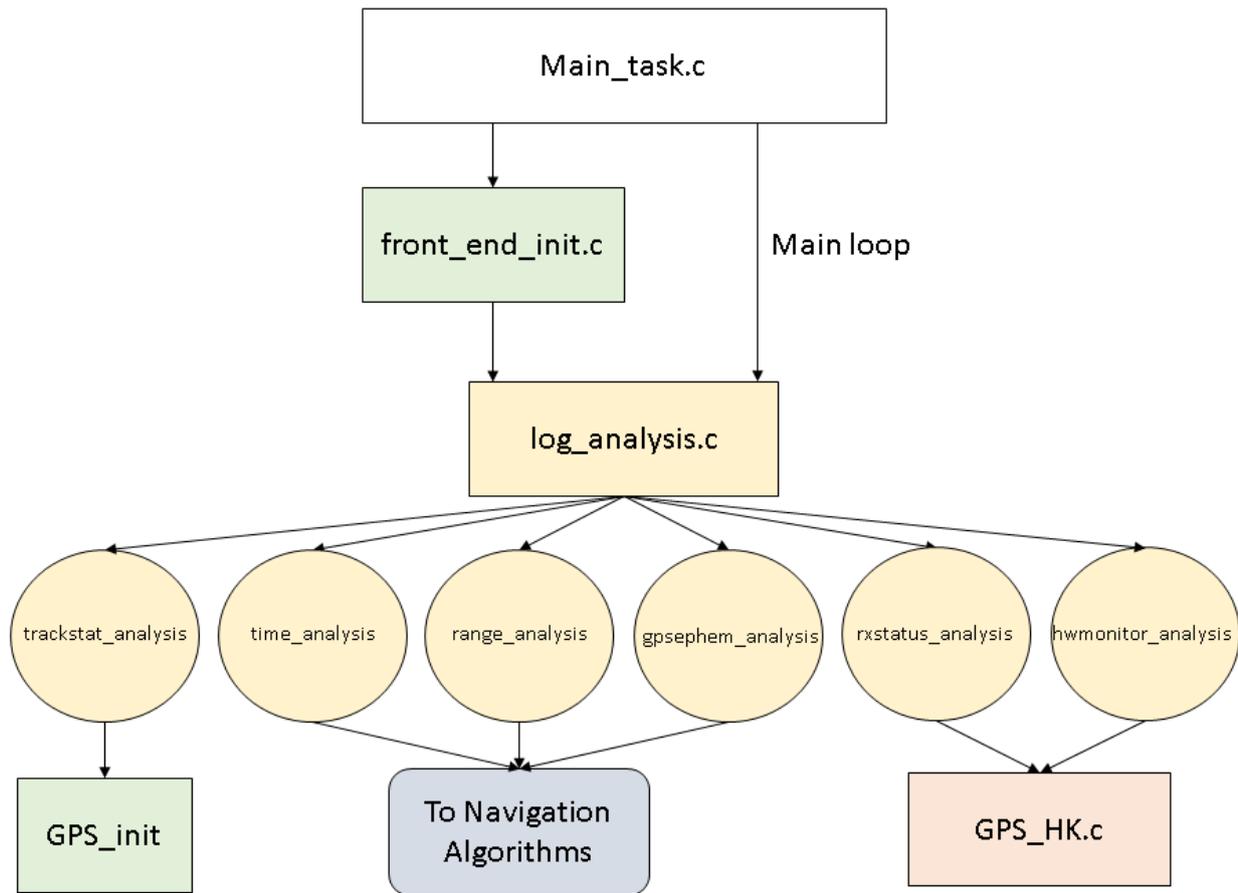
Figure 106: Data acquisition component interface with other software parts

As already mentioned before, for the ESEO mission a conservative time interval of 30 seconds between two consecutive epochs is set, in order to take in consideration hardware resources and position processing time. This means that every 30 seconds a fresh set of raw GPS observations is processed with one of the on-board algorithms and the satellite position is estimated. To regulate this "discrete" real-time operations the log itself is used: setting the log request timing interval to 30 seconds, the COTS front-end will provide the log with this precise interval, that is interpreted by the navigation computer as the sign to be ready to start a new position processing. This "available log detection" task is performed actively by polling the USART port buffer for available data. While this log detection method can introduce some delay from the actual log reception and the acquisition by the polling cycle, it is reasonably small to not represent an issue for 30 second of interval. As presented in Section 5.1.3, only TIME and RANGE logs are provided in regular intervals, while the GPSEPHEM log is obtained asynchronously with respect to the other logs. This means that it is possible that a new ephemeris set is received while the navigation software has already started position processing, but this is not a threat for the real-time activity, because they will be collected as soon as the processing is complete. However, even if the TIME and RANGE logs are usually provided consecutively, sometimes it is possible that a small random delay is introduced by the COTS front-end between the two messages. For this reason, for each of the two mission logs a flag is introduced and the processing part is enabled only when both flags are

set, meaning that the two logs required for the current epoch are available. At the end of the epoch processing, both flags are reset. Figure 107 shows the flow chart of the data acquisition process.
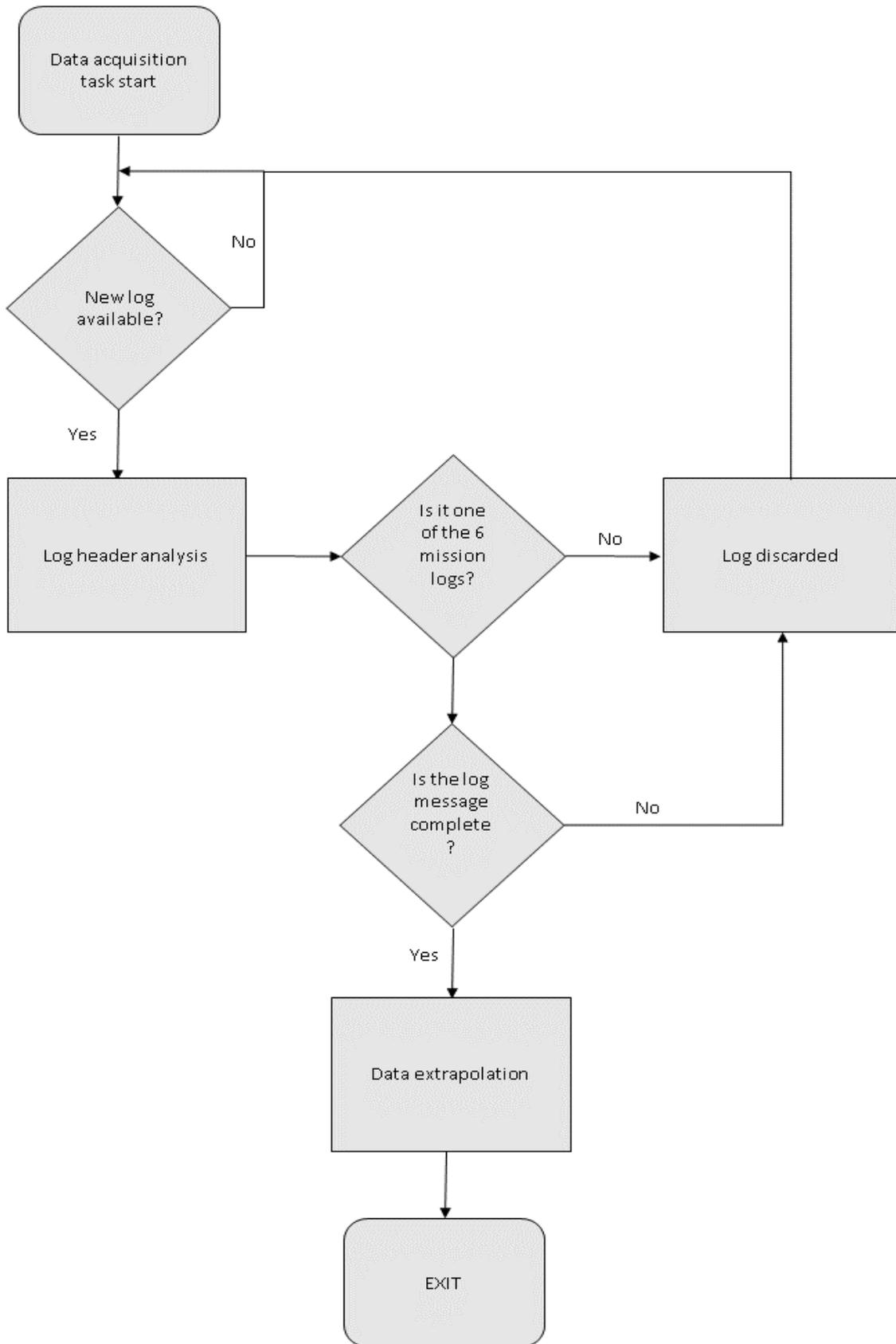
Figure 107: Data Acquisition Flow Chart

5.1.5   Kinematic positioning

The kinematic algorithm is the default navigation mode and implements a simple position estimator, which uses only the raw observations provided by the COTS front-end, without including in the estimation any a-priori information about the spacecraft trajectory. It is enabled after the navigation computer and front-end initialization, once a stable link with at least 4 GPS satellites is established. The observations, produced by the front-end every 30 seconds, are processed using a least squares minimization to estimate the receiver position and receiver clock offset [2]. The easiest position estimation method is based on the solution of a system of four equations with four unknowns: three coordinates of the receiver position and the clock error. The solution can be computed by using only the pseudorange raw information provided by the Novatel front-end. Pseudorange is a measure of the range between the receiver and a satellite of the GPS constellation, obtained by multiplying the velocity of propagation of the GPS signal, i.e. the speed of light, with the time between transmission and reception of the PRN code. The receiver computes this time by correlating the received code and a replica of the same code generated internally. However, this measurement is affected by clocks delays, related to the fact that the receiver and the transmitter clocks are not synchronized and that both present and offset with respect to the GPS system reference time. Since the GPS satellites clock offset information is known and can be obtained from the GPS broadcasted message, pseudorange ρ measurements can be expressed as functions of the receiver position and clock accuracy:

$$\rho = f(x_u, y_u, z_u, t_u) = r + e_c$$

where r is the distance between the receiver and a generic GPS satellite and e_c is the receiver clock error. Using the pseudorange provided by 4 different GPS satellites the following set of equations is obtained:

$$\rho_1 = \sqrt{(s_{11} - x_u)^2 - (s_{12} - y_u)^2 - (s_{13} - z_u)^2} + ct_u$$

$$\rho_2 = \sqrt{(s_{21} - x_u)^2 - (s_{22} - y_u)^2 - (s_{23} - z_u)^2} + ct_u$$

$$\rho_3 = \sqrt{(s_{31} - x_u)^2 - (s_{32} - y_u)^2 - (s_{33} - z_u)^2} + ct_u$$

$$\rho_4 = \sqrt{(s_{41} - x_u)^2 - (s_{42} - y_u)^2 - (s_{43} - z_u)^2} + ct_u$$

where ρ_i is the pseudorange between the i-th satellite and the receiver position, (s_{i1}, s_{i2}, s_{i3}) the i-th satellite position, (x_u, y_u, z_u) is the user position, c is the speed of light and t_u is the delay of the receiver clock. Solving this set of equations, it is easy to obtain the four receiver-related unknowns (u, t_u). Considering that the estimation of the user position clock is different from the real position by a small offset:

$$\Delta x_u = x_u - \hat{x}_u$$

$$\Delta y_u = y_u - \hat{y}_u$$

$$\Delta z_u = z_u - \hat{z}_u$$

$$\Delta t_u = t_u - \hat{t}_u$$

which leads to the following linearized expression of the pseudorange displacement, with respect to the i-th GPS satellite:

$$\Delta \rho_i = \rho_i - \hat{\rho}_i = a_{xi}\Delta x_u + a_{yi}\Delta y_u + a_{zi}\Delta z_u - c\Delta t_u$$

where (a_{xi}, a_{yi}, a_{zi}) are the direction cosines between the estimated user position and the i-th GPS satellite and are in the form of:

$$a_i = \left(\frac{s_{ix} - x_i}{\hat{r}_i}, \frac{s_{iy} - y_i}{\hat{r}_i}, \frac{s_{iy} - y_i}{\hat{r}_i} \right)$$

Considering the vectors of unknowns Δx, i.e. the receiver state, and the vector of measures $\Delta \rho$:

$$\Delta \rho = \begin{bmatrix} \Delta \rho_1 \\ \Delta \rho_2 \\ \Delta \rho_3 \\ \Delta \rho_4 \end{bmatrix} \qquad \Delta x = \begin{bmatrix} \Delta x_u \\ \Delta y_u \\ \Delta z_u \\ -c\Delta t_u \end{bmatrix}$$

the system can be expressed in matrix form:

$$\Delta \rho = H\Delta x$$

and then solved to find the four unknowns:

$$\Delta x = H^{-1}\Delta \rho$$

H being the observation matrix:

$$H = \begin{bmatrix} a_{x1} & a_{y1} & a_{z1} & 1 \\ a_{x1} & a_{y1} & a_{z1} & 1 \\ a_{x1} & a_{y1} & a_{z1} & 1 \\ a_{x1} & a_{y1} & a_{z1} & 1 \end{bmatrix}$$

Since more than 4 satellites are expected to be available every epoch, observations are processed with the least square method to obtain a better estimation of the receiver position. The LSQ method is used to find the solution Δx_0 that minimizes the loss function:

$$J(\Delta x) = (\Delta \rho - H\Delta x)^T (\Delta \rho - H\Delta x)$$

Calculating the derivative of the loss function in the point Δx_0, the following expression is obtained:

$$\Delta x_0 = (H^T H)^{-1} H^T \Delta \rho$$

Velocity of the spacecraft is estimated using the Doppler measurements, provided by the RANGE log, along with the pseudorange observable. As Doppler shift model, the following equation is considered:

$$D_i = -\frac{f_{Ti}}{c} [(\bar{v}_i - \bar{v}_u) * \bar{a}_i]$$

where f_{Ti} is the frequency of the signal transmitted by the i-th GPS satellite, $\bar{v}_i$ and $\bar{v}_u$ are, respectively, the i-th GPS satellite and user velocity and a_i is the already mentioned user-satellite line of sight vector.

Once that a new set of observations is available, psudorange, Doppler and GPS satellites orbital parameters are provided as input and the kinematic filter performs the following steps:

1. Estimation of the GPS satellites position and velocity at the current epoch, using orbital parameters provided by GPSEPHEM LOG.

2. Computation of $\Delta\rho$ differencing the psudorange measurements and its model, expressed as follows:

$$\rho = |r - r_{GPS}| + c \cdot (\delta t_c - \delta t_{GNSS})$$

$$\Delta\rho = p_m - \rho$$

   where r is receiver position, r_{GPS} is the position of the generic GPS satellite, δt_c and δt_{GNSS} are the receiver and the GPS satellite clock delays, respectively, and p_m is the pseudorange measurement obtained from RANGE log.

3. The algorithm performs observation residuals inspection, to discard observations with large errors (which generally happens when a new satellite becomes visible).

4. The algorithm checks for GPS satellites elevation, to discard observations of satellites with elevation below 5°.

5. The algorithm checks for GPS satellites geometry, by computing the Geometric Dilution Of Precision value. GDOP is a parameter that includes information about the relative position of the receiver and the GPS satellites in the field of view and provides useful indications about the quality of the processed position and clock delay. The matrix $(H^T H)^{-1} H^T$, used to calculate Δx inside the least-square solution, is a function of user - GPS satellites geometry and the GDOP value affects the final solution accuracy through this matrix. GDOP can be derived from the elements of the matrix:

$$(H^T H)^{-1} = \begin{bmatrix} D_{11} & D_{12} & D_{13} & D_{14} \\ D_{21} & D_{22} & D_{23} & D_{24} \\ D_{31} & D_{32} & D_{33} & D_{34} \\ D_{41} & D_{42} & D_{43} & D_{44} \end{bmatrix}$$

$$GDOP = \sqrt{D_{11} + D_{22} + D_{33} + D_{44}}$$

6. If the GPS satellites used to compute the solution of the least square problem are concentrated in a small portion of the space, from the receiver point of view, the quality of the solution will be lower and the GDOP is higher. If satellites are widely spread in the field of view and are far from each other, the GDOP is lower, meaning that the solution accuracy is higher. For the GPS Payload filter implementation, a threshold of 30 is used for the GDOP.

7. The elements of the H matrix are computed

8. Δx_0 is computed

9. The satellite position, velocity and clock are updated

10. The process is then iterated from phase 2, with the new satellite position and clock offset used to calculate the new $\Delta\rho$, until convergence is reached.

After the kinematic processing is completed, HK and SC data set are updated with the results of the least-square processing. Figure 108 shows the flow chart of the Kinematic Mode.
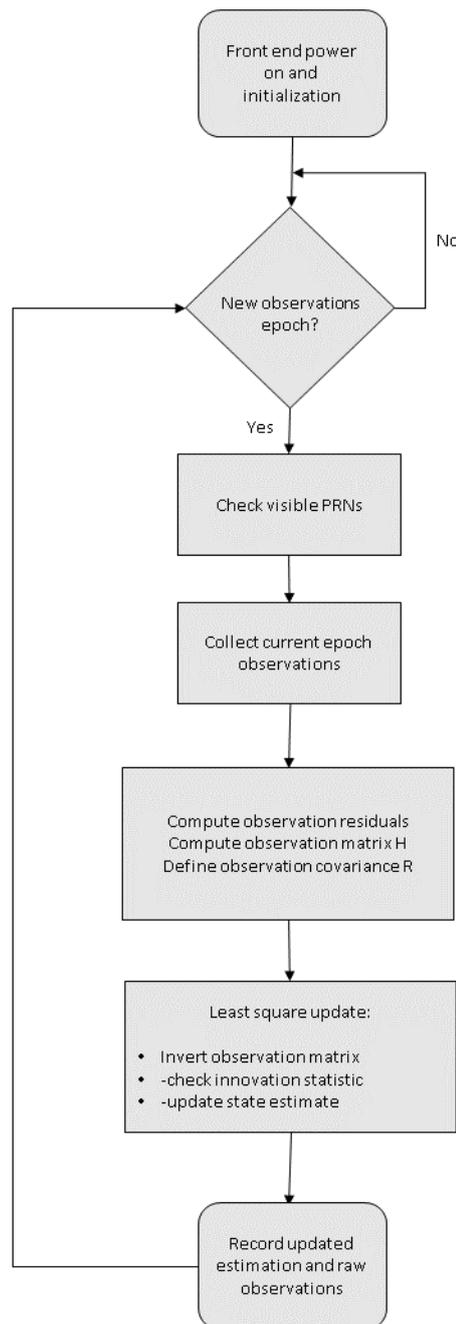
Figure 108: Kinematic Algorithm Flow Chart

5.1.6 Reduced dynamic positioning

To achieve better navigation performance with respect to the kinematic least squares based method, a second navigation mode was implemented in the embedded software. Differently from the Kinematic Mode, the Reduced Dynamic Mode receives as input both the raw GPS observables provided by the COTS front-end and the knowledge about the receiver trajectory, obtained from an accurate orbital model. These two sets of data are used to estimate the position within an extended Kalman filter. In the literature it is possible to find evidence of the possibility to achieve a meter-level accuracy with such an approach for LEO satellites and this level of accuracy is considered our target, too, during the ESEO mission [8]. This navigation mode is enabled only upon reception of a specific telecommand request, that provides to the application software the instruction to switch from the default Kinematic Mode, using the last processed state of the receiver (position, velocity and clock) to initialize the Kalman filter. Reduced Dynamics mode is considered the most critical part of the GPS Payload software, because of the difficulty to assess its actual performance on ground and to carry out a fine tuning of the filter, using simulated data. For this reason, several parameters of this navigation mode are covered by a dedicated telecommand, to achieve a high level of control and customization during the mission. In particular every parameter of the process matrix can be modified using separated telecommands and the entire Kalman filter can potentially be reset and reboot. Telecommands are the only way to apply some low level modifications to the GPS Payload code during the mission, since the ESEO platform is not designed to allow patch application to the payloads software. As happens for the Kinematic Mode, the frequency of the position fixes is fixed to 30 seconds, to provide a conservative processing time to the microprocessor, adequate to the computational resources. Reduced Dynamic software is basically composed of three main sub components: the extended Kalman Filter code, included in the source file called *EKF.c*, that is interfaced with the source files of orbit dynamics, *orbit.c*, and Runge-Kutta integrator, *RK.c*. It accesses also two external software components to perform matrix algebra and inversion.

The main reference frame adopted for the entire filter is an Earth fixed geocentric system, in order to allow for an easy use of the output position (no further conversion needed) and because the GPS measurements process would be easier in a reference frame compatible with the one used to generate the GPS satellites ephemeris. From the orbit model point of view, this translates in the conversion of the position of Moon and Sun to add their gravitational effect as third body perturbations and the need to include in the equation of motion non-inertial effects, namely Coriolis and centrifugal accelerations. For this reason, orbit model equations are expressed in the International Terrestrial Reference Frame (ITRF).

The entire processing is performed using the GPS time as reference time scale, because the broadcasted data and the receiver clock estimates inside the filter itself are expressed in this time frame. However conversion from other common time scales like International Atomic Time (TAI), Terrestrial Time (TT) and Coordinated Universal Time (UTC) is easy, because they are separated from the GPS time by a fixed number of seconds in the case of TT or by an integer amount of seconds that is slowly changing in time.

Figure 109 shows a functional scheme of the Kinematic Mode interface with other software components.
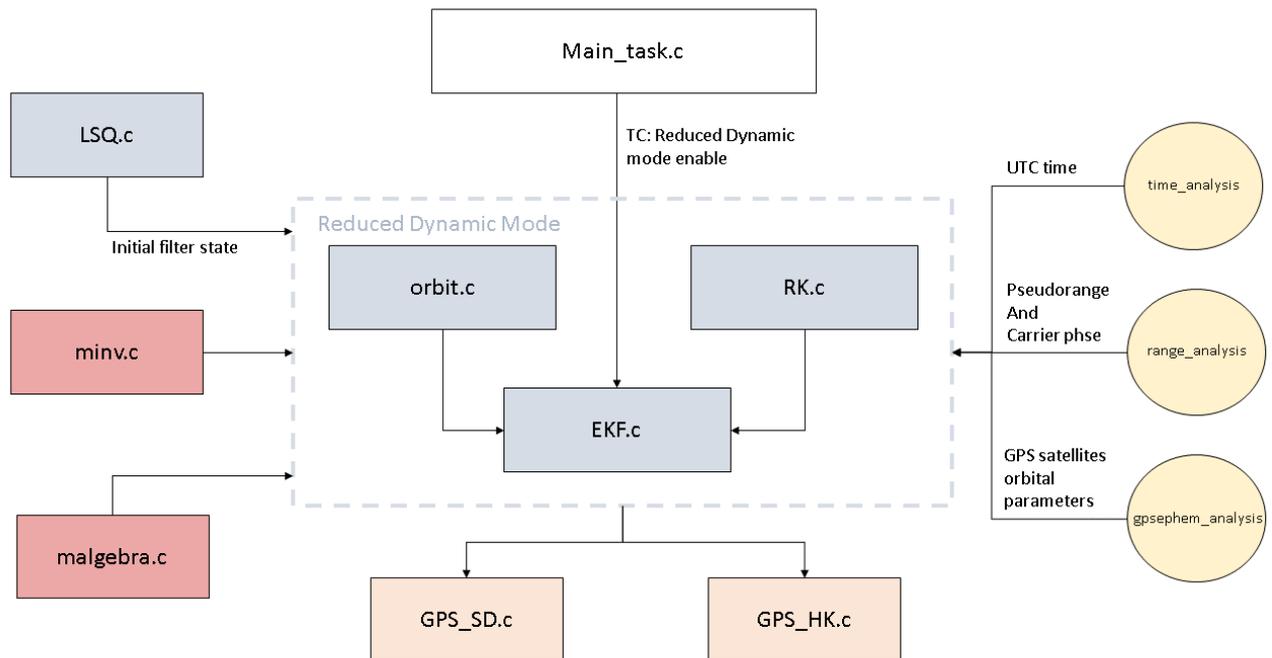
Figure 109: Reduced dynamic component interface with other software parts

5.1.6.1 Dynamic model

The implemented dynamic model accuracy is a trade-off between the computational limitation of the embedded application and the target navigation quality required as output. In this respect, the approach proposed by O. Montenbruck and E. Gill [1] was adopted for the implementation of the model. Target accuracy value used as a reference to select model components is 10^{-10} km/s^2, as proposed by Montenbruck et al. 2008 [8] and Montenbruck et al. 2009 [5] and, necessary to address real-time reduced dynamic navigation providing adequate constraints of GPS measurements. Figure 110 displays the typical contribution in terms of accelerations of the forces acting on a spacecraft in Earth orbit, as function of orbit radius. Using the target accuracy and an altitude around 500-600 km, it is possible to notice that the major perturbation effects are related to $J_{2,0}$, $J_{2,2}$, $J_{6,6}$, $J_{18,18}$, perturbations of the Earth gravitational field, Sun and Moon gravitational effects, atmospheric drag, solar radiation pressure, solid tides. Since the equations of motion of the spacecraft are expressed in an ECEF reference frame, apparent forces are also introduced. Other unmodelled effects are approximately accounted for in the filter by augmenting the state with the so-called empirical accelerations. Following, the mentioned orbit models are briefly presented and described, with a particular focus on their implementation inside the GPS Payload filter.
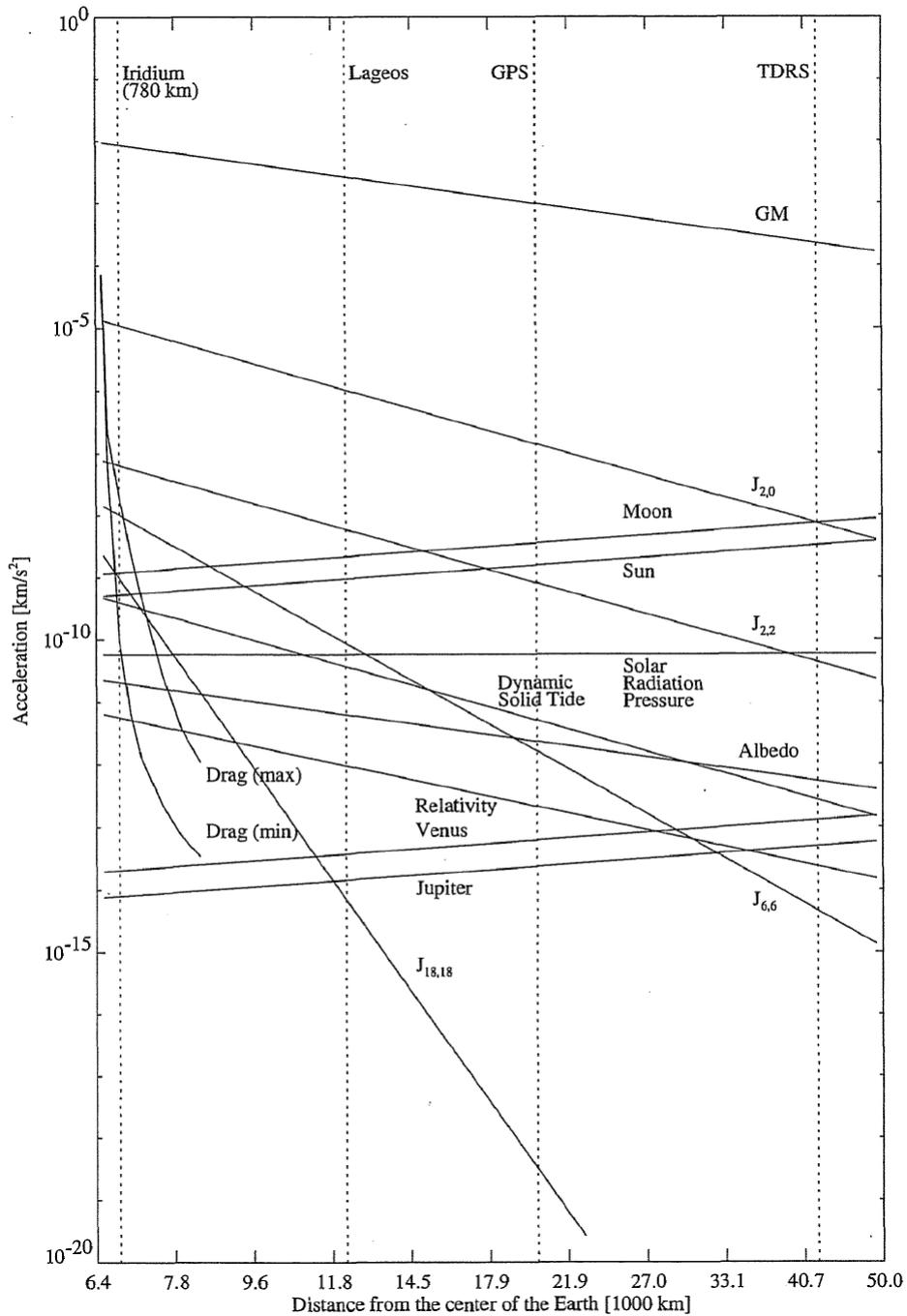
Figure 110: Perturbation effects acting on Earth orbiting spacecraft as function of altitude

Earth gravity field.

The motion of the spacecraft on an orbit around the Earth can be represented in first approximation by the Keplerian orbit model, where the total mass of the Earth is considered applied in its centre. However, the accuracy of this model is not adequate for most of the LEO applications, because it doesn't take into account the fact that the Earth is not a perfect sphere, neglecting major gravitational perturbations. In order to accurately describe the gravitational acceleration of the Earth, Legendre polynomial series expansion is used, using the spherical harmonics formulation:

123

$$\ddot{r} = \nabla \frac{GM_e}{r} \sum_{n=0}^{\infty} \sum_{m=0}^{n} \frac{R_e^n}{r^n} \bar{P}_{nm} sin(\phi) \left(\bar{C}_{nm} cos(m\lambda) + \bar{S}_{nm} sin(m\lambda) \right)$$

where GM$_e$ and R$_e$ are respectively the Earth gravitational parameter and radius; r is the distance from the centre of the Earth, $\bar{P}_{nm}$ are the normalized Legendre functions, $\bar{C}_{nm}$ and $\bar{S}_{nm}$ are the gravity field normalized geopotential coefficients, ϕ and λ are latitude and east longitude. The formulation of the gravitational acceleration used inside the filter is expressed normalized form, which is needed to reduce the high variation of un-normalized functions and parameters P$_{nm}$, C$_{nm}$ and S$_{nm.}$ The selected model is GGM03S released after the GRACE mission, referred to 1st January 2005 and valid up to an order of 130. However not all model coefficients are needed to compute the Earth gravity acceleration with an accuracy of 10^{-10} km/s^2: high order perturbations decrease faster with satellite altitude. According to the available embedded computational resources and to the target accuracy, model is computed up to 40x40 order, that is a good approximation for a spacecraft at an altitude between 500 km and 600 km, based on practical studies on real missions data [5]. The adopted normalization convention is expressed as:

$$\bar{P}_{nm} = \sqrt{\frac{(2 - \delta_{0m})(2n + 1)(n - m)!}{(n + m)!}} P_{nm}$$

$$\begin{Bmatrix} \bar{C}_{nm} \\ \bar{S}_{nm} \end{Bmatrix} = \sqrt{\frac{(n + m)!}{(2 - \delta_{0m})(2n + 1)(n - m)!}} \begin{Bmatrix} C_{nm} \\ S_{nm} \end{Bmatrix}$$

In order to compute Legendre polynomials and obtain accelerations a recursive procedure was implemented [1], by introducing the following parameters:

$$V_{nm} = \left(\frac{R_e}{r} \right)^{n+1} \cdot P_{nm} sin(\phi) \cdot cos(m\lambda)$$

$$W_{nm} = \left(\frac{R_e}{r} \right)^{n+1} \cdot P_{nm} sin(\phi) sin(m\lambda)$$

Starting from the values of V_{nm} and W_{nm} easily calculated at n=0 and m=0

$$V_{00} = \frac{R_e}{r}$$

$$W_{00} = 0$$

the recursive process can proceed by calculating all values with the same "m", and varying "n", using the following relations:

$$V_{nm} = \left(\frac{2n - 1}{n - m} \right) \cdot \frac{zR_e}{r^2} V_{n-1,m} - \left(\frac{n + m - 1}{n - m} \right) \cdot \frac{R_e^2}{r^2} V_{n-2,m}$$

$$W_{nm} = \left(\frac{2n-1}{n-m}\right) \cdot \frac{zR_e}{r^2} W_{n-1,m} - \left(\frac{n+m-1}{n-m}\right) \cdot \frac{R_e^2}{r^2} W_{n-2,m}$$

with x, y and z ITRF coordinates of the ESEO spacecraft.

Once that all terms for a fixed m are obtained, starting from the coordinates (n,m), $V_{n+1,m+1}$ and $W_{n+1,m+1}$ are computed using the following formulation:

$$V_{nm} = (2m-1) \cdot \left(\frac{xR_e}{r^2} V_{m-1,m-1} - \frac{yR_e}{r^2} W_{m-1,m-1}\right)$$

$$W_{nm} = (2m-1) \cdot \left(\frac{xR_e}{r^2} W_{m-1,m-1} - \frac{yR_e}{r^2} V_{m-1,m-1}\right)$$

The presented expressions show how all V_{nm} and W_{nm} parameters for n>m, for a fixed m, are recursive functions of the parameters calculated for n=m. At the same time all parameters $V_{n+1,m+1}$ and $W_{n+1,m+1}$, with n=m, depend only on the previous values V_{nm} and W_{nm}.

Using the calculated V_{nm} and W_{nm}, the acceleration can be derived in Earth fixed coordinates:

$$\ddot{x}$$
$$= \sum_{n,m} \begin{cases} (if\ m = 0) & \frac{GM}{R_e^2} \cdot \{-C_{n0}V_{n+1,1}\} \\ (if\ m > 0) & \frac{GM}{R_e^2} \cdot \frac{1}{2} \left\{ \left(-C_{nm}V_{n+1,m+1} - S_{nm}W_{n+1,m+1}\right) + \frac{(n-m+2)!}{(n-m)!} \cdot \left(C_{nm}V_{n+1,m-1} + S_{nm}W_{n+1,m-1}\right) \right\} \end{cases}$$

$$\ddot{y}$$
$$= \sum_{n,m} \begin{cases} (if\ m = 0) & \frac{GM}{R_e^2} \cdot \{-C_{n0}W_{n+1,1}\} \\ (if\ m > 0) & \frac{GM}{R_e^2} \cdot \frac{1}{2} \left\{ \left(-C_{nm}W_{n+1,m+1} + S_{nm}V_{n+1,m+1}\right) + \frac{(n-m+2)!}{(n-m)!} \cdot \left(-C_{nm}W_{n+1,m-1} + S_{nm}V_{n+1,m-1}\right) \right\} \end{cases}$$

$$\ddot{z} = \sum_{n,m} \frac{GM}{R_e^2} \cdot \{(n-m+1) \cdot (-C_{nm}V_{n+1,m} - S_{nm}W_{n+1,m})\}$$

Sun and Moon gravity field

Luni-solar third body perturbation is in the order of 10^{-9} km/s^2 for a spacecraft in LEO orbit. In this section only Sun and Moon gravitational accelerations affecting directly the satellite motion are considered. In order to compute the perturbation caused by the gravity of a third body in a Earth-centred coordinate system, the following equation can generally be used:

$$\ddot{r} = GM \left(\frac{s-r}{|s-r|^3} - \frac{s}{|s|^3}\right)$$

where r is the set of coordinates of the spacecraft and s and M are respectively coordinates and mass of the third body considered. The previous equation includes the first term referred to the direct gravitational effect on the spacecraft and a second contribution related to the fact that the Earth itself, and consequently the centre of the reference frame, is subject to an acceleration. Inside the filter a simplified version of the previous equation was implemented, that takes into account the fact that, for this application, the third body, Moon or Sun, is much more distant from the Earth with respect to the spacecraft:

$$\ddot{r} = \frac{GMr}{r^3}\left(-e_R + 3e_S(e_S \cdot e_R)\right)$$

with e_r and e_s unit vectors pointing in the direction of s and r.

Earth tides

Solid tides are small periodic deformations of the Earth shape, result of the gravitational effects of Sun and Moon. Their perturbation to the satellite motion is introduced in the filter not as a direct acceleration, but as a modification of some of the geopotential coefficients of the Earth gravity field, that depends from Sun and Moon position. This means that the Earth gravity field implemented is not static anymore, but is subject to periodic variations, depending on the position of the considered third body. The Earth gravity potential corrections can be calculated as function of the Love number k, a dimensionless parameter that provides information about the entity and effectiveness of shape variation effects, applied to a planetary body. Earth gravity field coefficients correction for can be computed in the following normalized form:

$$\Delta\bar{C}_{nm} - i\Delta\bar{S}_{nm} = \begin{cases} (for\ n = 2\ and\ n = 3) & \dfrac{k_{nm}}{2n+1}\displaystyle\sum_{j=2}^{3}\dfrac{GM_j}{GM_e}\left(\dfrac{R_e}{r_j}\right)^{n+1}\bar{P}_{nm}\sin(\Phi_j)e^{-im\lambda_j} \\[4mm] (for\ n = 4) & \dfrac{k_{2m}^{(+)}}{2n+1}\displaystyle\sum_{j=2}^{3}\dfrac{GM_j}{GM_e}\left(\dfrac{R_e}{r_j}\right)^{3}\bar{P}_{nm}\sin(\Phi_j)e^{-im\lambda_j} \end{cases}$$

with GM_e and R_e respectively gravitational parameter and equatorial radius of the Earth, GM_j gravitational parameter of Sun and Moon, r_j distance between the centre of the Earth and the third body, Φ_j and λ_j latitude and east longitude of Sun and Moon.

In the second equation, the term $k_{2m}^{(+)}$ represents the influence of degree 2 tides on degree 4 coefficients. A second set of Love parameters $k_{nm}^{(+)}$ was introduced because of the need to consider also flattening and Coriolis forces caused by Earth rotation. The used Love number for the computation of geopotential coefficients corrections can be found at IERS convention documentation released in 2010 [25]. For this project the tidal effect is approximated as elastic deformation only, resulting in real values for the Love numbers, neglecting the imaginary part. Solid Earth tides perturbation affect satellites motion with an acceleration around $2*10^{-10}$ km/s^2 for a user at 400 km of height. Ocean tides effect instead is 1 order of magnitude smaller than the solid tides contribution , and fort this reason was not implemented inside the filter.

Atmospheric Drag

This component of the orbit model represents one of the major contribution for low Earth orbit satellites. It is the results of the impact of atmosphere particles that can still be found at low altitudes with the satellite external surface exposed to the flux, normal to the velocity vector. Differently from gravitational effects, atmospheric drag is a surface force and is function of the ESEO spacecraft weight and orientation. The major challenge to assess the atmospheric effect on a satellite motion with the required level of accuracy is the density modelling and for this purpose many complex models of atmospheric density are available, that usually take into account many variables that needs to be constantly updated in time. However, considering the computational limitations of the embedded application studied in this project, the simple time-independent model proposed by Harris Priester was adopted. Despite its simplicity, this model is still widely used and allows for adequate approximation of the upper atmosphere density. This model is meant to only consider daily density variations due to the effect of solar radiation. The actual density value used at a certain altitude h, is calculated using the density computed at the apex and antapex of the atmospheric bulge caused by heating action of radiations, ρ_M and ρ_m, namely max and min density values. Their value can be obtained using the following equations:

$$\rho_m(h) = \rho_m(h_i)e^{\left(\frac{h_i - h}{H_m}\right)}$$

$$\rho_M(h) = \rho_M(h_i)e^{\left(\frac{h_i - h}{H_M}\right)}$$

Where h_i is the i-th tabulated value of height, with $h_i \leq h \leq h_{i+1}$, and H is the scale height, defined by:

$$H_m(h) = \frac{h_i - h_{i+1}}{\ln(\rho_m(h_{i+1})/\rho_m(h_i))}$$

$$H_M(h) = \frac{h_i - h_{i+1}}{\ln(\rho_M(h_{i+1})/\rho_M(h_i))}$$

Final density value can be obtained with the following relation:

$$\rho(h) = \rho_m(h) + \left(\rho_M(h) - \rho_m(h)\right) \cdot \left(\frac{1}{2} + \frac{e_r \cdot e_b}{2}\right)^3$$

with e_r and e_b are respectively satellite position and apex of the diurnal bulge unit vectors.

Once that the density value is calculated, atmospheric drag perturbation on the spacecraft can easily be computed with:

$$\ddot{r} = \frac{1}{2}C_D\frac{A}{m}\rho v^2$$

where A is the cross-section reference are of the spacecraft, m is its mass, v the velocity magnitude, C_D is the drag coefficient.

Solar radiation pressure

Similarly to the atmospheric effect, also the radiation pressure is a function of the spacecraft external layout, weight and attitude along the orbit. In particular solar panels disposition on the satellite external surfaces contribute to introduce this perturbation due to the impulse transferred by the photons, absorbed or reflected, that impact the spacecraft during the mission. While the atmospheric drag changes with altitude following the selected model, SRP effect can be considered almost constant along the orbit. This perturbation of the satellite motion is usually a small contribution with respect to other effects, in the order of 10^{-10} km/s^2 for a spacacraft with area to mass ratio of 0.01 m^2/kg. The resulting effect acting on a satellite moving inside the solar system is usually expressed as a pressure applied on the portion of external surface of the spacecraft exposed to the solar flux Φ, which is calculated, considering a complete absorbing satellite, as the ratio between the solar flux and the speed of light. The value of the solar flux can be assumed fixed to Φ=1367 Wm^{-2} for a spacecraft orbiting around the Earth, i.e. at 1 AU of distance from the Sun, and the corresponding solar radiation pressure can be considered constant for an absorbing external surface to the value $P = 4.56 \cdot 10^{-6} Nm^{-2}$. However for fully reflective surfaces the values of the pressure can be doubled and, in order to take into account all possible combinations of mixed reflective and absorbing surfaces, the reflectivity value ε is generally used. The resulting accelerations generated on the satellite is a function of the angle Θ between the direction of the Sun, i.e. the source of photons stream, and the vector normal to the surface of the satellite subjected to SRP. However since the orientation of the satellite can be assumed to be fixed, having the surfaces with solar panels always in the direction of the sun, to optimize on-board power management, an easier formulation was implemented, only dependent by satellite exposed surface A, mass m, reflectivity of the normal surface ε and distance from the sun d$_s$:

$$\ddot{r} = -P C_R \frac{A}{m} \frac{d_s}{d_s^3} AU^2$$

with C$_R$ = 1+ε, solar radiation pressure coefficient, that was included in the filter state in order to have the opportunity during the mission to leave it free to change, in case that the ESEO parameters interested by the SRP computation will change from the nominal conditions provided by the manufacturer of the platform.

Empirical accelerations

This contribution is introduced in the equations of motion in order to compensate for possible un-modelled forces or simplification errors [7]. This parameter is considered to be characterized by stochastic behaviour and is modelled using a first order Gauss-Markov process. This process time behaviour is based on and exponential autocorrelation formulation:

$$m_j = e^{-\left(\frac{t_{i+1}-t_i}{\tau_j}\right)}$$

with τ time constant of the autocorrelation process. Empirical accelerations are usually expressed in radial, along track and cross track components and they are included in the estimation process as part of the state. Based on similar study performed on LEO satellites, the expected value for the empirical acceleration module is of several 100 nm/s^2 for along-track and cross track components, and much smaller for radial part.

5.1.6.2 Filter architecture

For this filter, two types of basic GPS observations are used: pseudorange and carrier phase. As for the pseudorange measurement described in the previous chapter, carrier phase is still a GPS satellite-to-user range measurement but obtained in a different way. Considering the GPS signal as a carrier modulated with a PRN code, pseudorange measurement uses information provided by the code while the carrier phase counts the number of cycles of the RF carrier signal. While pseudorange measurement can bring noise in the order from centimeters up to some meters, carrier phase is a more accurate observable and its noise level can be as low as 1mm. However, these measurements implies the introduction in the filter of a new unknown: a bias value for every tracking channel. This unknown was added in the set of the receiver state and is estimated by the filter. One of the typical atmospheric effects to be taken into account for GPS-based navigation is the ionospheric delay, which applies also to space applications. It usually affects both pseudorange and carrier phase measurements with a delay characterized by the same absolute value, but applied with a different sign. In order to compensate for ionospheric effects inside the filter, considering the availability of only L1 GPS observations, the Group And Phase Ionospheric Combination (GRAPHIC) is considered the most suitable solution [9]. This combination mixes together pseudorange data (C/A) and carrier phase measurements (L1) and is defined as follows [24]:

$$\rho_{C1L1} = (\rho_{CA} + \rho_{L1})/2$$

where ρ_{C1L1} is the GRAPHIC combination, ρ_{CA} the pseudorange measurement and ρ_{L1} the carrier phase measurement. Although the attitude of the ESEO spacecraft is considered almost fixed and predictable for the entire mission, drag and solar pressure coefficients, that are function of the spacecraft surfaces orientation with respect to velocity and solar pressure vectors, are estimated inside the filter, in order to take into account the worst case scenario in which, for any reason, they are different from the design values. The state vector of the Kalman filter then includes 12 elements plus 1 extra entry per tracking channel (Table 25).

Table 25: State vector components

State parameter	Number of elements
User position [m]	3 elements, in ECEF coordinates
User velocity [m/s]	3 elements, in ECEF coordinates
Receiver clock offset [s]	1 element
Drag coefficient	1 element
Solar pressure coefficient	1 element
Empirical accelerations [nm/s^2]	3 elements, radial, tangential and normal coordinates
Bias parameters	N elements, where N is the number of tracking channels for the processed epoch

5.1.6.3 Kalman filtering of GPS raw observations

The Extended Kalman Filter (EKF) represents an adequate solution for applications that not includes strong non-linearities, like the orbit dynamics case. Although as a sequential filter it fits the real-time feature of this application, its solution will still be sub-optimal, because a linearization of the system around the last estimate is needed and the process and measurement noises are not Gaussian, i.e. white noise with zero mean, as required by the Kalman filter hypothesis. This linearization introduces a first order approximation, but as reported in the literature it is still a useful instrument for such an application and no other processing solutions were found to be valid alternative. Once activated, reduced dynamic mode replaces the kinematic mode, following its real-time operations: the application software first waits for new observables; if all necessary logs data are obtained, the estimation process is executed, followed by the update of HK and scientific data set. In order to have an adequate initial state for the Kalman filter, the kinematic solution is always processed before entering the reduced dynamic mode. The starting state is then introduced in a cycle of propagation and successive update, repeated every time that a new set of observations is available.

Process and measurements models can be generalized in the following non linear form:

$$x_{k+1} = f(x_k, u_k) + u_k$$

$$z_k = h(x_k, v_k) + v_k$$

with f and h discrete non-linear functions of time, u_k is the process error and v_k is the measurements noise. Since the Kalman filter application is based on linear system assumption, the non linear set of equations shall be linearized around the estimation of the previous epoch:

$$F(\hat{x}_k) = \left. \frac{\partial f(t, x)}{\partial x} \right|_{x=\hat{x}_k}$$

$$H(\hat{x}_k) = \left. \frac{\partial h(t, x)}{\partial x} \right|_{x=\hat{x}_k}$$

$$\phi_k = I + F(\hat{x}_k) T$$

with F_k and H_k respectively the linearized process and observation matrix, and ϕ_k is the transition matrix. The system can be then expressed in linearized form:

$$x_{k+1} = \varphi_k + u_k$$

$$z_k = H_k x_k + v_k$$

This linearization was needed because φ_k and H_k are necessary to compute of the Kalman gain K and the estimation error covariance matrix P. Propagation of position and velocity instead is performed by mean of numerical integration between two adjacent epochs of the complete non linear orbit model using a Runge-Kutta method.

Considering the k-th epoch, the current estimate of the state is expressed as $\hat{x}_k^+$ and the estimation error covariance matrix as P_k^+. State propagation is performed using the full set of orbital dynamics equations described in the previous section:

$$\begin{bmatrix} \dot{\hat{r}} \\ \dot{\hat{v}} \end{bmatrix} = f\left(t, \hat{r}, \hat{v}, \hat{a}_{emp}\right)$$

Empirical accelerations propagation is expressed by its exponentially correlated formulation presented before and all the remaining parameters are meant to be constant between two consecutive epochs. This set of equations provide the a priori state estimate at epoch k+1, $\hat{x}_{k+1}^-$. The propagation step is completed with the computation of the transition matrix and then the a priori estimation covariance matrix P_{k+1}^-, using the following formulation:

$$P_{k+1}^- = \phi_k P_k^+ \phi_k^T + Q_k$$

where Q_k is the process error covariance matrix. Before proceeding with the state update, a check is executed on the tracked GPS satellites and, if there is any variation with respect to the previous epoch, the ambiguity set and covariance are updated. The a-priori estimates of the state and covariance matrix are then corrected using the information obtained from the measurements: the residuals are computed, along with the observation and covariance matrices. The updating stage first starts from the computation of the Kalman gain:

$$K_{k+1} = P_{k+1}^- H_{k+1}^T R_{k+1}^{-1}$$

with K Kalman gain and R observation error covariance matrix. The residuals and innovation introduced by the new set of measurements is computed using the Kalman gain and then the a priori estimate of the state is updated:

$$i_k = K_k \left(z_k - H_k \hat{x}_k^-\right)$$

$$\hat{x}_k^+ = \hat{x}_k^- + i_k$$

State covariance update is performed using the following relation:

$$P_k^{-1}(+) = P_k^{-1}(-) + H_k^T R_k^{-1} H_k$$

The flow chart of the Reduced-Dynamics Mode is included in Figure 111.
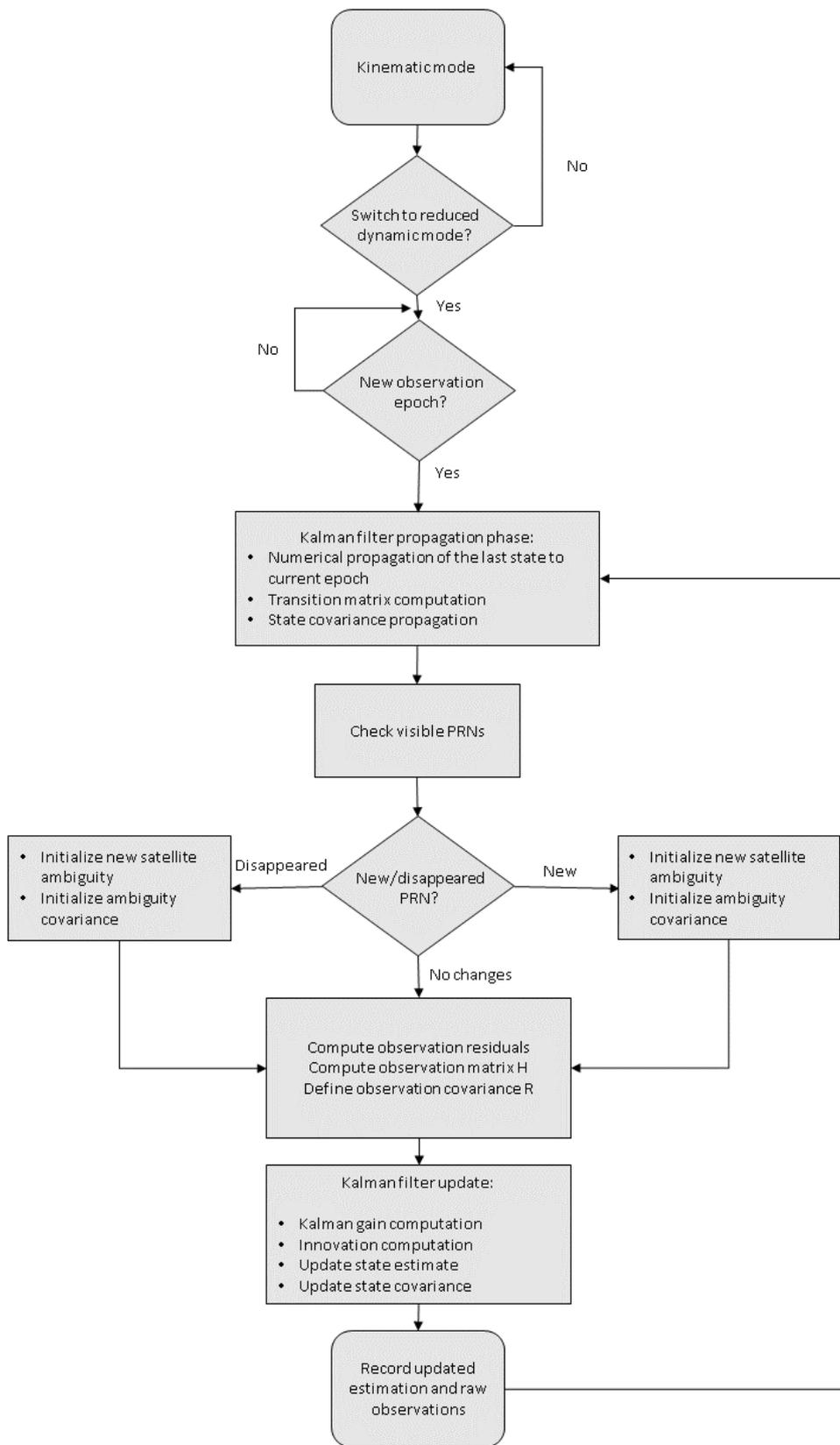
Figure 111: Reduced Dynamic Algorithm Flow Chart

5.1.6.4 Runge Kutta numerical integration

In order to propagate the receiver state between two consecutive epochs, the equation of motions of the ESEO spacecraft are numerically integrated using a 5th order Runge-Kutta method. While for offline processing the working load of the model equations integration is not an issue, this method was selected in order to fit the limited computational resources requirements of the embedded application. Considering a data rate of 30s even a simple integrator like the Runge-Kutta method proved sufficient to meet the target accuracy.

5.1.7 FDIR

Although in space missions the reliability requirements for the payloads are typically less stringent than those of the platform sub-systems, the application software shall perform some monitoring of the hardware and shall be able to quickly fix or isolate potential failures. This procedure is necessary to avoid that a payload failure propagates to the rest of the spacecraft and to guarantee the scientific outcomes from the experiment. A light Fault Detection Isolation and Recovery (FDIR) functionality is implemented inside the GPS Payload. It is focused on the COTS front-end behaviour, which is the critical part of the spacecraft architecture from both the mission goals and reliability points of view. This FDIR functionality represents the software support to the current limiting circuit described before and it is coupled and completed by the Safe Mode component, that performs isolation and recovery of the front-end operations, once the fault is detected. In the inconvenient scenario of a failure of the active front-end following a space radiation event on the board, an increasing current flow is expected, promptly limited by the CL circuit. At the same time, the higher the current demand the higher will be the voltage over a sensing resistor included in the CL circuit. The voltage value is read by the navigation computer microprocessor through the ADC converter and in case the voltage is below a threshold of 3V, the applications software stops immediately its operations and activates the Safe Mode that will perform troubleshooting activity. The software component involved in this task is FDIR_check, which is accessed from several points of the code in order to quickly react to the potentially detected problems, before the propagation to the rest of the payload or the satellite. In particular, this software component is activated right after every initialization phase and before and after the position processing at every epoch.

5.1.8 Safe mode

Once the FDIR software component detected an hardware problem to the active front-end, after the activation of the current limiting circuit, the Safe Mode is triggered, in order to avoid any possible propagation of the failure effects. When this scenario occurs, the time and last position are recorded, a single event counter is incremented and the HK data are updated in order to report that the safe mode is enabled. Inside the Safe Mode code, the software turns off the active front-end active and checks for the time elapsed since the last fail. If it is below a fixed threshold that means high frequency of failure event, the redundant front-end is marked as active and the front-end initialization procedure is executed again. In case two consecutive safe mode calls occurred with an interval lower than the threshold and they are referred to the functionality of the two different front-ends, it means that probably both devices have failed and it is not safe to enable any of them. In this case

the safe mode enters an infinite loop, waiting for instructions from ground. Once assessed on ground that the Safe Mode has entered the infinite loop, by checking the HK data, the procedure foresees to power-cycle the GPS Payload.

Figure 112 shows the flow chart of the data acquisition process.
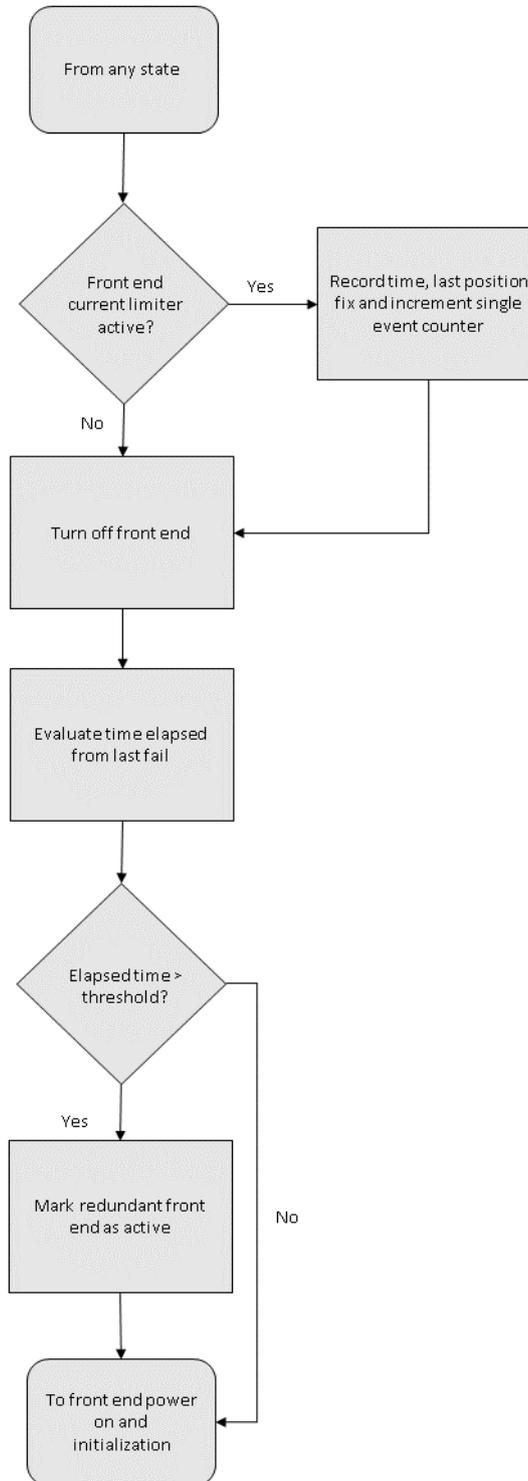
Figure 112: Safe Mode Flow Chart

5.1.9 Data storage, HK and TC Management

Typically, a spacecraft collects scientific and telemetry data during its mission and they are managed by the OBDH sub-system for the entire platform and payloads [28]. Telemetry data are set of values necessary for ground operators to assess the spacecraft health and correct operations. Scientific data set instead includes the outcomes of all active experiments on board and, once downloaded on ground, they are provided to payload developers and scientists in order to perform further analysis and to draw qualitative conclusions about the spacecraft mission. In order to perform data exchange with ground and to allow remote control of the payload operations from the ESEO control centre, the application software needs a series of auxiliary software components to interface externally with the ESEO OBDH. Furthermore, in order to optimize sub-systems performance during space missions, they are meant to be able to partially modify their operations and settings after the launch. Since once in orbit the spacecraft is to be considerate not manually accessible, it can only be accessed using telecommands sent from ground control stations to the spacecraft telecommunication subsystems. All commands for platform sub-systems and payloads are collected and then distributed again by the OBDH. This means that the Payload software development can benefit of the opportunity to implement a more flexible software during the mission, in order to test, for example, different data processing techniques or perform minor fixes in already identified critical parts. But, in order to take into account possible modifications, the software shall implement dedicated components to manage telecommands. They can be simple updates of application software values used to perform mission task or sometimes also modification of the software to exclude or include several parts of the code itself. For the GPS Payload, several aspects of the application software can be handled remotely using telecommands, as forcing to a specific operational mode, request transmission of data record or setting of navigation filters parameters. A pre-determined set of telecommands was implemented on board and the TC list was provided to the platform developer and to the mission control center: in fact, this set shall be implemented by both the instruments softwares that manages communications from space to ground and viceversa. Data exchange between the payloads and the OBDH is ruled by the CANOpen stack [27], that provides the main communication interface with the platform main data bus for most of the payloads on-board. It is commercial software component developed by Vector Informatik Gmbh. Interfaces of hardware and software with the CANOpen stack are implemeted respectively by the CAN software components and custom API, provided by the platform manufacturer to the payloads developer to encourage standardization of the communication driver. These API performs stack initialization and configuration, with a dedicated implementation for every subsystem. This solution allows the payalod to remain completely passive on the nodes of the data bus: scientific and housekeeping data are saved in the CANOpen stack internal structures created for every payload and then managed by the platform subsystems. To achieve all these tasks, this software task includes 3 sub-components [18]:

HK_update: updates the the housekeeping data set, including information provided by the rxstatus log and hwmonitor log. It collects data about: COTS receiver status and error; temperature measured on the external chassis, on the top surface of the navigation computer and on the front-end; time expressed in GPS time; COTS front-end clock status; front-end input voltage; GPS satellites in view. Then the CANOpen stack internal

structure dedicated to HK data is updated with the command *Cocan_Update_HK_Data*, so that it is ready to be transmitted to the OBDH upon explicit request, without any other action required to the GPS receiver application software. Further details about GPS Payload HK data are included in ANNEX 1.

SD_update: includes the real scientific outcomes of the GPS Payload experiment. It collects the outputs of the navigation algorithms and the raw observables before being processed. In particular the scientific data structure include: data availability flag, date of epoch, ESEO spacecraft position and velocity, COTS front-end clock, satellites in view and then for each of them PRN, psudorange, carrier phase, C/N0. Raw observables will be processed on ground to achieve a more precise determination of the orbit, to use as a reference to assess the actual performance of the GPS Payload. The CANOpen internal structure is then updated using the command *GPS_Update_Sci_Data,* to provide the data set ready to be transmitted to ground by the S-Band transceiver. The complete set of telecommands and description is included in ANNEX 2.

TC_management: it is the set of external instruction that can alter the payload mode and operations. They are meant to allow an high control from ground to the reduced dynamic navigation algorithm operations, because it is the most critical software component related to mission scientific goals and its validation on ground is not trivial. So several adjustments of model and measurements error covariance matrices are foreseen, after some processing is performed on first mission data. Also the orbit dynamic model can be modified by excluding some of the forces considered, in order to assess the payload performance with different levels of model accuracy. To maintain optimal functionality in time the navigation algorithm requires updated Earth Orbiting Parameters that are provided with a specific TC. Payload overall functionality can also be partially controlled by forcing the change to a specific software mode ot manually change and reset of the active front-end. Inside the TC checking routine, every address of the dedicated structure is accessed using the command *Cocan_Read_Cmd_Reg*, provided inside the CANOpen API. The complete set of telecommands and description is included in ANNEX 3. Figure 113 shows the relationship between HK, SC and TC management code with other software components, while Figure 114 shows the software flow chart.
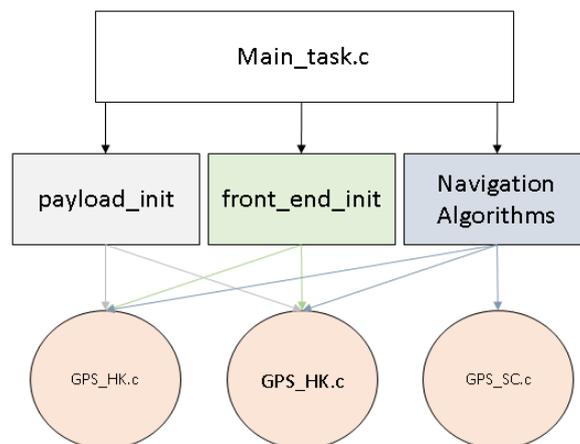
Figure 113: HK, SC and TC components interface with other software parts
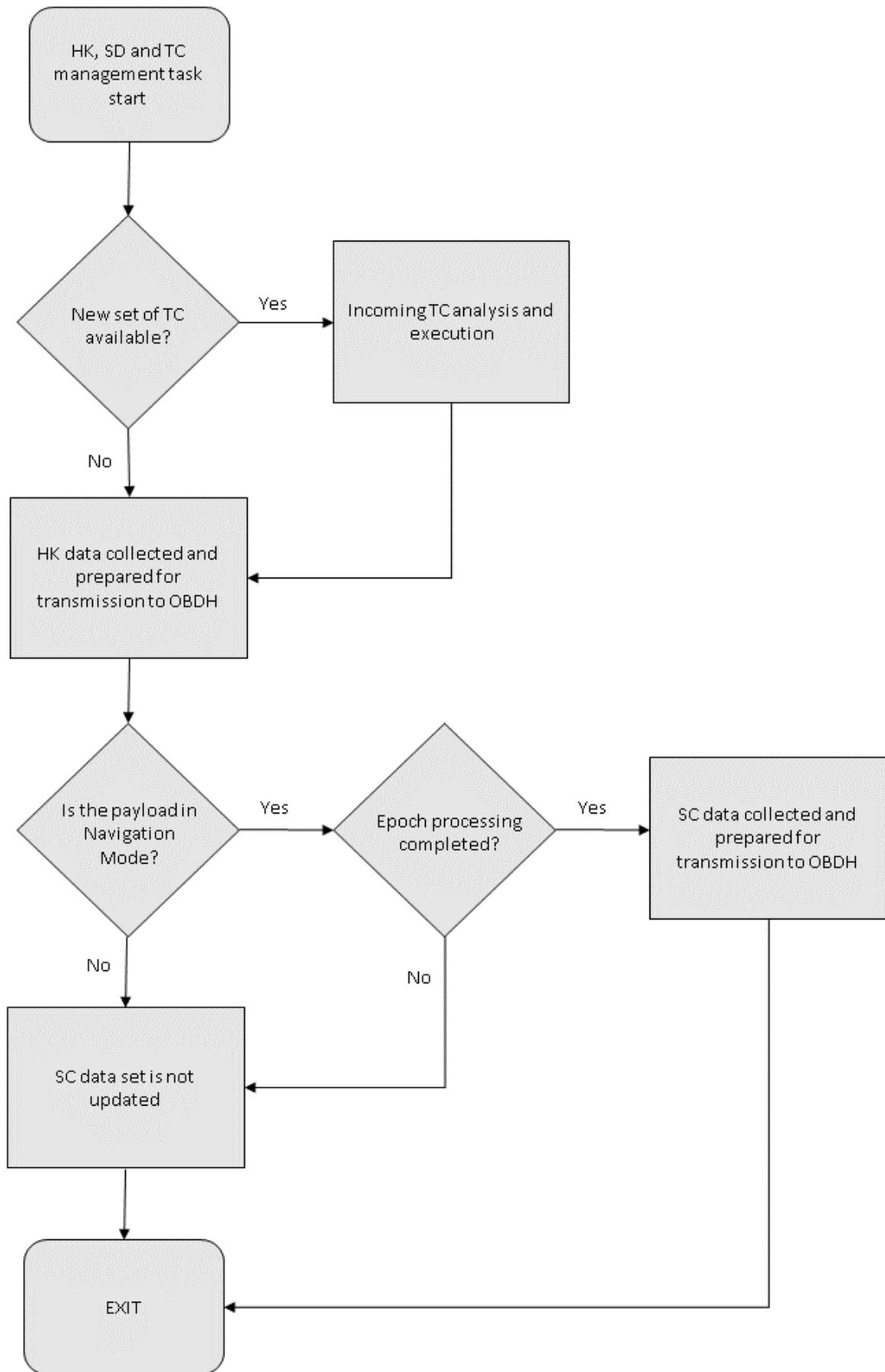
Figure 114: HK, SC and TC management component flow chart

These software components are called regularly in time and from several parts of the software. Since the HK, SC and TC management by the GPS receiver is passive and can only communicate with the OBDH upon explicit interrogation, it is necessary to continuously monitor and update these internal structures, in order to have data ready even if the request is received while the applications software is performing other tasks. For this reason HK data are updated at the end of the Payload Initialization Phase, at the end of the COTS Front-ends Initialization Phase, during Safe Mode and at every epoch, after the processing is complete. SD are updated only at the end of the epoch position processing, because they are meant to be completed only with spacecraft position and velocity data. TC monitoring is performed in many parts of the code, as happens for HK data updating.

5.2 Software validation

The issue of GPS Payload software validation was addressed through several consecutive test sessions. The main part of the code was progressively tested and debugged during the development, thanks to the availability of the EBB models of the Navigation Computer. This way, different software components were tested separately, that was acceptable for the preliminary development phase. The model of the COTS front-end was involved in the testing of the software, to verify the data acquisition routine functionality while interfacing with other software components. Some general verifications were performed on ground using also a model of the passive antenna, to assess real-time functionality of the application software while receiving space-like signal. Unfortunately, in order to test the actual navigation performance, ground testing or simulations are not enough. For this purpose, a GNSS Signal simulator is necessary to perform an acceptable validation of the algorithm performance [15]. While the Kinematic Algorithm could theoretically be tested also on ground, considering a static user, the Reduced Dynamics outputs would be meaningless if the "simulated user" is not moving in Low Earth Orbit, because of the orbit dynamics model information that is included in the processing of the position. In fact, in this case the algorithm would try to correct the position propagated with the dynamic model using GPS measurements related to a user on the surface of the Earth. However also for the Kinematic Mode a Signal Simulator aided validation is advisable, since the performance can slightly vary according to the different effect of DOP, ionosphere, troposphere and multipath. Besides the two navigation filters, also the signal acquisition component needed to be tested with a real "space" signal, in order to assess it efficiency and to tune its parameters. The ESEO spacecraft orbit model used for these tests was slightly different from the one used during the COTS front-end validation, because the hardware and software test campaigns were separated in time by two years, and then the orbit model provided by the platform developer company underwent some updates. The mentioned simulator-aided test sessions were carried out at:

- Istituto Superiore Mario Boella (ISMB), Turin, Italy: a NAVX–NCS GNSS simulator was kindly provided to perform preliminary complete software tests. Due to the lower precision of the orbit built in "spacecraft scenario" model, it was used only to validate the signal acquisition routine and to assess the Kinematic Algorithm performance.

- Nottingham Geospatial Institute (NGI), Nottingham, UK: to perform reliable Reduced Dynamic Algorithm verification and debug, the SPIRENT GNSS Signal Simulator was used, kindly granted by NGI. It allowed higher control and knowledge on the implemented dynamical model, which was used as a reference to calculate the estimated position residuals.

The problem of assessing the actual navigation performance of the payload raised the issue of the precision of the reference orbit implemented inside the simulator: although its model can be considered the "real world" within the simulation and from the GPS observables model point of view, it will always be an approximation of the real trajectory of the ESEO spacecraft. This is not of concern for the kinematic mode, since it only uses information from the GPS raw measurements and then it tries to estimate the orbit as it implemented inside

139

the simulator. The dynamic filter, instead, aims at obtaining a better estimation of the spacecraft position, mixing the observables generated by the simulator, starting from the internal created trajectory, with another orbit model, external and independent from the simulator model and meant to describe the real satellite motion the best way possible. This means that the calculated residuals does not provide real indications of actual performance of the reduced dynamics navigation filter, because the model used to generate the reference positions is an approximation of the real trajectories. Furthermore, even with the more accurate and customizable orbit model provided by the SPIRENT Simulator, a complete knowledge and insight is not available, adding uncertainty in the performance definition. For this reason, a fine-tuning of the filter during the test sessions was not an easy task. However, thanks to the possibility to perform the tuning of the filter during the mission, using dedicated telecommands, ground processing of raw and processed data obtained on-board are foreseen, as main activity in support of the GPS payload mission from ground. The updated parameters and orbit model details are included in Table 26 and Table 27.

Table 26: ESEO orbital parameters

ORBIT PARAMETERS	
Reference epoch	02/12/2017 00:00:00
SMA	6978.14 km
Eccentricity	0.001
Inclination	97.7513 deg
Right Ascension of the Ascending Node	206.355 deg (LTAN 15:05)
Argument of Perigee	90 deg
TA	0 deg

Table 27: ESEO dynamic model and attitute

ORBIT MODEL AND S/C ATTITUDE	
Earth Gravity Model	JGM3
Gravity order	70x70
Aerodynamic Cd	2.2
Cd reference surface	$0.2079 \ m^2$
Vehicle Mass	49.665 kg
Solar Radiation Pressure (Psr)	$4.56e-06 \ N/m^2$
SRP reference area	$0.189 \ m^2$
Reflection coefficient	1.26
S/C Fixed attitude	Earth pointing
Initial coordinate system	J2000
Earth rotation rate	7.29211585530E-5 rad/s
Earth gravitational constant	$398600.4415E+9 \ km^3/s^2$

Note that some of the entries in Table 27 are referred to explicit settings of the Spirent Simulator GUI software [35]: they were selected in order to obtain the most possible precise orbit model. No advanced settings on the spacecraft model were possible on the NAVX–NCS GNSS GUI. Results collected during the test sessions were included in a dedicated report and submitted to ESA for review purpose[32].

5.2.1 Acquisition routine testing

The first testing sessions took place at the Istituto Superiore Mario Boella (ISMB), Turin (Italy), using a NAVX–NCS GNSS simulator and the second EBB model of the Payload, with COTS front-end with removed COCOM limitations [Figure 115]. The first investigation was focused on the overall real-time behaviour of the application software and on the assessment of the acquisition routine performance, while working with GPS signal modelled as if the receiver is on-board a LEO spacecraft.
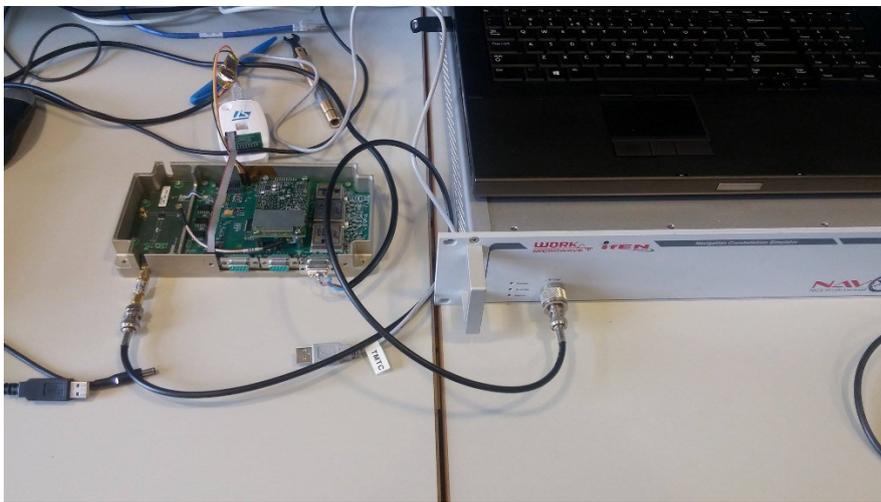
Figure 115 : Functional test with GPS signal simulator at ISMB, Turin

Following the results of similar tests, previously performed at the ESTEC facilities only on the COTS front-end (see Section 4.6.3), this time the entire payload in its final configuration was verified. After setting the scenario and powering on of the simulator, the GPS Payload was left free to perform autonomous setting of the tracking channels, following the GPS signal acquisition procedure foreseen also for the real mission and described in the details in Section 5.1.3. During this test, the acquisition process was visually monitored through the laptop terminal using the Putty software, thanks to the TRACKSTAT log message. The application software was set to transmit every log message received from the Novatel front end through the diagnostic serial communication port, in order to allow a fast real-time check of the Payload behaviour. A sample of the TRACKSTAT log obtained during one test session is the following (colours were added to highlight meaningful fields):

TRACKSTATA,COM1,0,66.0,UNKNOWN,0,90.000,006c0000,457c,12997;

INSUFFICIENT_OBS,NONE,5.0,20,

1,0,88008002,0.000,**-9332.000**,0.000,0.000,0.000,**NA**,0.000,

2,0,88008022,0.000,**6698.000**,0.000,0.000,0.000,**NA**,0.000,

3,0,88008043,0.000,**6855.000**,0.000,0.000,0.000,**NA**,0.000,

4,0,88008062,0.000,**-8700.000**,0.000,0.000,0.000,**NA**,0.000,

5,0,88008082,0.000,**3116.000**,0.000,0.000,0.000,**NA**,0.000,

6,0,880080a2,0.000,**2001.000**,0.000,0.000,0.000,**NA**,0.000,

7,0,880080c2,0.000,**2541.000**,0.000,0.000,0.000,**NA**,0.000,

8,0,880080e2,0.000,**-1214.000**,0.000,0.000,0.000,**NA**,0.000,

9,0,88008102,0.000,**-5594.000**,0.000,0.000,0.000,**NA**,0.000,

10,0,88008123,0.000,**4327.552**,0.000,0.000,0.000,**NA**,0.000,

11,0,88008143,0.000,**2016.000**,0.000,0.000,0.000,**NA**,0.000,

12,0,88008162,0.000,**-8520.000**,0.000,0.000,0.000,**NA**,0.000,

13,0,88008182,0.000,**-9817.000**,0.000,0.000,0.000,**NA**,0.000,

14,0,880081a2,0.000,**2752.000**,0.000,0.000,0.000,**NA**,0.000,

15,0,880089c4,0.000,**-8550.171**,52.440,14.600,0.000,**NA**,0.000*aa26effc

Since the previous sample was received at the beginning of the acquisition phase, right after the first log request was sent, it shows how none of the channels has locked any PRN signal. The first row is the header with the log name, which is used to recognize it from other logs and to address the message to the exact processing routine. The first field (in red) of the second row includes useful information about the solution status. In this case, the log reports "INSUFFICIENT_OBS", which means that the number of tracked PRN, if any, is not sufficient to process the solution. According to the COTS front-end firmware manual, the possible solution status words that can be obtained from the TRACKSTAT log are included in Figure 116. Once that at least 4 GPS satellites signals are obtained and no software or hardware problem occurres, the status word turns to "SOL_COMPUTED". Starting from the third row of the log message, a set of parameters for every channel is present: because of the initial setting of the routine, the first field of every channel set of parameters (in green) is the PRN number that is being tracked. The initial setting covers all PRN in numerical order from 0 to 15. As soon as a complete frequency range inspection is performed for a specific PRN number, it is changed to the next PRN in numerical order not yet assigned to another channel. For each channel, the fifth field (in yellow), is the instantaneous frequency error used to seek the GPS signal. At the beginning of the acquisition phase, every channel is set with 0Hz of frequency offset around the signal central frequency and 10kHz of

frequency error. As it is possible to see from the previous log message, every frequency value is included in the range of -10kHz and +10kHz, namely 10kHz around the central frequency.

Solution Status (Binary)	Solution Status (ASCII)	Description
0	SOL_COMPUTED	Solution computed
1	INSUFFICIENT_OBS	Insufficient observations
2	NO_CONVERGENCE	No convergence
3	SINGULARITY	Singularity at parameters matrix
4	COV_TRACE	Covariance trace exceeds maximum (trace > 1000 m)
5	TEST_DIST	Test distance exceeded (maximum of 3 rejections if distance >10 km)
6	COLD_START	Not yet converged from cold start
7	V_H_LIMIT	Height or velocity limits exceeded (in accordance with export licensing restrictions)
8	VARIANCE	Variance exceeds limits
9	RESIDUALS	Residuals are too large
13	INTEGRITY_WARNING	Large residuals make position unreliable
18	PENDING	When a FIX POSITION command is entered, the receiver computes its own position and determines if the fixed position is valid [a]
19	INVALID_FIX	The fixed position, entered using the FIX POSITION command, is not valid
20	UNAUTHORIZED	Position type is unauthorized - HP or XP on a receiver not authorized for it

Figure 116: Solution Status words

The third important parameter of the channel row, is the ninth field, that provides the observation status, using dedicated words, selected from the list in Table 28.

Table 28: Observation status words

GOOD	Observation is good
BADHEALTH	Satellite is flagged as bad health in ephemeris or almanac
OLDEPHEMERIS	Ephemeris >3 hours old
ELEVATIONERROR	Satellite was below the elevation cutoff
MISCLOSURE	Observation was too far from predicted value
NODIFFCORR	No differential correction available
NOEPHEMERIS	No ephemeris available
LOCKEDOUT	Satellite has been locked out
LOWPOWER	Satellite has low signal power
NOIONOCORR	No ionosphere delay correction was available
NOTUSED	Observation was not used in the solution
OBSL1	An L1 observation not directly used in the solution
NA	No observation available

Usually at the beginning of the acquisition phase, the status is "NA", since the PRN signal is not acquired yet. For the acquisition routine purpose, the channel is considered ready only when "GOOD" word is provided by the TRACKSTAT log. When this happens, that channel is excluded from parameters adjustment.

The following sample of TRACKSTAT log was acquired during the same test session but at the end of the routine.

#TRACKSTATA,COM1,0,70.0,FINE,1944,395280.000,00680000,457c,12997;

SOL_COMPUTED,SINGLE,5.0,20,

29,0,88008002,0.000,646.000,0.000,0.000,0.000,NA,0.000,

30,0,88008022,0.000,-9627.000,0.000,0.000,0.000,NA,0.000,

31,0,88008043,0.000,10256.000,0.000,0.000,0.000,NA,0.000,

5,0,88008062,0.000,8700.000,0.000,0.000,0.000,NA,0.000,

4,0,88008082,0.000,-6866.000,0.000,0.000,0.000,NA,0.000,

6,0,88009ca4,22479522.225,-16857.869,52.396,1185.220,-0.040,GOOD,0.172,

3,0,88009cc4,22147405.270,4808.221,52.421,25.060,0.010,GOOD,0.184,

2,0,880080e2,0.000,-10208.000,0.000,0.000,0.000,NA,0.000,

23,0,98009d04,21712371.991,-16318.001,52.416,262.300,0.049,GOOD,0.190,

1,0,88008122,0.000,-7397.000,0.000,0.000,0.000,NA,0.000,

11,0,88009d44,22200970.799,-21895.516,52.413,1174.960,-0.006,GOOD,0.183,

25,0,88008163,0.000,-31919.000,0.000,0.000,0.000,NA,0.000,

26,0,88008182,0.000,-33275.000,0.000,0.000,0.000,NA,0.000,

27,0,880081a2,0.000,-31628.000,0.000,0.000,0.000,NA,0.000,

28,0,880081c1,0.000,18000.000,0.000,0.000,0.000,NA,0.000,

27,0,08009de4,20336045.205,16998.635,52.408,12.490,-0.016,GOOD,0.209*ef9d8fe7

It is possible to notice the following variations with respect to the first message log:

- The first field of the seconds row (in red) reports, "SOL_COMPUTED", meaning that at least 4 GPS satellites signal was acquired.

144

- The observation status word (in blue) of PRN 6, 3, 23, 11, 27, tracked respectively by channels 5, 6, 8, 10, 15 reports "GOOD", meaning that for this PRN the observation is available and can be used to be processed by the navigation filters.

Table 29 includes the number of epochs used by the acquisition routine to lock the signal with at least 4 satellites during several test sessions. Scenario setting was modified in order to provide different starting condition of the GPS constellation: they were successive time intervals of the same long simulation or completely different periods.

Table 29: Acquisition time

VERIFICATION ISSUE	Number of epochs before acquisition complete	Seconds before acquisition complete
TEST #1	17	510s
TEST #2	15	450s
TEST #3	19	570s
TEST #4	20	600s
TEST #5	9	270s
TEST #6	17	510s
TEST #7	11	330s
TEST #8	8	240s
TEST #9	19	570s
TEST #10	25	750s
TEST #11	11	330s
TEST #12	19	570s
TEST #13	14	420s
TEST #14	27	810s
TEST #15	14	420s
TEST #16	18	540s
TEST #17	11	330s
TEST #18	8	240s
TEST #19	11	330s
TEST #20	18	540s
TEST #21	5	150s
TEST #22	6	180s
TEST #23	9	270s
TEST #24	10	300s
TEST #25	8	240s
TEST #26	15	330s
TEST #27	11	330s
TEST #28	12	360s

TEST #29	9	270s
TEST #30	10	300s
MEAN		402s (6.7m)
STD		163.3s
RMS		433.9s (7.23m)

Figure 117 shows the GPS satellites signal acquisition profile for TEST#1 and the related TRACKSTAT logs transcription is included in ANNEX 4.
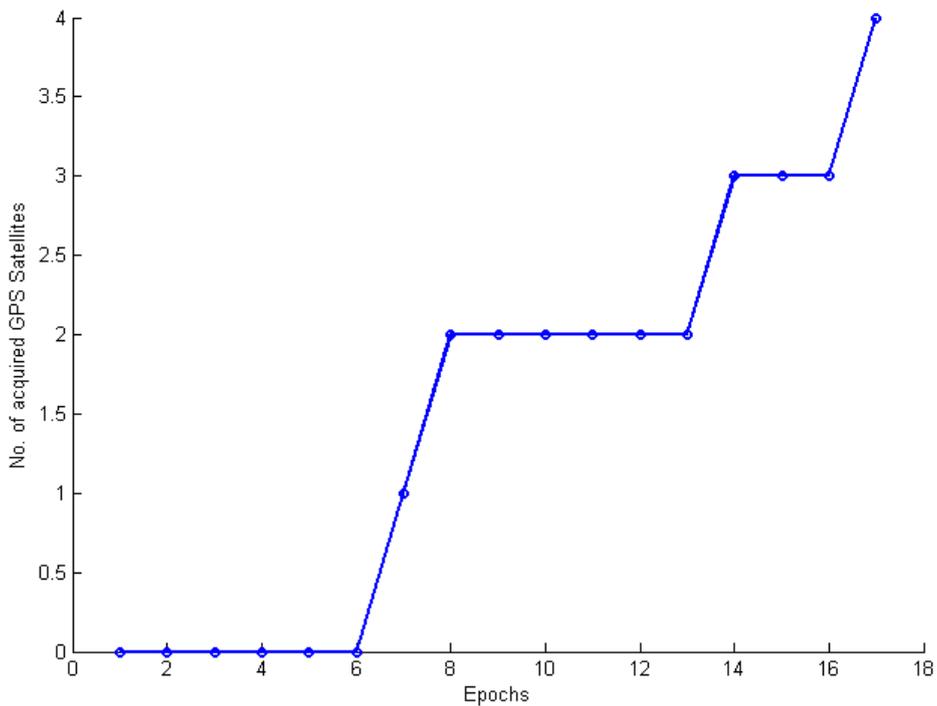
Figure 117: TEST #1 PRN acquisition profile

This test demonstrated the capability of the software to correctly lock and track the signal with a sufficient number of GPS satellite in a reasonable time: in over 30 verifications, the acquisition routine was always able to obtain a complete and stable link with acquisition time rms below 8 minutes.

5.2.2 Kinematic filter test

During the second phase of the software verification, the kinematic filter was tested and its outputs were processed and studied with the support of the signal simulator available at ISMB. As a reference, to assess the performance of the kinematic filter, the "real" position as provided by the simulator was used: the spacecraft scenario was prepared with the parameters included in Table 26 and the simulator was set to provide as output the data log, including spacecraft user positions in intervals of 1s. This series of tests at the simulator was also

146

very useful to perform an extensive debugging of the navigation filters, that would have been difficult to perform off line. Once that the final adjustments were applied to the code, some data acquisitions were performed, considering a position fix every 30 seconds. To perform processing of the kinematic filter results, the code was set to write to the diagnostic serial communication port the position computed every epoch by the active filter. The content of the Putty terminal was then saved in a txt file and processed using Matlab dedicated routines to calculate the positioning error in ECEF coordinates. The code was also set to maintain the Kinematic Mode for the entire length of the test sessions, without switching to reduced dynamic mode. During the test, the performance was assessed through visual inspection of the data received on the Putty log on the laptop, to obtain preliminary real-time information about the filter functionality and, in case behaviour not coherent with expectations, to allow to interrupt the simulation, inspect and fix errors, and then start again. The output statistics processing was performed off-line using the saved logs from the terminal. Besides the position provided by the active filter in ECEF coordinates and the reference spacecraft trajectory, other parameters were saved:

- GPS raw observations: epoch-wise pseudorange and carrier phase for each satellite in view

- GPS satellites ephemeris

- TIME log data

With this complete set of parameters, it was possible to reconstruct the test sessions off line, using the IAR embedded workbench capabilities to run the embedded software in "simulation mode", without the need of the hardware. All data usually provided by the front-end every epoch was simulated providing necessary parameters at the right epoch, extracted from the test logs using dedicated Matlab routines. This procedure allowed to perform further code debugging and filters adjustments and tuning, without the need to physically have the GPS signal simulator or GPS Payload hardware. In addition, part of the offline Kinematic filter testing was performed using data obtained also from the simulation sessions performed at NGI (see next Section).

The main results of the test sessions, performed in real-time or in off line post processing are summerized in the following tables and figures, along with the Kinematic Mode error statistics.

Session 1

- Data set length: 182 epochs (Table 30)

Table 30: Session 1 simulation time

	Start	End
Year	2017	2017
Month	4	4
Day	13	13
Hour	12	14

Minutes	56	27
Seconds	42	42

- Data set collected in: Turin

- Simulator: NAVX–NCS GNSS

- Real-time filter output: yes

The results of this test session, in terms of position accuracy, are displayed in Figure 118 while error statistics is included in Table 31.
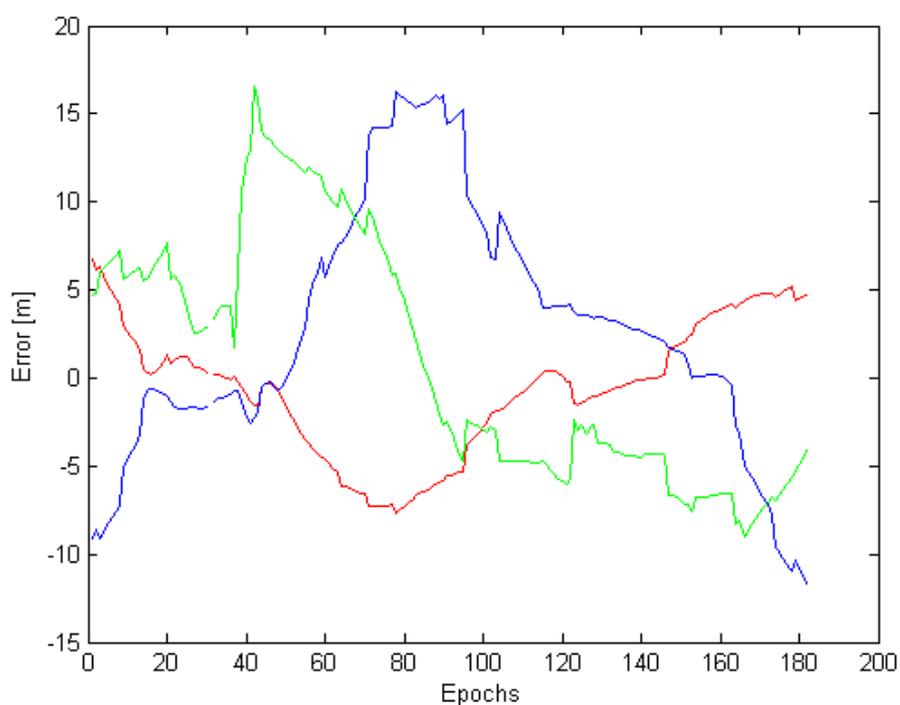
Figure 118: Tests Session 1 Error Plot in ECEF coordinates: x component (red), y component (blue) and the z component (green)

Table 31: Kinematic position error for one orbit

x position error mean (m)	-0.599
x position error STD (m)	3.719
y position error mean (m)	2.639
y position error STD (m)	7.065
z position error mean (m)	0.915
z position error STD (m)	6.943
3D RMS (m)	10.959

The position calculated by the kinematic mode has an accuracy of 10.959 m 3D RMS, that meets the expectations (<15m).

Session 2

- Data set length: 174 epochs (Table 32)

Table 32: Session 2 simulation time

	Start	**End**
Year	2017	2017
Month	7	7
Day	25	25
Hour	0	1
Minutes	9	36
Seconds	45	15

- Data set collected in: Nottingham

- Simulator: SPIRENT

The results of this test session are displayed in Figure 119 while error statistics is included in Table 33.
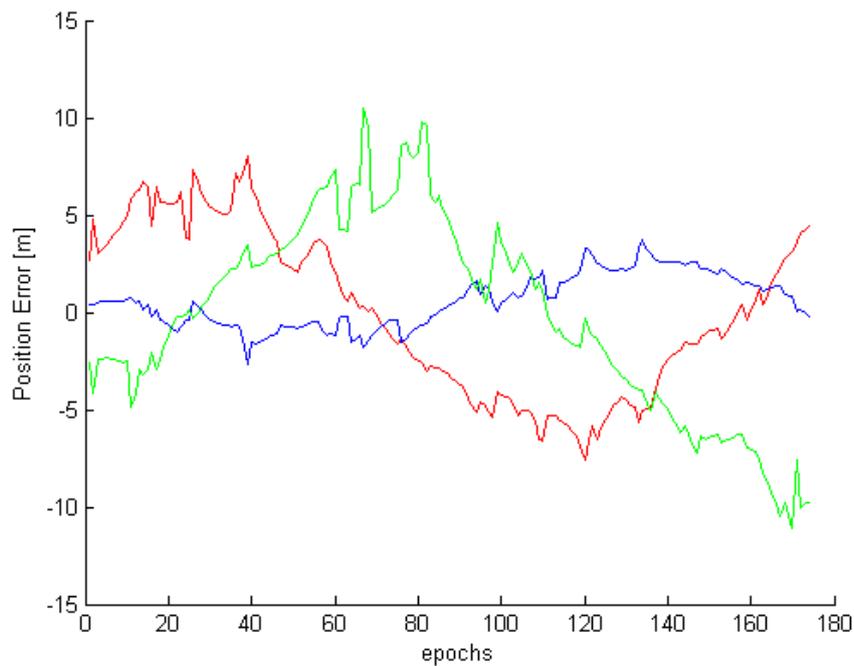
Figure 119: Tests Session 2 Error Plot in ECEF coordinates: x component (red), y component (blue) and the z component (green)

Table 33: Kinematic positioning error for one orbit

x position error mean (m)	-0.004
x position error STD (m)	4.230
y position error mean (m)	0.579
y position error STD (m)	1.360
z position error mean (m)	-0.254
z position error STD (m)	5.044
3D RMS (m)	6.753

The position calculated by the kinematic mode has an accuracy of 6.753 m 3D RMS, that meets the expectations (<10m).

5.2.3 Reduced dynamic filter test

Thanks to the high quality of the orbit model provided by the Spirent Simulator, the Reduced Dynamic Mode could be debugged and tested at the NGI facilities. As far as it is understood from to the Simgen Software User Manual, it is possible to achieve a level of accuracy in setting the orbital scenario that is suitable for assessing the performance of the Reduced Dynamic Filter. The simulator orbit model includes at least:

- Earth gravity model (order up to 70)

- Sun and Moon gravitational effects

- Solar radiation pressure

- Aerodynamic drag

As done during the previous tests, the output of the Dynamic Filter was collected through the diagnostic serial interface and then processed with dedicated Matlab routines. Before starting performing a complete acquisition session, several shorter tests were performed to fix bugs in the filter structure and orbit model, hard to detect without a complete application software test with realistic space-based observables. The simulator was set with the parameters included in Table 27. Since the purpose was also to test the entire application software, in its flight configuration, the starting navigation mode was the kinematic solution. The only difference from nominal conditions was represented by the software simulation of a telecommand to switch after two epochs to Reduced Dynamic Mode.

As initial tuning of the Kalman Filter Q matrix, the solution proposed by Avanzi et al. 2014 [6] for reduced dynamic studies on GRACE mission observables was used. Although the two spacecrafts, ESEO and GRACE,

are quite different in terms of physical properties, their orbit is sufficiently similar to use the process noise covariance matrix tuned for the latter, as a starting point to assess the orbit determination performance.

The simulation time of the session is included in Table 34.

Table 34: Reduced dynamic test session simulation time

	Start	End
Year	2017	2017
Month	7	7
Day	25	25
Hour	0	1
Minutes	9	36
Seconds	45	15

The preliminary results with initial tentative tuning of the Q matrix displayed an RMS of 7.631 m, which indicates an improvement with respect to the kinematic solution but also a need of appropriate tuning of the reduced dynamic filter, to rise its accuracy and reach the expected value (≈1m). The first real improvement in the performance was obtained by introducing a wider receiver clock error covariance, in order to take into account the poor clock accuracy of the COTS front-end. Finally, also the covariance of the empirical accelerations coordinates was extended to consider possible discrepancies between the filter model and the one included in the simulator and the error between the simulated model and the real world. Once completed this tuning procedure, a definitely more acceptable behaviour was obtained from the reduced dynamic solution, with a final 3D rms error of 1.378 m, after a transient of ~50 epochs as shown in Figure 120 and Table 35.
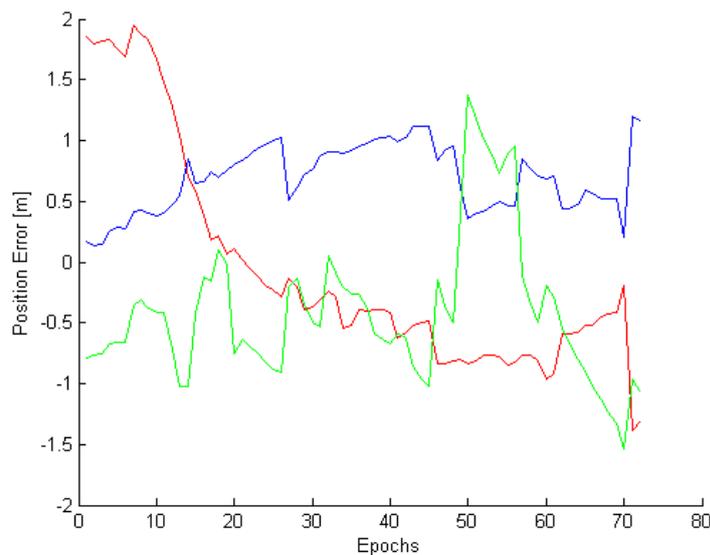
Figure 120: Reduced dynamic Error Plot in ECEF coordinates: x component (red), y component (blue) and the z component (green)

Table 35 Reduced dynamic positioning error for one orbit

x position error mean (m)	-0.063
x position error STD (m)	0.909
y position error mean (m)	0.685
y position error STD (m)	0.277
z position error mean (m)	-0.417
z position error STD (m)	0.590
3D RMS (m)	1.378

Although the final error rms is close to, but not lower than, the target threshold of 1m, the result of the last tuning procedure can be considered a good result, considering that GPS observations are simulated and the trajectory of the ESEO spacecraft is based on a simplified version of the real set of forces acting on the spacecraft. For this reason, the performance assessment of a navigation technique based on a different orbit model on ground, without real observations, is not an easy task. In fact, it implies the comparison of two models that have probably different errors with respect of the real world. However, this result can be considered a starting point to perform a successive finer tuning in real-time during the mission, after post processing of the data on ground. Unfortunately due to the tight schedule of the ESEO mission no further testing of the reduced dynamic filter was possible, e.g. for longer testing session. In fact the EBB and PFM models of the GPS Payload were required by SITAEL to perform the Test Readiness Review and qualification test.

6 CONCLUSIONS

This thesis presented the design, development and testing process of a GPS-based navigation sub-system for small satellite platforms. The proposed architecture is related to the specific version of this sub-system specifically prepared for ESEO microsatellite mission, sponsored by ESA Education office, but it can be adapted to different satellite platforms and missions with simple modifications to the hardware and software design. Since this PhD project was performed as part of a real space mission, it covered all the aspects and phases of the development of a sub-system for space applications, starting after the hardware preliminary design, previously performed by the author as part of his Master Thesis project. During the presentation of this work, the effort to adapt such a sub-system to small satellite missions, usually characterized by limited budget, internal volume, mass and power consumption, was highlighted. This thesis covered the following aspects:

- Hardware critical design

- Test campaign

- Application software development

- Software performance assessment

These topics are briefly summarized in the following sections and some conclusions are drawn in the end, drafting possible future developments of this project.

6.1 Hardware critical design

The ESEO GPS payload hardware design was covered entirely, considering both the custom electronic PCBs and the mechanical external enclosure. For what concerns the electronic design, a mixed configuration of COTS components and custom parts was selected, in order to meet the needs of small satellite missions in terms of low cost and fast development. The customized parts, namely the navigation computer and the amplification stage, were designed and routed taking into account the requirements of high reliability for every system that is meant to operate in space, due to the dangerous effect of space radiations on electronic devices. The front-end component was selected among the commercial receivers that implement the simplest architecture and is used inside the payload as a raw observation provider, leaving the position processing role to the navigation computer. The aluminum enclosure was designed to provide both the necessary mechanical interface with the ESEO platform and an adequate resistance to the launch dynamic stresses to the payload. Two EBB model were produced to perform hardware and software design validation, while the PFM model is currently used to perform the qualification test campaign and integration with ESEO spacecraft, in view of the preparations for launch.

6.2   Test Campaign

This thesis presented also a description of the procedures and results of the GPS Payload test campaign, that represents a critical and time-consuming part of the development of a sub-system for space applications. The thorough characterization of the payload functionality under the harsh external conditions is of outmost importance, due to the impossibility to perform fixing or replacement of damaged parts after the launch. To achieve the required level of confidence in the design, the payload parts were first tested separately and then fully assembled in flight configuration to obtain general baseline functionality of the device. The COTS front-end behaviour was characterized through several test sessions on ground and with the support of a GNSS simulator to generate the GPS signal as received from a user in space. Differently, the single navigation computer was electrically checked to verify its conformance with sub-system level requirements, due to the criticality of this custom component that manages power to all other parts of the payload. The whole payload, in flight configuration, was then subject to functional verification to assess its correct internal communication and two environmental tests, thermal and vibration, so to demonstrate the suitability of the device to operate on board a spacecraft.

6.3   Software development and testing

The third part of this project covered the development and validation of the application software hosted by the microprocessor of the navigation computer. It implements the software components needed to:

- handle the data exchange between the navigation computer and the two front-ends and between the payload and the on board data handling sub system of the ESEO platform;

- process the raw observations received from the Novatel receiver with two navigation algorithms;

- monitor the correct functionality of the two front-ends and control their operations;

- handle the telecommands received from the ground and translate them into payload mode changes or navigation filter parameters variation;

The two implemented navigation modes provide different level of accuracy: the Kinematic Mode includes the default navigation algorithm based on a least square solution, that uses only the code observables to compute the receiver position with an expected error below 10-15 m 3d rms; the Reduced Dynamic filter combines the information coming from a precise model of the spacecraft orbit with the pseaudorange and carrier phase measurements. The latter filter implements also the GRAPHIC ionospheric free combination of the two type of measurements with an expected error in the final position around 1m 3d rms. The application software validation was possible thanks to the availability of the GNSS simulators provided by Istituto Superiore Mario Boella and the Nottingham Geospatial Institute. Setting a scenario of a receiver moving along a low Earth orbit, the performance of both navigation algorithms was assessed, providing satisfactory results with respect

to the expectations. However, the final part of the Reduced Dynamic filter testing and tuning will be performed in orbit using real observations, as the GPS Payload main task.

6.4   Final Considerations

As a sub-system designed for a specific space mission, the development of the ESEO GPS Payload presented in this thesis includes all technical activities performed to produce a navigation device that is meant to be integrated inside a spacecraft to operate in space following a precise schedule. However the work linked to the GPS Payload cannot be considered concluded with the formal delivery of the sub-system, but will continue during the next years with mission operations and mission data processing. In fact, since the ESEO mission will be the first flight of this GPS receiver, its performance and behaviour shall be monitored, providing continuous support during the entire mission lifetime. In particular, as highlighted during previous sections, the processing of data collected during the mission are a critical part that will lead to further navigation filters adjustments. According to the current state of development of the GPS Payload, the final version of hardware and software will be delivered once the qualification test campaign, currently on-going on the proto-flight model, will be finished. Integration with the ESEO spacecraft will follow and the current project schedule foresees the launch in Q4 2018. After launch, the ESEO spacecraft will be operative for a minimum of 6 months, and during this period the scientific data produced by the GPS Payload will be constantly downloaded to the ground. Here these data will be analysed using, as a reference orbit, the trajectory obtained by processing the raw GPS observations generated on board. This data elaboration step will enable a fine- tuning of the Reduced Dynamic Filter, to finally assess the GPS Payload performance in real-time operations.

The work described in this thesis was partially described in the following conference papers:

- A. Avanzi, A. Locarini, P. Tortora, "Real-time precise orbit determination of the ESA ESEO spacecraft" 10th IAA Symposium on Small Satellites for Earth Observation, Berlin, Germany, April 20-24, 2015, paper: IAA-B10-1405P

- D. Modenini, M. Bosco, A. Locarini, P. Tortora, "Space Engineering and Small Satellites Education Activities at University of Bologna", 1st Symposium on Space Educational Activities, Padova, 9 – 10 December 2015

- A. Locarini, A. Avanzi, P. Tortora, "Development and Test Campaign of a GPS-Based Navigation Sub-System for the ESEO Mission", 3rd Metrology for Aerospace, Florence, Italy, 22 – 23 June 2016

- A. Locarini, A. Lucci, D. Modenini, P. Tortora, "Ground segment solutions for small satellites", AIDAA 2017 XXIV International Conference, Palermo/Enna, Italy, 18 – 22 September 2017

- A. Locarini, A. Avanzi, D. Modenini, P. Tortora, "On-board precise GPS navigation solution for small satellite missions", AIDAA 2017 XXIV International Conference, Palermo/Enna, Italy, 18 – 22 September 2017

Looking beyond the conclusion of the the ESEO mission, this project can be considered a first step in the development of a range of GNSS navigation sub-systems for small satellite platforms, including the following future developments:

- Replacement of Novatel front-end, with a custom baseband processor directly embedded in the navigation computer.

- Testing of the navigation device within small satellites missions that are high demanding in terms of position accuracy, such as formation flight.

- Scaling the sub-system to cubesat platforms, that represents a standard bus widely used in space industry and research, facing the even more limiting requirements in terms of volume, mass and power consumption.

- Implementation of the GALILEO constellation signal tracking, to improve the navigation performance.

ANNEX 1. HK data set

Table 36: GPS HK data

Label	Data type	Description	Default value	Monitor range	Monitor action	Scaling	Units	EDAC
GPS_REC_MODE	UNSINGED8	ESEO GPS receiver mode coded according to **GPS_REC_MODE value / Mode definition** 0x00 — Initialization sequence 0x01 — Diagnostic mode 0x02 — Front-end power up and configuration 0x04 — Kinematic positioning 0x08 — Reduced dynamic positioning 0x10 — Safe mode Table 38	0x00	NA	NA	NA	NA	
GPS_TEMPERATURE_1	SIGNED16	PCB mounted temperature sensor value	NA	-100 to 700		0.1	°C	
GPS_TEMPERATURE_2	SIGNED16	Chassis mounted temperature sensor value	NA	-100 to 700		0.1	°C	
GPS_FREND_M_VOLT	UNSIGNED16	Main COTS front-end input voltage	3300	0 to 3500		1.0	mV	
GPS_FREND_R_VOLT	UNSIGNED16	Redundant COTS front-end input voltage	3300	0 to 3500		1.0	mV	
GPS_FREND_M_STATUS	UNSIGNED32	Main COTS receiver status as defined in **Bit / COTS front-end status / Bit=0 / Bit=1** 0 — Error flag — No error — Error 1 — Temperature status — OK — Warning 2 — Voltage supply status — OK — Warning 3 — Antenna power status — Powered — Not Powered 4 — LNA Failure — —	0x00000000	NA	NA	NA	NA	

Within the GPS_REC_MODE value table:

GPS_REC_MODE value	Mode definition
0x00	Initialization sequence
0x01	Diagnostic mode
0x02	Front-end power up and configuration
0x04	Kinematic positioning
0x08	Reduced dynamic positioning
0x10	Safe mode

Within the GPS_FREND_M_STATUS table:

Bit	COTS front-end status	Bit=0	Bit=1
0	Error flag	No error	Error
1	Temperature status	OK	Warning
2	Voltage supply status	OK	Warning
3	Antenna power status	Powered	Not Powered
4	LNA Failure		

5	Antenna open flag	OK	Open
6	Antenna shorted flag	OK	Shorted
7	CPU overload flag	No overload	Overload
8	COM1 buffer overrun flag	No overrun	Overrun
9	COM2 buffer overrun flag	No overrun	Overrun
10	COM3 buffer overrun flag	No overrun	Overrun
11	Link overrun flag	No overrun	Overrun
12	Reserved		
13	Aux transmit overrun flag	No overrun	Overrun
14	AGC out of range		
15	Reserved		
16	Reserved		
17	Reserved		
18	Almanac flag/UTC known	Valid	Invalid
19	Position solution flag	Valid	Invalid
20	Position fixed flag	Not fixed	Fixed
21	Clock steering status	Enabled	Disabled
22	Clock model flag	Valid	Invalid
23	External oscillator locked flag	Unlocked	Locked
24	Software resource	OK	Warning
25	Reserved		
26	Reserved		
27	Reserved		
28	Reserved		
29	Auxiliary 3 status event flag	No event	Event
30	Auxiliary 2 status event flag	No event	Event
31	Auxiliary 1 status event flag	No event	Event

Table 39

158

GPS_FREND_R_STATUS	UNSIGNED32	Redundant COTS receiver status as defined in	0x00000000	NA	NA			

Bit	COTS front-end status	Bit=0	Bit=1
0	Error flag	No error	Error
1	Temperature status	OK	Warning
2	Voltage supply status	OK	Warning
3	Antenna power status	Powered	Not Powered
4	LNA Failure		
5	Antenna open flag	OK	Open
6	Antenna shorted flag	OK	Shorted
7	CPU overload flag	No overload	Overload
8	COM1 buffer overrun flag	No overrun	Overrun
9	COM2 buffer overrun flag	No overrun	Overrun
10	COM3 buffer overrun flag	No overrun	Overrun
11	Link overrun flag	No overrun	Overrun
12	Reserved		
13	Aux transmit overrun flag	No overrun	Overrun
14	AGC out of range		
15	Reserved		
16	Reserved		
17	Reserved		
18	Almanac flag/UTC known	Valid	Invalid
19	Position solution flag	Valid	Invalid
20	Position fixed flag	Not fixed	Fixed
21	Clock steering status	Enabled	Disabled
22	Clock model flag	Valid	Invalid
23	External oscillator locked flag	Unlocked	Locked
24	Software resource	OK	Warning
25	Reserved		
26	Reserved		
27	Reserved		
28	Reserved		

(NA, NA appear in the rightmost columns of the outer table)

29	Auxiliary 3 status event flag	No event	Event
30	Auxiliary 2 status event flag	No event	Event
31	Auxiliary 1 status event flag	No event	Event

Table 39

GPS_FREND_M_TIM_STAT | UNSIGNED8 | Main COTS receiver time status coded according to | 0x00 | NA | NA | | NA | NA |

GPS_FREND_X_TIM_STAT value (hex)	GPS Reference Time Status ASCII	Time status definition
0x14	UNKNOWN	Time validity is unknown
0x3C	APPROXIMATE	Time is set approximately
0x50	COARSEADJUSTING	Time is approaching coarse precision
0x64	COARSE	This time is valid to coarse precision
0x78	COARSESTEERING	Time is coarse set and is being steered
0x82	FREEWHEELING	Position is lost and the range bias cannot be calculated
0x8C	FINEADJUTING	Time is adjusting to fine precision
0xA0	FINE	Time has fine precision

160

		FINEBACKUPSTEERING	Time is fine and is being steered by the backup system						
		0xAA							
		FINESTEERING	Time is fine set and is being steered						
		0xB4							

Table 40

GPS_FREND_R_TIM_STAT	UNSIGNED8	Redundant COTS receiver time status coded according to			0x00	NA	NA		

GPS_FREND_X_TIM_STAT value (hex)	GPS Reference Time Status ASCII	Time status definition
0x14	UNKNOWN	Time validity is unknown
0x3C	APPROXIMATE	Time is set approximately
0x50	COARSEADJUSTING	Time is approaching coarse precision
0x64	COARSE	This time is valid to coarse precision
0x78	COARSESTEERING	Time is coarse set and is being steered
0x82	FREEWHEELING	Position is lost and the range bias cannot be calculated
0x8C	FINEADJUTING	Time is adjusting to fine precision

NA NA

		0xA0	FINE	Time has fine precision							
		0xAA	FINEBACKUPSTEERING	Time is fine and is being steered by the backup system							
		0xB4	FINESTEERING	Time is fine set and is being steered							

Table 40

GPS_WEEK	UNSIGNED16	GPS week				NA	NA	NA	NA	week	
GPS_SECONDS_OF_WEEK	UNSIGNED32	Seconds of the GPS week accurate to the millisecond				NA	NA	NA	NA	ms	
GPS_SATVIS	UNSIGNED32	Visible satellites according to				0x00000000	NA	NA	NA	NA	

Bit	GPS satellite PRN	Bit=0	Bit=1
0	01	Not visible	Visible
1	02	Not visible	Visible
2	03	Not visible	Visible
3	04	Not visible	Visible
4	05	Not visible	Visible
5	06	Not visible	Visible
6	07	Not visible	Visible
7	08	Not visible	Visible
8	09	Not visible	Visible
9	10	Not visible	Visible
10	11	Not visible	Visible
11	12	Not visible	Visible
12	13	Not visible	Visible
13	14	Not visible	Visible
14	15	Not visible	Visible
15	16	Not visible	Visible
16	17	Not visible	Visible
17	18	Not visible	Visible

162

		18	19	Not visible	Visible						
		19	20	Not visible	Visible						
		20	21	Not visible	Visible						
		21	22	Not visible	Visible						
		22	23	Not visible	Visible						
		23	24	Not visible	Visible						
		24	25	Not visible	Visible						
		25	26	Not visible	Visible						
		26	27	Not visible	Visible						
		27	28	Not visible	Visible						
		28	29	Not visible	Visible						
		29	30	Not visible	Visible						
		30	31	Not visible	Visible						
		31	32	Not visible	Visible						
		Table 41									
GPS_FIX_DAYS_J2000	UNSIGNED32	Current fix time, days past J2000				NA	NA	NA	NA	NA	
GPS_FIX_MS_OF_DAY	UNSIGNED32	Current fix time, milliseconds of day				NA	NA	NA	NA	NA	
GPS_FIX_X_ICRF	SIGNED32	Position fix in ICRF J2000, X axis				NA	NA	NA	NA	cm	
GPS_FIX_Y_ICRF	SIGNED32	Position fix in ICRF J2000, Y axis				NA	NA	NA	NA	cm	
GPS_FIX_Z_ICRF	SIGNED32	Position fix in ICRF J2000, Z axis				NA	NA	NA	NA	cm	
GPS_FREND_M_ERROR	UNSIGNED32	Main COTS receiver error as defined in				0x00000000	NA	NA	NA	NA	
GPS_FREND_R_ERROR	UNSIGNED32	Redundant COTS receiver error as defined in				0x00000000	NA	NA	NA	NA	
GPS_REC_ERROR	UNSGINED32	ESEO GPS receiver error coded according to				0x00000000	NA	NA	NA	NA	

Table 37: GPS_REC_MODE definition

GPS_REC_MODE value	Mode definition
0x00	Initialization sequence
0x01	Diagnostic mode
0x02	Front-end power up and configuration
0x04	Kinematic positioning
0x08	Reduced dynamic positioning
0x10	Safe mode

Table 38: COTS receiver status definition

Bit	COTS front-end status	Bit=0	Bit=1
0	Error flag	No error	Error
1	Temperature status	OK	Warning
2	Voltage supply status	OK	Warning
3	Antenna power status	Powered	Not Powered
4	LNA Failure		
5	Antenna open flag	OK	Open
6	Antenna shorted flag	OK	Shorted
7	CPU overload flag	No overload	Overload
8	COM1 buffer overrun flag	No overrun	Overrun
9	COM2 buffer overrun flag	No overrun	Overrun
10	COM3 buffer overrun flag	No overrun	Overrun
11	Link overrun flag	No overrun	Overrun
12	Reserved		
13	Aux transmit overrun flag	No overrun	Overrun
14	AGC out of range		
15	Reserved		
16	Reserved		
17	Reserved		
18	Almanac flag/UTC known	Valid	Invalid
19	Position solution flag	Valid	Invalid
20	Position fixed flag	Not fixed	Fixed
21	Clock steering status	Enabled	Disabled
22	Clock model flag	Valid	Invalid
23	External oscillator locked flag	Unlocked	Locked
24	Software resource	OK	Warning
25	Reserved		
26	Reserved		
27	Reserved		
28	Reserved		
29	Auxiliary 3 status event flag	No event	Event
30	Auxiliary 2 status event flag	No event	Event
31	Auxiliary 1 status event flag	No event	Event

Table 39: COTS receiver time status definition

GPS_FREND_X_TIM_STAT value (hex)	GPS Reference Time Status ASCII	Time status definition
0x14	UNKNOWN	Time validity is unknown
0x3C	APPROXIMATE	Time is set approximately
0x50	COARSEADJUSTING	Time is approaching coarse precision
0x64	COARSE	This time is valid to coarse precision
0x78	COARSESTEERING	Time is coarse set and is being steered
0x82	FREEWHEELING	Position is lost and the range bias cannot be calculated
0x8C	FINEADJUTING	Time is adjusting to fine precision
0xA0	FINE	Time has fine precision
0xAA	FINEBACKUPSTEERING	Time is fine and is being steered by the backup system
0xB4	FINESTEERING	Time is fine set and is being steered

Table 40: Satellite visibility definition

Bit	GPS satellite PRN	Bit=0	Bit=1
0	01	Not visible	Visible
1	02	Not visible	Visible
2	03	Not visible	Visible
3	04	Not visible	Visible
4	05	Not visible	Visible
5	06	Not visible	Visible
6	07	Not visible	Visible
7	08	Not visible	Visible
8	09	Not visible	Visible
9	10	Not visible	Visible
10	11	Not visible	Visible
11	12	Not visible	Visible
12	13	Not visible	Visible
13	14	Not visible	Visible
14	15	Not visible	Visible
15	16	Not visible	Visible
16	17	Not visible	Visible
17	18	Not visible	Visible
18	19	Not visible	Visible
19	20	Not visible	Visible
20	21	Not visible	Visible
21	22	Not visible	Visible
22	23	Not visible	Visible
23	24	Not visible	Visible
24	25	Not visible	Visible
25	26	Not visible	Visible
26	27	Not visible	Visible
27	28	Not visible	Visible
28	29	Not visible	Visible
29	30	Not visible	Visible
30	31	Not visible	Visible
31	32	Not visible	Visible

Table 41: COTS receiver error definition

Bit	COTS front-end error	Bit=0	Bit=1
0	DRAM status	OK	Error
1	Invalid firmware	OK	Error
2	ROM status	OK	Error
3	Reserved		
4	Electronic serial number access status	OK	Error
5	Authorization code status	OK	Error
6	Reserved		
7	Supply voltage status	OK	Error
8	Reserved		
9	Temperature status as compared against limits	OK	Error
10	MINOS status	OK	Error
11	PLL RF1 hardware status – L1	OK	Error
12	PLL RF2 hardware status – L2	OK	Error
13	Reserved		
14	Reserved		
15	NVM status	OK	Error
16	Software resource limit	OK	Error
17	Model not valid for this receiver	OK	Error
18	Reserved		
19	Reserved		
20	Remote loading has begun	OK	Error
21	Export restriction	OK	Error
22	Safe mode	OK	Error
23	Reserved		
24	Reserved		
25	Reserved		
26	Reserved		
27	Reserved		
28	Reserved		
29	Reserved		
30	Reserved		
31	Component hardware failure	OK	Error

ANNEX 2. Scientific data set

Table 42: GPS registers, scientific payload data accessed by S-band with GETP command

Sub-Address	Type	Byte 3								Byte 2								Byte 1								Byte 0							
		31	30	29	28	27	26	25	24	23	22	21	20	19	18	17	16	15	14	13	12	11	10	9	8	7	6	5	4	3	2	1	0
0x00	GETP	Don't care																								NEW_DATA_SET_AVAILABLE							
0x01	GETP	DATA_SET_DELIMITER_START																															
0x02	GETP	0x00								LAST_FIX_DAYS_PAST_J2000																							
0x03	GETP	LAST_FIX_MILLISECONDS_OF_DAY																															
0x04	GETP	ICRF_J2000_X_POSITION_CM																															
0x05	GETP	ICRF_J2000_Y_POSITION_CM																															
0x06	GETP	ICRF_J2000_Z_POSITION_CM																															
0x07	GETP	ICRF_J2000_X_VELOCITY_MMS																															
0x08	GETP	ICRF_J2000_Y_VELOCITY_MMS																															
0x09	GETP	ICRF_J2000_Z_VELOCITY_MMS																															
0x0A	GETP	CLOCK_OFFSET_CM																															
0x0B	GETP	0x00								OBSERVATIONS_SET_DAYS_PAST_J2000																							
0x0C	GETP	OBSERVATION_SET_MILLISECONDS_OF_DAY																															
0x0D	GETP	0x000000																								NUMBER_OF_VISIBLE_SATS							
0x0E	GETP	0x000000																								SAT_ID							
0x0F	GETP	CHANNEL_STATUS																															
0x10	GETP	PSEUDORANGE_HI																															
0x11	GETP	PSEUDORANGE_LOW																															
0x12	GETP	CARRIER_PHASE_HI																															
0x13	GETP	CARRIER_PHASE_LOW																															
0x14	GETP	C/No																															
..	..	Addresses from 0x0E to 0x014 are repeated 12 time, fore every receiver channel																															
0x62	GETP	DATA_SET_DELIMITER_END																															

- GPS Sub-Address 0x00:
  - Byte 0: Read 0xAA if a new data set is available, read 0x00 if no data set is available. Note that if this register reads 0xAA, it is cleared when reading register 0x62.
  - Byte 1 to 3: Read 0x000000.

- GPS Sub-Address 0x01:
  - Byte 0 to 3: Read 0xAABBAABB.

- GPS Sub-Address 0x02:
  - Byte 0 to 2: Last position fix days past J2000 specified as UNSIGNED24
  - Byte 3: Don't care.

- GPS Sub-Address 0x03:
  - Byte 0 to 3: Last position fix milliseconds of day specified as UNSIGNED32

- GPS Sub-Address 0x04:
  - Byte 0 to 3: Position fix X component, expressed in ICRF with reference to ecliptic and equinox of J2000, as a signed integer in centimeters.

- GPS Sub-Address 0x05:
  - Byte 0 to 3: Position fix Y component, expressed in ICRF with reference to ecliptic and equinox of J2000, as a signed integer in centimeters.

- GPS Sub-Address 0x06:
  - Byte 0 to 3: Position fix Z component, expressed in ICRF with reference to ecliptic and equinox of J2000, as a signed integer in centimeters.

- GPS Sub-Address 0x07:
  - Byte 0 to 3: Velocity fix X component, expressed in ICRF with reference to ecliptic and equinox of J2000, as a signed integer in millimeters per second.

- GPS Sub-Address 0x08:
  - Byte 0 to 3: Velocity fix Y component, expressed in ICRF with reference to ecliptic and equinox of J2000, as a signed integer in millimeters per second.

- GPS Sub-Address 0x09:
  - Byte 0 to 3: Velocity fix Z component, expressed in ICRF with reference to ecliptic and equinox of J2000, as a signed integer in millimeters per second.

- GPS Sub-Address 0x0A:
  - Byte 0 to 3: Clock error fix expressed in centimeters.

- GPS Sub-Address 0x0B:
  - Byte 0 to 2: Raw observation set days past J2000 specified as UNSIGNED24.
  - Byte 3: Read 0x00.

- GPS Sub-Address 0x0C:
  - Byte 0 to 3: Raw observation set milliseconds of day specified as UNSIGNED32.

- GPS Sub-Address 0x0D:
  - Byte 0: Number of visible GPS satellites.
  - Byte 1 to 3: Read 0x000000.

- GPS Sub-Address 0x0E:
  - Byte 0: Visible GPS satellite PRN number.
  - Byte 1 to 3: Read 0x000000.

- GPS Sub-Address 0x0F:
  - Byte 0 to 3: Channel status according to the following:
    - Bit 0 to 4: Tracking state:
      - > 1: Idle
      - > 2: Sky search

168

> 3: Wide frequency band pull-in
> 4: Narrow frequency band pull-in
> 5: Phase lock loop
> 6: Channel sttering
> 7: Frequency lock loop
> 9: Channel alignment
> 10: Code search
> 11: Aided phase lock loop
- Bit 5 to 9: SV channel number
- Bit 10: Phase lock flag (0 = Not locked, 1 = Locked)
- Bit 11: Parity known flag (0 = Not known, 1 = Known)
- Bit 12: Code locked flag (0 = Not locked, 1 = Locked)
- Bit 13 to 15: Correlator type:
  > 0: N/A
  > 1: Standard correlator: spacing = 1 chip
  > 2: Narrow correlator: spacing < 1 chip
  > 3: reserved
  > 4: Pulse aperture correlator
  > 5-6: Reserved
- Bit 16 to 18: satellite system:
  > 0: GPS
  > 1: GLONASS
  > 2: SBAS
  > 3: GALILEO
  > 4: Reserved
  > 5: QSZZ
  > 6: Reserved
  > 7: Other
- Bit 19: Reserved
- Bit 20: Grouping (0 = Not grouped, 1 = Grouped)
- Bit 21 to 25: Signal type (only GPS reported)
  > 0: L1 C/A
  > 5: L2 P
  > 9: L2 P codeless
  > 14: L5Q
  > 17: L2C
- Bit 26: Forward error correction (0 = Not FEC, 1 = FEC)
- Bit 27: Primary L1 channel (0 = Not primary, 1 = Primary)
- Bit 28: Carrier phase measurement (0 = Half cycle not added, 1 = Half cycle added)
- Bit 29: Reserved
- Bit 30: PRN lock flag (0 = PRN not locked)
- Bit 31: Channel assignment (0 = Automatic, 1 = Forced)

- GPS Sub-Address 0x10:
  o Byte 0 to 3: Raw pseudorange measurement, expressed as a signed integer in millimeters, highest four bytes.

- GPS Sub-Address 0x11:
  o Byte 0 to 3: Raw pseudorange measurement, expressed as a signed integer in millimeters, lowest four bytes.

- GPS Sub-Address 0x12:
  o Byte 0 to 3: Raw carrier measurement, expressed as a signed integer in 1e-3*cycles, highest four bytes.

- GPS Sub-Address 0x13:

- o Byte 0 to 3: Raw carrier measurement, expressed as a signed integer in 1e-3*cycles, lowest four bytes.
- GPS Sub-Address 0x14:
  - o Byte 0 to 3: Signal C/No, expressed as an unsigned integer in 1e-1*dB-Hz.

Registers from 0x0E to 0x14 repeats for up to 12 different channels.

- GPS Sub-Address 0x62:
  - o Byte 0 to 3: Read 0xAACCAACC. Note that when reading this address, the "new data set" flag is cleared.

ANNEX 3.   TC set

Table 43: GPS SC registers

Sub-Address	Type	Byte 3 (31–24)	Byte 2 (23–16)	Byte 1 (15–8)	Byte 0 (7–0)
0x00	GET	0x00	0x00	0x00	NODE ID
0x01	SETT	Don't care	DAYS PAST J2000		
0x02	SETT	MILLISECONDS OF DAY			
0x03	SET	Don't care			MODE
0x04	SET	Don't care			ACTIVE FRONT-END
0x05	SET	Don't care			RESET FRONT-END
0x06	SET	Don't care			AUTO_FIX_PERIOD
0x07	SET				KALMAN_FILTER_RESET
0x08	SET	KALMAN_FILTER_ENABLE_MODELS			
0x09	SET	KALMAN_FILTER_Q_DYNAMIC			
0x0A	SET	KALMAN_FILTER_Q_CLOCK			
0x0B	SET	KALMAN_FILTER_Q_AMBIGUITY			
0x0C	SET	KALMAN_FILTER_R_CURVE_PARAMETERS_CODE			
0x0D	SET	KALMAN_FILTER_R_CURVE_PARAMETERS_CARRIER			
0x0E	SET	CURRENT_UTC_TAI			
0x0F	SET	IERS_PARAMETERS_MJD			
0x10	SET	POLAR_MOTION_XP			
0x11	SET	POLAR_MOTION_YP			
0x12	SET	UT1_UTC			
0x13	SET	DPSI_1980			
0x14	SET	DEPS_1980			
0x15	SET				ADD_IERS_RECORD
0x16	SET	Don't care	NEW FIX DAYS PAST J2000		
0x17	SET	NEW FIX MILLISECONDS OF DAY			
0x18	SET				GENERATE_FIX
0x19	GET	FRONT_END_TIME_STATUS			

0x1A	GET	FRONT_END_ERROR
0x1B	SET	ENABLE_RECORDED_SET_DOWNLOAD
0x1C	GET	DEATH_REPORT_INDEX
0x1D	GET	DEATH_REPORT_DATA
0x1E	SET/GET	Reserved

- GPS Sub-Address 0x00:
  - Byte 0: NODE ID specified as UNSIGNED8
  - Byte 1: Always read 0x00
  - Byte 2: Always read 0x00
  - Byte 3: Always read 0x00

- GPS Sub-Address 0x01:
  - Byte 0 to 2: Days past J2000 specified as UNSIGNED24
  - Byte 3: Don't care.

- GPS Sub-Address 0x02:
  - Byte 0 to 3: Milliseconds of day specified as UNSIGNED32

- GPS Sub-Address 0x03:
  - Byte 0: Force receiver mode according to
    - > 0x00: Initialization sequence
    - > 0x01: Diagnostic mode
    - > 0x02: Front-end power up
    - > 0x04: Kinematic mode
    - > 0x08: Reduced dynamic mode
    - > 0x10: Safe mode
  - Byte 1 to 3: Don't care

- GPS Sub-Address 0x04:
  - Byte 0: Activate front-end according to
    - > 0x0A: Main front-end (default)
    - > 0xA0: Redundant front-end
  - Byte 1 to 3: Don't care

- GPS Sub-Address 0x05:
  - Byte 0: Active front-end is reset when 0xAA is written to this register, other values have no effect
  - Byte 1 to 3: Don't care

- GPS Sub-Address 0x06:
  - Byte 0: Automatic position fix generation period, expressed in seconds (default value is 30 seconds, valid range is 1 to 60)
  - Byte 1 to 3: Don't care

- GPS Sub-Address 0x07:
  - Byte 0: When in reduced dynamic filter mode, writing 0xAA to his register reset the Kalman filter
  - Byte 1 to 3: Don't care

- GPS Sub-Address 0x08:
  - Bit 0: Enable Precession (default value 1)
  - Bit 1: Enable Nutation (default value 1)
  - Bit 2: Enable Earth rotation respect to UT1 (default value 1)
  - Bit 3: Enable polar motion (default value 1)
  - Bit 4: Enable Sun gravity effect (default value 1)
  - Bit 5: Enable Moon gravity effect (default value 1)
  - Bit 6: Enable Earth harmonic gravity expansion up to 10x10 (default value 0)
  - Bit 7: Enable Earth harmonic gravity expansion up to 20x20 (default value 0)
  - Bit 8: Enable Earth harmonic gravity expansion up to 40x40 (default value 0)
  - Bit 9: Enable Earth harmonic gravity expansion up to 50x50 (default value 0)
  - Bit 10: Enable Earth harmonic gravity expansion up to 70x70 (default value 1)
  - Bit 11: Enable Earth tides correction (default value 1)
  - Bit 12: Enable solar radiation pressure model (default value 1)
  - Bit 13: Enable atmospheric drag model (default value 1)
  - Bit 14 to 31: Reserved

- GPS Sub-Address 0x09:
  - Byte 0 to 3: Standard deviation of the zero mean white noise process that models the empirical acceleration expressed as an integer value in $[nm/100*s^2]$. The Kalman filter requires this value to be expressed in nm/s^2 before being applied to the Q matrix computation; therefore the value assigned to this register is firstly divided by 100, and then used to compute the Q matrix. Its default value is 200. See the algorithm documentation for detailed information.

- GPS Sub-Address 0x0A:
  - Byte 0 to 3: Standard deviation of the clock model, integer value expressed in mm (the clock error is considered a range bias therefore expressed in unit of length). Default value is 3. See the algorithm documentation for detailed information.

- GPS Sub-Address 0x0B:
  - Byte 0 to 3: Standard deviation of the ambiguity model, integer value expressed in mm. Default value is 2. See the algorithm documentation for detailed information.

- GPS Sub-Address 0x0C:
  - Byte 0: Code R interpolation curve *a* parameter. See the algorithm documentation for detailed information.
  - Byte 1: Code R interpolation curve *b* parameter. See the algorithm documentation for detailed information.
  - Byte 2: Code R interpolation curve *c* parameter. See the algorithm documentation for detailed information.

- GPS Sub-Address 0x0D:
  - Byte 0: Carrier R interpolation curve *a* parameter. See the algorithm documentation for detailed information.
  - Byte 1: Carrier R interpolation curve *b* parameter. See the algorithm documentation for detailed information.
  - Byte 2: Carrier R interpolation curve *c* parameter. See the algorithm documentation for detailed information.

- GPS Sub-Address 0x0E:
  - Byte 0 to 3: Current number of leap seconds, expressed as UTC-TAI as a signed integer.

- GPS Sub-Address 0x0F:
  - Byte 0 to 3: MJD of the IERS parameters set that follows, in registers from 0x10 to 0x14.

- GPS Sub-Address 0x10:
  - Byte 0 to 3: IERS polar motion parameter xp, expressed as a signed integer in microarcseconds.

- GPS Sub-Address 0x11:
  - Byte 0 to 3: IERS polar motion parameter yp, expressed as a signed integer in microarcseconds.

- GPS Sub-Address 0x12:
  - Byte 0 to 3: IERS difference between UT1 and UTC expressed as a signed integer in 1e-4*ms.

- GPS Sub-Address 0x13:
  - Byte 0 to 3: IERS correction parameter dPsi1980, expressed as a signed integer in microarcseconds.

- GPS Sub-Address 0x14:
  - Byte 0 to 3: IERS correction parameter dEps1980, expressed as a signed integer in microarcseconds.

- GPS Sub-Address 0x15:
  - Byte 0: writing 0xAA to this register cause the IERS data set from register 0x10 to 0x14 to be recorded and included in the receiver collection of IERS parameters.
  - Byte 1 to 3: Don't care.

- GPS Sub-Address 0x16:
  - Byte 0 to 2: Days past J2000 specified as UNSIGNED24 of the fix to be generated on request.
  - Byte 3: Don't care.

- GPS Sub-Address 0x17:
  - Byte 0 to 3: Milliseconds of day specified as UNSIGNED32 of the fix to be generated on request.

- GPS Sub-Address 0x18:
  - Byte 0: writing 0xAA to this register cause the receiver to generate a new position fix at the time expressed by registers 0x16 and 0x17. Note that the time can be 60 seconds before or after the current time, otherwise the command is rejected.
  - Byte 1 to 3: Don't care.

- GPS Sub-Address 0x19:
  - Byte 0 to 3: Active front-end status as reported in

Bit	COTS front-end status	Bit=0	Bit=1
0	Error flag	No error	Error
1	Temperature status	OK	Warning
2	Voltage supply status	OK	Warning
3	Antenna power status	Powered	Not Powered
4	LNA Failure		
5	Antenna open flag	OK	Open
6	Antenna shorted flag	OK	Shorted
7	CPU overload flag	No overload	Overload
8	COM1 buffer overrun flag	No overrun	Overrun
9	COM2 buffer overrun flag	No overrun	Overrun
10	COM3 buffer overrun flag	No overrun	Overrun
11	Link overrun flag	No overrun	Overrun
12	Reserved		
13	Aux transmit overrun flag	No overrun	Overrun
14	AGC out of range		
15	Reserved		
16	Reserved		
17	Reserved		
18	Almanac flag/UTC known	Valid	Invalid
19	Position solution flag	Valid	Invalid
20	Position fixed flag	Not fixed	Fixed
21	Clock steering status	Enabled	Disabled
22	Clock model flag	Valid	Invalid

23	External oscillator locked flag	Unlocked	Locked
24	Software resource	OK	Warning
25	Reserved		
26	Reserved		
27	Reserved		
28	Reserved		
29	Auxiliary 3 status event flag	No event	Event
30	Auxiliary 2 status event flag	No event	Event
31	Auxiliary 1 status event flag	No event	Event

- o Table 39.
- GPS Sub-Address 0x1A:
  - o Byte 0 to 3: Active front-end time status as reported in

GPS_FREND_X_TIM_STAT value (hex)	GPS Reference Time Status ASCII	Time status definition
0x14	UNKNOWN	Time validity is unknown
0x3C	APPROXIMATE	Time is set approximately
0x50	COARSEADJUSTING	Time is approaching coarse precision
0x64	COARSE	This time is valid to coarse precision
0x78	COARSESTEERING	Time is coarse set and is being steered
0x82	FREEWHEELING	Position is lost and the range bias cannot be calculated
0x8C	FINEADJUTING	Time is adjusting to fine precision
0xA0	FINE	Time has fine precision
0xAA	FINEBACKUPSTEERING	Time is fine and is being steered by the backup system
0xB4	FINESTEERING	Time is fine set and is being steered

- o Table 40.
- GPS Sub-Address 0x1B:
  - o Byte 0 to 3: Writing 0xAAAAAAAA to this register cause the receiver to start providing recorded scientific data sets from the oldest one to newest one. The real-time fix is still computed and recorded but not provided as new data set.

- GPS Sub-Address 0x1C:
  - o Byte 0 to 3: The unit death report is composed of 24 32-bit registers containing information on the past receiver fault. Up to three death reports can be recorded. When this register value is 0x00000000, the next register at address 0x1D is reporting the number of valid death reports (from 0 to 3). If there is at least one valid death report, when the next register is read the index is automatically increased by one so that the next register read provides a new segment of death report data. When all valid death reports are read, the index register rolls over to 0x00000000.

- GPS Sub-Address 0x1D:
  - o Byte 0 to 3: Death report segment as identified by the previous register 0x1C.

- GPS Sub-Address 0x1E:

Byte 0 to 3: Reserved.

175

ANNEX 4. Trackstat log sample

=~=~=~=~=~=~=~=~=~=~=~= PuTTY log 2017.07.26 13:48:07 =~=~=~=~=~=~=~=~=~=~=~=

Ready for a command or log request

[COM1]#TRACKSTATA,COM1,0,91.5,COARSE,1959,172890.000,00680000,457c,12997;INSUFFICIENT_OBS,NONE,5.0,20,1,
0,88008001,0.000,-8000.000,0.000,0.000,0.000,NA,0.000,2,0,88008021,0.000,-
7000.000,0.000,0.000,0.000,NA,0.000,3,0,88008041,0.000,6000.000,0.000,0.000,0.000,NA,0.000,4,0,88008061,0.000,5000.000,0.0
00,0.000,0.000,NA,0.000,5,0,88008081,0.000,4000.000,0.000,0.000,0.000,NA,0.000,6,0,880080a1,0.000,-
2000.000,0.000,0.000,0.000,NA,0.000,7,0,880080c1,0.000,2000.000,0.000,0.000,0.000,NA,0.000,8,0,880080e1,0.000,1000.000,0.00
0,0.000,0.000,NA,0.000,9,0,88008101,0.000,10000.000,0.000,0.000,0.000,NA,0.000,10,0,88008121,0.000,9000.000,0.000,0.000,0.0
00,NA,0.000,11,0,88008141,0.000,8000.000,0.000,0.000,0.000,NA,0.000,12,0,88008161,0.000,7000.000,0.000,0.000,0.000,NA,0.0
00,13,0,88008181,0.000,6000.000,0.000,0.000,0.000,NA,0.000,14,0,880081a1,0.000,5000.000,0.000,0.000,0.000,NA,0.000,15,0,88
0081c1,0.000,-
3500.000,0.000,0.000,0.000,NA,0.000,22,0,080081e1,0.000,2393.000,0.000,0.000,0.000,NA,0.000,0,0,08022200,0.000,0.000,0.000,
0.000,0.000,NA,0.000,0,0,08022220,0.000,0.000,0.000,0.000,0.000,NA,0.000,0,0,08022240,0.000,0.000,0.000,0.000,0.000,NA,0.00
0,0,0,08022260,0.000,0.000,0.000,0.000,0.000,NA,0.000*b1fcb3d5

#TRACKSTATA,COM1,0,90.0,COARSE,1959,172920.000,00680000,457c,12997;INSUFFICIENT_OBS,NONE,5.0,20,1,0,880080
01,0.000,4750.000,0.000,0.000,0.000,NA,0.000,2,0,88008021,0.000,-4250.000,0.000,0.000,0.000,NA,0.000,3,0,88008041,0.000,-
3500.000,0.000,0.000,0.000,NA,0.000,4,0,88008061,0.000,-3250.000,0.000,0.000,0.000,NA,0.000,5,0,88008081,0.000,-
3250.000,0.000,0.000,0.000,NA,0.000,6,0,880080a1,0.000,3500.000,0.000,0.000,0.000,NA,0.000,7,0,880080c1,0.000,-
3250.000,0.000,0.000,0.000,NA,0.000,8,0,880080e1,0.000,3000.000,0.000,0.000,0.000,NA,0.000,9,0,88008101,0.000,-
2750.000,0.000,0.000,0.000,NA,0.000,10,0,88008121,0.000,-2500.000,0.000,0.000,0.000,NA,0.000,11,0,88008141,0.000,-
2000.000,0.000,0.000,0.000,NA,0.000,12,0,88008161,0.000,-1750.000,0.000,0.000,0.000,NA,0.000,13,0,88008181,0.000,-
1500.000,0.000,0.000,0.000,NA,0.000,14,0,880081a1,0.000,-1250.000,0.000,0.000,0.000,NA,0.000,15,0,880081c1,0.000,-
1000.000,0.000,0.000,0.000,NA,0.000,15,0,080081e1,0.000,1514.000,0.000,0.000,0.000,NA,0.000,0,0,08022200,0.000,0.000,0.000,
0.000,0.000,NA,0.000,0,0,08022220,0.000,0.000,0.000,0.000,0.000,NA,0.000,0,0,08022240,0.000,0.000,0.000,0.000,0.000,NA,0.00
0,0,0,08022260,0.000,0.000,0.000,0.000,0.000,NA,0.000*9d8088a8

#TRACKSTATA,COM1,0,87.5,COARSE,1959,172950.000,00680000,457c,12997;INSUFFICIENT_OBS,NONE,5.0,20,1,0,880080
02,0.000,-
9650.000,0.000,0.000,0.000,NA,0.000,2,0,88008021,0.000,9500.000,0.000,0.000,0.000,NA,0.000,3,0,88008041,0.000,8500.000,0.0
00,0.000,0.000,NA,0.000,4,0,88008061,0.000,-
8500.000,0.000,0.000,0.000,NA,0.000,5,0,88008081,0.000,8250.000,0.000,0.000,0.000,NA,0.000,6,0,880080a1,0.000,-
8000.000,0.000,0.000,0.000,NA,0.000,7,0,880080c1,0.000,8250.000,0.000,0.000,0.000,NA,0.000,8,0,880080e1,0.000,-
7500.000,0.000,0.000,0.000,NA,0.000,9,0,88008101,0.000,7750.000,0.000,0.000,0.000,NA,0.000,10,0,88008122,0.000,-
6626.000,0.000,0.000,0.000,NA,0.000,11,0,88008141,0.000,7250.000,0.000,0.000,0.000,NA,0.000,12,0,88008161,0.000,6750.000,0
.000,0.000,0.000,NA,0.000,13,0,88008181,0.000,6750.000,0.000,0.000,0.000,NA,0.000,14,0,880081a1,0.000,-
6000.000,0.000,0.000,0.000,NA,0.000,15,0,880081c1,0.000,6250.000,0.000,0.000,0.000,NA,0.000,6,0,080081e1,0.000,-
406.000,0.000,0.000,0.000,NA,0.000,0,0,08022200,0.000,0.000,0.000,0.000,0.000,NA,0.000,0,0,08022220,0.000,0.000,0.000,0.000,
0.000,NA,0.000,0,0,08022240,0.000,0.000,0.000,0.000,0.000,NA,0.000,0,0,08022260,0.000,0.000,0.000,0.000,0.000,NA,0.000*6b1
d3621

[COM1]#TRACKSTATA,COM1,0,90.0,COARSE,1959,172980.000,00680000,457c,12997;INSUFFICIENT_OBS,NONE,5.0,20,1,
0,88008001,0.000,15500.000,0.000,0.000,0.000,NA,0.000,2,0,88008021,0.000,14500.000,0.000,0.000,0.000,NA,0.000,3,0,8800804
1,0.000,13500.000,0.000,0.000,0.000,NA,0.000,4,0,88008061,0.000,12500.000,0.000,0.000,0.000,NA,0.000,5,0,88008081,0.000,11

500.000,0.000,0.000,0.000,NA,0.000,6,0,880080a1,0.000,10500.000,0.000,0.000,0.000,NA,0.000,7,0,880080c1,0.000,19500.000,0.0
00,0.000,0.000,NA,0.000,8,0,880080e1,0.000,18500.000,0.000,0.000,0.000,NA,0.000,9,0,88008101,0.000,17500.000,0.000,0.000,0.
000,NA,0.000,10,0,88008121,0.000,16500.000,0.000,0.000,0.000,NA,0.000,11,0,88008141,0.000,15500.000,0.000,0.000,0.000,NA,
0.000,12,0,88008161,0.000,14500.000,0.000,0.000,0.000,NA,0.000,13,0,88008181,0.000,7000.000,0.000,0.000,0.000,NA,0.000,14,
0,880081a1,0.000,8000.000,0.000,0.000,0.000,NA,0.000,15,0,880081c1,0.000,9000.000,0.000,0.000,0.000,NA,0.000,7,0,080081e1,
0.000,-
5073.000,0.000,0.000,0.000,NA,0.000,0,0,08022200,0.000,0.000,0.000,0.000,0.000,NA,0.000,0,0,08022220,0.000,0.000,0.000,0.00
0,0.000,NA,0.000,0,0,08022240,0.000,0.000,0.000,0.000,0.000,NA,0.000,0,0,08022260,0.000,0.000,0.000,0.000,0.000,NA,0.000*6e
c54827

#TRACKSTATA,COM1,0,91.0,COARSE,1959,173010.000,00680000,457c,12997;INSUFFICIENT_OBS,NONE,5.0,20,1,0,880080
01,0.000,6250.000,0.000,0.000,0.000,NA,0.000,2,0,88008021,0.000,14000.000,0.000,0.000,0.000,NA,0.000,3,0,88008041,0.000,13
500.000,0.000,0.000,0.000,NA,0.000,4,0,88008061,0.000,13250.000,0.000,0.000,0.000,NA,0.000,5,0,88008081,0.000,7250.000,0.0
00,0.000,0.000,NA,0.000,6,0,880080a1,0.000,13000.000,0.000,0.000,0.000,NA,0.000,7,0,880080c1,0.000,7750.000,0.000,0.000,0.0
00,NA,0.000,8,0,880080e1,0.000,7750.000,0.000,0.000,0.000,NA,0.000,9,0,88008101,0.000,12000.000,0.000,0.000,0.000,NA,0.000
,10,0,88008121,0.000,12000.000,0.000,0.000,0.000,NA,0.000,11,0,88008141,0.000,11750.000,0.000,0.000,0.000,NA,0.000,12,0,88
008161,0.000,11500.000,0.000,0.000,0.000,NA,0.000,13,0,88008181,0.000,11250.000,0.000,0.000,0.000,NA,0.000,14,0,880081a1,
0.000,11000.000,0.000,0.000,0.000,NA,0.000,15,0,880081c1,0.000,10500.000,0.000,0.000,0.000,NA,0.000,22,0,080081e1,0.000,-
196.000,0.000,0.000,0.000,NA,0.000,0,0,08022200,0.000,0.000,0.000,0.000,0.000,NA,0.000,0,0,08022220,0.000,0.000,0.000,0.000,
0.000,NA,0.000,0,0,08022240,0.000,0.000,0.000,0.000,0.000,NA,0.000,0,0,08022260,0.000,0.000,0.000,0.000,0.000,NA,0.000*e45
f1cbb

#TRACKSTATA,COM1,0,91.5,COARSE,1959,173040.000,00680000,457c,12997;INSUFFICIENT_OBS,NONE,5.0,20,1,0,880080
01,0.000,19000.000,0.000,0.000,0.000,NA,0.000,2,0,88008021,0.000,19250.000,0.000,0.000,0.000,NA,0.000,3,0,88008041,0.000,1
250.000,0.000,0.000,0.000,NA,0.000,4,0,88008061,0.000,1500.000,0.000,0.000,0.000,NA,0.000,5,0,88008081,0.000,18000.000,0.0
00,0.000,0.000,NA,0.000,6,0,880080a1,0.000,2000.000,0.000,0.000,0.000,NA,0.000,7,0,880080c1,0.000,2500.000,0.000,0.000,0.00
0,NA,0.000,8,0,880080e1,0.000,17500.000,0.000,0.000,0.000,NA,0.000,9,0,88008101,0.000,2750.000,0.000,0.000,0.000,NA,0.000,
10,0,88008121,0.000,3000.000,0.000,0.000,0.000,NA,0.000,11,0,88008141,0.000,3000.000,0.000,0.000,0.000,NA,0.000,12,0,88008
161,0.000,3500.000,0.000,0.000,0.000,NA,0.000,13,0,88008181,0.000,3500.000,0.000,0.000,0.000,NA,0.000,14,0,880081a1,0.000,
3750.000,0.000,0.000,0.000,NA,0.000,15,0,880081c1,0.000,15500.000,0.000,0.000,0.000,NA,0.000,17,0,080081e1,0.000,-
2000.000,0.000,0.000,0.000,NA,0.000,0,0,08022200,0.000,0.000,0.000,0.000,0.000,NA,0.000,0,0,08022220,0.000,0.000,0.000,0.00
0,0.000,NA,0.000,0,0,08022240,0.000,0.000,0.000,0.000,0.000,NA,0.000,0,0,08022260,0.000,0.000,0.000,0.000,0.000,NA,0.000*ac
ff3b9c

[COM1]#TRACKSTATA,COM1,0,89.5,COARSE,1959,173070.000,00680000,457c,12997;INSUFFICIENT_OBS,NONE,5.0,20,1,
0,88009c04,24710041.007,21631.459,46.585,16.550,0.000,NOIONOCORR,0.000,2,0,88008021,0.000,24500.000,0.000,0.000,0.000
,NA,0.000,3,0,88008041,0.000,23500.000,0.000,0.000,0.000,NA,0.000,4,0,88008061,0.000,22500.000,0.000,0.000,0.000,NA,0.000,
5,0,88008081,0.000,21500.000,0.000,0.000,0.000,NA,0.000,6,0,880080a1,0.000,20500.000,0.000,0.000,0.000,NA,0.000,7,0,880080
c1,0.000,29500.000,0.000,0.000,0.000,NA,0.000,8,0,880080e1,0.000,28500.000,0.000,0.000,0.000,NA,0.000,9,0,88008101,0.000,27
500.000,0.000,0.000,0.000,NA,0.000,10,0,88008121,0.000,26500.000,0.000,0.000,0.000,NA,0.000,11,0,88008141,0.000,25500.000,
0.000,0.000,0.000,NA,0.000,12,0,88008161,0.000,24500.000,0.000,0.000,0.000,NA,0.000,13,0,88008181,0.000,17000.000,0.000,0.
000,0.000,NA,0.000,14,0,880081a1,0.000,18000.000,0.000,0.000,0.000,NA,0.000,15,0,880081c1,0.000,19000.000,0.000,0.000,0.00
0,NA,0.000,15,0,080081e1,0.000,-
2000.000,0.000,0.000,0.000,NA,0.000,0,0,08022200,0.000,0.000,0.000,0.000,0.000,NA,0.000,0,0,08022220,0.000,0.000,0.000,0.00
0,0.000,NA,0.000,0,0,08022240,0.000,0.000,0.000,0.000,0.000,NA,0.000,0,0,08022260,0.000,0.000,0.000,0.000,0.000,NA,0.000*d
dd24ea5

#TRACKSTATA,COM1,0,88.5,COARSE,1959,173100.000,00680000,457c,12997;INSUFFICIENT_OBS,NONE,5.0,20,1,0,88009c04,24587891.137,21155.850,46.628,46.550,0.000,NOIONOCORR,0.000,2,0,88008021,0.000,24000.000,0.000,0.000,0.000,NA,0.000,3,0,88008041,0.000,23250.000,0.000,0.000,0.000,NA,0.000,4,0,88008062,0.000,23790.000,0.000,0.000,0.000,NA,0.000,5,0,88008081,0.000,22500.000,0.000,0.000,0.000,NA,0.000,6,0,880080a2,0.000,22220.000,0.000,0.000,0.000,NA,0.000,7,0,880080c1,0.000,17500.000,0.000,0.000,0.000,NA,0.000,8,0,880080e1,0.000,22500.000,0.000,0.000,0.000,NA,0.000,9,0,88008101,0.000,22250.000,0.000,0.000,0.000,NA,0.000,10,0,88008121,0.000,18250.000,0.000,0.000,0.000,NA,0.000,11,0,88008141,0.000,21250.000,0.000,0.000,0.000,NA,0.000,12,0,88008161,0.000,21250.000,0.000,0.000,0.000,NA,0.000,13,0,88008181,0.000,21250.000,0.000,0.000,0.000,NA,0.000,14,0,88009da4,25428621.482,25924.602,46.302,22.550,0.000,NOIONOCORR,0.000,15,0,880081c1,0.000,20750.000,0.000,0.000,0.000,NA,0.000,17,0,080081e1,0.000,-2000.000,0.000,0.000,0.000,NA,0.000,0,0,08022200,0.000,0.000,0.000,0.000,0.000,NA,0.000,0,0,08022220,0.000,0.000,0.000,0.000,0.000,NA,0.000,0,0,08022240,0.000,0.000,0.000,0.000,0.000,NA,0.000,0,0,08022260,0.000,0.000,0.000,0.000,0.000,NA,0.000*9dffa9a5

#TRACKSTATA,COM1,0,89.0,COARSE,1959,173130.000,00680000,457c,12997;INSUFFICIENT_OBS,NONE,5.0,20,1,0,88009c04,24468534.270,20654.279,46.794,76.550,0.000,NOIONOCORR,0.000,2,0,88008021,0.000,29250.000,0.000,0.000,0.000,NA,0.000,3,0,88008041,0.000,28500.000,0.000,0.000,0.000,NA,0.000,4,0,88008061,0.000,12250.000,0.000,0.000,0.000,NA,0.000,5,0,88008081,0.000,27500.000,0.000,0.000,0.000,NA,0.000,6,0,880080a1,0.000,27750.000,0.000,0.000,0.000,NA,0.000,7,0,880080c1,0.000,27500.000,0.000,0.000,0.000,NA,0.000,8,0,880080e1,0.000,12500.000,0.000,0.000,0.000,NA,0.000,9,0,88008101,0.000,12500.000,0.000,0.000,0.000,NA,0.000,10,0,88008121,0.000,26750.000,0.000,0.000,0.000,NA,0.000,11,0,88008141,0.000,26500.000,0.000,0.000,0.000,NA,0.000,12,0,88008161,0.000,26250.000,0.000,0.000,0.000,NA,0.000,13,0,88008181,0.000,13750.000,0.000,0.000,0.000,NA,0.000,14,0,88009da4,25282314.667,25326.219,46.618,52.550,0.000,NOIONOCORR,0.000,15,0,880081c1,0.000,14250.000,0.000,0.000,0.000,NA,0.000,15,0,080081e1,0.000,2000.000,0.000,0.000,0.000,NA,0.000,0,0,08022200,0.000,0.000,0.000,0.000,0.000,NA,0.000,0,0,08022220,0.000,0.000,0.000,0.000,0.000,NA,0.000,0,0,08022240,0.000,0.000,0.000,0.000,0.000,NA,0.000,0,0,08022260,0.000,0.000,0.000,0.000,0.000,NA,0.000*e0ec6e42

[COM1]#TRACKSTATA,COM1,0,90.5,COARSE,1959,173160.000,00680000,457c,12997;INSUFFICIENT_OBS,NONE,5.0,20,1,0,88009c04,24352126.359,20124.154,46.604,106.550,0.000,NOIONOCORR,0.000,2,0,88008021,0.000,35500.000,0.000,0.000,0.000,NA,0.000,3,0,88008041,0.000,34500.000,0.000,0.000,0.000,NA,0.000,4,0,88008061,0.000,33500.000,0.000,0.000,0.000,NA,0.000,5,0,88008081,0.000,32500.000,0.000,0.000,0.000,NA,0.000,6,0,880080a1,0.000,31500.000,0.000,0.000,0.000,NA,0.000,7,0,880080c1,0.000,30000.000,0.000,0.000,0.000,NA,0.000,8,0,880080e1,0.000,39500.000,0.000,0.000,0.000,NA,0.000,9,0,88008101,0.000,38500.000,0.000,0.000,0.000,NA,0.000,10,0,88008121,0.000,37500.000,0.000,0.000,0.000,NA,0.000,11,0,88008141,0.000,36500.000,0.000,0.000,0.000,NA,0.000,12,0,88008161,0.000,35500.000,0.000,0.000,0.000,NA,0.000,13,0,88008181,0.000,26000.000,0.000,0.000,0.000,NA,0.000,14,0,88009da4,25139518.382,24696.248,46.309,82.550,0.000,NOIONOCORR,0.000,15,0,880081c1,0.000,27000.000,0.000,0.000,0.000,NA,0.000,17,0,080081e1,0.000,2000.000,0.000,0.000,0.000,NA,0.000,0,0,08022200,0.000,0.000,0.000,0.000,0.000,NA,0.000,0,0,08022220,0.000,0.000,0.000,0.000,0.000,NA,0.000,0,0,08022240,0.000,0.000,0.000,0.000,0.000,NA,0.000,0,0,08022260,0.000,0.000,0.000,0.000,0.000,NA,0.000*3044455b

#TRACKSTATA,COM1,0,89.0,COARSE,1959,173190.000,00680000,457c,12997;INSUFFICIENT_OBS,NONE,5.0,20,1,0,88009c04,24238809.872,19568.754,46.670,136.550,0.000,NOIONOCORR,0.000,2,0,88008021,0.000,26000.000,0.000,0.000,0.000,NA,0.000,3,0,88008041,0.000,26500.000,0.000,0.000,0.000,NA,0.000,4,0,88008061,0.000,26750.000,0.000,0.000,0.000,NA,0.000,5,0,88008081,0.000,27000.000,0.000,0.000,0.000,NA,0.000,6,0,880080a1,0.000,33000.000,0.000,0.000,0.000,NA,0.000,7,0,880080c1,0.000,27250.000,0.000,0.000,0.000,NA,0.000,8,0,880080e1,0.000,32750.000,0.000,0.000,0.000,NA,0.000,9,0,88008101,0.000,28000.000,0.000,0.000,0.000,NA,0.000,10,0,88008121,0.000,28250.000,0.000,0.000,0.000,NA,0.000,11,0,88008141,0.000,32000.000,0.000,0.000,0.000,NA,0.000,12,0,88008161,0.000,31750.000,0.000,0.000,0.000,NA,0.000,13,0,88008181,0.000,31500.000,0.000,0.000,0.000,NA,0.000,14,0,88009da4,25000392.928,24037.773,46.427,112.550,0.000,NOIONOCORR,0.000,15,0,880081c1,0.000,31000.000,0.000,0.000,0.000,NA,0.000,15,0,080081e1,0.000,2000.000,0.000,0.000,0.000,NA,0.000,0,0,08022200,0.000,0.000,0.000,0.000,0.

000,NA,0.000,0,0,08022220,0.000,0.000,0.000,0.000,0.000,NA,0.000,0,0,08022240,0.000,0.000,0.000,0.000,0.000,NA,0.000,0,0,08022260,0.000,0.000,0.000,0.000,0.000,NA,0.000*9ccce385

#TRACKSTATA,COM1,0,89.5,COARSE,1959,173220.000,00680000,457c,12997;INSUFFICIENT_OBS,NONE,5.0,20,1,0,88009c04,24128739.955,18987.867,46.715,166.550,0.000,NOIONOCORR,0.000,2,0,88008021,0.000,39500.000,0.000,0.000,0.000,NA,0.000,3,0,88008041,0.000,21750.000,0.000,0.000,0.000,NA,0.000,4,0,88008061,0.000,21750.000,0.000,0.000,0.000,NA,0.000,5,0,88008081,0.000,21750.000,0.000,0.000,0.000,NA,0.000,6,0,880080a2,0.000,37036.000,0.000,0.000,0.000,NA,0.000,7,0,880080c1,0.000,37750.000,0.000,0.000,0.000,NA,0.000,8,0,880080e1,0.000,22000.000,0.000,0.000,0.000,NA,0.000,9,0,88008101,0.000,37250.000,0.000,0.000,0.000,NA,0.000,10,0,88008122,0.000,36288.000,0.000,0.000,0.000,NA,0.000,11,0,88008141,0.000,23000.000,0.000,0.000,0.000,NA,0.000,12,0,88008161,0.000,23250.000,0.000,0.000,0.000,NA,0.000,13,0,88008181,0.000,23250.000,0.000,0.000,0.000,NA,0.000,14,0,88009da4,24865109.406,23351.340,46.383,142.550,0.000,NOIONOCORR,0.000,15,0,880081c1,0.000,23750.000,0.000,0.000,0.000,NA,0.000,32,0,080081e1,0.000,-5000.000,0.000,0.000,0.000,NA,0.000,0,0,08022200,0.000,0.000,0.000,0.000,0.000,NA,0.000,0,0,08022220,0.000,0.000,0.000,0.000,0.000,NA,0.000,0,0,08022240,0.000,0.000,0.000,0.000,0.000,NA,0.000,0,0,08022260,0.000,0.000,0.000,0.000,0.000,NA,0.000*fed3cb10

[COM1]#TRACKSTATA,COM1,0,90.5,COARSE,1959,173250.000,00680000,457c,12997;INSUFFICIENT_OBS,NONE,5.0,20,1,0,88009c04,24022063.023,18381.189,46.632,196.550,0.000,NOIONOCORR,0.000,2,0,88008021,0.000,-4500.000,0.000,0.000,0.000,NA,0.000,3,0,88008041,0.000,-5500.000,0.000,0.000,0.000,NA,0.000,4,0,88008061,0.000,-6500.000,0.000,0.000,0.000,NA,0.000,5,0,88008081,0.000,-7500.000,0.000,0.000,0.000,NA,0.000,6,0,880080a1,0.000,-8500.000,0.000,0.000,0.000,NA,0.000,7,0,880080c1,0.000,-10000.000,0.000,0.000,0.000,NA,0.000,8,0,880080e1,0.000,-500.000,0.000,0.000,0.000,NA,0.000,9,0,88008101,0.000,-1500.000,0.000,0.000,0.000,NA,0.000,10,0,88008121,0.000,-2500.000,0.000,0.000,0.000,NA,0.000,11,0,88008141,0.000,-3500.000,0.000,0.000,0.000,NA,0.000,12,0,88008161,0.000,-4500.000,0.000,0.000,0.000,NA,0.000,13,0,88008181,0.000,-14000.000,0.000,0.000,0.000,NA,0.000,14,0,88009da4,24733827.385,22637.166,46.551,172.550,0.000,NOIONOCORR,0.000,15,0,880081c1,0.000,-7500.000,0.000,0.000,0.000,NA,0.000,29,0,080081e4,0.000,559.984,46.712,5.340,0.000,NA,0.000,0,0,08022200,0.000,0.000,0.000,0.000,0.000,NA,0.000,0,0,08022220,0.000,0.000,0.000,0.000,0.000,NA,0.000,0,0,08022240,0.000,0.000,0.000,0.000,0.000,NA,0.000,0,0,08022260,0.000,0.000,0.000,0.000,0.000,NA,0.000*0965783b

#TRACKSTATA,COM1,0,90.0,COARSE,1959,173280.000,00680000,457c,12997;INSUFFICIENT_OBS,NONE,5.0,20,1,0,88009c04,23918916.869,17749.357,46.802,226.560,0.000,NOIONOCORR,0.000,2,0,88008021,0.000,-5750.000,0.000,0.000,0.000,NA,0.000,3,0,88008041,0.000,-13250.000,0.000,0.000,0.000,NA,0.000,4,0,88008061,0.000,-7000.000,0.000,0.000,0.000,NA,0.000,5,0,88008081,0.000,-13000.000,0.000,0.000,0.000,NA,0.000,6,0,880080a1,0.000,-6750.000,0.000,0.000,0.000,NA,0.000,7,0,880080c1,0.000,-7000.000,0.000,0.000,0.000,NA,0.000,8,0,880080e1,0.000,-7250.000,0.000,0.000,0.000,NA,0.000,9,0,88008101,0.000,-12000.000,0.000,0.000,0.000,NA,0.000,10,0,88008121,0.000,-7750.000,0.000,0.000,0.000,NA,0.000,11,0,88008141,0.000,-8000.000,0.000,0.000,0.000,NA,0.000,12,0,88008161,0.000,-11500.000,0.000,0.000,0.000,NA,0.000,13,0,88008181,0.000,-8500.000,0.000,0.000,0.000,NA,0.000,14,0,88009da4,24606695.789,21896.189,46.450,202.550,0.000,NOIONOCORR,0.000,15,0,880081c1,0.000,-9000.000,0.000,0.000,0.000,NA,0.000,29,0,18009de4,23883816.577,-952.744,46.695,35.340,0.000,NOIONOCORR,0.000,0,0,08022200,0.000,0.000,0.000,0.000,0.000,NA,0.000,0,0,08022220,0.000,0.000,0.000,0.000,0.000,NA,0.000,0,0,08022240,0.000,0.000,0.000,0.000,0.000,NA,0.000,0,0,08022260,0.000,0.000,0.000,0.000,0.000,NA,0.000*6c022573

#TRACKSTATA,COM1,0,88.5,COARSE,1959,173310.000,00680000,457c,12997;INSUFFICIENT_OBS,NONE,5.0,20,1,0,88009c04,23819455.467,17090.326,46.753,256.560,0.000,NOIONOCORR,0.000,2,0,88008021,0.000,-750.000,0.000,0.000,0.000,NA,0.000,3,0,88008041,0.000,-2250.000,0.000,0.000,0.000,NA,0.000,4,0,88008061,0.000,-18250.000,0.000,0.000,0.000,NA,0.000,5,0,88008081,0.000,-1750.000,0.000,0.000,0.000,NA,0.000,6,0,880080a1,0.000,-

1500.000,0.000,0.000,0.000,NA,0.000,7,0,880080c1,0.000,-2000.000,0.000,0.000,0.000,NA,0.000,8,0,880080e1,0.000,-17500.000,0.000,0.000,0.000,NA,0.000,9,0,88008101,0.000,-17250.000,0.000,0.000,0.000,NA,0.000,10,0,88008121,0.000,-2750.000,0.000,0.000,0.000,NA,0.000,11,0,88008141,0.000,-3000.000,0.000,0.000,0.000,NA,0.000,12,0,88008161,0.000,-4000.000,0.000,0.000,0.000,NA,0.000,13,0,88008184,0.000,-14158.094,45.423,11.460,0.000,NA,0.000,14,0,88009da4,24483876.757,21126.439,46.639,232.550,0.000,NOIONOCORR,0.000,15,0,880081c2,0.000,-4169.000,0.000,0.000,0.000,NA,0.000,29,0,18009de4,23893572.878,-2466.161,46.730,65.340,0.000,NOIONOCORR,0.000,0,0,08022200,0.000,0.000,0.000,0.000,0.000,NA,0.000,0,0,08022220,0.000,0.000,0.000,0.000,0.000,NA,0.000,0,0,08022240,0.000,0.000,0.000,0.000,0.000,NA,0.000,0,0,08022260,0.000,0.000,0.000,0.000,0.000,NA,0.000*1ad4c238

[COM1]#TRACKSTATA,COM1,0,87.5,COARSE,1959,173340.000,00680000,457c,12997;INSUFFICIENT_OBS,SINGLE,5.0,20,1,0,88009c04,23723834.724,16404.406,46.932,286.560,0.000,NOTUSED,0.000,2,0,88008021,0.000,-14500.000,0.000,0.000,0.000,NA,0.000,3,0,88008041,0.000,-15500.000,0.000,0.000,0.000,NA,0.000,4,0,88008061,0.000,-16500.000,0.000,0.000,0.000,NA,0.000,5,0,88008081,0.000,-17500.000,0.000,0.000,0.000,NA,0.000,6,0,880080a1,0.000,-18500.000,0.000,0.000,0.000,NA,0.000,7,0,880080c1,0.000,-20000.000,0.000,0.000,0.000,NA,0.000,8,0,880080e1,0.000,-10500.000,0.000,0.000,0.000,NA,0.000,9,0,88008101,0.000,-11500.000,0.000,0.000,0.000,NA,0.000,10,0,88008121,0.000,-12500.000,0.000,0.000,0.000,NA,0.000,11,0,88008141,0.000,-13500.000,0.000,0.000,0.000,NA,0.000,12,0,88008161,0.000,-14500.000,0.000,0.000,0.000,NA,0.000,13,0,88008184,0.000,-14207.844,45.664,9.440,0.000,NA,0.000,14,0,88009da4,24365531.945,20329.354,46.681,262.550,0.000,NOTUSED,0.000,15,0,880081c1,0.000,-23000.000,0.000,0.000,0.000,NA,0.000,31,0,18009de4,21310376.952,-803.549,47.625,23.440,0.000,NOTUSED,0.000,0,0,08022200,0.000,0.000,0.000,0.000,0.000,NA,0.000,0,0,08022220,0.000,0.000,0.000,0.000,0.000,NA,0.000,0,0,08022240,0.000,0.000,0.000,0.000,0.000,NA,0.000,0,0,08022260,0.000,0.000,0.000,0.000,0.000,NA,0.000*a31ad5d2

#TRACKSTATA,COM1,0,88.5,COARSE,1959,173370.000,00680000,457c,12997;SOL_COMPUTED,SINGLE,5.0,20,1,0,88009c04,23632207.374,15692.083,46.922,316.560,0.000,GOOD,0.187,2,0,88008021,0.000,-16000.000,0.000,0.000,0.000,NA,0.000,3,0,88008041,0.000,-16000.000,0.000,0.000,0.000,NA,0.000,4,0,88008061,0.000,-16750.000,0.000,0.000,0.000,NA,0.000,5,0,88008081,0.000,-17000.000,0.000,0.000,0.000,NA,0.000,6,0,880080a1,0.000,-16750.000,0.000,0.000,0.000,NA,0.000,7,0,880080c1,0.000,-17250.000,0.000,0.000,0.000,NA,0.000,8,0,880080e1,0.000,-17500.000,0.000,0.000,0.000,NA,0.000,9,0,88008101,0.000,-17500.000,0.000,0.000,0.000,NA,0.000,10,0,88008121,0.000,-21750.000,0.000,0.000,0.000,NA,0.000,11,0,88008141,0.000,-18000.000,0.000,0.000,0.000,NA,0.000,12,0,88008161,0.000,-18500.000,0.000,0.000,0.000,NA,0.000,13,0,88009d84,28287051.229,-14253.140,45.472,39.440,0.000,GOOD,0.004,14,0,88009da4,24251816.815,19505.566,46.694,292.550,0.000,GOOD,0.173,15,0,880081c1,0.000,-18750.000,0.000,0.000,0.000,NA,0.000,31,0,18009de4,21320329.635,-2681.439,47.650,53.440,0.000,GOOD,0.219,0,0,08022200,0.000,0.000,0.000,0.000,0.000,NA,0.000,0,0,08022220,0.000,0.000,0.000,0.000,0.000,NA,0.000,0,0,08022240,0.000,0.000,0.000,0.000,0.000,NA,0.000,0,0,08022260,0.000,0.000,0.000,0.000,0.000,NA,0.000*e927a1f2

BIBLIOGRAPHY

[1]. O. Montebruck, E. Gill "Satellite Orbits: Models, Methods and Applications", Springer, First Edition, Berlin, Germany, 2000

[2]. Kaplan E. D., Hegarty C. J., "Understanding GPS: principles and applications", Artech House, Second Edition, Norwood, MA, USA, 2006

[3]. NovAtel Inc. "OEM6 Family Firmware Reference Manual", NovAtel Inc, rev 7, 2014, om-20000129

[4]. Parkinson, B. W., and J. J. Spilker. "Global Positioning System: Theory and Applications, vol. 2, ch. 21, (P. Zarchan, editor-in-chief)." Progress in Astronautics and Aeronautics 164.

[5]. Montenbruck et al. "Onboard Real-Time Navigation for the Sentinel-3 Mission" ION-GNSS-2009, 22 Sep. -25 Sep. 2009, Savannah, USA (2009).

[6]. Avanzi A., Garcia A., and Tortora P., "Implementation and Tuning of LEO Satellites Real-time Navigation Algorithm Based on Single Frequency GPS Measurements" NAVITEC 2014, Noordwijk, 3-5 December 2014

[7]. Montenbruck et al. "Reduced dynamic orbit determination using GPS code and carrier measurements". Aerospace Science and Technology 9 (2005) 261–271

[8]. Montenbruck et al. "Precision real-time navigation of LEO satellites using global positioning system measurements" GPS Solutions (2008) 12:187–198

[9]. Bock H. et al. "GPS single-frequency orbit determination for low Earth orbiting satellites" Advances in Space Research 43 (2009) 783–791

[10]. A. Locarini, "Design of a GNSS receiver for the ESEO Mission", MsC Thesis, University di Bologna

[11]. A. Locarini, "GPS Payload Design Definition File", University of Bologna, Forlì, 2016.

[12]. A. Locarini, "GPS Payload Test Plan", University of Bologna, Forlì, 2016.

[13]. A. Locarini, "GPS Payload GPS Electrical Test Procedure", University of Bologna, Forlì, 2016.

[14]. A. Locarini, "GPS Payload GPS Front-End Functionality Test Procedure", University of Bologna, Forlì, 2016.

[15]. A. Locarini, "GPS Payload Navigation Test Procedure", University of Bologna, Forlì, 2016.

[16]. A. Locarini, "GPS Payload Software Architectural Design Document", University of Bologna, Forlì, 2016.

[17]. A. Locarini, "GPS Payload User Manual", University of Bologna, Forlì, 2016.

[18]. A. Locarini, "GPS Receiver HK and TC List", University of Bologna, Forlì, 2016.

[19]. AS-12_005-MIS-PAP-01_v1.0, ESEO Product Assurance Plan

[20]. http://www.sensorantennas.com/antenna_pdf/GPS/1575-20,-39,-49,-59.pdf

[21]. http://www.novatel.com/assets/Documents/Papers/OEM615.pdf

[22]. NovAtel Inc. "NovAtel PC Utilities: User Manual", NovAtel Inc, rev 1, 2013, GM-14915117

[23]. Montenbruck et al. "GPS Orbit Determination for Micro-Satellites – The PROBA-2 Flight Experience" AIAA Guidance, Navigation, and Control Conference 2 - 5 August 2010, Toronto, Ontario Canada.

[24]. Yunck T.P. "Orbit Determination", in B.W. Parkinson and J.J. Spilker Jr. (eds.), Global Positioning System: Theory and Applications, Vol. II, Ch. 21 (AIAA, Washington, D.C., 1996.

[25]. http://www.iers.org/nn_11216/IERS/EN/Publications/TechnicalNotes/tn36.html

[26]. Ashkenazi, V., W. Chen, C J. Hill, T. Moore, D. Stanton and D. Fortune, "GPS for Real-Time Autonomous Orbit Determination of LEO Satellites", Proceeding GNSS '97, First European Symposium on Global Navigation Satellite. Systems, pp 657 - 665, Munich

[27]. A.Avanzi, "ESEO Software Interface Control Document", SITAEL, Forlì, 2016

[28]. A.Avanzi, "OBDH Subsystem Level Software Architectural Design Document", SITAEL, Forlì, 2016

[29]. A. Corbelli, "ESEO GPS Vibration Test Report", SITAEL, Forlì, 2016

[30]. A. Locarini, "GPS Payload GPS Electrical Test Report", University of Bologna, Forlì, 2016.

[31]. A. Locarini, "GPS Payload GPS Front-End Functionality Test Report", University of Bologna, Forlì, 2016.

[32]. A. Locarini, "GPS Payload Navigation Test Report", University of Bologna, Forlì, 2016.

[33]. SpaceWorks_Nano_Microsatellite_Market_Forecast_2017

[34]. A. Locarini, "GPS Payload Experiment Interface Document", University of Bologna, Forlì, 2016.

[35]. SimGEN USER MANUAL, SPIRENT Communications, 2008

[36]. J.R. Wertz, W. Larson, "Space Mission Analysis and Design", Space Technology Library 3rs edition

[37]. ECSS_Q_ST_70_02C

[38]. MIL-DTL-5541 Type I, Class 3

[39]. T. Irvine, "Extending Steinberg's Fatigue Analysis of Electronics Equipment Methodology to a Full Relative Displacement vs. Cycles Curve", 2013

AKNOWLEDGMENTS

First of all, I am grateful to Professor Tortora for the opportunity he gave me to be part of this interesting PhD project and to keep following my professional dreams. This experience meant a lot to me and has been extremely formative both from a professional and personal point of view. During these 3 years, I had the opportunity to discover and study the topic of satellites navigation and to deepen knowledge and practice with satellites sub-systems design and development and I hope to keep working and study in this interesting field.

ESA Education office is greatly acknowledged for the opportunity offered to European students to constantly involved in interesting and challenging project, like ESEO.

I wish to thank Alessandro Avanzi and all SITAEL Forlì team for their constant technical support during these three years. They helped me gaining an important and great experience in the professional field that I love.

I wish to sincerely acknowledge Prof. Fabio Dovis and Prof. Gianluca Marucco, along with all the GNSS team of the Istituto Superiore Mario Boella, for their precious contribution in providing the GNSS simulator for the critical testing phase.

I wish to thank also Prof. Terry Moore and the Nottingham Geospatial Institute for hosting me during my period abroad, giving me the opportunity to gain professional experience in such an importantcentre of excellence for satellite navigation and to work side by side with great professionals.

A huge thank to all my laboratory mates for the nice moments spent together and for being friends, before being colleagues.

Grazie mia madre, che mi ha sempre incoraggiato in ogni scelta della mia vita e non mi ha mai fatto mancare il suo sostegno durante questi anni. È grazie ai suoi enormi sacrifici se sono giunto dove sono ora ed è grazie a lei se ho imparato a sognare e a seguire i miei obiettivi con risolutezza.

Grazie di cuore Valentina, compagna di vita e, molto presto, moglie, per aver condiviso con me tutte le gioie professionali e non, di questi anni, ma anche per avermi sempre sostenuto nei momenti duri e stressanti, cercando di infondermi coraggio e buonumore. Grazie di credere sempre in me.